A Parametric Study of Combustion System Design for a Light Duty Diesel Engine

Steven Higginson

A thesis submitted in partial fulfilment of the requirements of the University of Brighton for the degree of Doctor of Philosophy

School of Computing Engineering and Mathematics (SCEM)

In collaboration with

Delphi Diesel Systems (DDS) and Ricardo Consulting Engineers

Declaration

I declare that the research contained in this thesis, unless otherwise formally indicated within the text, was the original work of the author. The thesis has not been previously submitted to this or any other university for a degree, and does not incorporate any material already submitted for a degree.

Signed:

Dated:

Abstract

This thesis documents the characterisation of the performance of a range of Diesel combustion systems derived from two conventional and two unconventional piston bowl designs used in combination with production and prototype piezoelectric fuel injection equipment (FIE).

The effect of injector tip protrusion was studied in order to evaluate the importance of spray targeting on the performance of each piston bowl. All but one bowl, optimised for the same tip protrusion, resulted in an isFC improvement of up to 2.4 % at part load. At full load, the isFC for the unconventional bowls deteriorated by up to 7.4 % as the tip protrusion was increased.

All bowls were tested over a range of part and full load key points and the unconventional bowls had consistently lower isFC (up to 2.5 % lower) but higher isNOx, particularly at part load. Both unconventional bowls performed identically at part load, with one of them performing better at full load.

Both conventional solenoid and prototype piezoelectric injectors were tested on a single conventional bowl. The combustion rate was shown to be slower for the conventional injectors, resulting at part load in better fuel consumption due to less heat transfer. The faster mixture formation and combustion process that the prototype injection system generated was beneficial at the higher load condition.

The effect of the number of injector holes was studied with the prototype piezoelectric injection system. An increase in the number of holes showed an improvement at one of the part load key points, but resulted in reduced performance at the full load points.

A pilot injection study was carried out. Adding a pilot reduced the emission of HC and CO significantly (more than 10 %) while improving the fuel consumption. Adding a pilot and retarding the injection timing at part load resulted in a low temperature combustion mode, which led to a simultaneous reduction in NOx (20 %) and smoke (45 %). This demonstrated the potential of the unconventional bowl designs for use with low temperature combustion strategies.

Contents

List of Tables

List of Figures

Nomenclature

Acronyms

AFR	Air-to-Fuel Ratio
AFRs	Stoichiometric Air-to-Fuel Ratio
aHRR	Apparent Net Heat Release Rate
ATDC	After Top Dead Centre
B1	Baseline Bowl
B2	Narrow Bowl
B3	Shallow Bowl
B4	Ramped Bowl
B5	Stepped Bowl
CAD	Computer Aided Design
CARB	California Air Resources Board
CFD	Computational Fluid Dynamics
CO	Carbon Monoxide
CO2	Carbon Dioxide
CoV	Coefficient Of Variance
DI	Direct Injection
DPF	Diesel Particulate Filter
ECU	Engine Control Unit
EGR	Exhaust Gas Recirculation
FIE	Fuel Injection Equipment
FL	Full Load
HC	Hydrocarbon
HCCI	Homogenous Charge Compression Ignition
HPV	High Pressure Valve
HTHR	High Temperature Heat Release
ICE	Internal Combustion Engine
IDI	Indirect Injection
IFP	Institut Français du Pétrole
IMV	Inlet Metering Valve
KP	Key Point
LNT	Lean Nox Trap
LTC	Low Temperature Combustion
LTHR	Low Temperature Heat Release
MK	Modulated Kinetics
N2	Nitrogen
NADI	Narrow Angle Direct Injection
NEDC	New European Drive Cycle
NOx	Oxides of Nitrogen
O2	Oxygen
PCCI	Premixed Charge Compression Ignition
PCI	Premixed Lean Combustion
PM	Particulate Matter
PPCI	Partially Premixed Compression Ignition

PREDIC	Premixed Lean Diesel Combustion
PRF	Primary Reference Fuel
SCR	Selective Catalyst Reduction
SI	Spark Ignition
SOIm	Start of Main Injection Timing
TDC	Top Dead Centre
UNIBUS	Uniform Bulky Combustion
VCO	Valve Covered Orifice

Greek Symbols

η_{fc}	Fuel Conversion Efficiency	[%]
ϕb	Piston Bowl Diameter	[mm]
ϕ	Equivalence Ratio	[-]
γ	Ratio of specific heats	

Roman Symbols

BMEP	Brake Mean Effective Pressure	[bar]
BSFC	Brake Specific Fuel Consumption	[g/kWh]
Di	Internal Nozzle Hole Diamter	[mm]
Do	External Nozzle Hole Diameter	[mm]
GIMEP	Gross Indicated Mean Effective Pressure	[bar]
HL,exh	Heat Loss to Exhaust	[kW]
HL,ht,c	Heat Loss to Heat Transfer and Crevice	[kW]
IMEP	Indicated Mean Effective Pressure	[bar]
isCO	Gross Indicated Specific Carbon Monoxide	[g/kWh]
isFC	Gross Indicated Specific Fuel Consumption	[g/kWh]
isHC	Gross Indicated Specific Hydrocarbons	[g/kWh]
isNOx	Gross Indicated Specific Oxides Of Nitrogen	[g/kWh]
K	Nozzle Hole K-Factor	[-]
Ki	Critical Flow Nozzle Calibration Coefficient	[-]
L	Nozzle Hole Length	[mm]
Oi	Critical Flow Nozzle Activation Coefficient	[-]
Pin	Critical Flow Nozzle Inlet Pressure	[mbar]
Tin	Critical Flow Nozzle Inlet Temperature	[K]
W,I,g	Gross Indicated work	[kW]

Acknowledgements

From the University of Brighton I would like to thank my supervisors Dr David Mason and Dr Guillaume De Sercey, Professor Morgan Heikal, the technical staff Brain Maggs, Peter Rayner and Ken Marris and all of the other staff members that helped me on my way, too numerous to mention. I would also like to thank Delphi Diesel systems Ricardo consulting engineers and the EPSRC for their input into this project.

I would like to thank all of my fellow research students; Lars, Lyndon, Benoit, Angad and Thiago, who suffered and succeeded with me in equal measure.

I would also like to thank my family and friends for supporting me over the last five years. I must make a special mention of my parents; Sue and Jim. The belief they have in me is astounding and I am grateful for it.

Katrin Oberin.

1 Introduction

1.1 Project Context

The work in this thesis is focused on an experimental study into the influence of piston bowl geometry and fuel injector type on optimal fuel injection strategies for clean high efficiency operation. Clean, efficient operation is necessary for the Diesel internal combustion engine (ICE) to meet future European emission regulations. The work in this thesis is relevant to Diesel engines used in passenger car applications, referred to as category M_1, which is defined in the European directive (2001/116/EC).

Emission regulations were first applied to new passenger cars in the 1970's in America by the California Air Resources Board (CARB) (70/220/EEC) and since then the regulations have gone through a series of amendments and updates. The driver for the updates and amendments has come from two distinct external pressures; the availability of the non-renewable fuel source and the effect of pollutant emissions on the environment. At the beginning of this research project the European emission standard in force was Euro IV. Euro V was then introduced, which enforces a limit of 0.180 g/km of Oxides of Nitrogen (NOx) and 0.005 g/km of Particulate Matter (PM). The legislation proposed for 2014, is Euro VI which mandates a reduction of NOx by 56 %, whilst maintaining the PM level. These regulations apply to all new production vehicles. The following Table 1.1 details the regulated levels.

Tier	Date	Tail pipe emission				
	yyyy-mm	CO	HC	NOx	HC+NOx	PM
		g/km	g/km	g/km	g/km	g/km
Euro I	1992-07	2.72	-	-	0.97	0.140
Euro II	1996-01	1.00	-	-	0.70	0.080
Euro III	2000-01	0.64	-	0.50	0.56	0.050
Euro IV	2005-01	0.50	-	0.25	0.30	0.025
Euro V (current)	2009-09	0.50	-	0.18	0.23	0.005
Euro VI (future)	2014-09	0.50	-	0.08	0.17	0.005

Table 1.1 European emission regulations for Diesel powered passenger car vehicles ≤ 3,500kg

The European commission has also proposed a fleet averaged limit on carbon dioxide (CO_2) emissions. The target proposed in 2007 is to meet 120g/km of CO_2 by 2012 (2007/0297 (COD)). Emissions of CO_2 are intrinsically linked to the fuel consumption of an engine because the ideal process for oxidising a hydrocarbon leads to the production of CO_2, water vapour (H_2O) and nitrogen (N_2). Reducing fuel consumption, therefore, reduces the CO_2 emission. To this date the CO_2 target is not a legal requirement of a vehicle manufacturer, however if this becomes a law, then this represents an additional challenge to overcome.

Experts within the automotive industry and engine research groups state it will be difficult to achieve the NOx limits for Euro VI without aftertreatment. Installing NOx aftertreatment systems such as selective catalyst reduction (SCR) or a lean NOx trap (LNT) represents the least risk in getting a vehicle into production (Bickerstaffe, 2009). Aftertreatment systems, whilst effective in removing unwanted emissions from the exhaust gas, typically have added cost, complexity and fuel consumption penalties, which are unattractive for vehicle manufactures thus providing a driver for research into the reduction of engine out pollutant emissions. Engine out pollutant emissions are measured directly as they exit the combustion chamber, prior to any chemical and thermal influence in the exhaust system. The production of engine out emissions is influenced by the in-cylinder mixture formation processes. The mixture formation process is controlled by the rate of fuel addition and energy in the in-cylinder air motion. The fuel addition is governed by fuel pressure, injector type and nozzle design and the energy in the airflow is governed by the engine inlet air pressure, inlet port shape and activation, as well as the piston bowl shape.

For this reason the present study takes two steps with engine hardware to reduce engine out emission; firstly 4 different piston bowls were designed, two conventional and two unconventional in shape and secondly a prototype fuel injection system was developed, with direct needle actuation. The piston bowls were designed and evaluated by Ricardo Consulting Engineers using Computational Fluid Dynamic (CFD) technology to assess the in-cylinder flow regimes and fuel spray targeting. The conventional type refers to typical, re-entrant, toroidal piston bowls, which have become an industry standard. The first unconventional design was adopted from a heavy duty applications and the second was an evolution of this design based on CFD evaluation and analysis of the potential fuel spray

pattern. The prototype fuel system was developed by Delphi Diesel Systems (DDS) based on the development of new piezo technologies. The design employs a piezo actuator to move the needle directly which shows an improvement in Diesel fuel spray formation. The fuels spray pattern with various nozzles has been studied but the effect on combustion is not fully understood.

Both elements of the hardware have new concepts for the Diesel combustion system. Although there has been substantial research into Diesel combustion system configurations, there is still scope for developing the understanding of the effect of conventional and unconventional hardware on the combustion process. This thesis shows the results of the experiments that were carried out with the new hardware, with recommendations for the use of the hardware designed in this study.

1.2 Thesis Structure

The next chapter, chapter 2, has the literature review of the fundamentals of the combustion process and emissions formation, of the design of engine hardware and of the existing knowledge of the effect of this hardware on the combustion process. Understanding the fundamentals of the combustion process and emission formation is important because it helps to identify the reasons why one piston bowl behaves differently to another. Understanding the effects of the design of the hardware also assists in the understanding of the in-cylinder processes that are occurring. Chapter 3 shows the experimental equipment used in this study including the hardware and the instrumentation. Within the chapter there is an assessment of the suitability and limitations of the experimental facility, hardware and instrumentation. Chapter 4 shows the experimental process used to optimise the spray targeting and to characterise the piston bowls and fuel injectors. The experimental procedure ensured experiments were repeatable and that the comparisons between each piston bowl were made on the same basis. Chapters 5 to 7 present the results and the discussion of the characterisation of the piston bowls. This chapter includes the results of the spray targeting and the results of the characterisation process. This chapter is important in identifying why the bowls perform differently and identifies the characteristic differences between the conventional and unconventional bowl designs. In this chapter the best performing bowl is selected with justification given for the

selection. Chapter 8 shows the results of further testing. This further testing examines the effect of multiple injection strategies and attempts to further reduce the engine emissions output based on the knowledge gained from the characterisation process and the understanding of the mixture formation requirements. The final chapter comprises the conclusions and recommendations for further work.

2 Diesel Combustion System Development Literature Survey

In this chapter the literature related to modern Diesel engine combustion systems is reviewed. Combustion system design was examined to identify the different design concepts that have been developed and classify their key features and relevance to future combustion systems. The evaluation is focused on developments in combustion chamber design and fuel injection systems. Following this, experimental and computational investigations into Diesel combustion and emissions are reviewed.

2.1 Diesel Combustion Systems

In this study the combustion chamber geometry and fuel injection equipment and their configuration are referred to as the combustion system. These two hardware elements create and support the combustion process. Diesel engines have developed two distinct types of combustion system, the indirect injection (IDI) and the direct injection (DI) combustion system.

2.1.1 Indirect Injection

The indirect injection Diesel engine is characterised by the existence of a separate chamber linked to the main chamber by a gas flow passage. Within this separate chamber, the air and fuel mix before the combustion process. This causes an increase in local pressure, forcing the combustion products and un-burnt fuel back into the main combustion chamber.

Various configurations of the IDI Diesel engine have been developed. An early example, called the Comet, was developed by Ricardo in the 1930's. The Comet used an almost spherical combustion chamber integrated into the cylinder head with a pathway running between it and the main combustion chamber (Heisler, 2002, Bosch, 2000). This chamber is known as the pre chamber. It generates rotational air motion induced by the tangential arrangement of the flow path and the injector.

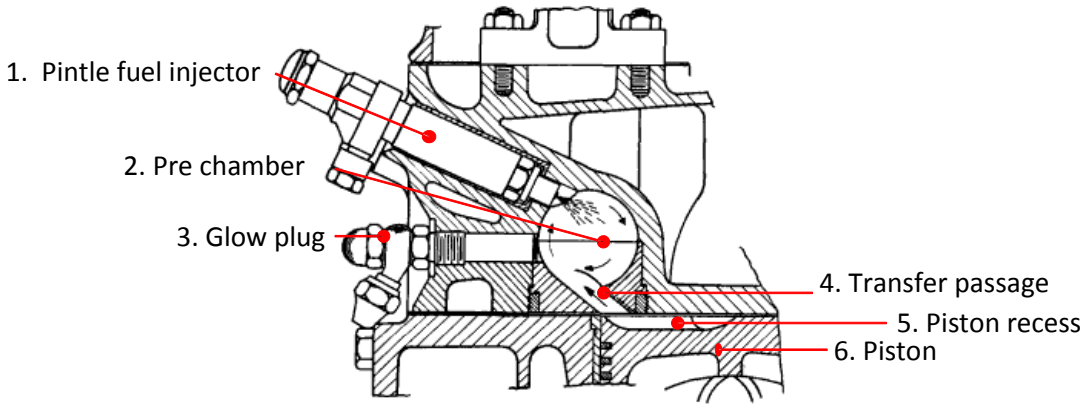

Figure 2.1 Ricardo Comet IDI Diesel engine (Carr, 2014)

Figure 2.1 shows the pre chamber (2) contains a pintle type fuel injector (1) and glow plug (3). The piston (6) in the main chamber is flat, with two small recesses (5). The fuel injector is a single hole, conical pintle injector, with a tangential orientation. The injector location and the shape of the pre chamber both encourage air and fuel mixing before the start of the combustion event. A low pressure injection system of 100 bar was used because the turbulence of the air is sufficient to assist mixture formation. The fuel spray was targeted at the hot walls of the pre chamber to enhance vaporisation and entrain the mixture (Heisler, 2002). The glow plug is located to aid heating of the pre chamber under cold start conditions, so that the air would reach the auto ignition temperature whilst the engine is in the early stages of warming up (Bosch, 2000).

During the first stage of the combustion process, rich combustion products such as carbon monoxide (CO) and particulates form due to the poorly atomised fuel spray. As heat is released the temperature and pressure increases inside the pre chamber and a flow reversal occurs forcing the gas into the main combustion chamber. At this point the combustion products and any un-burnt fuel mix with the remaining oxygen due to additional turbulence caused by the piston recess in the main combustion chamber. The piston recess forces the gas into a rotary motion with the air leading to further oxidation. The remaining combustion gases mix and oxidises as the piston expansion process begins.

The oxidation of the combustion gases that occur in the pre chamber can be assisted by distributing the combustion gases amongst the fresh air within the cylinder. The Mercedes

variant in Figure 2.2 used a different concept for the indirect injection combustion system (Bosch, 2000, Heisler, 2002).

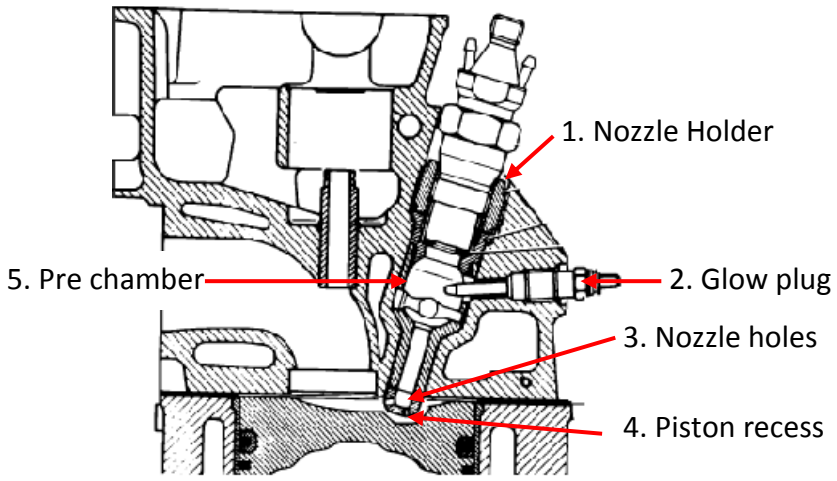

Figure 2.2 Mercedes IDI Diesel engine cross section (Davis, 2011)

The pathway that links the pre chamber (5) to the main chamber with the piston recess (4) had distributed nozzle holes (3) at the inlet and exit. This allowed the combustion to be distributed through the main chamber with a greater probability of locating oxygen in the fresh charge. This design can be compared to a direct injection configuration with a multi-hole nozzle injection system. In this case, the pre chamber acts as the combustion medium regulator, analogous to the fuel pressurising system and the nozzle holes in the pathway are analogous to a fuel injector with multiple nozzle holes.

The motion of the air induced into the combustion chamber can be controlled to assist the combustion product and air mixing in addition to using the pre chamber to mix the fuel and air. The intake arrangement of the Mercedes variant of the indirect injection system was designed to encourage in-cylinder swirl motion (Heisler, 2002). Swirl is tangential air motion induced by either incorporating a helical port, which encourages to gas to rotate around the valve trumpet, or by deactivating a port (in an engine with more than one port) to bias the airflow tangentially in the cylinder. Generating swirl by shaping the inlet ports has been shown to have a negative effect on engine breathing and volumetric efficiency. Swirl ratio is a dimensionless number proportional to engine speed. Deactivating one port on multiple inlet valve engines reduces the flow area available and also reduces the volumetric efficiency. Therefore a trade-off exists between a design which allows the fuel and air to mix

more efficiently, with swirl, and a design which negates poor mixing by increasing the charge density by inducing more air into the cylinder.

The need for a pre chamber, a transfer path and increased combustion gas turbulence on the indirect injection Diesel engine increases the heat transfer losses. For the same engine displaced volume, the surface area is greater than direct injection variants. Heat transfer losses are also exaggerated by the need to induce high turbulence in both the pre chamber and the main combustion chamber. A special insert made of Nimonic, a material with low thermal conductivity and a high temperature tolerance, is used as the pre chamber to reduce these parasitic losses however the concept was fundamentally flawed and could not achieve low specific fuel consumption.

Indirect injection systems allow the fuel to be injected from the beginning of the compression stroke, allowing more time for the mixture formation process. The benefit of this is that the maximum engine speed can increase, which enables the engine to be operated with power densities suitable for automobiles. The weakness of the indirect injection engine is poor fuel efficiency (Middlemiss, 1978, Heywood, 1988, Stone, 1999, Bosch, 2000, Heisler, 2002), whilst the main benefit of this type of combustion system is the reduction in the kinetic energy required in the fuel spray for good air-fuel mixing. As a result the fuel injection system could be operated at low pressures thus simplifying the system and reducing its cost and minimising parasitic losses.

With the Comet engine, turbulence is created within the combustion system, reducing the dependency on port design to promote air motion. This benefited engine volumetric efficiency. Finally the rate of oxidation of the combustion products in the main chamber reduced the rate of pressure rise and the noise associated with Diesel knock is reduced (Heywood, 1988, Stone, 1999). There are some aspects of the mixture preparation of the indirect injection system that are similar to a port fuelled gasoline engine; the combustion system design must ensure sufficient fuel vaporisation and droplet break up.

Both of these IDI combustion systems have high turbulence and a high surface area to volume ratio, which increase the convective heat transfer losses. The additional surface area comes from the pre chamber and transfer passages. With the development of electronically

controlled common rail fuel systems and improved turbo charging technology, the direct injection engine has becomes a viable alternative.

2.1.2 Direct Injection

The direct injection (DI) combustion system, shown in Figure 2.3, is made up of a single combustion volume enclosed within the cylinder head and piston. The fuel injection system is located to deliver the fuel directly into the enclosed volume. With a modern cylinder head layout containing four valves per cylinder the injector is generally mounted vertically in the centre of the combustion chamber. For two valves per cylinder arrangements the injector is usually mounted at an angle.

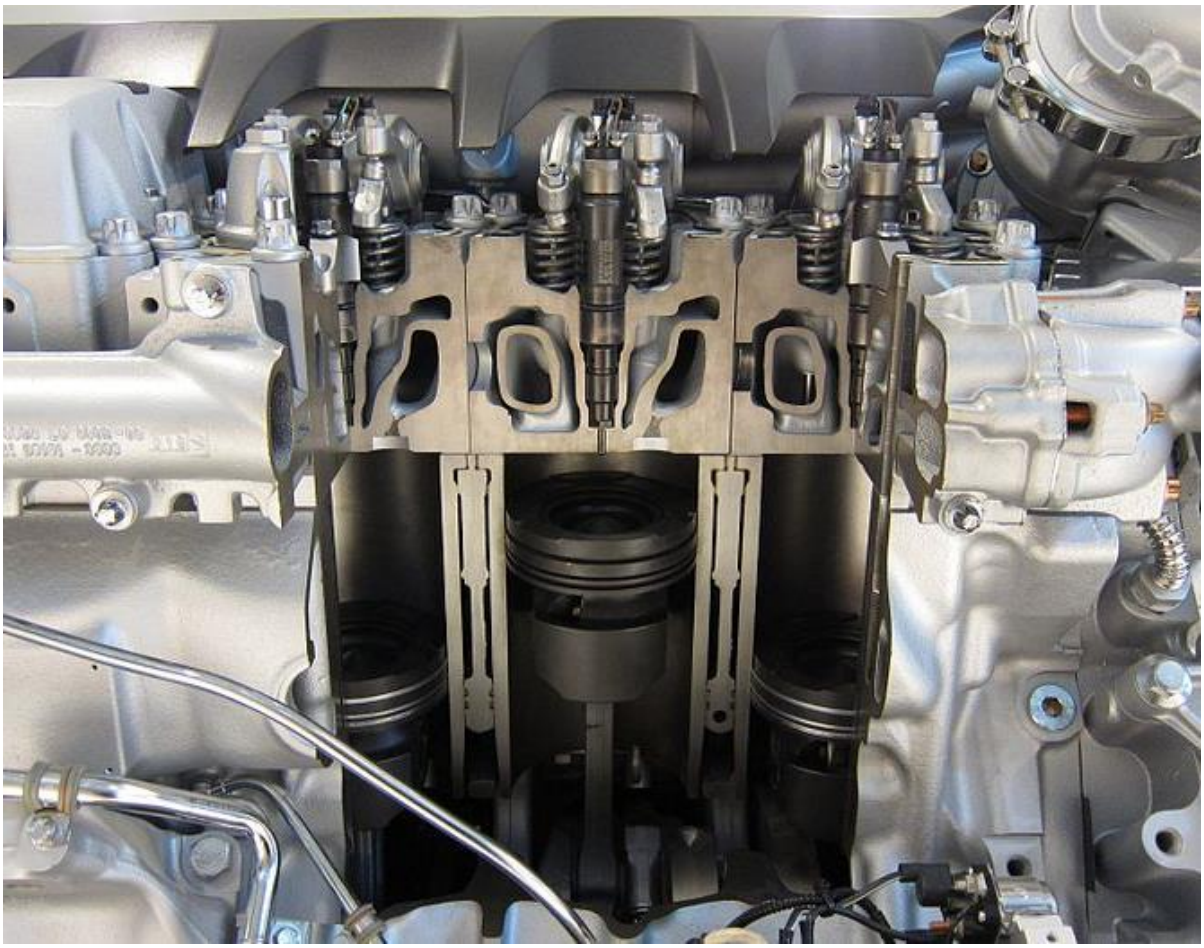

Figure 2.3 DI Diesel engine with a centrally mounted fuel injector (Cleynen, 2011)

The design requirements for the DI combustion system vary depending upon the size and the speed of the engine. These systems are usually classified according to displaced volume and relative operating speed of the engine (Stone, 1999).

Heavy duty Diesel engines have been used in both marine applications and power generation. They employ both two-stroke and four stroke modes of operation, with speed ranges from 100 – 1800 revolutions per minute (Heywood, 1988, Stone, 1999). The application of low speed Diesel for power generation is sensible, as the larger the displaced volume of the engine results in a significantly lower surface area to volume ratio. This is hugely beneficial for reducing the thermal losses from the combustion system and improving fuel efficiency. One of the largest Diesel engines used for container ship propulsion is the Wartsila-Sulzer RTA96C. It has a displaced volume of 1820 litres per cylinder and with multi-cylinder configurations producing 84 MW with a fuel efficiency of 171 g/kWhr (Doug). The maximum speed of the engine was determined by mean piston speed. The RTA96C has a maximum piston speed of 8.5 m/s, which equates to a running speed of 102 RPM and a stroke of 2.5 m (Doug).

The low engine speed of the RTA96C means that there is more time per cycle for the mixture formation process to occur. The length of time available and the limited speed range of the engine simplified the design of the combustion system. The fuel injection equipment is optimised to provide maximum fuel spray pressure, without the need for variation over a wide speed range. A mechanical unit injection is ideal for this combustion system.

The design of the piston bowl shown in Figure 2.4 is kept as wide and shallow as possible to accommodate the fuel spray formed using high injection pressures. Minimal air motion is created both internally and externally (Bosch, 2000, Heywood, 1988). In heavy duty Diesel engines it is more effective to optimise the inlet for maximum air consumption because adequate time exists for the mixture formation process using the kinetic energy in the fuel spray.

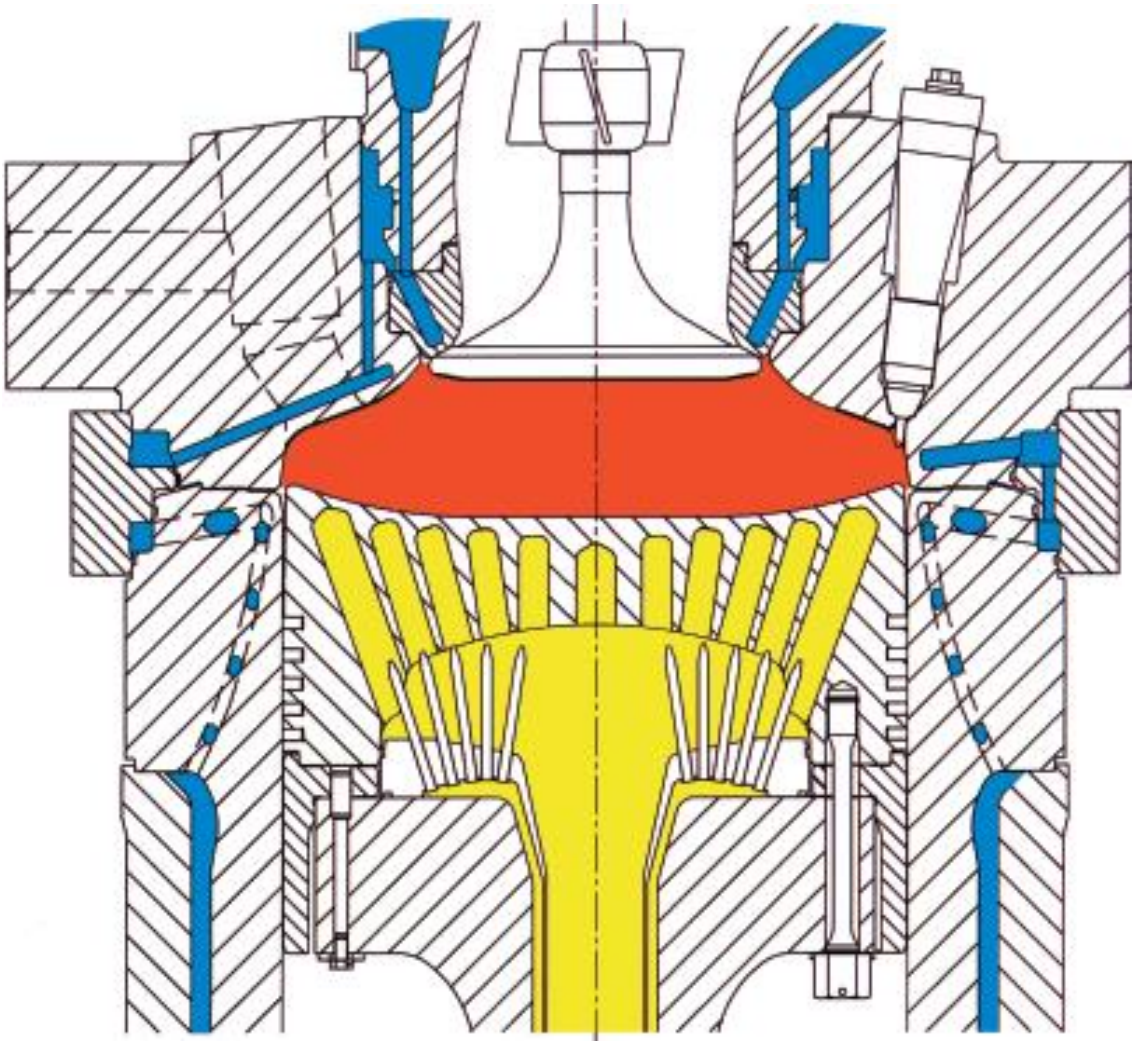

Figure 2.4 Engine cross section detailing piston design (Doug, 2009)

At the other end of the scale is the light duty Diesel engine. Light duty Diesel engines are usually operated with high swirl rates to assist the mixture formation process. These engines are required to work over a large speed range, with the maximum speed up to and over 4000 RPM (Stone, 1999, Bosch, 2000). In comparison to the heavy duty Diesel, the mixture formation and combustion process in a light duty Diesel engine has less time to occur. Comparing the maximum engine speeds of a light duty application to a heavy duty application (4000 RPM compared with 100 RPM), the time for one engine cycle is 40 times shorter. Mixture formation is assisted by using high injection pressures; however this needed to be available over a wide range of engine speed and loads.

The move towards the use of light duty DI engines began because of the need for improved fuel consumption versus the IDI variant. The compromise between the DI and IDI systems is

having a light weight, high speed system (IDI) and a system with minimal thermal losses and greater refinement (DI). Smaller combustion systems have inherently high heat transfer losses associated with the larger surface area to volume ratio. However the benefit of the smaller system is that it can be easily packaged into a vehicle platform due to its size and weight.

In comparison to the heavy duty Diesel engine, light duty Diesels utilise narrower and deeper piston bowl shapes in order to promote more turbulent air motion. This is demonstrated by the DI MAN combustion system shown in Figure 2.5. The MAN piston bowl is deep and is combined with a pintle injector which directs the fuel flow on to the bowl wall to enhance the mixture formation process (Stone, 1999).

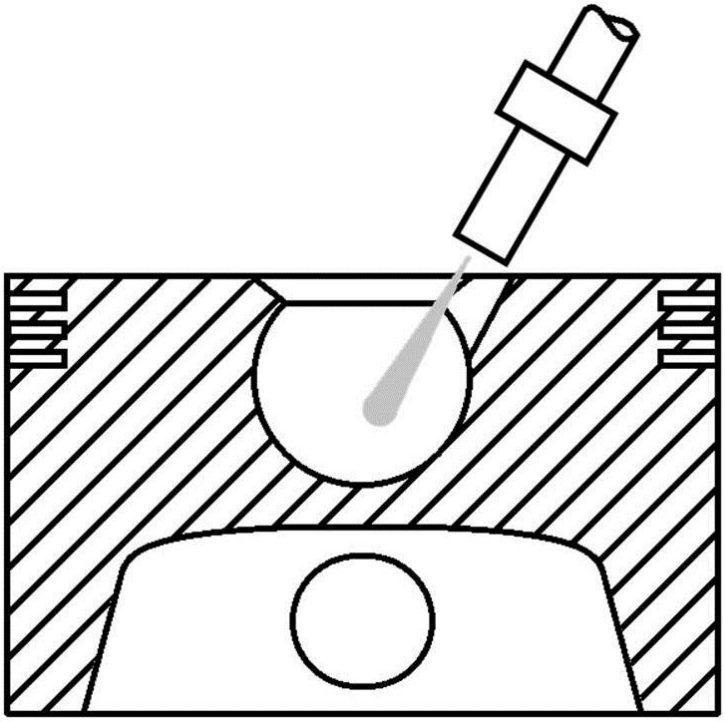

Figure 2.5 Schematic of the MAN spherical combustion system design concept

The turbulence generated by a narrow piston bowl design is called squish. This is the flow of gas forced into the piston bowl at top dead centre and is more pronounced in a narrow piston design. Internally generated turbulence enhances the mixture formation process, but leads to greater convective heat transfer losses (Stone, 1999). Internal turbulence creation is necessary to help the combustion process where the engine operation has to occur over a broad range of speed and load conditions.

Generating the energy for the mixture formation process becomes more challenging over a wide range of speeds and load conditions. At low speeds there is less air swirl and fuel pressure available (depending on the fuel system configuration). Swirl is often proportional to the engine speed, as the engine rotational speed increases, so does the swirl rotational speed. At low speed low load conditions with low thermal energy in-cylinder, there is a reduction in the heat transfer temperature gradient and convective heat transfer losses are reduced.

At low speed, high load, the mixture formation is limited by the lack of air motion. At medium to high speed the swirl turbulence increases and the available pressure within the fuel system is greater. Both of these enhance the mixture formation process. There is a limit to the engine speed because the cycle time reaches a minimum for mixture formation and combustion to occur. The time available to add the fuel to the combustion system and control the burning process is too short. This results in the fuel injection event and the combustion process extending into the expansion stroke therefore reducing the engine efficiency at higher speeds.

The viability of the DI engine in a vehicle application has come through developments of the engine sub systems. Improved cylinder head designs, allowing higher in-cylinder pressures, turbo charging and improved fuel system design have made mixture formation possible within the short times available. The benefit of reduced heat transfer losses mean that the DI Diesel engine is a viable alternative to the IDI variant in order to meet fuel economy targets.

However, further development of the DI Diesel combustion systems are required in order to meet future, stringent emissions standards. The move towards advanced combustion modes requires better understanding in terms of the way the mixture formation process evolves. This includes understanding the best way to accommodate and mix the fuel spray within the piston bowl design.

2.1.3 Diesel Piston Bowl Design

Piston bowl design has been the subject of several research projects both experimental and computational, for over forty years (Middlemiss, 1978). The research projects have focused

on the shape of the cross section of the piston bowl and the effect of changing the dimensions of the major features on the combustion process. The effects on the combustion process are interlinked by the way in which the major features interact with the fuels spray; through in-cylinder air motion development and by surface interactions with the fuel spray.

The DI Diesel piston bowl has a complex cross section design developed to enhance impingement the mixture formation process. Research carried out in the past has developed the design of the piston bowl into a toroidal, re-entrant design that uses squish flow and swirl flow to enhance the mixture formation. Typically the piston is a flat surface parallel with the cylinder head fire deck and the bowl is machined out of the piston blank. A schematic is shown in Figure 2.6

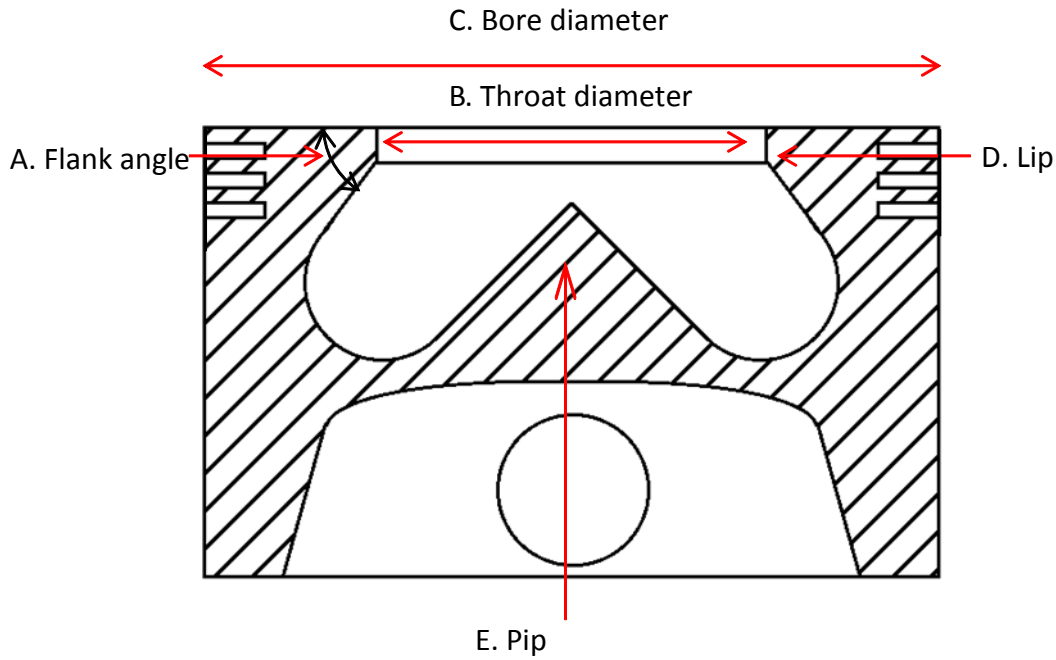

Figure 2.6 Schematic layout of a DI piston bowl showing some of the parameters used in (Middlemiss, 1978) study

A study conducted by (Middlemiss, 1978) experimentally demonstrated that the re-entrant combustion chamber with a central pip could sustain rapid combustion at more retarded combustion timings than open bowls meaning that NOx could be reduced, without a large penalty on fuel consumption. Improvements in specific fuel consumption of around 11 % were achieved at equivalent NO outputs with a marginal reduction in smoke number at the

most retarded injection timing. The role of the pip is to occupy the space where the velocities are lower and to increase the velocity at the periphery of the chamber to enhance fuel and air mixing. This central pip encourages more turbulence than an open bowl design.

A design guide for piston bowls was developed by (Middlemiss, 1978). The emissions outputs and fuel measurements were used to understand the effect of the bowl design on the combustion process. Although in-cylinder information was available this study demonstrated that it was possible to draw considered conclusions from careful analysis of the emissions behaviour without necessity for pressure measurement.

Some of the parameters investigated by Middlemiss are shown in Figure 2.6. Throat diameter (B) should be around a third of the piston bore (C) for the ideal operation. Larger re-entrant bowls begin to behave like open chambers and smaller throat diameters suffer from high NOx levels and poor fuel consumption due to convective heat transfer losses. Varying the compression ratio affects ignition delay and the NOx and smoke emissions trade-off. At a high compression ratio a retarded timing has low NOx and high smoke. Specific fuel consumption was lowest at 17:1 and Middlemiss recommended using the highest value that could be achieved within the smoke limit. Finally the lip shape (D) and flank angle (A) were less distinct; sharp lips with a flank angle of 70° resulted in low smoke without a NOx penalty, but in general in order to reduce smoke, impingement with the lips and the bowl was to be avoided. Flank angles in the order of 30-50° were recommended, large flank angles approximated the open chamber behaviour

(Saito et al., 1986) tested a re-entrant chamber and found that, as Middlemiss recommended, a re-entrant bowl with a throat that was roughly a third of the bore diameter performed the best compared to the conventional open chambers of the time. Computational analysis showed that there were high temperature regions found on the lip section which were identified as helping to reduce the ignition delay. Spray targeting was such that this high temperature region was used to control the combustion behaviour of the engine.

The high wall temperatures and high squish velocities allows combustion timing to be retarded without sacrificing fuel consumption and smoke emissions. Indeed at one test

point, the re-entrant bowl has shown an improvement in Brake Specific Fuel Consumption (BSFC) of 4 % whilst simultaneously reducing NOx and smoke by 10 % and 39 % respectively. Compared to the deep open bow used, the re-entrant bowl was 6 % better in fuel consumption and 60 % better in smoke number with only a 14 % penalty on the NOx emission. The squish flow which assisted the combustion was calculated to be 50 % higher than the deep open chamber that was tested, which although increased the NOx emission, meant that the fuel consumption and smoke number were both improved.

(Ikegami et al., 1990) indicated through in-cylinder studies that the role of the lip in the re-entrant chamber was to suppress the flow of bowl based combustion products and un-burnt fuel into the squish regions. Back flow that occurred during the combustion event forced the combustion products and un-burnt fuel into a region that was low in temperature and turbulence. This led to high specific fuel consumption and smoke number, although in general NOx is lower. Comparing the deep bowl of the time with the re-entrant bowl, even though the re-entrant bowl was 14 % worse on NOx, it was 7 % better on BSFC, 60 % better on particulates and 75 % better on smoke number. Combustion with the deep bowl was more varied across the range of injection timings tested, whereas the re-entrant bowl could tolerate being retarded with little change in fuel consumption and emissions.

(Kidoguchi et al., 1999) studied the effects of the re-entrant design with experimental engine testing on an engine instrumented with an endoscope and CFD calculations to further understand the in-cylinder processes. As with previous work the comparison was made against a standard open bowl and a selection of re-entrant designs with parametric variation of features such as compression ratio and throat diameter. The results of this work indicated that although the NOx levels converged on the same values for all bowls as the injection timing was retarded, the re-entrant bowls were better in terms of specific fuel consumption and particulate emissions. A two stage combustion process was identified where a short ignition delay and diffusive combustion was retained in the piston bowl whilst being supported by highly turbulent squish and swirl flows. This hypothesis was supported by endoscopic measurements, which identified yellow emitted light indicative of soot luminosity within the piston bowl region. The intensity was observed sooner and within the region of the piston bowl, during the early phase of combustion.

Having attempted to understand the effect of combustion chamber geometry on engine performance, research attention also focussed on the fundamental behaviour in-cylinder. (Montajir et al., 2000) used an adapted engine with a square combustion chamber that allowed undistorted photographs to be taken of the fuel spray spreading over the surface of the combustion chamber. A fuel spray path length and an equivalent fuel spray diameter were calculated based upon the area that the fuel spray had spread over the bowl wall. The characteristics were used to demonstrate the effect of lip radius, spray targeting, bowl diameter and toroidal radius. The study showed that a round lip reduces the energy lost due to the impact of the fuel spray with the bowl wall leads to a greater spread of fuel spray and fuel volume at the bottom of the bowl after impingement. The targeting and bowl diameter has to be such that the fuel distribution is balanced between flow into the squish regions and flow concentrated at the bottom of the bowl. A radius corner in the bottom of the bowl helps with fuel distribution; however the authors demonstrated that a radius that was too large leads to a long spray path length. Overall, the interaction of the fuel spray and the piston bowl presents a trade-off in the process of mixture formation.

The Narrow angle direct injection NADI piston bowl concept can be seen in the study by Institut Français du Pétrole (IFP) (Walter and Gatellier, 2002) The piston bowl is narrow and deep and coupled with a narrow spray angle fuel injector. This allows the fuel to be injected very early in the cycle to allow time for premixing to occur before the onset of combustion. This mixture formation strategy with this bowl and injector combination is unusual and is a move away from the previous studies. It relies less on the turbulence generated in-cylinder for the mixture formation process by allowing more time for premixing the fuel and air. With such an unusual arrangement the authors make a comparison of the NADI combustion system with the baseline engine at full load because the unusual combustion system could have compromised the engine performance at full load.

The majority of bowl studies have shown that a circular, re-entrant bowl type with a toroidal piston bowl works the best for stable, retarded combustion, that result in low NOx and smoke without a large penalty on fuel consumption. The toroidal re-entrant designs are considered to be of a conventional type of design that has been accepted as an industry standard for many years. The NADI concept (Walter and Gatellier, 2002), which uses

advanced combustion modes, challenges the way that the mixture formation process can be changed for clean and efficient combustion. The application of advanced combustion modes means that unconventional piston bowl design may be required for future Diesel engines.

2.2 Diesel Fuel Injector Design

Common rail fuel injection systems are designed to supply each injector with the same fuel pressure over a range of engine conditions. The common rail serves as a high pressure fuel reservoir replenished by a separate fuel pump operated by the engine crank shaft. This allows the flexible operation of the injection system over a range of operating conditions (Bosch, 2000, Mollenhauer.K and Tschoeke.H, 2010).

Typically, each injector within the common rail system is actuated electronically. Electronically actuated fuel injection systems have revolutionised the Diesel engine design. This is because the fuel injection event can be controlled without mechanical restrictions related to engine speed as with a unit injector. There are two types of injector actuator currently in use; solenoid actuator or piezo electric actuator. In current production vehicles the actuator is used to control a valve in the body of the injector. This valve controls the flow of fuel through the injector. Opening the flow valve causes a pressure difference across the injector needle and forces the needle to lift.

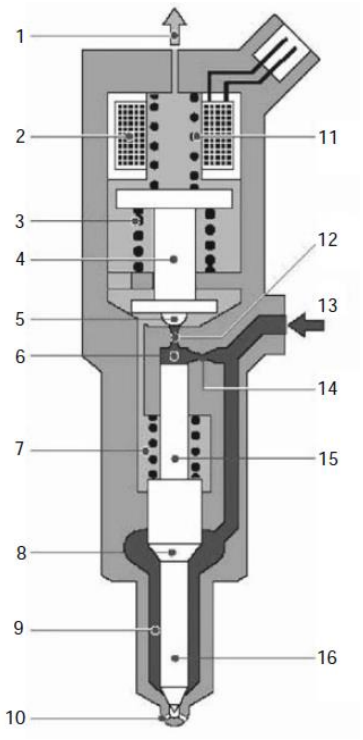

1. Fuel return (spill flow)
2. Solenoid coil
3. Over lift springs
4. Solenoid armatures
5. Valve ball
6. Valve control chamber
7. Nozzle spring
8. Nozzle needle pressure shoulder
9. Chamber volume
10. Spray hole
11. Solenoid valve spring
12. Outlet throttle
13. High pressure port
14. Inlet throttle
15. Valve piston
16. Nozzle needle

Figure 2.7 Solenoid valve injector design (adapted from (Mollenhauer.K and Tschoeke.H, 2010))

Figure 2.7 shows the solenoid variant of the Bosch system. The flow through the injector is controlled by the movement of the valve ball, by the activation of the solenoid. This opens the flow passage from the valve control chamber to the fuel return. The piezo injector seen in Figure 2.8 uses a piezo electric actuator with an amplifier to operate the control valve. Fuel still flows through the injector in order to lift the needle, however the system has a faster response time, having a delay between electrical signal and hydraulic response of 150 microseconds (Mollenhauer.K and Tschoeke.H, 2010). These injectors can be integrated easily into existing common rail systems.

The above two injection systems work well with a common rail fuel system as there was a readily available supply of high pressure fuel which can be utilised to lift the needle and control the injection event. Refining the flow through the injector can improve the injector response time as seen with the piezo electric actuator and precise metering of the fuel can be achieved.

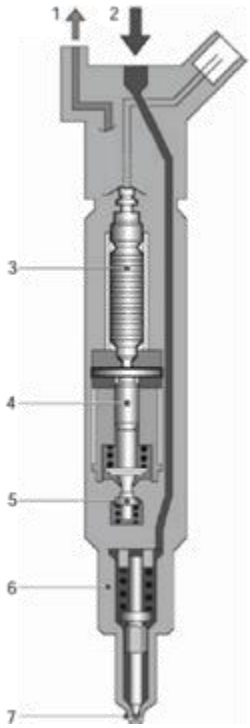

1. Fuel return (spill flow)
2. High pressure port
3. Piezo actuator module
4. Hyraulic coupler (amplifier)
5. Servo valve (control valve)
6. Nozzle module with nozzle needle
7. Spray hole

Figure 2.8 Bosch piezo inline injector design (adapted from (Mollenhauer.K and Tschoeke.H, 2010))

The disadvantage of the injectors operating with a spill flow with the common rail system is that the needle lift is indirect and is influenced by the response of the needle to the

changing forces in the system. Needle lift then becomes a parameter dictated by the construction of the hardware that cannot be altered dynamically and is limited by the rail pressure.

Actuating the needle directly reduces the hydraulic effects on the injection event and therefore improving the response of the injector but it additionally removes the requirement for the fuel return into the rail.

Figure 2.9 shows a direct acting injector, which has completely eliminated the requirement for a return flow through the injector. The needle actuation occurs as a result of direct hydraulic coupling between the needle and the piezo electric actuator. The piezo electric actuator is sealed from the high pressure fuel, and the stack compensates for the thermal and hydrostatic loads introduced by the pressurised fuel (Schöppe and Zülch, 2009).

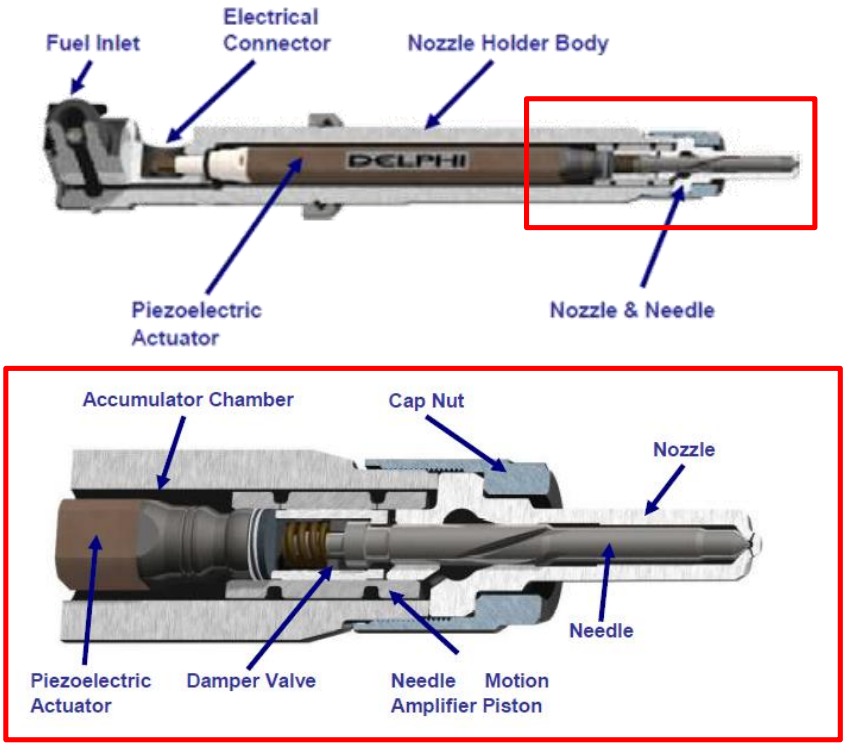

Figure 2.9 Delphi DFI3 direct acting fuel injector (adapted from (Schöppe and Zülch, 2009))

There are several benefits to this system, the first of which is the reduction in the hydraulic power requirement associated with the return flow through the injector. This also benefits the thermal loading on the fuel circuit, helping to reduce the fuel temperature in the system. The design of the body of the injector allows a residual amount of fuel to exist

inside the accumulator chamber, thus increasing the pressurised volume available for injection. The response time was also improved between the electrical demand and the hydraulic event, and was in the order of 100 microseconds. The result is a fast response with a 'square' injection rate profile, regardless of the fuel pressure used when compared to conventional solenoid or valve operated piezo systems (Schöppe and Zülch, 2009). A 'square' rate profile results in the largest injected mass per second.

The direct acting injector is a step change in the design of the Diesel fuel injector. Systems have existed in the past that have been capable of delivering high fuel pressures, however, the operation of the injection equipment is based upon return flow principle and therefore the hydraulic performance is affected making the system less efficient. The improvement in spray momentum as a result of the high fuel pressure at the point of needle lift and the maintenance of this pressure during the injection event improve the fuel spray atomisation and air entrainment. Also the fast opening and closing times allow precise and repeatable control of very small injection quantities and multiple injection events allowing for novel injection strategy development to achieve clean and efficient combustion.

2.2.1 Fuel Injector Nozzles

Figure 2.9 shows the fuel injector nozzle for a common rail system. Nozzles are incorporated into the nozzle holder assemblies for the common rail system. The nozzle is the boundary between the fuel system and combustion chamber, and the design of the nozzle heavily influences the mixture formation process. The function of the nozzle is to direct the fuel spray to the desired location and to create the shape of the spray plume. The definition of the nozzle parameters for the piston bowl being used is important as these cannot be changed and spray targeting can only then be adjusted by changing the injector position. The last function of the injection needle is to seal the fuel system. This is a vital function as any of the high pressure and temperature combustion entering the fuel system could cause damage. The damage could manifest itself either as mechanical fatigue of the components or by leaving deposits in the system (Mollenhauer.K and Tschoeke.H, 2010).

Nozzle designs vary depending on the design of the combustion system. A combustion system is developed based on the size and speed of the engine, as a result the mixture formation requirements change. This means that inherently, the fuel injection nozzle design

is part of the combustion system hardware and is as important as the piston bowl design to the output and emissions of the engine.

Multi-hole nozzles use the needle to restrict the fuel flow to more than one orifice. The systems can be direct orifice closing as in the valve covered orifice (VCO) whereby the orifice was covered by the needle itself, or a system which uncovers a volume that feeds the nozzle orifices as in the sac design. The two types are shown in Figure 2.10.

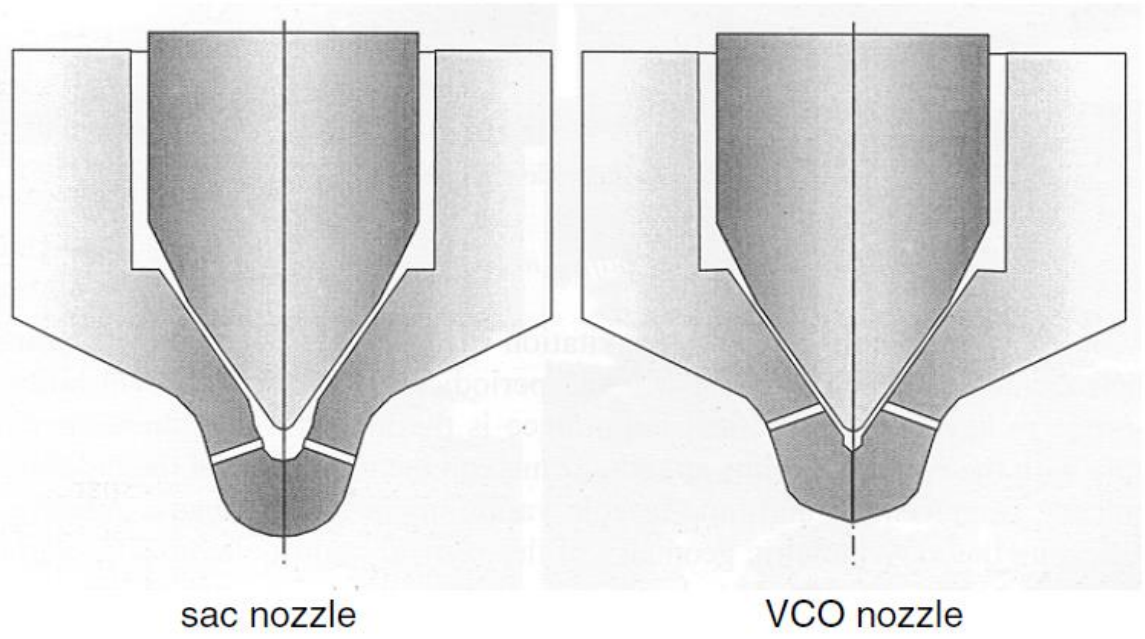

Figure 2.10 Multi-hole nozzle types; left sac, right VCO (Martynov, 2005)

In a VCO system, during the early stage of needle lift, the flow area will be smaller than the orifice flow areas. In this circumstance, the pressure distribution around the needle seat can be uneven. The pressure distribution will have an effect on the needle motion which in turn changes the distribution of fuel to each orifice. Some systems have double needle guides to assist the stability of the needle motion (Bae et al., 2002). Other systems force a swirl motion of the fuel as it begins to flow through the nozzle, to centre the needle as it lifts (Karimi, 2007).

The restriction in the nozzle orifices means that the fuel volume in the nozzle is minimized at the end of the injection event. In this respect the VCO is a better nozzle design because less residual fuel finds its way to the combustion chamber. If the residual fuel at the end of

injection, with low momentum, finds its way to the chamber under non combusting conditions, the fuel will be emitted as un-burnt hydrocarbons.

In a sac nozzle the needle uncovers a volume from which the nozzle orifices are fed. The sac design can be conical or cylindrical in design. The sac nozzle allows the distance between two nozzle holes to be reduced, which means more holes can be machined into the nozzle. The number of holes depends upon the combustion system design and the strategy for the mixture formation (Mollenhauer.K and Tschoeke.H, 2010).

2.2.1.1 Hole size

The size of a nozzle hole has an influence on the fuel spray formation. The hole size affects the atomisation and fuel spray cavitation as well as the fuel spray penetration into the combustion chamber. The size of the hole also influences the rich regions in a fuel spray by changing the fuel flow area.

For a fixed number of holes, changing the size of the hole results in a change in the fuel flow rate. Maintaining the volumetric flow rate by adjusting the number of holes is typical when the discharge coefficient of the nozzle hole can be maintained. This was seen in the study of Lechner, where the reduction in hole size was used to reduce the flow rate for the same number of nozzle holes (Lechner et al., 2005). The nozzle was a flow device with a differential pressure between the in-cylinder conditions and the rail pressure.

Hole sizes can be produced reliably down to diameters of 0.08 mm (Payri et al., 2008). This was the smallest size that can be drilled as suggested in (Minato et al., 2004) where the authors applied an 18 hole nozzle to maintain the fuel flow rate and mixing time required in their combustion investigation. For the same flow rate a smaller hole means the need for more holes, which increases the probability of spray interactions. Spray interactions have a negative effect in the mixture formation process by forming rich regions in the fuel spray (Abraham et al., 1999, Amagai et al., 2003).

2.2.1.2 K factor

K factor is defined as the ratio of the difference in internal, di, and external nozzle hole diameter, do, divided by the length of the nozzle hole, l.

$$k = 100\left(\frac{d_i - d_o}{l}\right)$$

Equation 2.1: definition of nozzle k factor

K factor gives a measure for the profile of an injector nozzle hole. A number less than 0 means that the hole diverges, equal to 1 is a cylindrical hole and greater than 1 is a converging hole. Simulations and experiments have shown that converging nozzles can help reduce cavitation within the nozzle hole (Martynov, 2005, Payri et al., 2008, Payri et al., 2011). The discharge coefficient of the injector nozzle can be affected by cavitation in the nozzle, which requires more fuel pressure to maintain the flow. Although nozzle holes with different k factors were employed in this study the influence of k factor on combustion system performance was not investigated as part of this work. Typical k factors used in this study ranged from 1.5 to 2.5.

2.3 Diesel Combustion and Emissions

There are two distinct types of combustion applied in Diesel engines; traditional mixing controlled combustion and low temperature combustion. Traditional Diesel combustion will be a limiting factor for manufacturers trying to meet future emissions regulations without expensive aftertreatment systems (Dec, 2009). Due to this, low temperature combustion at part load operating conditions, can help to reduce engine out emissions without sacrificing efficiency. There are however issues with the control of the combustion event (Iida et al., 2004, Zheng and Yao, 2009, Dec, 2009) and the increase in other emitted species such as CO and HC (Sjöberg and Dec, 2005, Miles, 2007, Kim et al., 2008, Miles, 2010).

Both forms of combustion will be presented to aid the understanding of the combustion process and the limitations that currently exist for the Diesel engine to operate in these modes.

2.3.1 Traditional Diesel Combustion

In a traditional direct injection Diesel combustion process, the combustion occurs over four distinct phases with the majority of the heat release process occurring in two distinct phases (Heywood, 1988). The four phases of the combustion process shown in Figure 2.11 are defined to occur no earlier than the start of the injection event (a.) and are as follows; ignition delay (a. to b.), premixed combustion (b. to c.), diffusion or mixing controlled combustion (c. to d.) and finally late cycle oxidation or tail combustion (d. to e.).

Ignition delay is defined as the time from the start of the fuel injection process to the turning point on the cumulative heat release curve. Ignition of the fuel is dependent upon the temperature and equivalence ratio, thus ignition delay can be influenced by various parameters such as compression ratio, injection pressure and Exhaust Gas Recirculation (EGR) rate. Premixed combustion is characterised by a rapid pressure rise, linked to the heat release from fuel that has reached the temperature to auto-ignite. The ignition delay directly influences the premixed proportion of the combustion process as it changes the amount of time available for the fuel and air to mix to ignitable conditions. In traditional Diesel combustion, a short ignition delay was preferred to limit the pressure rise rate (Heywood, 1988).

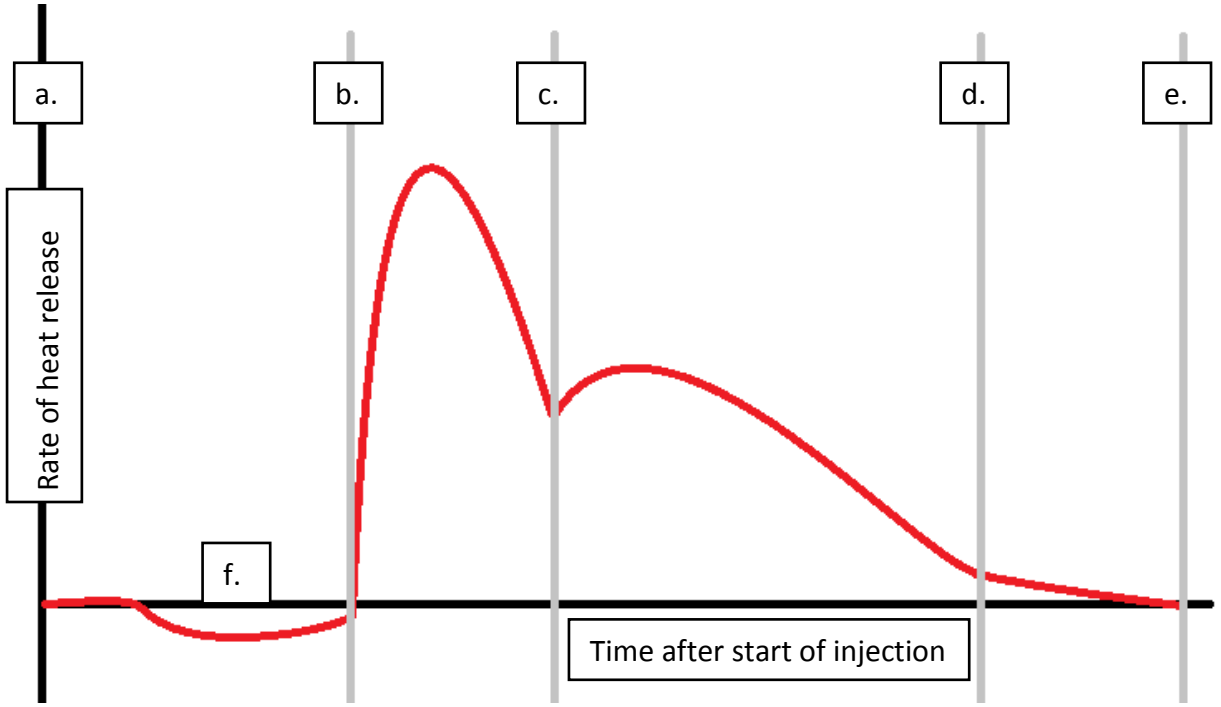

Figure 2.11 Traditional diesel combustion schematic

Once the initial portion of the fuel has combusted in a premixed manner, the heat release is then governed by the diffusion of fuel from the core of the fuel jet, to the jet periphery, where combustion occurs as the fuel and air mixes (Dec, 1997). The mixing rate is governed by the following mixture formation strategies; high fuel pressure or high levels of in-cylinder turbulence such as swirl and squish. The characteristic nature of traditional Diesel combustion process was the formation of soot or particulate matter. If the temperature was high enough, greater than 1500 K, and the equivalence ratio higher than one within the fuel spray then particulate matter will be formed (Frenklach and Wang, 1994, Akihama et al., 2001, Kitamura et al., 2002).

The tail combustion event occurs relatively late in the combustion cycle and this was where further heat release occurs due to the oxidation of un-burnt and partially formed species such as CO, HC and soot. In a Diesel combustion system where it is operated with excess air, the oxidation occurs as the combustion species react with radicals formed during the combustion process and the remaining oxygen (CO reaction with OH radicals in the table of (Zheng and Yao, 2009)).

Work has been done to build an understanding of the phenomena involved in the conventional Diesel combustion process. Over a decade ago, in the late 90's, Dec applied laser based techniques on a fuel spray in order to build up a schematic representation of the different zones of the fuel spray during the combustion process (Dec, 1997). As a result a schematic of the Diesel combustion process was developed, which was used to inform a phenomenological model of the combustion process.

Later, Dec carried out a review on advanced compression ignition engines and states that traditional Diesel combustion will not be sufficient to meet the more stringent emissions regulations (Dec, 2009). A lot of work has been done to enhance the mixture formation process without harming the performance of the Diesel engine but a move towards low temperature combustion will be required. This will be achieved by developing Diesel combustion systems and the understanding of the mixture formation processes.

The limitation for traditional Diesel combustion exists because the formation of NOx and PM is not limited in the combustion process. Late cycle oxidation is responsible for oxidising the species of the rich combustion process such as PM, CO and HC. Reducing the formation of NOx was possible with the use of EGR. The effect of EGR is twofold; the peak temperature reduces due to the increase in specific heat capacity of the exhaust gas constituents and the oxygen concentration reduces for the same manifold pressure conditions (Stone, 1999). As a result of the reduction in oxygen content, less late cycle oxidation can occur. Any further increase in EGR will suppress the formation of NOx, however a secondary effect was to limit the oxidation of the rich combustion products. This was where a trade-off between NOx and PM occurs.

In order to mitigate the side effect of EGR reducing the oxygen content, a necessary requirement in order to reduce NOx, work must be done to reduce the formation of PM during the combustion process. This was why the move towards low temperature combustion modes was required, as the formation of PM was prevented by suppressing the in-cylinder temperature. Both NOx and PM formation zones can be avoided if the temperature was suppressed below 1500 K.

2.3.2 Alternative Diesel Combustion Strategies

A reduction in Oxides of Nitrogen can be achieved by the use of exhaust gas recirculation (Heywood, 1988). However, a trade-off is also well established whereby the reduction of the oxygen content in the cylinder due to the displacement of air leads to an increase in the output of PM.

In recent years, studies have shown the potential for a simultaneous reduction in PM and NOx in a Diesel engine, whilst at the same time, maintaining good efficiency (i.e. low emissions of CO_2). Since the turn of the century several authors have referred to Low Temperature Combustion (LTC) in which the energy was released from the fuel either by combustion under highly diluted low temperature conditions or under highly premixed lean conditions. Work has been conducted to develop the understanding of the in-cylinder processes involved (Thring, 1989, Akagawa et al., 1999, Kimura et al., 1999, Kimura et al., 2001, Akihama et al., 2001, Walter and Gatellier, 2002, Shimazaki et al., 2003, Hasegawa and Yanagihara, 2003, Minato et al., 2004, Okude et al., 2004, Iida et al., 2004, Lechner et al., 2005, Kook et al., 2005, Laguitton et al., 2007, Ryan, 2007, Fang et al., 2008b, Kim et al., 2008).

2.3.2.1 HCCI – Homogeneous Charge Compression Ignition

Homogeneous Charge Compression Ignition (HCCI) is a combustion technique developed as an alternative to traditional Diesel combustion. In this mode the charge is highly diluted with EGR and the fuel is injected in an advanced manner in order to form a Homogeneous charge. HCCI was first observed over three decades ago and described as a combustion process differing both from normal Diesel and gasoline processes (Onishi et al., 1979). In HCCI, the fuel and intake charge (air plus EGR) form an homogenous cloud in which the equivalence ratio (ϕ) is uniform and lean throughout. Equivalence ratio is defined as the ratio of the measured Fuel to Air ratio to the stoichiometric Fuel to Air ratio (FAR_s). This value is the inverse of lambda, with rich values being greater than one and lean values being less than one.

$$\varphi = \frac{\frac{Fuel}{Air}_{measured}}{\frac{Fuel}{Air}_{Stoichiometric}} = \frac{1}{\lambda}$$

The ignition occurs simultaneously at all locations in the mixture provided that the correct pressure and temperature are achieved towards the end of the compression stroke of the engine. HCCI with gasoline was investigated by Thring, 1989, which found lower fuel consumption compared to normal Diesel operation, however the engine has to be modified to allow the fuel and air to be premixed and autoignite. In a Diesel engine, in order to provide sufficient time for the air fuel mixture to homogenise, some approaches use very advanced injection timings (Akagawa et al., 1999) and double injections with high concentrations of EGR (Hasegawa and Yanagihara, 2003).

The development of HCCI combustion was thought of as being more viable with fuels other than typical Diesel fuel, such as gasoline, and primary reference fuels (PRF) of different composition (PRF80 was composed of 80 % of the primary reference fuel iso-octane and then 20 % of n-heptane). Diesel fuel is prone to auto ignition due to its high cetane number whereas HCCI relies on longer ignition delays to enable the air and fuel to mix after the completion of the injection event before the onset of combustion (Ryan et al., 2004). The emissions characteristics of HCCI is that there was a simultaneous reduction in the amount of NOx and Particulate matter (PM) produced (Yao et al., 2009), this is due to both a temperature reduction and a reduction in rich equivalence ratios. The downside was the increase in HC and CO as a result of incomplete combustion that occurred.

(Lü et al., 2005) reference the initial research into what is now commonly accepted as the combustion mode HCCI. They identify the factors which limit the full scale production of engines operating solely in HCCI mode. These factors include; the extension of the operating range of HCCI to that above the lowest of the part load conditions, improved control of the combustion event and a reduction in the un-burnt hydrocarbon (UHC) and Carbon monoxide (CO) emissions.

2.3.2.2 Low Temperature Combustion (LTC)

Applications of the HCCI technique in the Diesel engine and the associated issues with the application has focussed research into Diesel combustion with a highly premixed charge (Iida et al., 2004), rather than a fully homogeneous charge. There are various names that exist for premixed charge combustion systems, some examples are shown in the following Table 2.1.

Name	Acronym	Authors	Mixture formation
Premixed lean Diesel combustion	PREDIC	(Akagawa et al., 1999)	Early injection low load No EGR Water injection
Modulate Kinetics	MK	(Kimura et al., 1999)	Swirl number 3-5 Retarded timing High EGR rate
Uniform bulky combustion system	UNIBUS	(Hasegawa and Yanagihara, 2003)	Early pilot Late main injection
Premixed lean Diesel combustion	PCI	(Minato et al., 2004)	High injection pressure
Partially premixed compression ignition	PPCI	(Lechner et al., 2005)	Narrow spray angle High EGR rates Compression ratio16:1 Double injection
Premixed charge compression ignition	PCCI	(Laguitton et al., 2007)	Low compression ratio 13.5:1

Table 2.1 List of different names for alternative LTC modes to HCCI

There is a mode of LTC operation known as premixed charge compression ignition (PCCI) (Laguitton et al., 2007) or partially premixed compression ignition (PPCI) (Lechner et al., 2005, Kim et al., 2008). This is similar to combustion in a spark ignition (SI) engine in which heat release occurs through a high proportion of premixed charge. Premixed combustion is the initial part of typical Diesel combustion which precedes diffusion combustion (Heywood, 1988). Increasing the ratio of premixed combustion can be achieved through a reduction in compression ratio (Laguitton et al., 2007), increase of cooled EGR (Kimura et al., 1999) and modified injection timings (Lechner et al., 2005).

Operating an engine in an LTC mode, thus far has focused on controlling the cylinder conditions externally, by varying the amount and condition of air and EGR supplied to the engine. Fuel injection strategies have also been investigated as well as the effect of forcing the air motion in the cylinder through the use of swirl or tumble port designs. There are a number of techniques with fuel injection strategies that allow LTC modes to be used. The techniques can be classified as either very early direct-injection LTC or Near Top Dead Centre (TDC) direct-injection LTC by (Dec, 2009).

2.3.2.2.1 Very Early direct-Injection LTC

Injecting into the cylinder earlier has proved an issue in terms of wetting the cylinder liner as a result of increased penetration. The penetration is due to the lower in-cylinder pressures experienced when injecting part way along the compression stroke. Injectors with hole numbers greater than 7 holes employing more disperse sprays produce better early injection results (Akagawa et al., 1999). Conventional Diesel injectors allow switching to traditional injection regimes for full load conditions, however when used for early injection the impingement and wetting as mentioned was a significant problem. Using narrower spray cone angles can reduce liner wetting, however there was still the issue of the wall wetting of the piston bowl (Walter and Gatellier, 2002, Fang et al., 2008a, Fang et al., 2008c).

2.3.2.2.2 Near TDC direct-injection LTC

The premixing required to achieve LTC can also be achieved with this near and post TDC injection. This result is the ignition is less reliant on the chemical kinetics and more closely related to the injection event. The technique known as Modulated Kinetics was a method in which the injection event occurs in the expansion stroke (Kimura et al., 1999). As such, the expansion of the gas volume leads to slowing of the auto-ignition process. The use of highly cooled EGR and reduced compression ratio are often applied to increase the ignition delay (Laguitton et al., 2007). Increased ignition delay is beneficial and leads to an increase in the premixed phase of combustion, as it allows more of the air and fuel to mix prior to combustion.

One of the problems is the lack of time for the mixing to occur before the auto-ignition process and the combustion occurs in a mixing-controlled process. EGR is required to keep the local peak-combustion temperatures low, thus helping with the NOx formation whilst at the same time increasing the ignition delay (Kook et al., 2005).

The effect of early and late injection timings was demonstrated by carrying out a sweep of injection timings at different levels of EGR and at a fixed load point of 3 bar Indicated Mean Effective Pressure (IMEP). When the injection timing is retarded the NOx level reduces. The peak temperature was lower, and there was more time for premixing before the combustion event. The expansion of the in-cylinder gas due to the retarded injection also

leads to quenching of the NOx producing reactions after the start of combustion. Soot production is also suppressed in this operating mode because the in-cylinder temperatures are low enough for the fuel to combust in fuel rich regions without leading to soot formation. The oxygen concentration is low and in-cylinder temperatures are reduced is detrimental to soot oxidation; however the amount of soot produced is significantly less. This is an important aspect of LTC, the balance between the formation and oxidation of combustion products such as PM HC and CO.

CO and HC emissions under these operating conditions are noted to increase with the substantial reduction of soot and NOx (Miles, 2007, Kim et al., 2008, Miles, 2010). These levels are above that of traditional Diesel combustion, however it has been observed that these levels are less than the very early direct-injection LTC due to the reduced homogeneity and reduced penetration.

The main difference in LTC and traditional Diesel combustion does not come from the premixing phase; indeed the author states that the Diesel jet was much the same as observed in traditional Diesel combustion (Dec, 1997, Dec, 2009). Moreover the author goes on to explain that the main reason for the differences in emissions with the combustion modes was that the combustion event was occurring while the fuel was being injected, due to the improved ignition delay, meaning the mixture became lean much more quickly.

2.3.3 Soot Formation

Soot formation is reduced in the advanced combustion modes such as LTC and HCCI, even when the equivalence ratio is low. Soot formation is at a maximum at 1800K and between 1500K and 2300K as suggested in (Kamimoto and Bae, 1988) from experiments carried out in shock wave tubes. Soot is not formed above temperatures of 2300K regardless of the oxygen content, as it breaks down into gaseous hydrocarbons faster than it would form soot. The equivalence ratio effect can be explained in a similar way to that suggested by (Kamimoto and Bae, 1988) where a limit to the formation of particles exists when a the ratio of carbon to oxidant is less than one. Stable species such as H20 and CO2 are formed. Low compression ratio may help the soot formation region because the lower in-cylinder pressures reduce the width of the soot peaks as suggested in (Kamimoto and Bae, 1988).

The move away from conventional Diesel combustion towards the low temperature, clean combustion, discussed in the previous section has been prompted by the demonstration of the operation of the combustion engine with low soot and NOx performance without heavy losses in efficiency or the need for aftertreatment.

In the work of Akihama et al. (Akihama et al., 2001), the mechanisms for the suppression of soot in the low temperature operating mode were investigated further in order to identify the factors contributing to this improvement. Based on the work the authors have carried out to develop the combustion system, their hypothesis was that either; the presence of EGR causes a reduction in the combustion flame temperature, thus reducing the effects of rich combustion of the fuel, or that the presence of EGR leads to an improvement in the mixing process. To investigate this, Akihama et al. (Akihama et al., 2001) used a CFD package, KIVA 2 code, and a zero dimensional chemical kinetics model developed by Frenklach and Wang (Frenklach and Wang, 1994). The methodology described was such that the two processes used were applied independently, to determine equivalence ratio (ϕ) and temperature (T) profiles. The chemical kinetics tool was used to define the region of sooting conditions in terms of a, Equivalent ratio versus Temperature (ϕ-T) map, and the in-cylinder conditions were defined by CFD.

The result of the investigation is that the leading mechanism for the suppression of soot is the suppression of the combustion temperature. The distribution of the ϕ-T profiles in the CFD cell volumes was such that they are displaced to the left hand side of the soot peak when compared to the conventional combustion.

The ϕ-T map shown in the following Figure 2.12, demonstrates regions of NOx and soot formation and tries to indicate the conventional Diesel combustion distribution as well as the regions of operation for advanced low temperature combustion techniques. The map is based upon previous research and is summarised in (Dec, 2009).

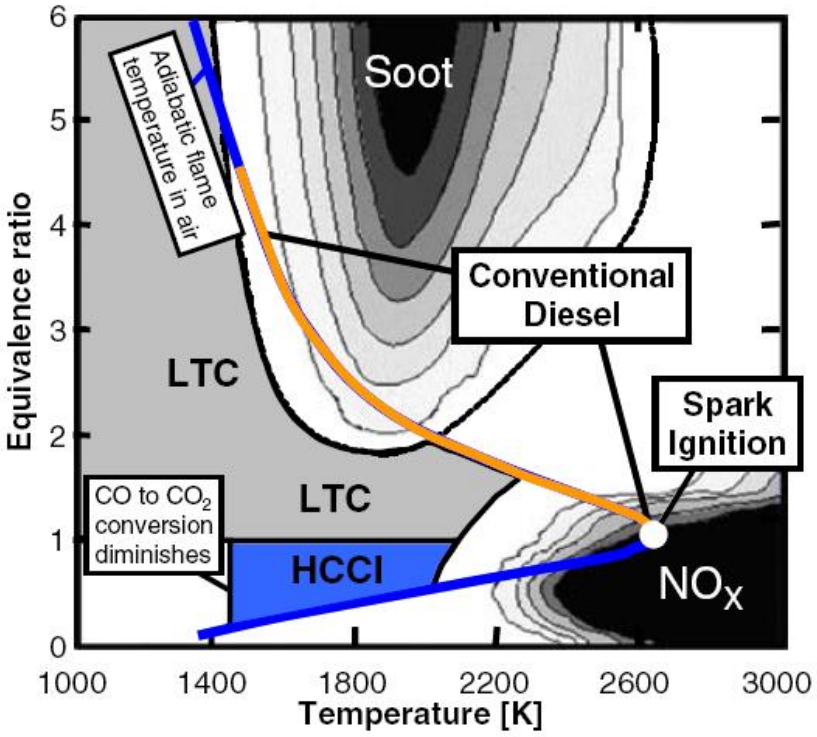

Figure 2.12 Equivalence ratio (ϕ) versus temperature (T) map (Dec, 2009)

2.4 Multiple Injections

The advances in the electrically controlled common rail Diesel fuel systems has allowed for precise metering of fuel over a wide range of injection timings independent of the engine speed. Multiple injections can be characterised by their relationship to the main injection event. For example injections that are before the main injection of fuel are known as pilot injections and injections that occur after the main injection are known as post injections.

Multiple injections are common place for modern direct injection (DI) Diesel engines operating with a common rail fuel system (Tanaka et al., 2002) for traditional Diesel combustion and LTC. A multiple injection process can be used to control the heat release process and therefore has an influence on mixture formation, engine output and emissions. Additionally, due to the modification of the heat release process (relative to a single injection) the pressure rise rate can be controlled to reduce combustion noise and make the Diesel engine more refined. It is now rare for an engine to be operated with a single injection other than under full load conditions.

Multiple injection strategies are also employed in order to achieve advanced combustion modes that result in a simultaneous reduction in oxides of Nitrogen (NOx) and smoke as mentioned in the previous chapter. Usually this is coupled with an increase in the emissions output of CO and HC (Miles, 2010) due to the overall lower temperature in-cylinder and the increased lean regions within the fuel spray. The fuel spray becomes leaner due to an increase in ignition delay and longer fuel spray penetration.

Simultaneous reductions in smoke and NOx were achieved with split injections demonstrated by (Han et al., 1996). The injection was split with the majority of fuel in the pilot and meant that the fuel that would have been injected in a rich mixture was separated from the combustion process. A greater spatial distribution of the fuel during the combustion process was achieved. The use of a small pilot in leads to an increase in the smoke produced for the same fuelling conditions. The temperature increase that has occurred through the use of a pilot injection and the late injection of the greatest quantity of fuel leads to short ignition delay and long combustion duration without the time or temperature to oxidise the combustion products. Splitting the injection process can lead to an increase in the entrainment of air into the fuel spray. This is the case as long as the

ignition delay of the main injection is not reduced by the pilot. The interaction of the pilot and main heat release should be separated for to achieve good air entrainment prior to the start of combustion.

2.5 Combustion System Development Conclusions

The direct injection Diesel engine needs to improve engine out emissions in order to meet future, stringent emission standards. Currently the direct injection Diesel engine equipped with a common rail fuel system is the most suitable system. It offers the required fuel efficiency, has the flexibility to operate at a variety of speeds and loads and has the required power density for the passenger car market. The need to install expensive aftertreatment systems to achieve emissions targets means that research must be done into reducing engine out emissions. The engine hardware that forms the combustion system, discussed previously, needs to be experimentally investigated with the application of typical and alternative Diesel combustion modes. The need for the change in thinking for the hardware is to accommodate combustion in highly pre mixed regions, with EGR rates greater than 50% or AFR tending towards the Stoichiometric Air-to-Fuel Ratio (AFRs), where a simultaneous reduction of NOx and PM can be achieved. This study aims to discover whether there is a combination of engine hardware, conventional or unconventional that can achieve low emission and fuel consumption.

The development of combustion system strategies for a modern clean Diesel engine must be based upon the flexibility of the system to switch modes. For example, operating in HCCI mode requires the mixture formation process to begin in such a way that the fuel and air mix before the onset of the combustion process. This satisfies the requirements of the regulated emissions levels; however optimising the hardware for part load emissions performance can compromise performance at the unregulated full load running condition. The importance of full load is debateable, as the vehicle cannot be put into production if it does not satisfy the part load regulated emissions criteria. However, the benchmark power output figure is more marketable to the consumer and specific power outputs are desirable for engine downsizing. This study also aims to discover whether conventional and unconventional hardware can be optimised to achieve low engine out emissions without an impact on high specific power outputs.

Existing investigations of advanced combustion modes use existing hardware both in terms of fuel injection equipment and piston bowl designs. The important aspect for future development is having an improved strategy for the design and interaction of the

combustion chamber shape and the fuel injection spray. Injection strategies help as the metering of the fuel into the chamber affects the emission formation and combustion process; however the chamber interactions are not optimised for the fuel spray. The same can be said for traditional Diesel combustion; the limitations have been established with existing hardware designs and the conventional knowledge of the mixture formation process. This study aims to show whether conventionally and prototype designed Fuel Injection Equipment (FIE) can be used to control the fuel metering and combustion process. In particular, this study aims to show whether new injection hardware requires a different thinking about the design of the injector nozzle.

Understanding the performance of conventional and unconventional combustion system designs with traditional and advanced Diesel combustion modes will be important to achieve a reduction in pollutant emissions from the engine, whilst at the same time maintaining low levels of fuel consumption associated with modern Diesel engines. Information gathered from testing the hardware in this study will be used to show the limitations and also the requirements of the mixture formation process for both types of Diesel combustion.

The piston bowls selected represent industry standard and unconventional designs that will influence the thermal behaviour of the engine and the mixture formation process. The piston bowls will be tested at a representative set of engine operating conditions. The results generated by the conventional designs will serves as a reference for the unconventional combustion systems. The assessment of suitability of the unconventional designs will be based upon the delta to the conventional systems. Previous studies show marginal improvements with the change in bowl characteristic for the same conventional system. There is the potential for a step change in the efficiency and emission output for the unconventional systems, this study aims to establish whether this is an useful improvement or a deterioration not worth pursuing. Without any information on conventional designs it is difficult to assess the impact of the unconventional combustion systems and whether they will be suitable in light duty Diesel engines.

3 Experimental Equipment

This chapter describes the experimental facility used in this research project. A description of the experimental engine hardware and fuel system is given along with a description of the test bed services and systems. The instrumentation used is described along with the data acquisition systems to build a picture of the capabilities and limitations of the experimental facility.

3.1 Hardware Specification

This experimental study is based around a single cylinder Diesel engine and fuel injection equipment (FIE) including fuel injectors with solenoid and piezo electric actuation. Four different bowl designs and two types of injector were tested. The experimental programme investigates the relationship between combustion chamber geometry, defined by the piston bowl and fuel spray shape governed by the injector nozzle design. A description of the experimental hardware follows.

3.1.1 Single Cylinder Diesel Research Engine

The engine used in this experimental investigation was a light duty four stroke single cylinder direct injection Diesel engine. The engine was based upon an established Ricardo Hydra crank case design with an aluminium cylinder head. The peak in-cylinder pressure limit of this particular design, for safe operation, was 200 bar. The use of an aluminium cylinder head was a choice that reflects the current practice for production engines. The specification of the engine is given in the following table, Table 3.1.

The design employs four valves per cylinder, two inlet valves and two exhaust valves with the fuel injector mounted vertically in the centre of the cylinder. The valves are also vertically mounted in the cylinder head which avoids the need for cut outs in the piston to accommodate the valves during the opening process at top dead centre.

Parameter	Value
Number of cylinders, ncyl	1
Operating cycle	4
Bore	84 mm
Stroke	90 mm
Displaced volume, Vd	0.498 litres
Bore/Stroke ratio	0.93
Compression ratio with the baseline bowl B1	16.6
Cylinder pressure limit	200 bar
Cylinder head swirl ratio (variable)	1.75-4.58
Maximum injection pressure	2000 bar
Specific torque target	>200 Nm/litre
Specific power target	>40 kW/l

Table 3.1 Engine specification

The engine was designed with one helical swirl port and one straight port to create the variable swirl ratio. The two ports have different shaped inlet runners to enhance the air motion prior to entering the combustion chamber. One port has a helical port, which encourages a helical flow around the trumpet of the valve which translates in the axial rotation of the air in the combustion chamber. The inlet valve arrangement is shown in Figure 3.1. The helical port can be deactivated with a throttle, which diverts flow to the tangential, straight port to increase the swirl ratio.

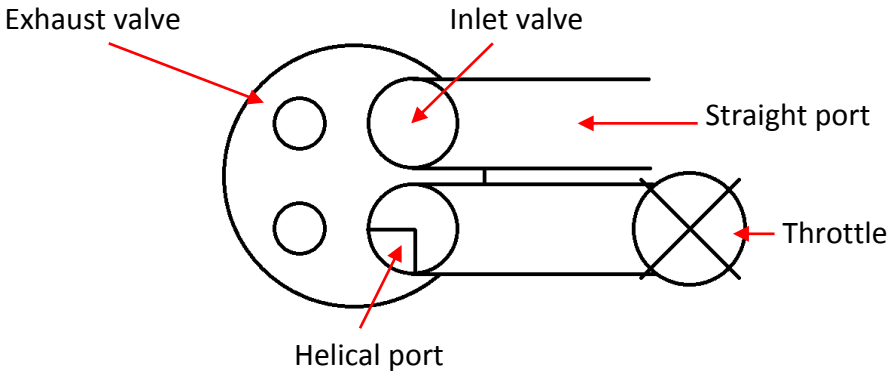

Figure 3.1 Port deactivation strategy for enhancing in-cylinder air motion

Each of the pistons used in this study were machined out of a blank, cast aluminium production piston. The piston includes an oil gallery to help with cooling of the hot surfaces. The oil was supplied by a single nozzle jet, which sprays oil up through the gallery and over the underside of the piston.

The swirl ratios for the individual bowls are not defined. The variation of the swirl ratio shown in the table is due to the port deactivation throttle and was measured on a steady state flow rig. The steady state flow rig gives a representation of the potential swirl ratios, at maximum valve lift. Variation in the bowl geometry will have an influence on the swirl ratio in cylinder, but without measurement or calculation by CFD, individual bowl swirl ratio is unknown.

The cylinder head includes recesses for both a glow plug and a pressure transducer. The glow plug was not fitted on the research engine; however a blank of the shape of the glow plug was installed. There were two reasons for this; to maintain the combustion volume and therefore the compression ratio, and to simulate the protrusion and interaction of the glow plug with the fuel spray. The latter was important, as the dispersion angle of the fuel spray needs to be such that fuel was not being deposited on to the glow plug surface.

The cut out for the pressure transducer was such that the transducer was mounted as flush as possible to the combustion chamber. The packaging limitation for the complete cylinder head means that the transducer was mounted at an angle to the cylinder head surface. There was a small volume between the face of the transducer and the combustion chamber. Previous experience suggests that this difference would result in a measurement uncertainty smaller than that of the sensor itself.

3.1.2 Piston Bowl Library

The piston bowl designs used in this study include conventional design concepts as well as unconventional designs. The piston outlines are shown in the following figure, Figure 3.2.

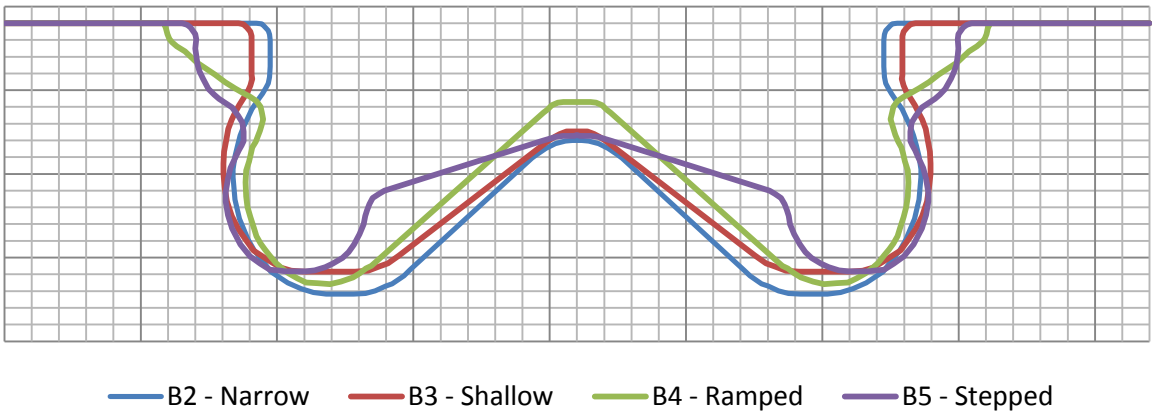

Figure 3.2 Overlay of piston bowl design

The conventional bowl shapes (B2 and B3) have variations in aspect ratios of bowl width to bowl depth, whereas the unconventional designs (B4 and B5) move away from the conventional re-entrant squish lip design towards a 'stepped' design. The removal of the re-entrant squish lip leads to a secondary 'pip' within the piston volume. The secondary 'pip' refers to the bump that is created by the cutaway lip from the unconventional bowls. Each piston has been characterised by its major dimensions, best described by the following schematic, Figure 3.3 and presented in Table 3.2.

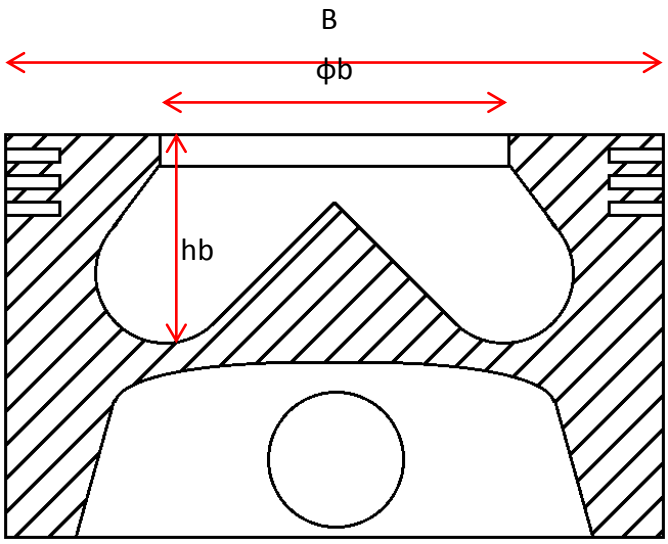

Figure 3.3 Piston bowl major dimensions schematic

Where B was the diameter of the piston, ϕb represents the diameter of the piston bowl and hb was the distance from the top of the piston to the combustion chamber floor. The bowl diameter was measured in the same way for both conventional piston bowls and stepped piston bowls. It was measured across the edge of the flat surface of the piston. The difference in piston diameter B and bowl diameter ϕb can be used to calculate the squish area. The dimensions displayed in the following table were generated using CAD packages and measurements of the piston bowls. Whilst the parameters that define the geometry of the piston bowl were adjusted, the bowl volume was maintained to ensure that the compression ratio was maintained the same.

Bowl	Name	Compression ratio	Piston diameter B	Description	Bowl diameter ϕb	Bowl depth hb	Aspect ratio ϕb/hb	Bowl to bore ratio ϕb/B	Bowl surface area SA	Bowl volume V	Bowl SA/V	TDC SA/VTDC
-	-	-	mm		mm	mm	-	-	mm^2	mm^3	1/mm	1/mm
B2	Narrow	16	83.074	Toroidal, re-entrant	47.1	16.2	2.91	0.57	4331	26602	0.163	0.59
B3	Wide	16	83.074	Toroidal, re-entrant	49.8	14.8	3.36	0.60	4326	26602	0.163	0.59
B4	Ramped	16	83.074	Toroidal, stepped	60.6	15.7	3.86	0.73	4805	26597	0.181	0.57
B5	Stepped	16	83.074	Toroidal, stepped	58.0	14.9	3.89	0.70	4860	26562	0.183	0.58

Table 3.2 Major parameters for each piston bowl

The stepped combustion chambers allow an effective increase in the ratio of the piston bowl diameter, ϕb. As a result there was a significant increase in the aspect ratio of the piston bowl as it was possible to maintain a large bowl depth for the same bowl volume.

The, wide and open nature of the unconventional bowls B4 and B5 means there is a difference in characteristic of the design compared to the conventional designs. The bowl occupies a greater proportion of the piston bore (10% more), thus reducing the flat portions of the piston bowl. This means that the surface area to volume ratio is better (in terms of heat transfer) for the unconventional bowls, than the conventional bowls. Bowl B4 has the lowest ratio of 0.57. It is not clear at this stage how the characteristic difference in SA/VTDC will affect the thermal efficiency of the engine because air motion also has an influence on heat transfer losses.

The effect of increasing the protrusion of the injector nozzle tip was assumed to be insignificant. Reducing the volume at TDC by the volume of a cylinder with the injector nozzle diameter (7 mm) and the height of the maximum protrusion change (2 mm), changes the compression ratio by less than 0.1 making this change insignificant and within the uncertainty of the combined measurements used to calculate the compression ratio.

3.1.3 High Pressure Common Rail Fuel System

The fuel injection system was based upon a common rail fuel system. The system was comprised of the standard components of a common rail system taken from a production system. The system was used up to a maximum of 2000 bar fuel rail pressure.

The baseline configuration of the fuel system used in the study employed a balanced valve solenoid injector. This was included in the test programme to provide a reference for comparison with the direct acting fuel injectors. The injector was the only component in the fuel system that was changed along with the hardware and software necessary to control the fuel injector.

The high pressure fuel pump that feeds the fuel rail was driven by a dedicated electric motor rather than the engine crankshaft as it would be in a production vehicle. This arrangement provided the flexibility to drive the fuel pump independently of the speed of the engine without imposing constraints on the engine power output. In a typical test the controller

governing the speed of the motor driving the fuel pump would act to maintain the pump speed at a fixed fraction of the engine speed (usually half the engine speed).

The fuel pump itself was a two piston pump, with a low pressure fuel feed, inlet metering valve (IMV) and injector return flow connection. The inlet metering valve was used to reduce the volume of flow passed through the pump. This provides one means of regulating the fuel rail pressure. The return from the solenoid injector to the pump was blocked when changing between injector types because the direct acting piezo system does not have a return flow.

The type of fuel pump employed in this study will produce variations in the fuel rail pressure due to the pulsing nature of the fuel delivery. For a crankshaft driven pump the pulses arrive in the rail at the same point in the engine cycle. Initial tests with the experimental system showed a slow change (over a period of 10 minutes) in the phase of the pulses at a steady engine speed. In order to mitigate this effect an additional fuel rail was installed between the pump and rail supplying the fuel injectors. This proved capable of damping these pulsations thus minimising the variation of fuel pressure for successive fuel injection events.

The fuel rail on the experimental facility had no modifications before being installed. As it was taken from a multi-cylinder production system, the other injector connections are plugged off with one used as a location to mount an additional rail pressure sensor. The ends of the rail were plugged with a high pressure valve (HPV) at one end and a pressure sensor located at the other. The output of the rail pressure sensor was the feedback to the rail pressure controller, which modified the spill characteristic of the high pressure valve.

An Emtronix injector driver system was used to control the injection events for the tests with the solenoid fuel injector. A dedicated engine control unit (ECU) was supplied by DDS and was used to control the injection timing of the direct acting injection system. The purpose built ECU for the direct acting injector was also used to control the fuel pressure for the solenoid system, but not the injection timing. This was preferred as the system operates both the IMV and HPV in a closed loop manner. There were two benefits to this; the temperature of the fuel in the system was reduced, and the pressure pulsations from the

two piston pump were damped out. This was particularly important for precise metering of fuel when the fuel pump was driven by the dedicated motor.

3.1.4 Injector Nozzle Library

The direct acting injectors were supplied with a range of nozzle geometry variations. Table 3.3 lists the injector nozzle geometries available for the study. As the table shows the geometry fixes a number of parameters including flow rate and cone angle. In order to maintain the injector flow rate when changing the injector hole size, the number of holes was increased. In order to increase the flow rate the hole size was increased without changing the hole number.

Nozzle	Description					
	Actuator	Post hone vol flow	Hole size	Holes	Cone angle	k-factor
ID	Type	(cm3/min)	mm	-	°	-
N0	Solenoid	770	0.131	7	155	2
N1	Piezo	760	0.131	7	155	2.5
N2			0.123	8		
N3			0.116	9		
N4			0.131	7	145	
N5			0.123	8		
N6			0.116	9		
N15		860	0.141	7	155	
N7			0.131	8		
N8			0.123	9		
N16		860	0.141	7	145	
N9			0.131	8		
N10			0.123	9		
N11		760	0.131	7	155	1.5
N12			0.123	8		
N13		760	0.131	7	145	
N14			0.123	8		

Table 3.3 Injector nozzle library

There were two characteristic cone angles used in this study, which were fixed for each set of nozzles. The nozzles with a cone angle of 155° were used for the conventional bowls (B2 and B3) and the 145° cone angles were used for the unconventional bowls (B4 and B5). These cone angles were determined by Ricardo prior to the design of the piston bowls

based upon their analysis of the fuel spray pattern and air motion using CFD software. The angles are the optimum required to target the spray at the lip and secondary 'pip' for the conventional and unconventional systems respectively.

3.2 Engine Test Bed

The engine test bed was comprised of several systems; with a number of the systems being unique to the experimental facility used in this study. The general layout and operation of the test bed have been described by earlier studies (Laguitton, 2005, Mason et al., 2008). The following section focuses on the modifications that were made to some of the systems.

3.2.1 Air System

A diagram of the air supply system can be seen in Figure 3.4. As stated the system was inherited from a previous study, and was modified to improve the precision and speed of the testing process. The air supply was provided by two Ingersoll Rand compressors via a 3 m^3 pressure vessel. The system was designed to supply ambient temperature compressed air at gauge pressures up to 10 bar and mass flow rates up to 0.15 kg/s. There was no air dryer in the system and so variations in humidity of the fresh air supplied to the engine could occur with changes in the weather conditions. In order to monitor this, the relative humidity of the intake air was measured.

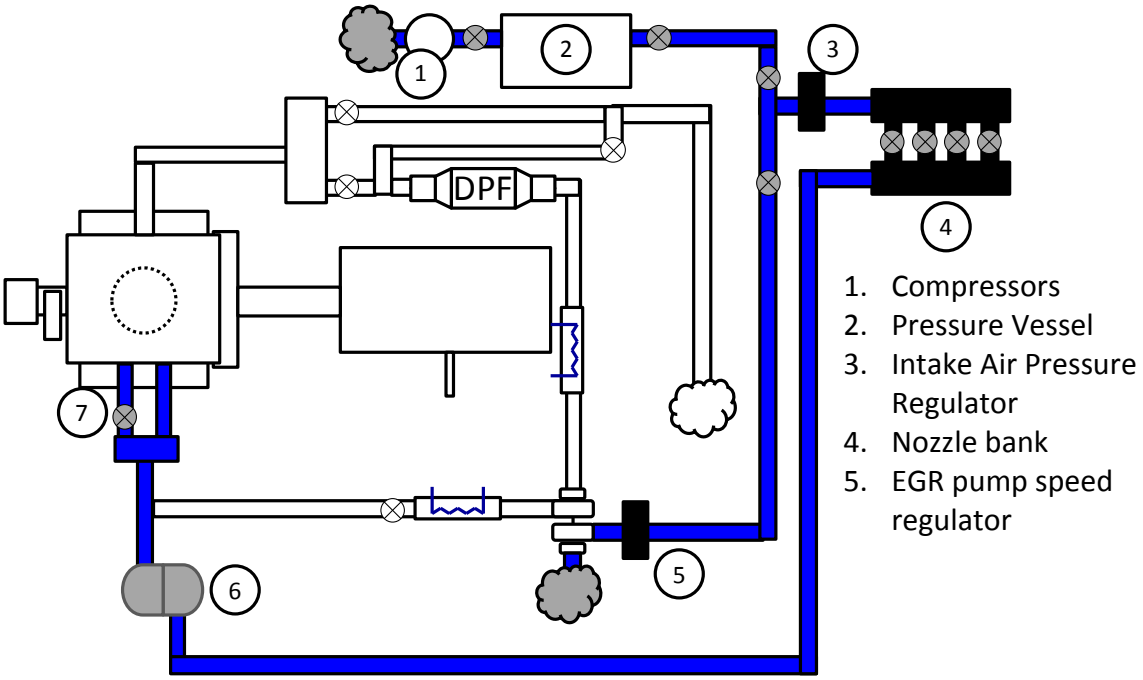

Figure 3.4 Air system schematic

The pressure vessel was used as a damping volume separating the compressors from the engine. The compressors were setup to maintain the pressure in the vessel within one of two ranges (9.0 to 10 bar, or 4.0 to 10 bar). For this work the first range was used. The operation of the compressors was such that the pressure vessel was continuously replenished to its maximum capacity. This negates the time response characteristic of the compressor control system in regulating the pressure inside the vessel. This was of particular importance under high air flow conditions used during full load operation.

As part of this work the system to control and measure the air mass flow rate delivered to the engine was changed. The compressed air supplied from the pressure vessel was regulated at location three, Shown in Figure 3.4. The regulator was operated from the engine test cell and was used to control the pressure supplied to the nozzle bank at location four in Figure 3.4.

The nozzle bank indicated in the air system schematic contains a set of four critical flow Venturi nozzles that are designed based upon the British standard for such a device (BS EN ISO 9300:2005). The nozzle bank consists of two plenums, upstream and downstream of

each nozzle, with a pressure and temperature tapping on the upstream plenum. The plenums are linked by the nozzles and each nozzle has an isolating valve which required manual operation. Provided that the pressure ratio between the downstream plenum and upstream plenum was kept below a critical value then the nozzles were choked and the air mass flow rate only depended the upstream pressure, temperature and the area of the throat of the nozzle. This prevents pressure waves travelling upstream from the engine (caused by the pulsating nature of the engine air flow) affecting the control and measurement of the air flow rate. The air mass flow rate can be computed from:

$$\dot{m} = \sum_{i=1}^{4} o_i k_i \frac{p_{in}}{\sqrt{T_{in}}}$$

Equation 3.1 mass flow calculation for the critical flow nozzles (BS EN ISO 9300:2005)

Were k_i is a coefficient that depends upon the nozzle installation, shape and throat area. If the nozzle valve was open then $o_i = 1$ otherwise 0. A method for computing k_i was given (BS EN ISO 9300:2005). The set of nozzles were specified with increasing diameters so that when used individually or in groups they could deliver the required air flow for the engine over its entire operating map. The British standard was such that a calculation for the mass flow rate through the orifice can be made based upon the pressure, temperature and hardware characteristics of the nozzle (discharge coefficient, flow area surface roughness etc.). In this case however each nozzle and combination of nozzles was calibrated with an Endress and Hauser, thermal mass flow meter under steady flow conditions. The coefficients calculated for each nozzle combination from this calibration were then used to compute the air mass flow rate based upon the pressure and temperature upstream of the nozzle bank.

After the air passes through the critical flow nozzles, the air passes through an air heater which could be was used to further condition the air in order to meet the required specified intake manifold conditions. Previously, the plenum which houses the heating element also acted as a damping volume to reduce the pulsations observed when the EGR circuit was used. The use of critical flow nozzles meant that this function was no longer required. The

air then passes into the engine through the manifold and intake ports, which were described in section 3.1.1.

3.2.2 Fuel System

As described in section 3.1.3, new fuel system components were supplied for this study. As this hardware comes from a fuel system adapted from a production system it was straight forward to integrate it into the existing fuel system in the engine test cell. The existing fuel system was based upon a Ricardo design, which allows the conditioning and measurement of the fuel flow (Laguitton, 2005).

As Figure 3.5 shows, the cooling water on the fuel circuit was conditioned by an external cooling tower. This allowed the heat generated in the fuel circuit to be dissipated, and the fuel temperature to be regulated. The regulated fuel temperature applies to the fuel on the low pressure side, i.e. fuel that was sent along track C to the high pressure fuel pump at the engine.

The fuel was pumped around the system which was replenished by a tank located on the external wall of the test bed. The tank was equipped with a float sensor to determine when the level of the tank was low. This was visually inspected on each test day through a sight glass on the tank. The system included an AVL 733 fuel meter, which was used to measure the mass of fuel consumed. When the fuel meter is operated it isolates the supply from the fuel tank and as a result fuel was circulated by the pump around the rest of the fuel circuit.

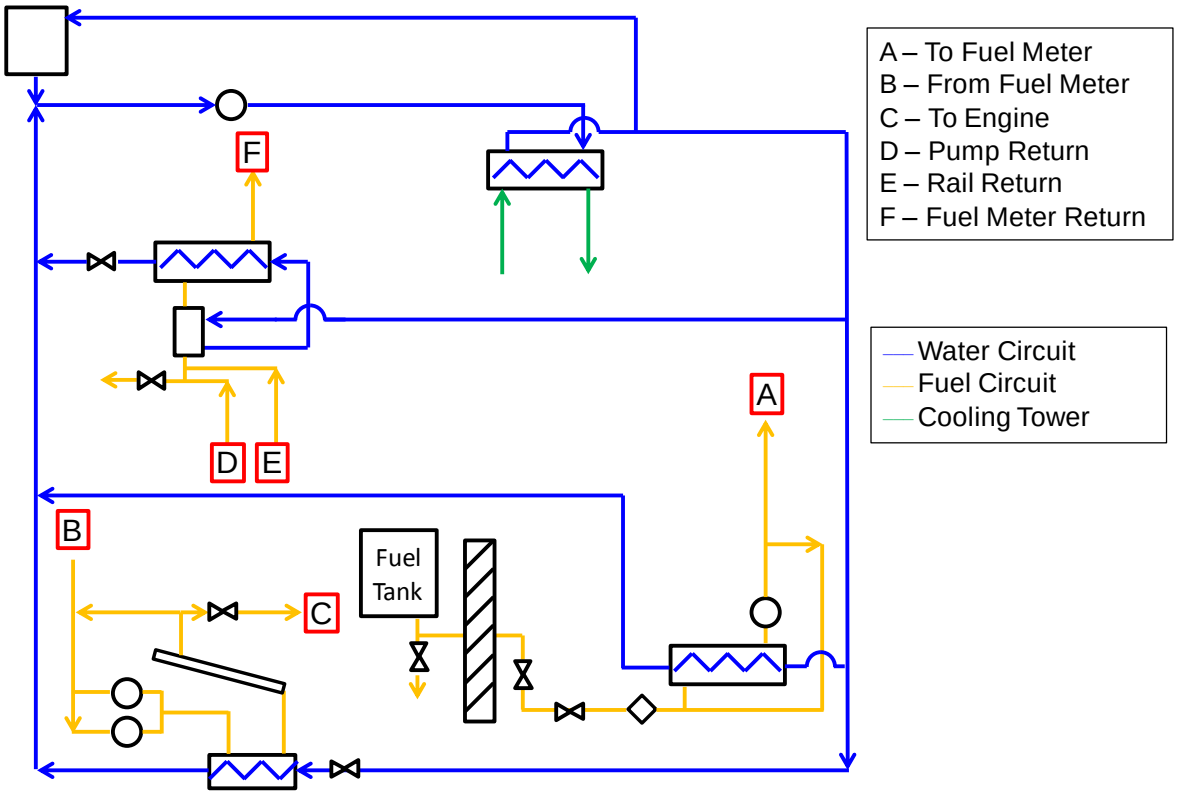

Figure 3.5 Low pressure fuel system schematic

Figure 3.6 shows the integration of the new hardware into the existing fuel system. The connections from the fuel rail and the fuel pump manage the spill flow from the high pressure valve and inlet metering valve respectively. Figure 3.6 also shows the difference in system configuration for the solenoid and piezo systems, with the removal of the leak back flow to the pump from the injector and the removal of the depression gauge. The practical implementation of this system meant that the leak connection was plugged and left disconnected when using the piezo system. This was possible due to the location of the connection between the injector and fuel pump on the fuel pump itself. It exposed the return line to a vacuum meaning there was always a depression in this line. This was necessary to allow the interchange to take place between each fuel injector type.

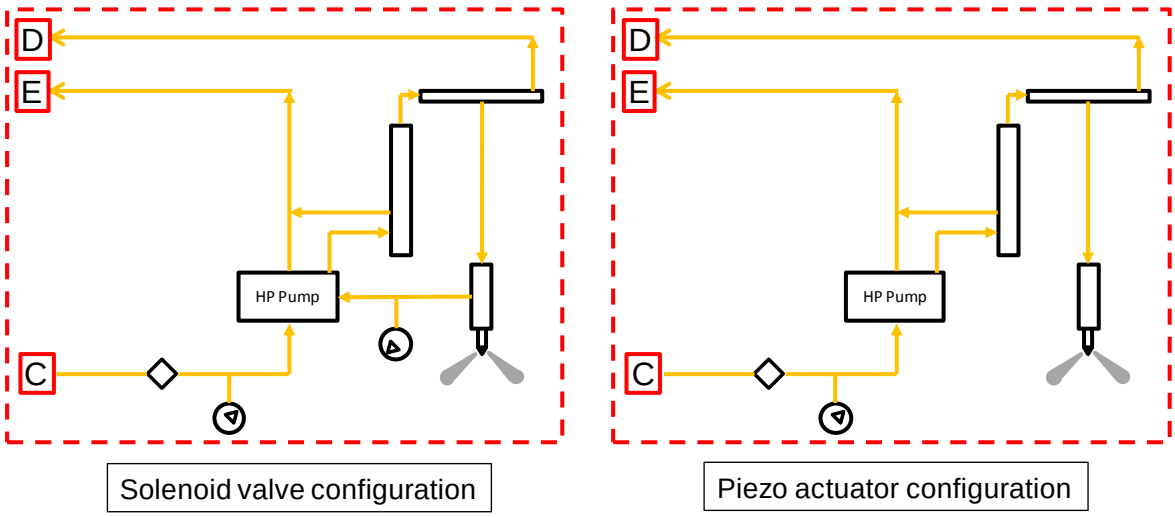

Figure 3.6 High pressure fuel system schematic

The filter indicated in Figure 3.6 was specified for the operation of the piezo system. The filter was finer than that shown in Figure 3.5. It was necessary to reduce the probability of any small particles in the fuel or accumulated from the components in the fuel system, affecting the performance of the piezo electric actuator as this was exposed to the fuel within the body of the injector.

The fuel used for this study was a primary reference fuel with no biodiesel content (B0) called Carcal 725A. The specification can be found in the Appendix A. Example data from the specification is shown in Table 3.4.

Property	Units	Specification		Result
		Max	Min	
Cetane number	-	52	54	52.8
Density @ 15 °C	g/ml	0.833	0.837	0.8348
Viscosity @ 40 °C	cSt	2.3	3.3	2.7
Sulphur Content	mg/kg	6	10	9.3
H/C Atomic Ratio	-	-	-	1.88
Gross Calorific Value	MJ/kg	-	-	45.62
Net Calorific Value	MJ/kg	-	-	42.75

Table 3.4 Table showing the fuel specification of the reference fuel Carcal 725A (see Appendix A)

3.2.3 Exhaust System

The exhaust system was unique to the engine test cell used in this study. Since previous studies it has been modified according to the work done in (Mason et al., 2008), with only minor changes, which will be described here.

The exhaust system was modified and divided into a full load route and a part load route. The need for discrimination was for two purposes; to help control the thermal energy radiated from the exhaust pipe and to lower the minimum back pressure under full load conditions. Each route was joined before passing by the sample point for the emissions analyser and both routes are connected to the external flue running out of the test cell to the surroundings. Figure 3.7 shows the exhaust system arrangement, with each route indicated.

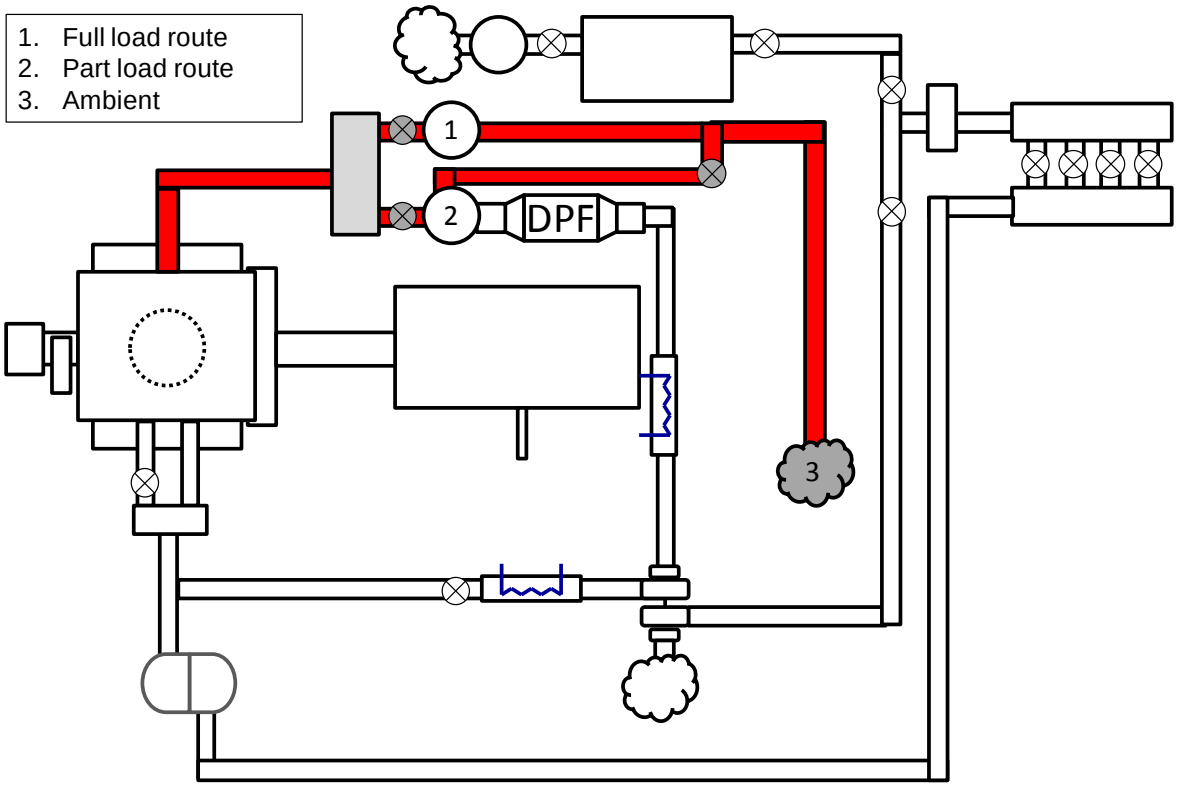

Figure 3.7 Exhaust system schematic

The full load route was fitted with an orifice plate in order to create a flow restriction to increase the back pressure on the engine as it pumps the gas through the system. The size of the orifice plate was selected to produce back pressures similar to a high specific power

turbocharged Diesel engine. The full load route had an isolating valve to allow the switch over to the part load operation.

The part load system was used when the gas flow and temperature was lower than the full load condition as well as containing the pipe work used in the EGR circuit as will be described in the following section. The part load route was equipped with two mechanically operated valves, one of which can be operated solely to change the back pressure level set on the engine and the other one operated to affect the back pressure and the restriction on the EGR circuit. These valves are used to isolate the system when switching to the full load route.

3.2.4 Exhaust Gas Recirculation System

The EGR system was integrated into the part load route of the engine exhaust system. This was the major modification made in previous work (Mason et al., 2008), which was necessary in order to deliver low temperature EGR with the aim of achieving low NOx. Prior to that point there was a short circuit system with a cooled stream and an un-cooled stream that were mixed prior to being added to the intake system. The existing system is shown in Figure 3.8. As described there are a series of valves which are used to modulate the pressure and flow rates of the gas in the system.

The valve indicated by number four was an electronically actuated valve, controlled from the test cell. The valve was a poppet type that reveals a flow curtain for the exhaust gas. This valve was modified with an insert to reduce the effective flow area and to allow finer regulation of the exhaust gas. The length of the EGR system causes a significant heat loss from the exhaust gas by the time it was returned to the intake manifold, particularly at the low load conditions. The heat exchangers shown could be used to heat up the exhaust gas under these conditions.

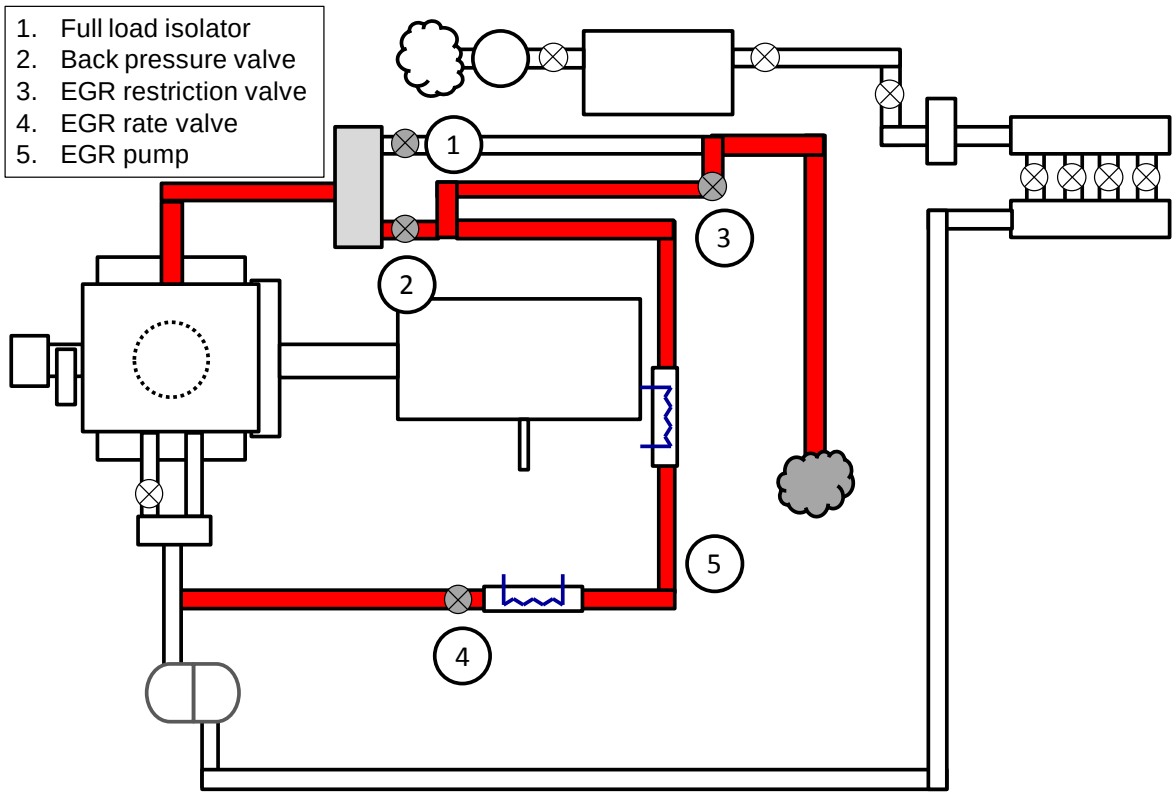

Figure 3.8 EGR circuit schematic

3.2.5 Oil and Water System

The oil and water supplies for the engine were both managed independently by the test cell controller. The oil was contained in the crankcase and circulated around the engine to provide lubrication to the valve system, the crankshaft and the piston. The oil circuit had its own pump and heat exchanger configuration to regulate its temperature and it was equipped with a pressure level switch. The switch was linked to a test bed controller, which if tripped would turn off the fuel, air and dynamometer systems as a safety measure. The oil temperature was regulated at a temperature of 85°C.

The water system carries the coolant through the engine. The coolant was stored in a tank in the engine test cell and the circuit has a pump and heat exchanger to regulate the temperature of the coolant. The coolant was also controlled to a temperature of 85°C.

3.3 Data Logging

The data recorded at each test point in this study was an averaged value made over the acquisition period. The acquisition period was dependent upon the type of data logged. Sensors were logged by either the low speed or high speed data acquisition system. Low speed data logging was made over a fixed time period and sampled at 1 Hz. The high speed data was acquired over 300 consecutive engine cycles.

3.3.1 Low Speed Logging

The instruments which make up the low speed log file are indicated in Table 3.5. The measuring duration was linked to the fuel meter sampling time, in normal operation this was set to 100 seconds. Therefore the instruments logged at 1 Hz will include 100 values for each channel in the low speed log file. Some instruments recorded in the low speed log operated in a command mode. For example the smoke meter which requested three samples, which were recorded and averaged. The fuel meter was requested to make one measurement for the measurement duration. The fuel mass consumed was used to compute the average fuel mass flow rate and average injected mass.

Once acquired, analysis was performed on the low speed data file, with the average and standard deviation computed for each of the channels. The average value was used in the summary file for a data set. In most cases two test logs were made for each test condition.

3.3.2 High speed Data

High speed data was distinguished from the low speed data by the time response of the transducer. The fast time response of these instruments allows them to be logged at crank angle resolution. High speed data refers to the channels indicated in Table 3.5 and they are logged over 300 engine cycles.

The data was synchronised with the crank angle encoder with has a resolution of half a degree crank angle. The software used to log the high speed data was used to interpolate between these crank angle marks, over a specified window around TDC, to give a finer resolution for the combustion process. The result was a data file, with both raw outputs and calculated values based on the signals measured. The majority of the calculated values used are combustion calculations were based on the measured in-cylinder pressure.

3.4 Instrumentation

The instrumentation used in this study has been specified based upon the best response characteristic and accuracy for the application. The locations of the sensors used on the engine test bed are shown in Figure 3.9 and Table 3.5 has the corresponding key.

The pressure and temperature sensors for the gas flow in and out of the engine were kept as close as possible to the engine. In the case of item 5, the intake high speed Kistler, this had to be located up stream of the separate intake runners, as indicated in Figure 3.9. The instrument was also located after the EGR connection, to take a measurement of the mixed intake stream.

A crank shaft encoder was used to synchronise the measurement of the fast responding sensors with the motion of the engine crank shaft. It has marks of half degree increments, which can be interpolated between using the high speed software.

All of the thermocouples used on the test bed were k-type thermocouple. They were used for two purposes; to monitor the performance of the engine and the gas exchange process and to monitor the condition of the oil and coolant supplies to the engine. In each flow location they are inserted so that the tip of the thermocouple was aligned to the central axis of the pipe. This was to ensure the thermocouples are away from the walls and that the measurement was of the gas temperatures and not influenced by any conduction from the pipe walls.

The load cell was used to measure the brake torque of the engine and hence compute the brake mean effective pressure (BMEP).The load on a single cylinder engine was specified in terms of the gross indicated mean effective pressure (GIMEP), since the friction characteristic was not representative of a multi cylinder engine due to the specific number of bearings per cylinder. The load cell measurement was used as an indicator to determine whether the GIMEP measurement varied greatly.

No.	Type	Description	Make	Model	Range	Unit	Accuracy	Log speed
1	Pressure	Air supply pressure	Druck	PMP-317	0-10	barA	0.15%	Low
2	Temperature	Air supply temperature	K-type		0-100	°C	1°	Low
3	Humidity	Relative humidity	Rotronic	i4000	0-100	%		Low
4	Temperature	Pre EGR temperature	K-type		0-200	°C	1°	Low
5	Pressure	Intake pressure	Kistler	4045A5	0-5	barA	0.30%	High
6	Temperature	Swirl temperature	K-type		0-100	°C	1°	Low
7	Pressure	Straight port intake pressure	Druck	PMP-317	0-4	barA	0.15%	Low
8	Temperature	Straight port intake temperature	K-type		0-100	°C	1°	Low
9	Encoder	Crank angle encoder	Leine and Linde		0-360	°	0.5°	High
10	Pressure	Fuel pressure	Kistler	4067A3000	0-3000	barA		High
11	Pressure	In-cylinder pressure	Kistler	6125C	0-300	bar	0.40%	High
12	Current	Current trace			0-50	A		High
13	Pressure	Exhaust pressure	Kistler	4045A5	0-5	barA	0.30%	High
14	Temperature	Exhaust temperature	K-type		0-1400	°C	1°	Low
15	Pressure	Exhaust pressure	Druck	PMP-317	0-4	barA	0.15%	Low
16	Temperature	EGR coolant in	K-type		0-200	°C	1°	Low
17	Temperature	EGR pump temperature	K-type		0-200	°C	1°	Low
18	Temperature	EGR coolant out	K-type		0-200	°C	1°	Low
19	Temperature	EGR temperature	K-type		0-200	°C	1°	Low
20	Emissions	Raw emissions (various)	Horiba	MEXA 7170DEGR	-	Ppm		Low
21	Temperature	Sample point temperature	K-type		0-1400	°C	1°	Low
22	Emissions	Smoke	AVL	415s	0-10	FSN	0.05FSN	Low
23	Load	Torque			-30-110	Nm		Low
24	Mass flow	Fuel measurement	AVL	733	0-54	kg/h	0.01kg/h	Low

Table 3.5 Sensor identification and description

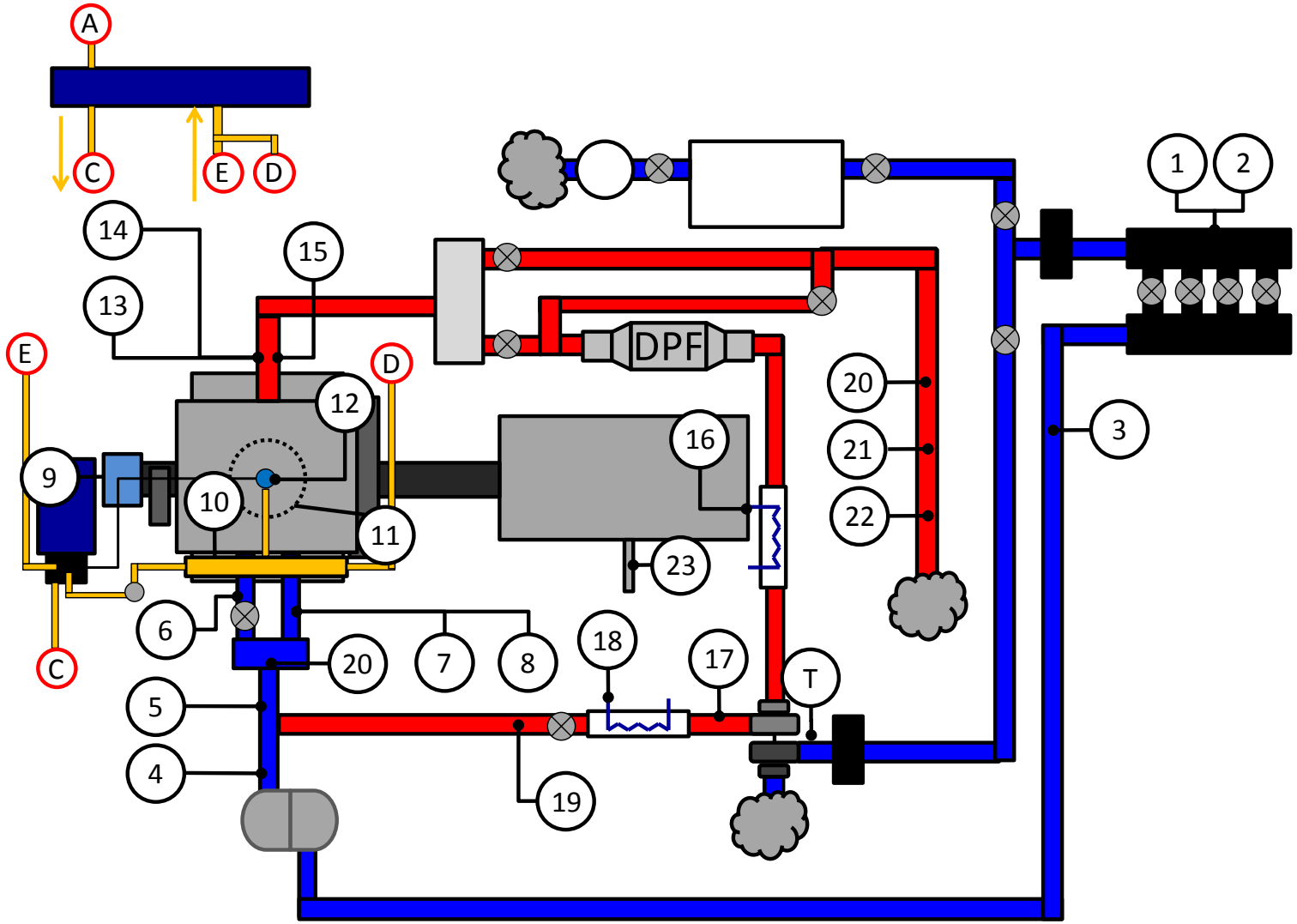

Figure 3.9 Test bed schematic

3.4.1 Emissions Measurement

The emissions measurements made on the test bed are both gaseous and particulate. The European legislation for a Diesel vehicle requires the regulation of particulate matter from the exhaust pipe. The system on the test bed has been inherited from previous studies with only minor modifications to the sampling point locations (Laguitton, 2005).

3.4.1.1 Gaseous

The emissions analyser has several measuring devices and two sampling lines used to measure the individual species in the exhaust gas and intake gas. The outputs of the individual measuring devices are collated and displayed by the main control unit. The species that are measured in the exhaust system are not only regulated emissions, but they are also to establish the operating condition of the engine. From these measured values operating parameters such as air to fuel ratio and the EGR rate were computed.

EGR rate is defined as the ratio of the concentration of CO2 in the exhaust stream, to the concentration of CO2 in the intake manifold, after the air and the EGR have mixed. In the calculation the presence of CO2 in the air is accounted for.

$$\frac{\left(\mathrm{CO}_{2,\mathrm{int}} - \mathrm{CO}_{2,\mathrm{air}}\right)}{\left(\mathrm{CO}_{2,\mathrm{exh}} - \mathrm{CO}_{2,\mathrm{air}}\right)} = \%_{EGR} = \frac{\dot{m}_{EGR}}{\dot{m}_{air} + \dot{m}_{EGR}}$$

Once the EGR rate has been calculated, it is possible to calculate the mass flow rate of EGR from the air flow. Rearranging the above equation leads to:

$$\dot{m}_{EGR} = \dot{m}_{air} \frac{\%_{EGR}}{(1 - \%_{EGR})}$$

The total flow into the engine can then be calculated:

$$\dot{m}_{Total} = \dot{m}_{air} \frac{1}{(1 - \%_{EGR})}$$

The accuracy of the measurement of the CO2 will affect the uncertainty of the calculation of the EGR rate. When a calculation is a quotient, the relative uncertainty of the measured values can be summed to give the uncertainty of the calculation. As a result based on the worst case quoted uncertainty of the sensors the error in the EGR rate calculation is 4 %.

The following table shows the typical uncertainty of the calculated EGR rate based on the accuracy of the CO2 measurement, at typical engine operating conditions.

Key point	Absolute Uncertainty	Min	Nominal	Max
KP1	2%	43%	45%	47%
KP2	2%	36%	38%	40%
KP3	1%	28%	29%	30%

No.	Type	Description	Measurement	Model	Range	Unit	Accuracy	Repeatability	Time response (T90)	Condition Temperature	Condition humidity
1	Carbon Dioxide	Non dispersive infrred detector	Direct	AIA-723	0-20	%	smallest: 1% FS or 2% reading	0.50%	1.5s	Room temp	Cooler dried
2	Carbon Monoxide	Non dispersive infrred detector	Direct	AIA-723	0-3	%	smallest: 1% FS or 2% reading	0.50%	1.5s	Room temp	Cooler dried
3	Oxides of Nitrogen	Chemiluminescence Detector	Direct	CLA-720M	0-500, 0-10000	ppm	smallest: 1% FS or 2% reading	0.50%	2s	Heated sample	Cooler dried
4	Oxygen	Magneto-pneumatic	Direct	MPA-720	0-25	%	smallest: 1% FS or 2% reading	0.50%	1.5s (O2>5%), 2s (O2<5%)	Room temp	Cooler dried
5	Total Hydrocarbon	Flame ionisation detector	Direct	FIA-725A	0-500, 0-50000	ppm	smallest: 1% FS or 2% reading	0.50%	1.5s	Heated sample	Wet

Table 3.6 Emissions analyser performance

The above Table 3.6 shows the type of analyser and its performance. The measurements made by the analyser are direct measurements of the exhaust stream. Each analyser conditions the gas depending upon its requirements. Where the analyser was a heated sample it was maintained to 191°C, as dictated by the configuration of the Horiba emissions hardware. This was regulated by the heated line and the analyser itself. There was an additional heated oven in line between the exhaust pipe and heated sample line, which was maintained at 191°C. This oven was inherited from previous studies and serves to maintain the temperature of the sample gas and to remove the particulate matter from the sample. The cooler used to dry the sample gas was located in the control unit of the analyser rack. The sample gas in these analysers was at room temperature.

As the study was carried out at steady state conditions the response time of the sensors was sufficient to cope with changes in the output of the engine. Following the selection of a new test point the gaseous emissions were monitored and test points were only logged once fluctuations in readings have fallen below a predetermined threshold.

3.4.1.2 Particulate Matter

The means for determining the mass of particulate matter flowing out of the engine was a calculation based on a correlation between particulate concentration and filter smoke number (FSN). The measurement of smoke number was based on the principle of drawing a sample of the exhaust gas through filter paper. The deposits of particulate matter discolour the filter paper and the opacity of the discolouration was measured. The conversion from the paper blackening to a filter smoke number was based upon the opacity of the paper and the amount of time or volume of the sample gas.

There was an optimum paper blackening that the opacity sensor can operate at for the best measurement accuracy. This involves sampling a different amount of gas depending upon the concentration of particulates in the exhaust. The smoke meter can be operated in this way in automatic mode, and it was capable of determining the sample volume required for the optimum paper blackening. It was found that taking an average of three samples minimised measurement uncertainty and produced repeatable results.

3.4.2 Fuel measurement

The fuel measurement made on the engine test bed was a direct measurement of the mass of fuel consumed. The fuel meter weighs the mass lost from the system over a specified period. The specified time period can be adjusted between fifteen and 100 seconds. This measurement of mass consumed was then used for the calculation of fuel consumption as a mass flow rate.

The Device has a weighing bucket with a 900 g capacity and was capable of measuring up to 50 kg/h (approximately 900 g of fuel consumed over 60 seconds). The maximum fuel flow expected on the single cylinder engine at the highest fuel flow conditions was around 7 kg/h (depending upon engine speed). At this order of fuel mass flow rate the most fuel mass lost from the system was around 195 g, which was approximately 22 % of the total mass of the measuring bucket. Under the part load conditions with an expected fuel mass flow rate of 0.6 kg/h this equates to less than 2 % of the total bucket mass.

With that in mind the sampling time was kept to its maximum of 100 seconds to allow the largest mass of fuel under any test condition, to be consumed. This was done to minimise the effect of the uncertainty in the measurement of fuel mass on the computed fuel mass flow rate.

3.5 Engine Test Points Drive Cycle Analysis

The engine test points used in this study were based upon key points selected from an analysis of engine load variations for a vehicle driven over the New European Drive Cycle (NEDC). Additionally, there were two tests points for full load operation, one at maximum torque (2000FL) and one at maximum speed (4000FL) as an assessment of peak torque and peak power. Table 3.7 summarises the key points identified, the names of each key point and the key points used in the tests to determine nozzle protrusion. The test process will be described in more detail in the following chapter.

Test point	Speed	GIMEP	Used in Protrusion test
-	RPM	bar	-
KP1	1500	3	
KP2	1500	6	
KP3	2000	9	P
2000FL	2000	24	P
4000FL	4000	21.4	P

Table 3.7 Test points used in the study

The table shows that there are 3 key points for the protrusion test. Nozzle protrusion was altered by adding washers of varying thicknesses to the injector. The points tested have different requirements for the mixture formation process which may result in a different optimisation for the protrusion test. The full load key points are not regulated by the emissions legislation; however they still remain important in terms of achieving high specific power outputs. The test carried out at 4000FL, where peak power occurred, was an additional check for the optimisation at the part load condition. The washer selection at KP3 should not affect the engine performance at the other operating conditions, so it was important to understand how the engine responded at other test points. Protrusion – 2000FL, where peak torque occurred, is at the same speed as Protrusion – KP3 but at an increased boost pressure and load target. The combustion process changes compared to KP3, because of the increase in the fuel required to meet the load target. Combustion is generally more diffusive at this point when compared to KP3.

3.6 Measurement Error and Uncertainty Analysis

In the presentation of experimental results, consideration was given to the measurement uncertainty of the calculated values. Appropriate sensors were selected to reduce error and therefore the resulting uncertainty of the calculated values used in the analysis. Where the error of a measurement was unknown, analysis based on the deviation of the measurement was used.

The parameters that required a calculation of the uncertainty were the indicated specific emissions values, and the fuel consumption. Other variables such as rate of heat release and combustion burn angles were either taken as the sensor value or the deviation of the experimental measurement. The deviation of the measurement was taken because the uncertainty calculation was too complicated, or involved a numerical integration, which in theory results in large uncertainty. The experimental deviation approach was a practical solution, without which it would be difficult to draw useful conclusions.

3.6.1 Calculating uncertainty

When a calculated value is a sum, then the absolute uncertainty of the measured values are summed together to give the overall uncertainty. When the calculated value is a product, then the relative uncertainty of the measured values are summed together. This method can be summarised in the following equations:

When a calculation is as follows; $a = b + c$

The absolute uncertainty is; $\partial a = \partial b + \partial c$

Where a is the sum calculated from the measured values b and c. ∂a is the uncertainty of the calculated vale a, ∂b is the error in the measurement b and ∂c is the error in measurement c. An example of this application is the calculation of exhaust flow from the fuel flow and air flow as follows:

$$\dot{m}_{exh} = \dot{m}_{fuel} + \dot{m}_{air}$$

Where $\dot{m}_{exh}$is the calculated mass flow of exhaust gas, $\dot{m}_{air}$ is the calculated mass flow of air and $\dot{m}_{fuel}$ is the measured mass flow rate of fuel. At an operating condition typical of KP3 with EGR flowing the error in the fuel measurement is 0.004 kg/h, the uncertainty in the

airflow calculation is 0.63 kg/h therefore the uncertainty in the flow of exhaust is the sum of these two values, 0.634 kg/h or 0.63 kg/h to 2 significant figures. The relative uncertainty for the mass flow of exhaust (used in the emissions calculations later) at KP3 is as follows:

$$\frac{\partial \dot{m}_{exh}}{\dot{m}_{exh}} = \frac{0.63}{(27.6 + 1.4)} = 2.2\%$$

When the calculation is as follows; $a = bc$

The relative uncertainty is; $\frac{\partial a}{a} = \frac{\partial b}{b} + \frac{\partial c}{c}$

Where a is the product calculated from the measured values b and c. ∂a is uncertainty of the calculated vale a, ∂b is the error in the measurement b and ∂c is the error in measurement c as for the previous case. The calculation of air flow is a product of the two measured values, fuel flow and AFR as follows:

$$\dot{m}_{air} = \dot{m}_{fuel} AFR$$

Where $\dot{m}_{air}$ is the calculated mass flow of air, $\dot{m}_{fuel}$ is the measured mass flow rate of fuel and AFR is the air to fuel ratio. At KP3 the relative error in the fuel measurement is 0.3%, and the relative error of the AFR calculation from the emissions analyser is 2%. As a result the relative uncertainty of the air flow calculation is 2.3% (0.63 kg/h).

For other measurements such as the burn angles the standard deviation of the measured or calculated value was used to represent the spread of data. This takes account of the variability of each test point on a specific day but does not consider the effects of the sensor error. As a means to validate this approach, measurements were taken for a daily check point to build up a picture of certainty about the sensors being used. An example of the cross check process can be given using the performance of the cylinder pressure sensor, which was used for all of the combustion calculations that fed the analysis. When the daily check point was tested, a motored curve was analysed for the variation of cyclinder pressure over the course of the testing. This accounts for the long term effect of sensor error.

3.6.2 Representing Uncertainty

In order to simplify the application the worst case error was taken to represent the maximum difference observed for each point shown in the test data. This was a conservative approach and a means for a quick reference for the performance of each combustion system configuration tested. The following Table 3.8 shows the uncertainties for the commonly occurring parameters used in the analysis.

		Test point				
Calculation	Uncertainty	KP1	KP2	KP3	4000FL	2000FL
isCO	%	8.8%	7.4%	6.9%	6.3%	6.4%
isHC	%	8.8%	7.4%	6.9%	6.3%	6.4%
isNOx	%	8.8%	7.4%	6.9%	6.3%	6.4%
isFC	%	2.9%	1.5%	1.0%	0.4%	0.5%
50% angle	%	3.0%	2.0%	2.0%	2.0%	2.0%
90% angle	%	3.0%	3.0%	3.0%	3.0%	2.0%
Smoke	FSN	0.05				

Table 3.8 Calculated and measured uncertainties for the common emissions results displayed in the results section

3.7 Daily Check Point Analysis

In order to verify the experimental equipment was working normally and to diagnose any issues after a piston change, a daily check point was tested prior to testing each day. The daily check point was based on an open loop engine condition that generated an expected output. The engine was also motored at each part load key point because an injector change could influence the engine output for an open loop condition making it impossible to compare check point conditions.

3.7.1 Motored Test Points

The engine oil and coolant was heated up before the engine started. The target temperature prior to starting the engine was 85 °C. Once up to temperature the engine was motored at each of the three key point conditions this was used to check the variation in maximum cylinder pressure and other test set up conditions. The inlet and exhaust conditions were set and the motored pressure curve and the torque measurement were taken to check for variation.

		Average			Standard Deviation			CoV %		
Parameter	Units	KP1	KP2	KP3	KP1	KP2	KP3	KP1	KP2	KP3
Speed	RPM	1501	1501	2000	5	4	4	0.3%	0.3%	0.2%
Intake pressure	barA	1.028	1.161	1.428	0.005	0.005	0.012	0.4%	0.4%	0.8%
Intake temp	°C	30.4	30.6	30.0	1.4	1.2	0.9	4.7%	4.0%	3.2%
Pmax	Bar	37.3	42.2	56.0	0.6	0.6	0.6	1.5%	1.5%	1.1%
Pmax angle	ATDC	-0.9	-0.9	-0.7	0.1	0.1	0.1	-11.1%	-11.7%	-14.9%
Exhaust pressure	barA	1.304	1.385	1.984	0.017	0.022	0.043	1.3%	1.6%	2.1%
Air flow	kg/h	21.1	24.4	40.7	0.5	0.4	0.4	2.6%	1.5%	1.0%

Table 3.9 Motored check point statistics

The table shows the average, standard deviation and coefficient of variance for each of the measured values for the duration of the testing programme. Figure 3.10 shows the parameters for each test where the x-axis was the number of test points. There were more than 200 test logs for each motored key point that contribute to the calculation for each measurement (some were discounted due to mistakes in the set up).

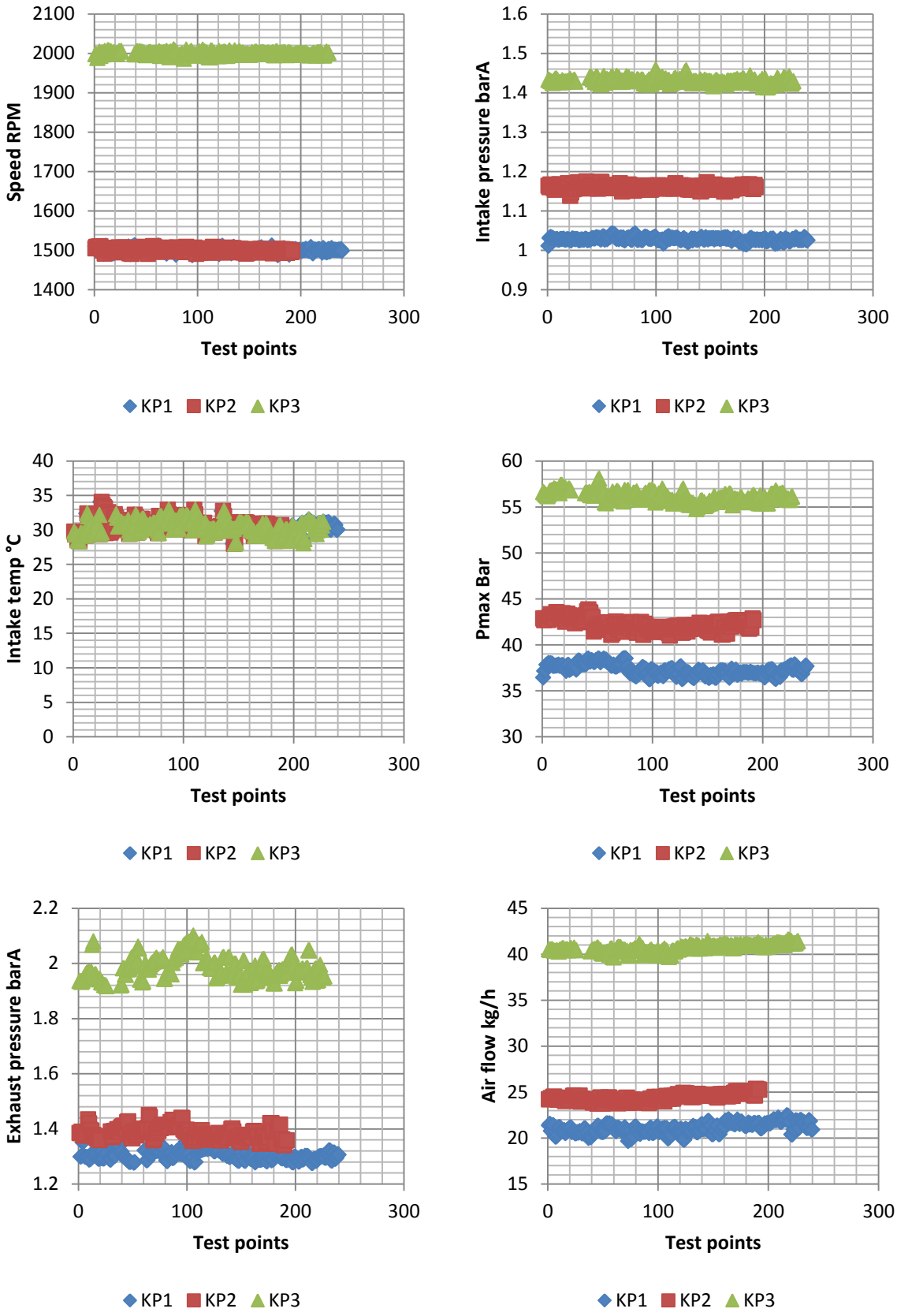

Figure 3.10 Motored check point test plots

Taking the cylinder pressure PMax measurement as an example; when the test was set up in the same way the measured parameters varied no more than 0.6 bar in all cases for one standard deviation The maximum CoV on this value was 1.5 % due to the relatively low maximum cylinder pressure at KP1.

The cylinder pressure measurement was an important parameter for the combustion calculations so ensuring that experimental error and variation was reduced was important. When the experimental variation was reduced it was possible to say that any variation in engine performance was due to hardware changes rather than error in the measurements. The figure shows that there were no step changes in any of the parameters tested, when bowls or injectors were changed. There is random scatter with no discernable long term trend indicating that data taken later in the programme could be compared with data acquired in the early stages.

3.7.2 Daily Check Point

Once each of the motored tests was completed, the engine was set into the 'open loop' condition. The following tables show the set up parameters and expected outputs.

As Table 3.10 and Table 3.11 show, the variation in the daily check point outputs for each bowl was minimal. The largest CoV observed in the set up was the intake temperature. The variation was a maximum of 4.3% for bowl B3 although this only represented 1.3 °C and in absolute temperature terms (°K) the variation was less than 0.5 %. GIMEP varied with a change in piston bowl (due to efficiency changes). As a result the fuel system set up was differently. The daily check point formed part of the zero EGR testing conditions

The results of the daily check point test gave confidence that the piston changes didn't affect the engine operation above and beyond the changes to the combustion process. It allowed the conclusions about the hardware design changes to be drawn with confidence in the variation of the results. Throughout the testing phase of the project this condition was successfully used to diagnose faults with the emissions measuring equipment, a cylinder head failure and issues with sensors and measuring equipment.

Test set up		
Parameter	Setting	Units
Speed	2000	RPM
Intake P	1.47	barA
Intake T	30	°C
Rail pressure	1050	bar
SOIm	-9	°C
Inj Dur (bowl dependent)	≈ 700	µs

Table 3.10 Open loop daily check point set up

		Average				Standard Deviation				CoV %			
Parameter	Units	B2	B3	B4	B5	B2	B3	B4	B5	B2	B3	B4	B5
Speed	RPM	2003	2001	2001	1997	4	4	8	6	0.2%	0.2%	0.4%	0.3%
Intake pressure	barA	1.469	1.470	1.471	1.467	0.004	0.003	0.007	0.004	0.3%	0.2%	0.5%	0.3%
Intake temp	°C	32.7	31.2	32.3	31.6	0.7	1.3	0.4	0.6	2.3%	4.3%	1.1%	1.8%
Rail pressure	Bar	1040.2	1043.5	1036.5	1044.1	2.5	5.6	3.0	2.4	0.2%	0.5%	0.3%	0.2%
Inj Dur	µs	694.1	699.7	681.5	677.1	1.9	1.9	6.6	3.0	0.3%	0.3%	1.0%	0.4%
SOIm	ATDC	-7.0	-9.0	-9.0	-9.0	0.0	0.0	0.0	0.0	-0.1%	0.0%	-0.2%	0.0%
Fresh air mass flow	barA	40.6	41.1	41.0	41.1	0.3	0.2	0.4	0.1	0.7%	0.6%	0.9%	0.1%
Fuel flow	kg/h	1.44	1.45	1.42	1.41	0.01	0.01	0.01	0.02	0.7%	0.7%	0.7%	1.4%
GIMEP	bar	9.06	9.01	8.98	9.06	0.07	0.04	0.07	0.04	0.8%	0.4%	0.7%	0.4%

Table 3.11 Open loop daily check point output and variation

4 The Effect of Injector Nozzle Protrusion on Combustion and Emissions

This chapter presents the initial testing to determine the injector tip protrusion. The injector tip protrusion is an important parameter in a Diesel engine for the relationship of the fuel spray with the piston bowl. The injector tip protrusion will be optimised for each bowl and fixed for the characterisation of each piston bowl.

The tip protrusion modifies the relationship of the fuel spray with the combustion chamber. This is known as spray targeting as it uses the combustion chamber geometry to influence the mixture formation process. This is similar in concept to a 'wall guided' Gasoline Direct Injection (GDI) in which the combustion chamber walls are used to disperse the fuel to a more a favourable location (Bosch, 2000). The interaction with the combustion chamber modifies the spray penetration (Pickett and Lopez, 2005, Pickett et al., 2005), the atomisation process (Amagai et al., 2003, Fang et al., 2008a), the jet interactions (Abraham et al., 1999, Amagai et al., 2003, Pickett and Lopez, 2005), the flame lift off length (Pickett et al., 2005, Som et al., 2011), heat transfer losses due to surface evaporation and ultimately has an influence on the mixture formation process and fuel efficiency. Therefore, being able to understand and optimise the surface, which can be modified further by changing the injector protrusion. Assumptions have to be made about the in-cylinder conditions relating to the engine operation that influence the liquid and vapour spray penetration. This makes the optimisation of protrusion necessary, first to check the assumptions about the fuel spray behaviour, but also to accommodate the wide range of in-cylinder conditions the engine is spray targeting is of particular interest and importance.

The main hardware parameters that influence the spray targeting are: the injector tip protrusion, the injector spray angle, and the geometry of the piston bowl. Once the shape of the piston bowl is defined, the spray angle of the injector nozzle can be selected to interact with a region on the bowl.

4.1 Experimental Results

When the engine was first assembled, the nozzle tip protrusion of fuel injector N0 was measured without a washer (Moukaideche, 2009), dimension c in Figure 4.1. This was used as a reference point for establishing the fuel spray path with the injector in the engine. The relative displacement of the injector, from having no washer fitted to the point where the injector was clamped into the engine, was measured with a dial gauge when the engine was cold. The position of the injector nozzle when the clamping torque was applied could now be established allowing a close approximation to the real spray targeting compared to the assumed value based on CAD geometry. The data presented in the results section uses the displacement of the fuel injector spray centre relative to the cylinder head gas face as a reference, dimension b in Figure 4.1.

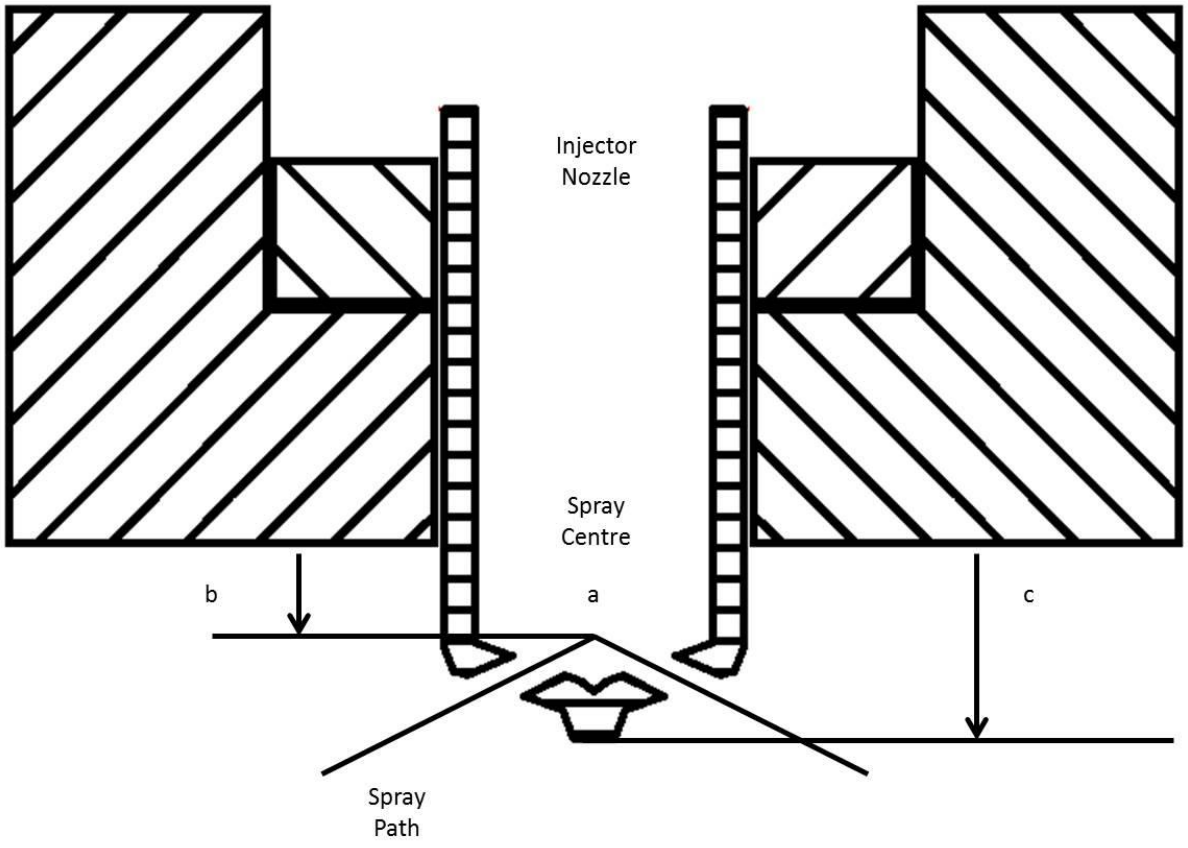

Figure 4.1 Schematic representation of the displacement of the injector with the change in protrusion. Arrows represent the positive displacement of the spray centre (b) and the nozzle tip (c).

The addition of a washer to the fuel injector reduces the displacement of the spray centre from the gas face. Thus the thinnest washer represents the furthest distance for the spray centre below the gas face. Protrusion was changed from least to most protrusion in 3 steps. The relationship between the spray centre height and washer thickness, with the clamping torque (26 Nm) applied is given in Table 4.1.

Washer	Spray centre height
mm	mm
3.1 mm	0.18
2.6 mm	0.61
2.1 mm	1.18
1.6 mm	1.60

Table 4.1 The relationship of washer thickness and spray centre height

Some of the analysis in this section includes an energy balance. Based upon the assumption that the heat input, the fuel conversion efficiency, heat transfer and crevice losses can be lumped together, then it was possible to calculate an energy balance based on heat release data and other measured parameters. The following description can best be illustrated in the following Figure 4.2. The maximum fuel energy per cycle, defined by the fuel consumption and the lower heating value ($q_{lhv,f}$) of the fuel gives a maximum amount of energy that can be extracted from the fuel (Q_{fuel}). The fuel conversion efficiency (η_{fc}) accounts for the fuel that has not contributed to the heat release process completely and was calculated from the emissions output, air flow and fuel consumption (Heywood, 1988). The maximum gross heat release (HR_{gross}) then becomes the product of the maximum fuel energy and the fuel conversion efficiency. The difference between the gross and net heat release (HR_{net}) accounts for the heat transfer and crevice losses ($HL_{ht,C}$) (Heywood, 1988). The difference between the indicated work (W_i) and the net heat release was the heat rejected through the exhaust (HL_{exh}).

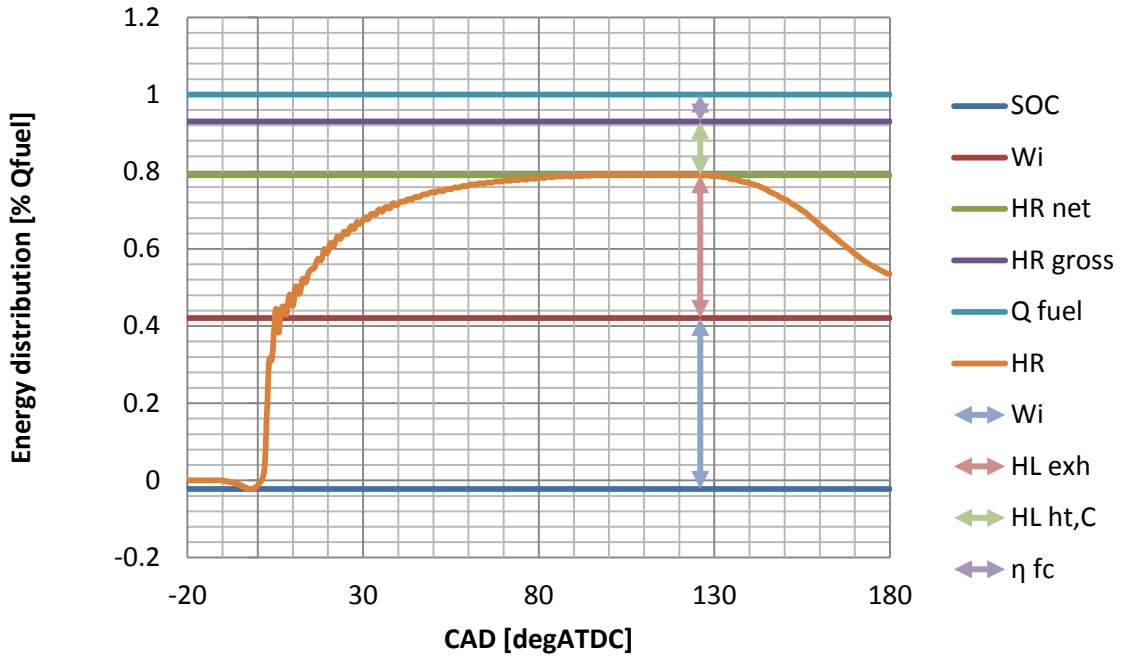

Figure 4.2 Schematic for heat release from fuel and subsequent identification of losses based on Heywood

The above explanation can be quantified with simple analysis. The maximum heat input was equal to the maximum fuel energy supplied, Q_{fuel} where:

$$Q_{fuel} = \frac{cycle}{2}\frac{\dot{m}_{fuel}}{N} q_{\mathrm{lhv},f}$$

Equation 4.1

Where; N was the engine speed expressed in rev.s^{-1}, $\dot{m}_{fuel}$ was the mass flow rate of fuel in kg.s^{-1}. The fuel conversion efficiency can be calculated from the combustion losses by taking into account the enthalpy of formation of various emitted species that do not contribute to the heat release process and can be quantified in the following equation.

$$\eta_{fc} = 1 - \frac{\sum_i x_i Q_{\mathrm{lhv},i}}{[\dot{m}_f/(\dot{m}_a+\dot{m}_f)]Q_{\mathrm{lhv},f}}$$

Equation 4.2

Where; x_i represents the mass fractions of the individual constituents, $Q_{\mathrm{lhv},i}$ the enthalpy of formation of the individual constituents, $Q_{\mathrm{lhv},f}$ was the lower heating value of the fuel, $\dot{m}_a$

was the air mass flow rate and $\dot{m}_f$ was the fuel mass flow rate. The final two parameters should be expressed in equivalent units of mass flow rate, kg.s^{-1} or g.h^{-1} for example.

Based on the schematic in Figure 4.2, the maximum gross heat release, HR_{gross} can be calculated as the product of the maximum heat input of the fuel, Q_{fuel} and the fuel conversion efficiency, η_{fc}.

$$HR_{gross} = Q_{fuel} \times \eta_{fc}$$

Equation 4.3

The maximum net heat release value (HR_{net}) can be calculated from the magnitude of the heat release from the start of combustion (SOC) to the value of heat release at the crank angle of exhaust valve opening (HR_{θ}). SOC was defined at the minima of the heat release profile that indicates a turning point from fuel evaporation into heat rise due to combustion.

$$HR_{\mathrm{net}} = \mathrm{HR}_{\theta} - \mathrm{HR}_{\mathrm{SOC}}$$

Equation 4.4

Therefore the heat losses through heat transfer and crevice losses, lumped together in this analysis can be taken as the difference between the maximum values for HR_{gross} and net heat release, HR_{net} respectively.

$$HL_{HT,C} = HR_{gross} - HR_{net}$$

Equation 4.5

The difference between HR_{net} and the indicated work output (W_i) results in the heat that was lost through the exhaust.

$$HL_{\mathrm{exh}} = HR_{net} - \mathrm{W_i}$$

Equation 4.6

As a result an energy balance can be produced, which helped to identify where the fuel energy was being lost and what effect bowl geometry had on this distribution.

4.1.1 Protrusion – KP3 Test

Protrusion – KP3 was tested with piezo injector N1 for the conventional bowls (B2 and B3) and N4 for the unconventional bowls (B4 and B5) as described in the nozzle library in chapter 3.1.4. The following Table 4.2 shows the test settings that were used for the protrusion conditions, with the Start of Main Injection Timing (SOIm) being retarded in steps of two° starting at -9°ATDC. The rail pressure was fixed along with the intake conditions. Fuelling demand was varied to maintain the load (GIMEP) as the injection timing was varied.

Test Settings									
Test name	Speed	Load GIMEP	Intake temp	Intake pressure	EGR rate	EGR temp	Pilot SOI	Rail pressure	SOI_m
	RPM	bar	°C	bar A	%	°C	°ATDC	bar	°ATDC
Protrusion - KP3	2000	9	41	1.47	26	70	NA	1050	-9, -7, -5, -3

Table 4.2 Protrusion – KP3 test settings

The results in Figure 4.3 show an increasing trend in Indicated Specific Fuel Consumption (isFC) with increasing protrusion for all bowls apart from B5. Bowl B3 is the most sensitive to changes in protrusion resulting in an 8.7 % increase in fuel consumption when changing from the 3.1 mm to the 1.6 mm washer. Specific CO_2 emission follows this trend for all bowls indicating that for all but B5, the effect of increasing protrusion is to increase fuel consumption. Bowl B5 goes through a turning point in fuel consumption and CO_2, from the 3.1 mm to the 2.1 mm washer indicating unique behaviour for this unconventional system.

Smoke and CO follow the fuel consumption trend; Bowls B4 and B3 show a significant increase in smoke and CO with the 1.6 mm washer. The smoke number of bowl B4 changes from 0.16 FSN to 4.4 FSN, and CO changes from 1.28 g/kWh to 21.1 g/kWh. Bowl B5 smoke improves from 0.28 FSN with the 3.1 mm washer to 0.19 FSN with the 2.6 mm washer eventually increasing to 1.85 FSN with the 1.6 mm washer. isCO stays the same for B5 with the 3.1 mm and 2.6 mm at washer 1.28 g/kWh, increasing to 7.59 g/kWh with the 1.6 mm washer. The increase in smoke number would mean a large change in the exhaust opacity and a resulting increase in particulate filter loading. Smoke and CO are good indicators of rich combustion.

isNOx reduces with increasing protrusion. This effect is consistent across all bowls. At the smallest protrusions conventional bowls have lower isNOx levels than the unconventional bowls. As with CO and smoke, the isNOx emission indicated that the combustion becomes rich as the protrusion increases.

The results indicate that the biggest effect of protrusion is to reduce air entrainment into the fuel spray prior to combustion. The combustion process is sensitive to the spray targeting towards a particular point on the combustion chamber surface. As a result, the combustion duration increases with protrusion, as shown by the 90 % angle in Figure 4.3. Bowl B3 and B4 are affected the most, with the 90 % angle changing from approximately 40°ATDC to 57°ATDC. 17° change represents a significant increase in burn duration, increasing heat rejection into the exhaust and reducing efficiency.

The combustion process at Protrusion – KP3 was premixed, with the fuel injection demand completed before the onset of the combustion process. In order to avoid both slow combustion duration and rich product formation the fuel must be well distributed. When the isFC and indicators of rich combustion deteriorate with protrusion changes, one can assume that poor mixing of the air and fuel has occurred before combustion.

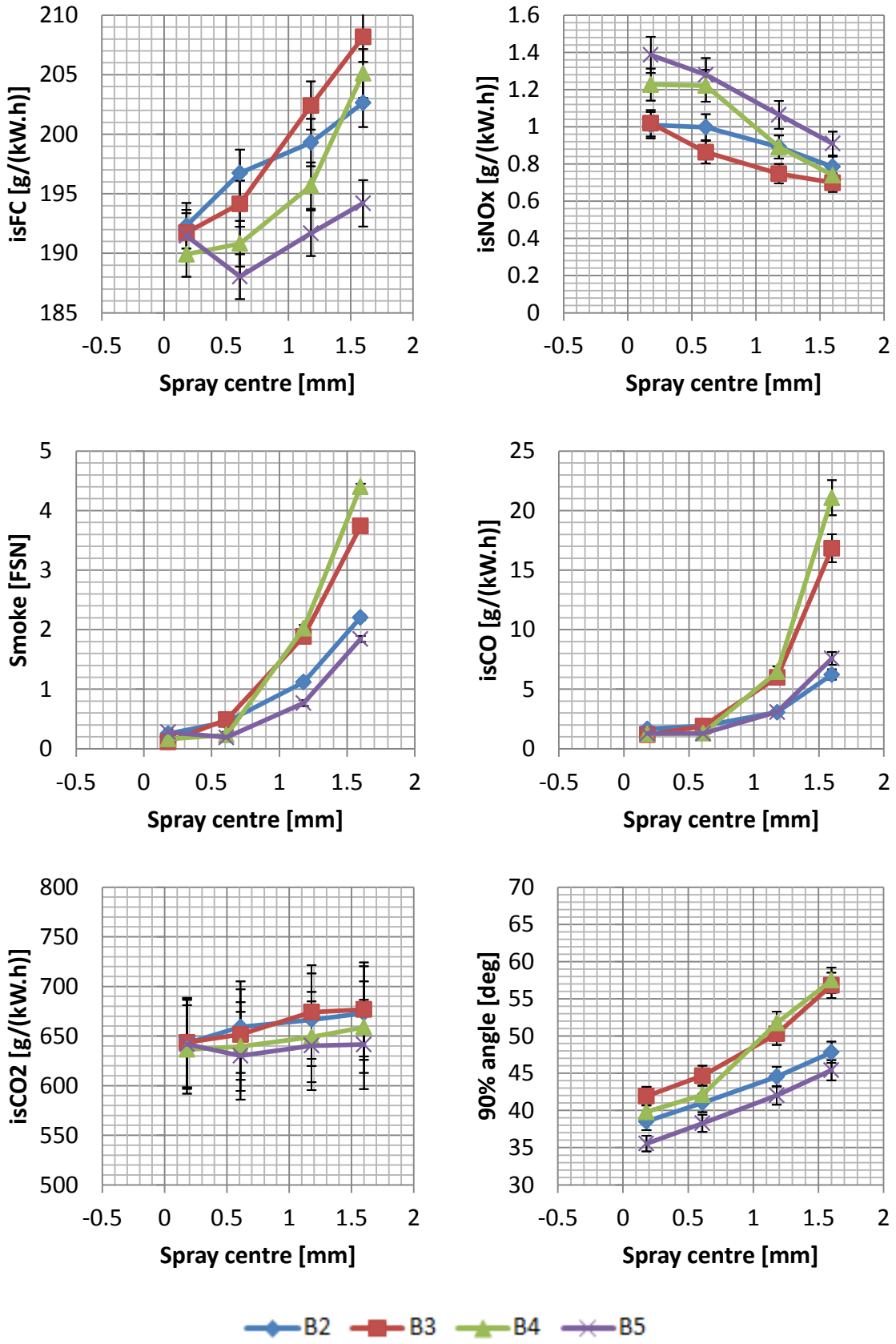

Figure 4.3 Effect of protrusion for all bowls at protrusion – KP3. Plots show spray centre below gas face for the selected SOIm of -9 °ATDC.

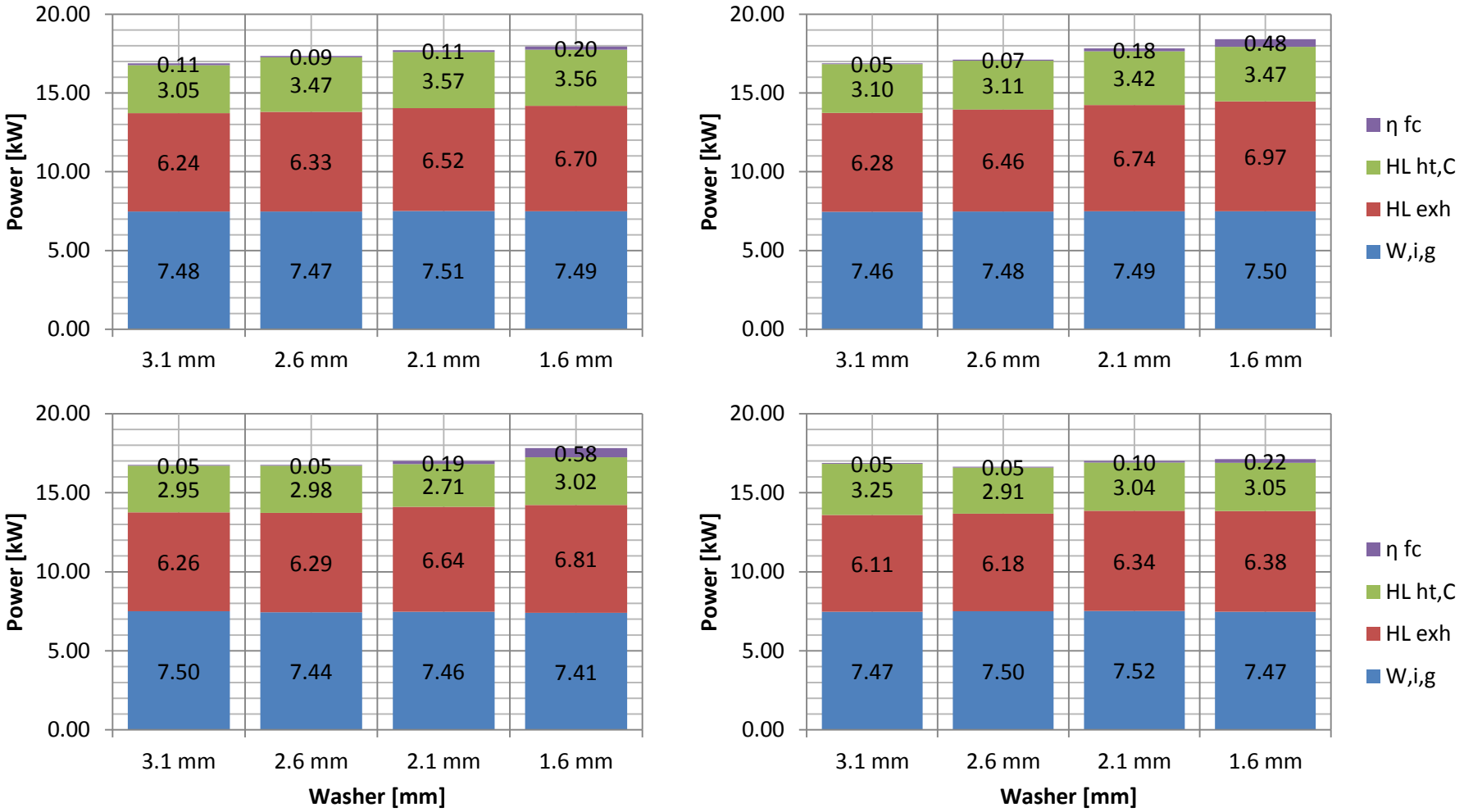

Figure 4.4 Fuel energy distribution for all bowls. Protrusion – KP3 with SOIm set at -9 °ATDC. From top left B2, top right B3 bottom left B4, Bottom right B5

An energy balance was performed in order to gain more insight into the mechanisms affecting the thermal efficiency of each bowl. Figure 4.4 shows an energy balance for each bowl and washer at -9°ATDC (for a description of the calculation see Appendix B Energy balance). The indicated work (W,I,g) was maintained approximately constant by changing the fuelling to meet the load target. What this demonstrates is that as protrusion increased, the heat rejection (HL,exh) to the exhaust increased. This is consistent for all bowls, with bowl B3 having the largest change (11 %) from the 3.1 mm to the 1.6 mm washer. Bowls B2 and B5 have the smallest change in heat rejection at 7 % and 4 % respectively.

A difference in heat transfer and crevice losses (HL,ht,C) is visible between the conventional and unconventional bowls. For the conventional bowls as the protrusion increases the heat transfer and crevice losses increases. The increase overall is 17 % for B2 and 12 % for B3. This may be due to an increase in turbulence that results from the combustion being contained in the bowl region.

The unconventional bowls do not show this trend. The results show that there is some variation as the protrusion increases. Apart from the 2.1 mm washer, the losses for B4 are consistent, averaging 2.98 kW with a CoV of less than 1 %. For bowl B5 the highest heat transfer and crevice loss is with the 3.1 mm washer. The remaining losses average 3 kW with a CoV of 2 % .This may indicate the influence of the secondary pip on the behaviour of the combustion system heat losses.

The heat loss differences between combustion systems may be a result of the fact the air supported conventional systems encourage swirl and squish. Combustion may be contained within the bowl region by the re-entrant lip (Kidoguch et al, 1999) and thus increase turbulent air motion resulting in higher heat transfer losses. The wider unconventional bowls, which have reduced squish regions, may be relatively stagnant and heat losses may be insensitive to protrusion changes.

The overall fuel efficiency is related to the work conversion efficiency. At this key point the influence of protrusion strongly affects the mixture formation process, which then affects the heat release process. In the case of the 3.1 mm washer, the heat release process is completed sooner (refer to the 90 % burn angle plot, Figure 4.3) leading to better work

conversion efficiency. This results in the minimum heat rejection through the exhaust and the highest fuel conversion efficiency assuming the heat lost in heat transfer is not significant.

Looking at the fuel spray targeting of the piston bowl features for the protrusions used at protrusion – KP3 helps to explain some of the behaviour observed from the experimental results. Figure 4.5 shows the piston at the start of injection and the two liquid spray plumes show the spray targeting with the thickest (3.1 mm) and thinnest (1.6 mm) washers.

The spray angles are different for the conventional (155°) and unconventional bowls (145°) and this is reflected in the figure by the direction of the fuel spray. The figure itself represents a section of half of a piston with a centre line on the right hand side of the figure. The lines that form the fuel spray include a centre line and a diverging line that represents a 13° cone angle based on observations of liquid fuel spray by (Karimi, 2007).

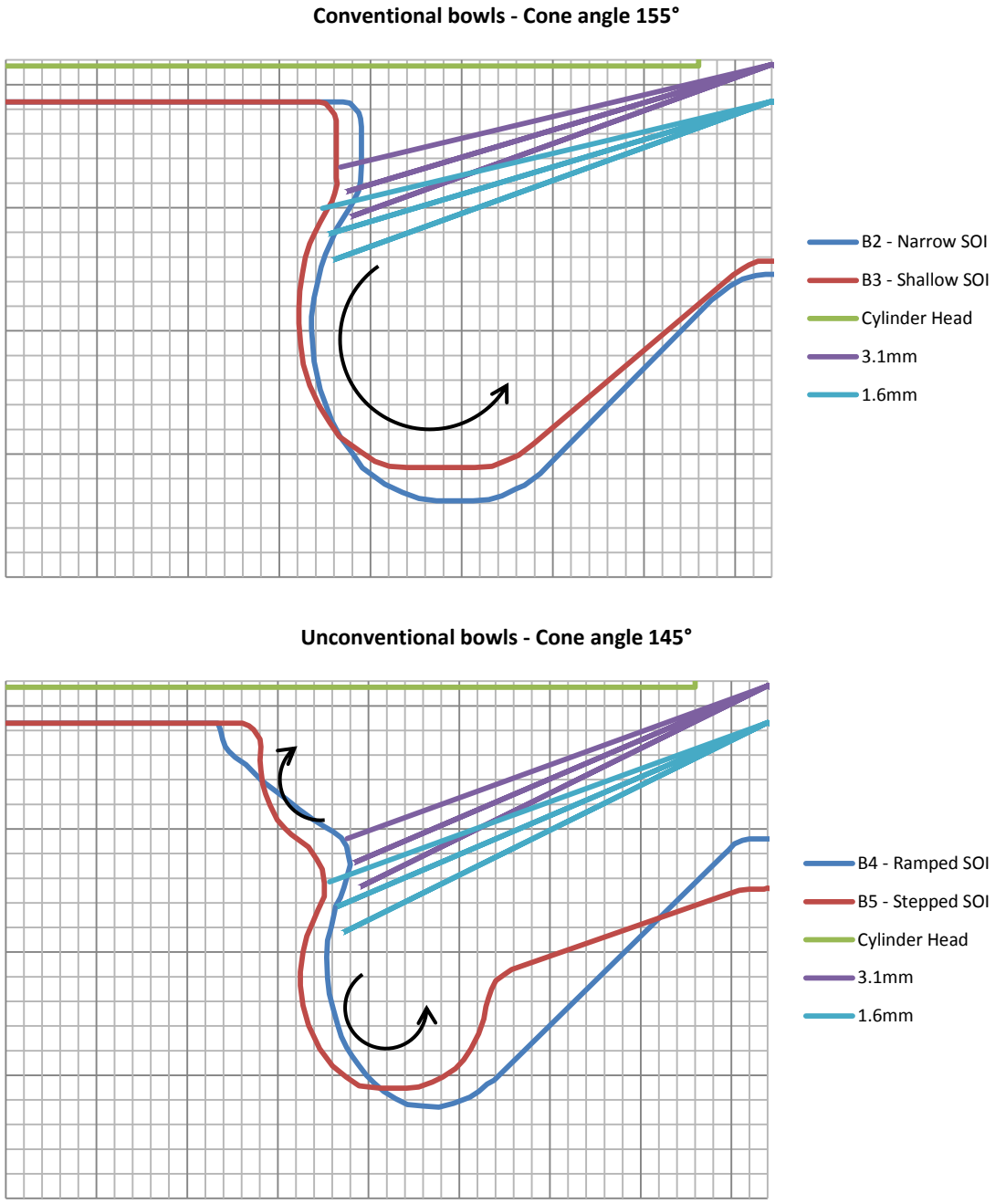

Figure 4.5 Fuel spray piston bowl relationships for conventional (top) and unconventional (bottom) piston bowls. SOIm was -9°ATDC, injection duration 0.7 ms. Arrows representing potential spray distribution as influenced by the piston shape looking at a section of the engine from the front. Cone angles are based on liquid fuel (Karimi, 2007).

At 2000 RPM the piston displacement for the injection durations typical of the operating condition is approximately 8° or 0.7 mm. At this test condition, the assumption is that these

figures represent the effective bowls and spray relationships prior to the onset of combustion and therefore allow a judgement to be made about how the fuel is distributed.

Because the majority of the mixing occurs with 0.7 mm piston displacement before the onset of combustion, the mixture formation relies on the distribution of fuel by the combustion chamber walls. For the conventional systems an increase in protrusion reduces the impact angle with the lip and can cause a downward flow of the fuel into the bowl region, therefore reducing the amount of air that can be entrained into the fuel spray.

In previous research by Middlemiss (1978), this was a positive effect because the result of creating rich regions of fuel and air was that combustion became more diffusive, resulting in a reduction in Indicated Specific Oxides of Nitrogen (isNOx). High swirl and squish flows helped to oxidise the products formed by rich combustion. Rich fuel regions were apparent in the measured emissions in the experiments and the longer combustion durations were reflected in the fuel consumption and the increase in HL_{exh} with protrusion, indicating that this was the behaviour of the conventional bowls.

The fuel consumption and emissions differences observed between the conventional bowls can be attributed to the location of fuel spray interaction with the piston bowl wall. Because bowl B3 is wider, the fuel spray effectively interacts with the lip lower down the face of the lip, changing the effective protrusion required to target the same place on the bowl lip. Because the protrusion has been shown to be an important parameter in terms of mixture formation and combustion efficiency, bowl B3 would be expected to show a marginal improvement in the output emissions with a slightly thicker washer.

The spray targeting effect is different for the unconventional systems. As the protrusion increases for these bowls, the spray targeting moves to a different region on the secondary pip. As this occurs, fuel distribution changes from being split between the upper and lower portions to being concentrated within the bowl region in a similar way to the conventional systems. Because the lower bowl region is smaller in volume for the unconventional bowls (necessary to maintain the compression ratio), there is less volume for the fuel and air to mix. This could lead to richer regions being formed, which may explain the significant deterioration of the combustion with the last step of protrusion, particularly with bowl B4.

The volume of the upper portion of the bowl and the radius of the upper portion curvature influences the fuel spray distribution and mixing. The difference between these unconventional bowls could be the way that the fuel spray is forced into a more intense vortex with the tighter curvature of the upper region of bowl B5. Additionally, the lower region in bowl B5 encourages a more intense swirling motion relative to bowl B4 enhancing fuel mixing and further product oxidation.

There is an upper limit observed for the protrusion of the unconventional systems which could be a result of the fuel making its way into the squish regions. Figure 4.5 shows that with the thickest washer, the fuel could have penetrated into the squish regions before and during combustion. The squish region is typically cooler than the main chamber region, which could lead to poor combustion and oxidation of combustion products.

4.1.2 Protrusion – 4000FL Test

At this higher engine speed, the cycle time is reduced as well as the time for mixture formation and formed product oxidation. This test point was used to ensure that the optimisation of the protrusion at Protrusion – KP3 did not compromise full load in terms of cylinder pressure, exhaust temperature and smoke number.

Test Settings									
Test name	Speed	Load	Intake temp	Intake pressure	EGR rate	EGR temp	Pilot SOIm	Rail pressure	SOI_m range
	RPM	GIMEP	°C	barA	%	°C	-	bar	°ATDC
Protrusion – 4000FL	4000	21.4 (approx 35 kW)	45	2.4	NA	NA	NA	2000	-19, -17, -15, -13

Table 4.3 Test settings used for 4000FL

The test setting used can be seen in Table 4.3 above. For each bowl, the protrusion was set and the test condition was run. Once the load target was achieved a timing swing was carried out from the most advanced to the most retarded SOIm timing. The limiting factors at this condition were the maximum cylinder pressure, the maximum exhaust temperature and the smoke number. In some tests the limits were reached before the load target was achieved so no meaningful data could be logged for comparison with other bowls.

Prior to testing the load target was reduced for bowl B4 because there was some uncertainty as to whether the load target of 21.4 bar GIMEP would be met with the unconventional bowls. In order to gather comprehensive data for the response to timing and protrusion the load target was set at 19.4 bar GIMEP. This has to be considered when looking at the following plots. Once the characterisation had been run for B4 at the higher load target it was clear that the load target was achievable so bowl B5 was tested at the higher load level at protrusion – 4000FL.

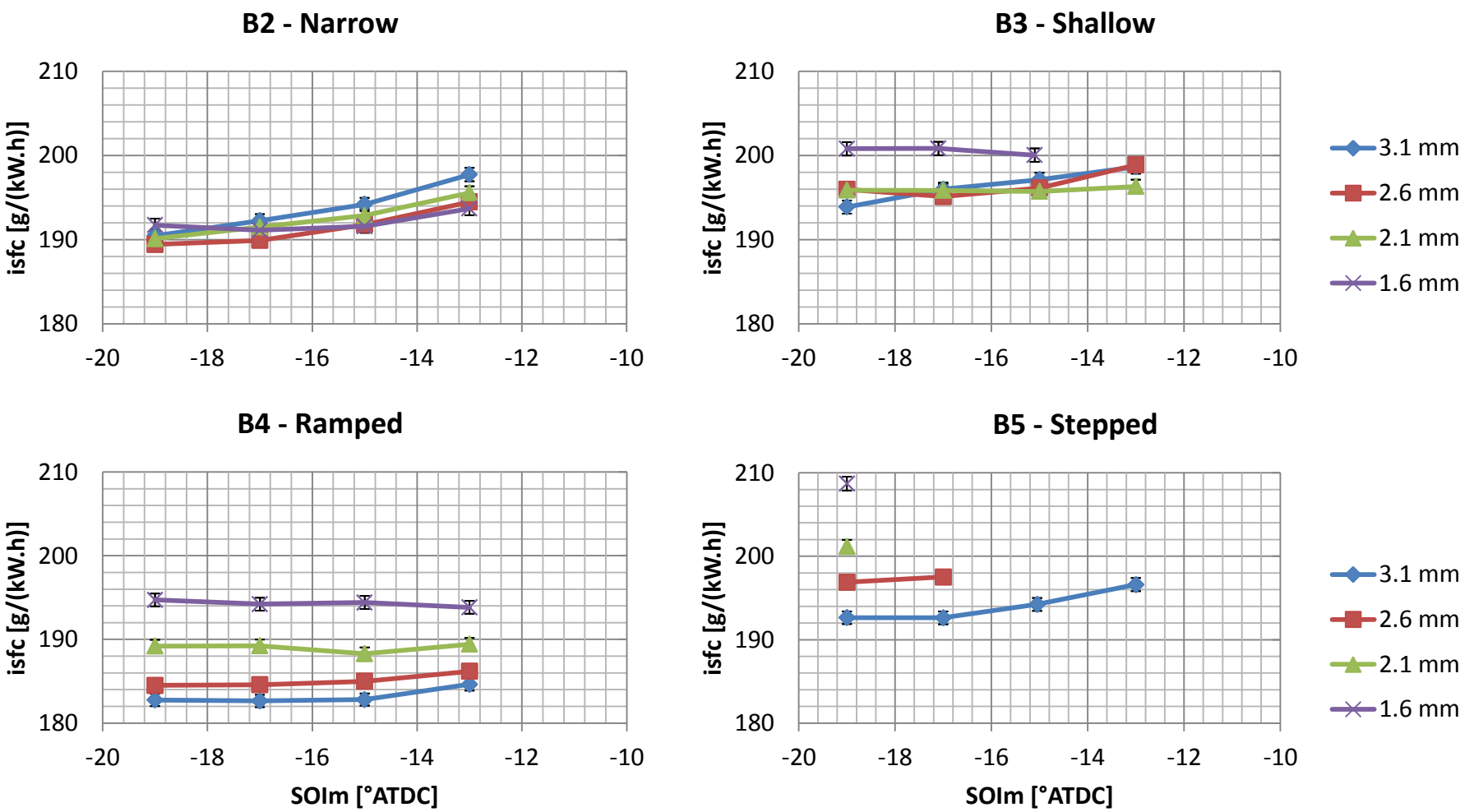

Figure 4.6 The effect of protrusion on isFC at Protrusion – 4000FL. Plots showing the SOIm swing at a fixed load.

As Figure 4.6 shows, the trend for the response to protrusion at this test point differs between the conventional and unconventional designs. For the unconventional designs the response is similar to that observed at Protrusion – KP3, in that the isFC deteriorates with an increase in protrusion. For bowl B4 the difference between the 3.1 mm washer and the 1.6 mm washer is approximately 6 % across the range of SOIm used. For bowl B5, at the most advanced SOIm timing the difference is 7.7 %. For the conventional bowls the effect of protrusion on isFC is not as significant as it is with the unconventional bowls. B3 shows the biggest difference, around 3 %, with the 1.6 mm washer.

With Protrusion – KP3 the response to a change in protrusion has the same trend for each SOIm tested for each of the conventional and unconventional bowls. With Protrusion – 4000FL however the trends with a protrusion change are different for the conventional bowls.

The limiting parameters were reached before it was possible to log any test data for bowl B5. Hence, as the protrusion increased and the SOIm retarded for bowl B5, the exhaust temperature limit was reached and therefore test points were not logged. The trend however at the most advanced SOIm is for the deterioration of the combustion process with an increase in protrusion as observed for bowl B4. This shows a consistent response for the unconventional bowls.

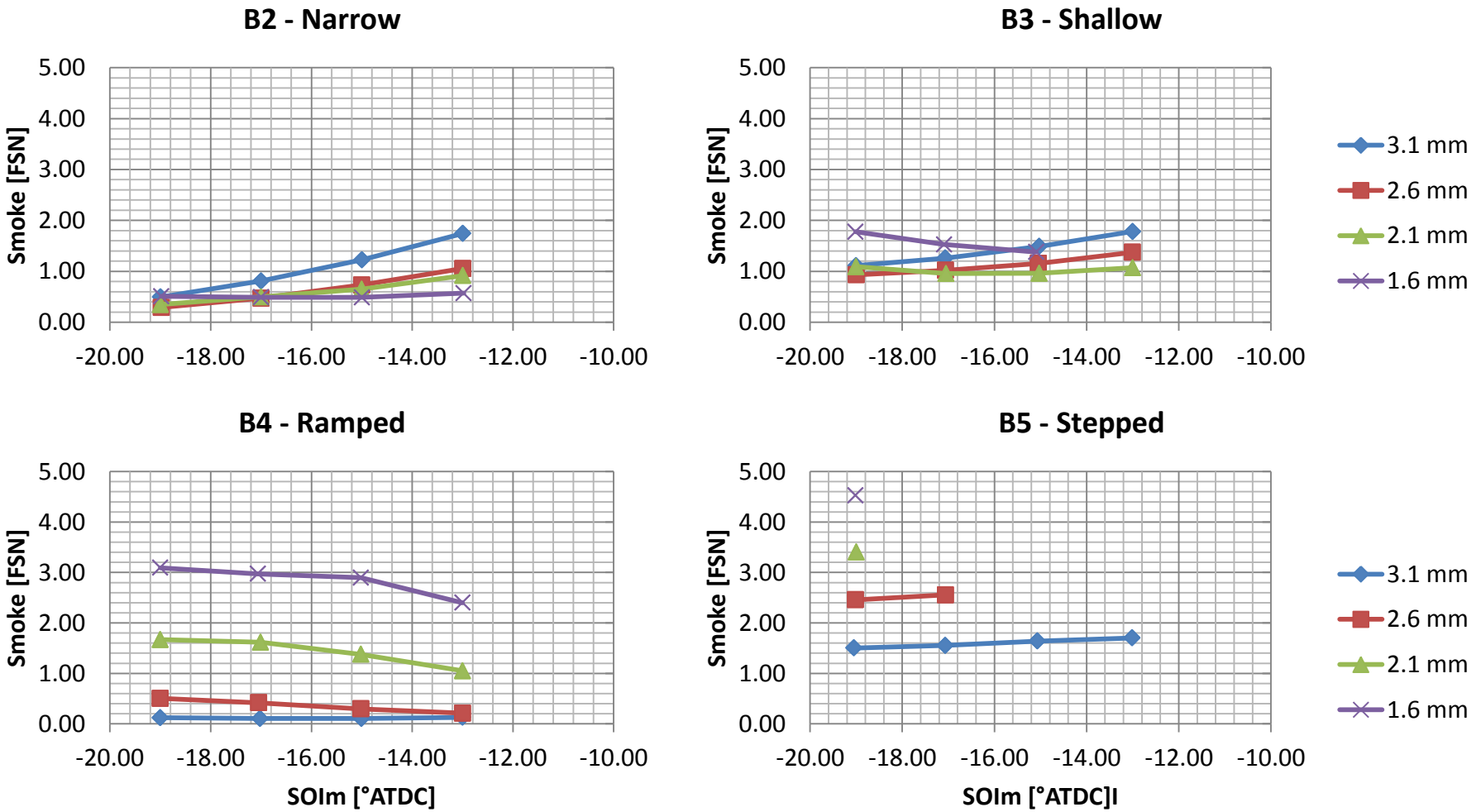

Figure 4.7 The effect of protrusion on smoke number at Protrusion – 4000FL. Plots showing the SOIm swing at a fixed load.

The smoke number shown in Figure 4.7 follows the isFC trend for all bowls. The biggest differences with a change in protrusion are observed for the unconventional bowls. Bowl B5 increases from 1.5 FSN with a 3.1 mm washer to 4.53 FSN with a 1.6 mm washer. The differences for the conventional bowls are less severe, with the biggest difference for B2 occurring at the most retarded timing (3.1 mm - 1.74 FSN and 1.6 mm - 0.57 FSN).

Swirl and squish velocities are proportional to engine speed. The air supported conventional systems potentially vary less when the protrusion is changed because the turbulence in the air has a stronger influence on the air fuel mixing than the spray targeting. Conversely, the unconventional systems, where one would assume the squish flow is less intense, rely more on the targeting of the spray at a particular region of the piston bowl.

Examining the spray targeting at this key point helps interpret these results. At this engine speed (4000 RPM) and injection duration (max 1400 µs) the piston moves through 33°. The piston displacement at this speed (5 mm) is approximately 7 times larger than the displacement at protrusion – KP3 (0.7 mm) because of the increased speed and increased injection duration required to meet the increased load. As the piston displacement is relatively large, the interaction of the fuel spray and bowl wall evolves relative to the SOIm, however some assumptions can be made about the distribution of the fuel.

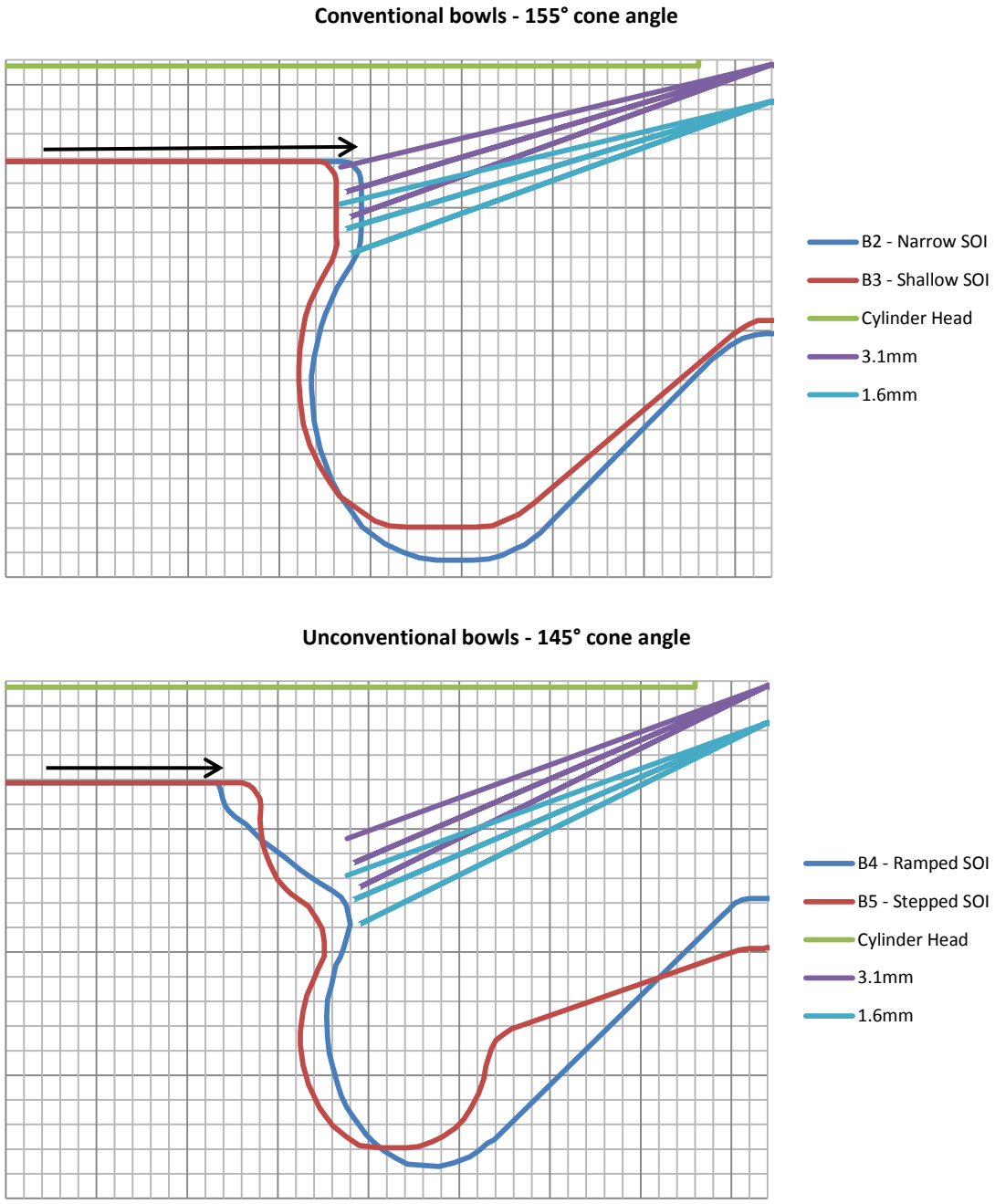

Figure 4.8 Fuel spray piston bowl relationships for conventional (top) and unconventional (bottom) piston bowls. SOIm was -19 °ATDC, injection duration 1.4 ms. Arrows representing potential squish flow velocity differences between each bowl.

Figure 4.8 shows the spray targeting for 3.1 mm and 1.6 mm washers with a SOIm of -19 °ATDC. As with KP3 – Protrusion, the assumption is that these figures represent the effective bowls and spray relationships prior to the onset of combustion and therefore allow a judgement to be made about how the fuel is distributed. As the protrusion increases for

the conventional bowls the spray targeting moves down the face of the lip and into the bowl region. Unlike protrusion – KP3, the strong squish flow encouraged by the relatively narrow bowl throat makes the conventional bowls less sensitive to the precise location of the spray targeting.

The unconventional bowls are more reliant on the interaction with the bowl wall. With the 3.1 mm washer, less fuel is focussed into the bowl region during the injection process. This indicates that there is potential to encourage better air entrainment by distributing the fuel between the upper and lower portions of the bowl.

Considering the energy balance in Figure 4.9, the differences between the conventional bowls appears to be the magnitude of the heat transfer and crevice losses ($HL_{ht,C}$). The difference between B2 and B3 with the 3.1 mm washer is more than 10 % for each washer selected. This is with comparable exhaust heat rejection values. For bowl B3 with the 1.6 mm washer, the load target was not met (34.6 kW) however the maximum fuel input (82.1 kW) was more than with the 3.1 mm washer (81.1 kW). The load target was exhaust temperature limited. For B3, when the 1.6 mm washer was used more of the heat energy was being rejected through heat transfer instead of contributing to work output.

The behaviour of B5 is similar to B3; when the load target was not met for the equivalent heat input, an increase in $HL_{ht,C}$ is observed. The poor combustion associated with the 1.6 mm washer means that the exhaust temperature limit was achieved before the load target could be met. Bowl B4 seems to indicate that the heat losses through the exhaust and heat transfer increases with protrusion. This is in line with the fuel consumption response. The smoke indicates that the mixture formation was poor as the protrusion increased, indicating the importance of spray targeting for the unconventional bowls compared to the conventional bowls.

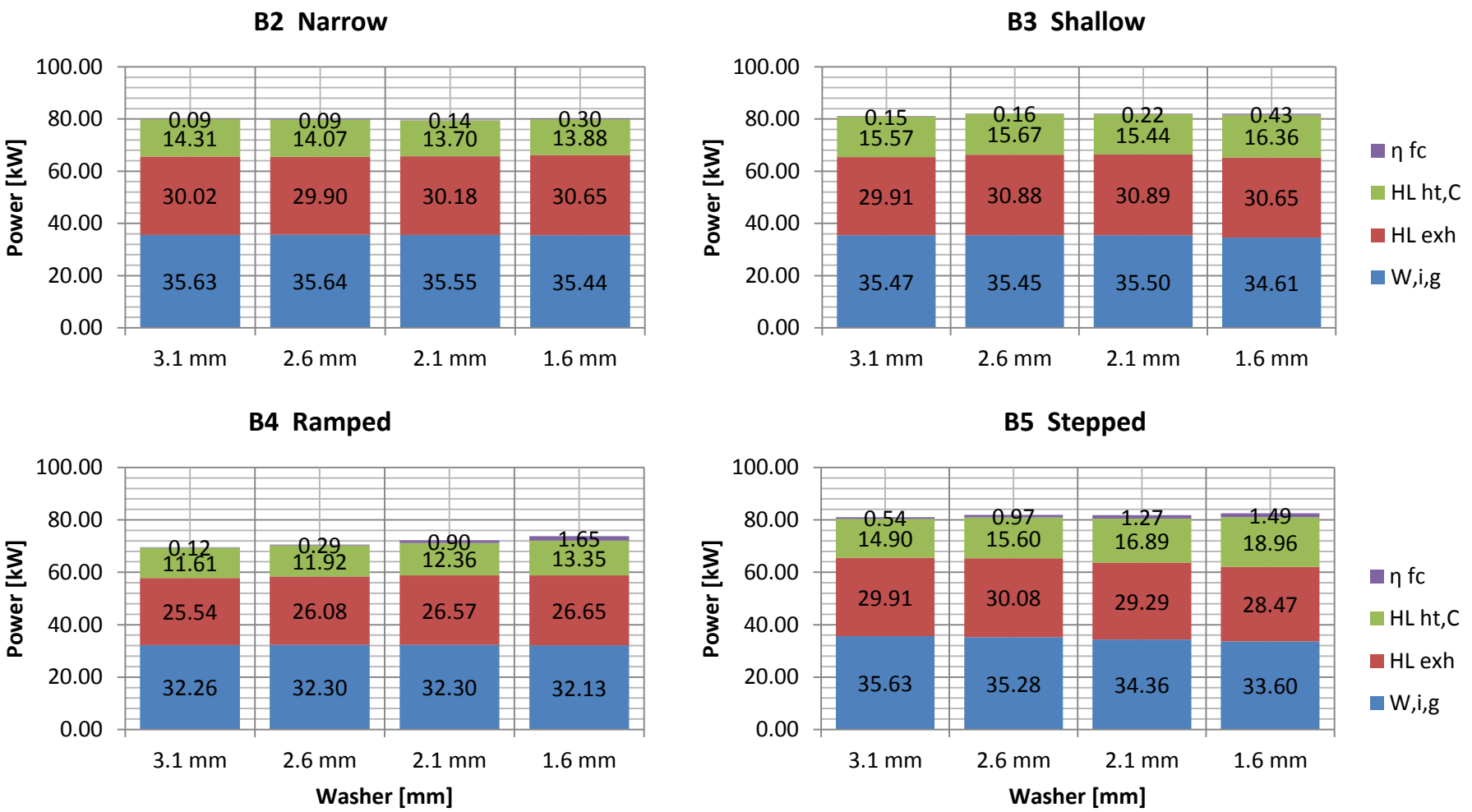

Figure 4.9 Energy balance top left to bottom right B2 to B5

4.1.3 Protrusion – 2000FL Test

Because protrusion – 2000FL was a full load condition the emissions are not regulated and hence the only important aspect was that the load target could be achieved within the boundaries of exhaust temperature, cylinder pressure and smoke number without a significant penalty on fuel consumption.

Test Settings									
Test name	Speed	Load	Intake temp	Intake pressure	EGR rate	EGR temp	Pilot SOIm	Rail pressure	SOIm range
	RPM	GIMEP	°C	barA	%	°C	-	bar	°ATDC
Protrusion – 2000FL	2000	24	50	2.4	NA	NA	NA	2000	-8, -6, -4, -2

Table 4.4 Protrusion – 2000FL test settings

The test setting used can be seen in Table 4.4. For each bowl, the protrusion was set and the test condition was run. The procedure was the same as with protrusion – 4000FL. Once the load target was set, at this condition a timing swing was carried out from the most advanced to the most retarded SOIm timing.

As seen in Figure 4.10, for all combustion chamber configurations, isFC deteriorates with increasing protrusion at each SOIm tested. Bowl B3 seems to show the smallest deterioration (approx. 4 % across all SOIm timings) from the 3.1 mm to the 1.6 mm washer, however the isFC is higher than all other bowls with the 3.1 mm washer (above 200 g/kWh for all SOIm tested).

The unconventional bowls are insensitive to the first step change in protrusion; however as with the conventional bowls further changes of protrusion lead to an increase in fuel consumption. What is observed immediately is that the thinnest washer is consistently poor for all of the combustion systems tested. This was also observed at protrusion – KP3. For the conventional bowls this indicates that, when the engine speed is reduced and the turbulence is lower, the sensitivity of the spray targeting increases compared to protrusion 4000FL. For the unconventional bowls, where squish is potentially lower, the spray targeting remains the governing parameter for the combustion quality.

Figure 4.11 shows that the smoke number increases for all bowls using the thinnest washer. This is the strongest indicator of a deterioration of the combustion due to poor fuel air

mixing. Bowls B2 and B4 seem to suffer with the highest smoke number when the thinnest washer is used achieving 1.5 FSN and 2.37 FSN respectively.

The energy balance is shown in Figure 4.12. With an increase in protrusion, in general, there is an increase in both $HL_{th,C}$ and HL_{exh} as well as fuel conversion efficiency losses. Bowl B4 has the biggest change from the 3.1 mm washer to the 1.6 mm washer of around 27 %. With the thinnest washer the combustion process breaks down and released heat is lost without contributing to the work output.

The bowl and spray relationship is similar to protrusion – KP3 at the start of injection event. The initial spray formation is affected by the fuel being biased more into the piston bowl with the thinnest washer. The piston displaces further than at protrusion – KP3 due to the longer injection event, however this is not sufficient to help entrain the available air into the fuel spray and combustion gasses. The initial spray formation and therefore spray targeting is the dominant parameter for the combustion process.

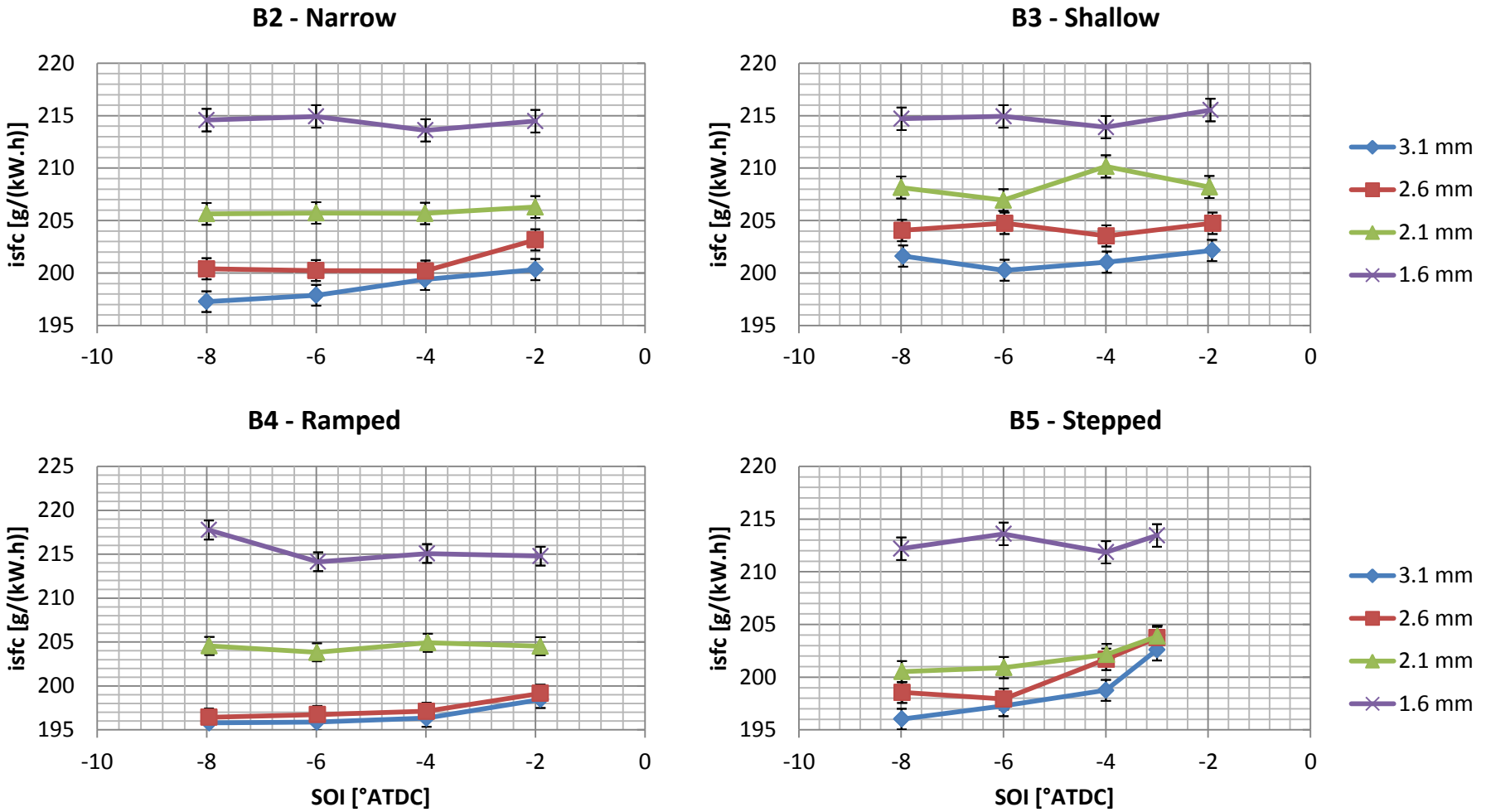

Figure 4.10 The effect of protrusion on fuel consumption at 2000FL. Top left bowl B2, top right B3, bottom left B4 and bottom right B5

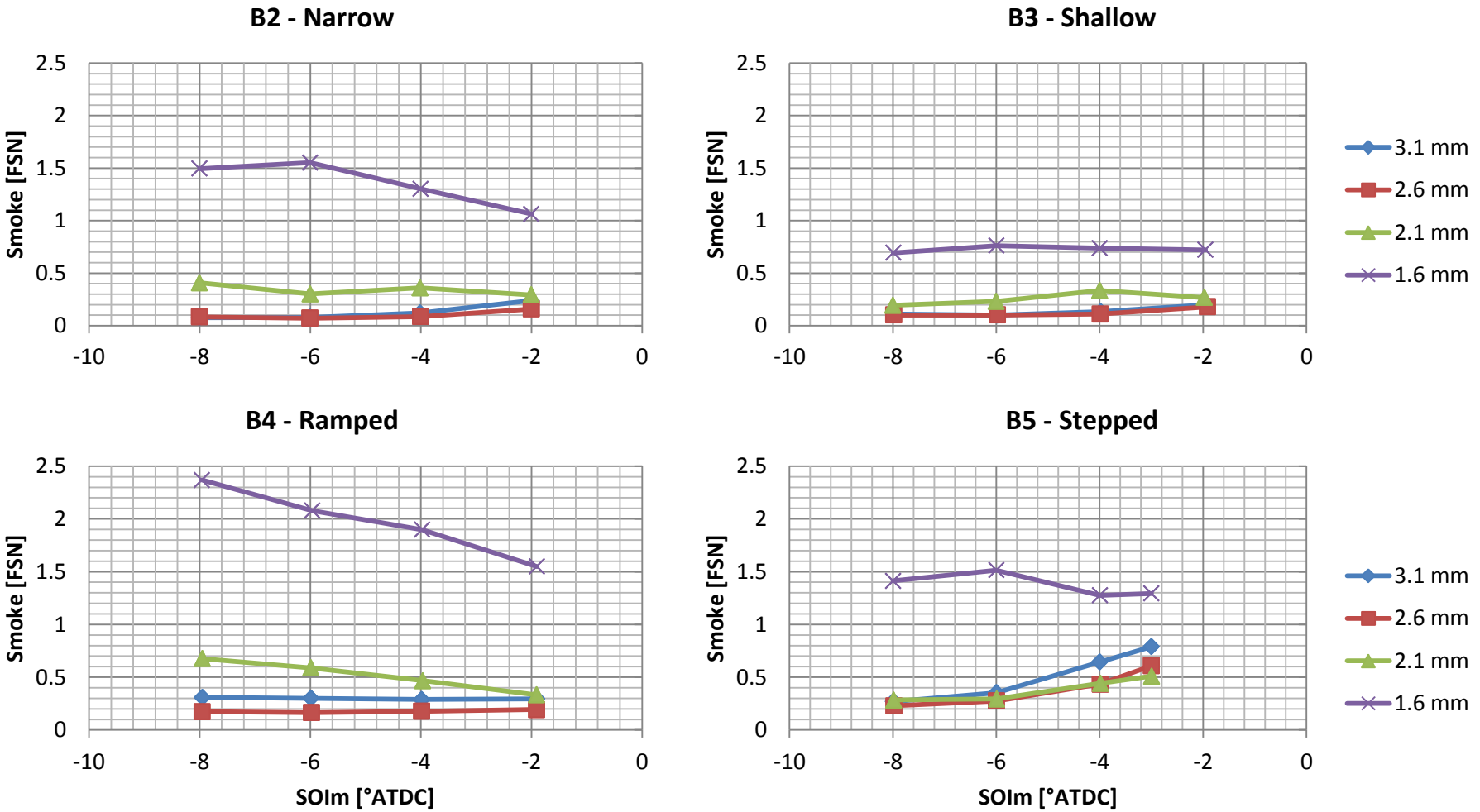

Figure 4.11 The effect of protrusion on smoke number at 2000FL. Top left bowl B2, top right B3, bottom left B4 and bottom right B5

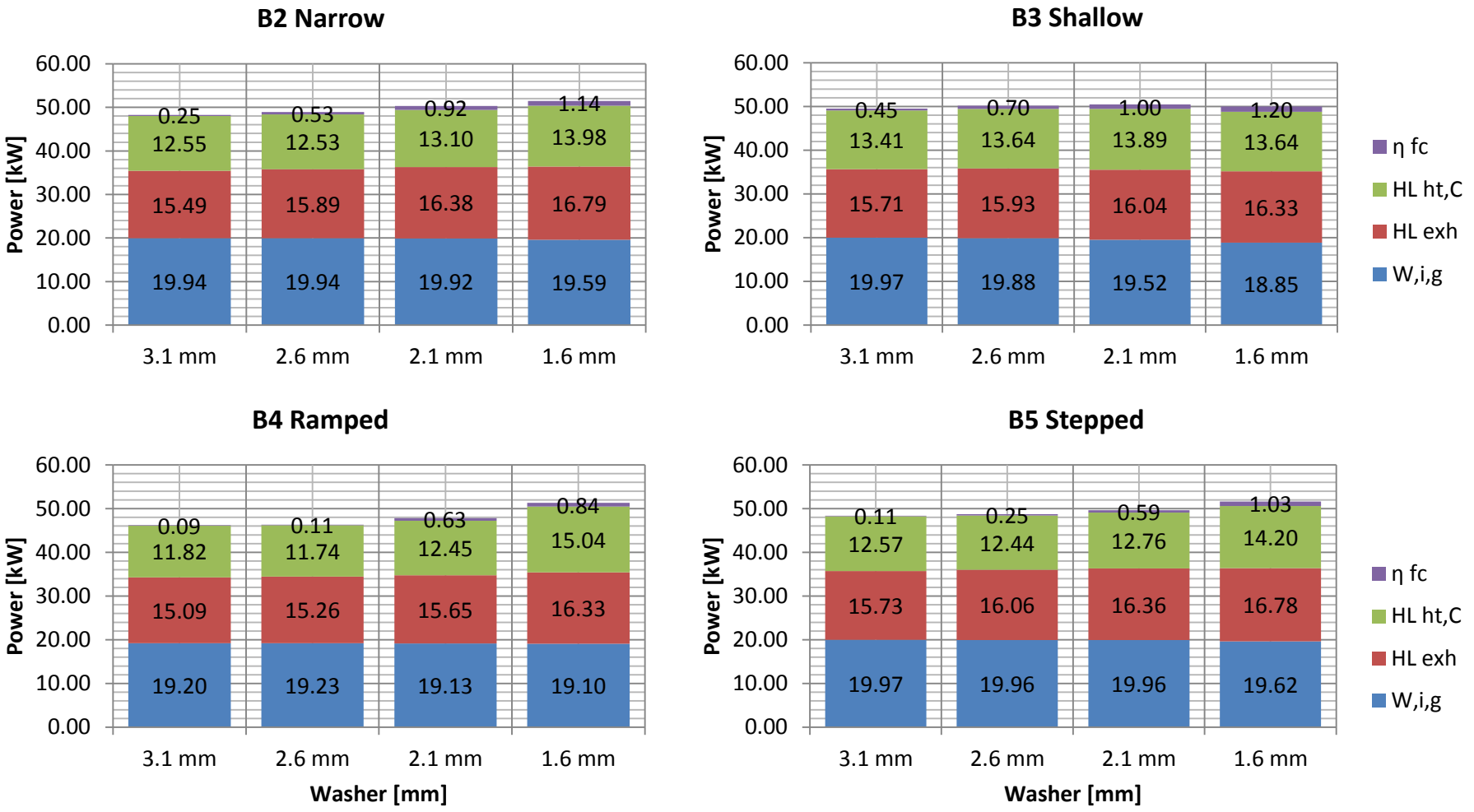

Figure 4.12 Energy balance protrusion 2000FL

4.2 Conclusions of Protrusion Optimisation

Based upon the above analysis and discussion a washer was selected for each combustion chamber. As demonstrated previously, there are trends and behaviours that occur with a change in protrusion that are consistent across all of the bowls and some that are unique to either the conventional or unconventional systems. A comparison of the sensitivity of each bowl to injector protrusion has identified trends and behaviours that explain the behaviour of each combustion system. The protrusion selections are summarised and presented in the following Table 4.5.

Bowl	Injector	Selected washer
B2 - Narrow	N1	3.1 mm
B3 - Shallow		3.1 mm
B4 - Ramped	N4	3.1 mm
B5 - Stepped		2.6 mm

Table 4.5 Selected washers for each combustion system based on the protrusion results

The majority of the combustion systems are optimised with the 3.1 mm washer. That includes conventional and unconventional combustion systems. The exception to this is bowl B5, which optimises with the 2.6 mm washer. Optimising with the 3.1 mm washer to benefit of Protrusion – 4000FL would have sacrificed a fuel consumption improvement of approximately 1.6 % at Protrusion – KP3.

Discriminating between the first two protrusions is straight forward for the conventional systems. The optimisation focuses on low isFC and smoke adding emphasis to the distribution of the fuel spray that reduces the locally rich concentration of air to fuel ratio. It appears that concentrating the fuel away from the piston bowl is beneficial for the combustion process for Bowl B2 and B3.

Discriminating between the first protrusion step is harder for the unconventional bowls. At protrusion – KP3 bowl B5 could optimise with the 2.1 mm washer with no discernible isFC penalty. This is a change from the characteristic behaviour of the conventional bowls. The response at Protrusion – 4000FL shows the isFC and smoke deteriorate with increasing protrusion. Even though this is not a regulated emissions point, combustion performance and engine integrity limits are a secondary requirement that have to be respected. The

selection of the 2.6 mm washer limited the range of SOIm timings that could be used before the engine integrity limits were met.

One response that is consistent across all combustion systems at Protrusion – KP3 and 2000FL is that the injector can be 'over protruded'; i.e. the thinnest washer performs the worst regardless of piston bowl, test point and SOIm timing. However a difference in behaviour between conventional and unconventional combustion systems can be seen at Protrusion – 4000FL; fuel consumption deteriorates with an increase in protrusion for both of the unconventional bowls whereas the relationship is more complicated for the conventional combustion systems, showing no real trend across the range of SOIm timings used. In general, when the spray targeting is at the lowest point of the interacting feature, (piston bowl lip for the conventional bowl and mid-ramp pip for the unconventional system) then the mixing process is sufficiently poor for this washer to be disregarded.

Spray targeting is essential for the ideal preparation of the air and fuel before the onset of combustion at 2000 RPM. All of the bowls 'guide' the fuel changing its distribution and air entrainment prior to the onset of combustion. This is to be expected from the literature however the effect on combustion could not have been predicted, particularly as there is no reference for the unconventional systems. Targeting the bowl lip and avoiding a downward flow of the fuel into the bowl region is vital for the conventional systems. The impact of fuel on the lip aids the fuel mixing process.

Spraying the fuel into the bowl region is also detrimental to the performance of the unconventional systems bowls; additionally with these unconventional bowls an upper limit can be observed. It is important to spray fuel onto the secondary pip in the right location. The turnover in the response observed with B5 could be due to the negative effect of spraying fuel into the squish regions, where temperatures and turbulence may be too low for production oxidation and rapid combustion.

There is an additional geometric limit to the nozzle extraction; the spray impingement onto the cylinder head for all bowls, which can lead to poor air entrainment. Cylinder head spray impingement limits oxidation of any the combustion products (Park and Reitz, 2009). Spray impingement with the cylinder head occurs as a result of the divergence of the fuel spray cone.

Finally, the unconventional systems achieve the performance requirements at the higher load conditions. As these combustion systems are experimental, there may have been a point where the mixture formation process could have been compromised by a lack of in-cylinder turbulence encouraged by the traditional re-entrant design suggested by Middlemiss (1978). This is not the case, and even though the mixture formation strategy is different between the conventional and unconventional systems, they both work successfully over the range of engine conditions tested in the protrusion experiments.

Protrusion – KP3 is a medium load point where combustion temperatures are high enough to enable the formation of particulate matter if the fuel and air are poorly mixed. Fuel needs to be well distributed to avoid rich air-to-fuel ratios and thus avoid forming particulates. The remaining points tested in the characterisation include two key points at lower load (reduced fuelling), which are leaner overall compared to protrusion – KP3. This may have a bearing on the protrusion optimisation. With increasing protrusion at protrusion - KP3 the mixture became overly rich as the fuel was concentrated in the piston bowl region. If the mixture were leaner (due to reduced fuelling), then it is possible that optimising the protrusion with a thinner washer (increased protrusion) is optimal. This would help to avoid poor combustion associated with overly lean combustion.

It is important to try and understand the impact of the protrusion optimisation at the remaining key points. The optimisation has been carried out to achieve the greatest fuel distribution at a medium load point. Selection of a relevant key point for protrusion optimisation requires careful thought as to the available strategies for emissions reduction in-cylinder (pilot injection, cooled EGR).

5 The Effect of Bowl Geometry on Combustion and Emissions

Once the protrusion testing was completed, the washer selection was fixed and the characterisation of each bowl commenced. The characterisation process was used to evaluate how the mixture formation demands were affected by bowl geometry at each test condition. This chapter demonstrates the effect of bowl geometry on engine performance. The comprehensive testing of each bowl in the characterisation consisted of carrying out combined EGR and SOIm swings at part load and SOIm swings at full load. This testing was carried out with standard flow (760 cm^3/min) and high flow (860 cm^3/min) injectors. Each injector required a combined 56 test points (three part load and two full load conditions) per bowl and each bowl was tested with 4 different injectors in order to comprehensively test the response of the hardware. The conventional bowls were tested with N1-N3 and N8 and the unconventional bowls were tested with N4-N6 and N10.

Nozzle	Description					
	Actuator	Post hone vol flow	Hole size	Holes	Cone angle	k-factor
ID	Type	(cm3/min)	mm	-	°	-
N0	Solenoid	770	0.131	7	155	2
N1	Piezo	760	0.131	7	155	2.5
N2			0.123	8		
N3			0.116	9		
N4			0.131	7	145	
N5			0.123	8		
N6			0.116	9		
N15		860	0.141	7	155	
N7			0.131	8		
N8			0.123	9		
N16			0.141	7	145	
N9			0.131	8		
N10			0.123	9		
N11		760	0.131	7	155	1.5
N12			0.123	8		
N13		760	0.131	7	145	
N14			0.123	8		

5.1 Experimental results

All of the following results were generated with the piezo injectors, for the conventional bowls the 7 holes nozzle N1, was used and for the unconventional bowls nozzle the 7 holes nozzle, N4 was used. The part load tests were EGR swings, with four EGR conditions, which started at zero and went to a lower limit of isNOx. At each EGR level a timing swing was tested as an additional measure of the engine response. Figure 5.1 illustrates the timing swing and EGR swing; the points show the timing swing, the furthest right being the most advanced SOIm. The different sets of points show the different EGR rates tested. The part load tests show the complete EGR swing with emphasis at the lower end of the isNOx emissions.

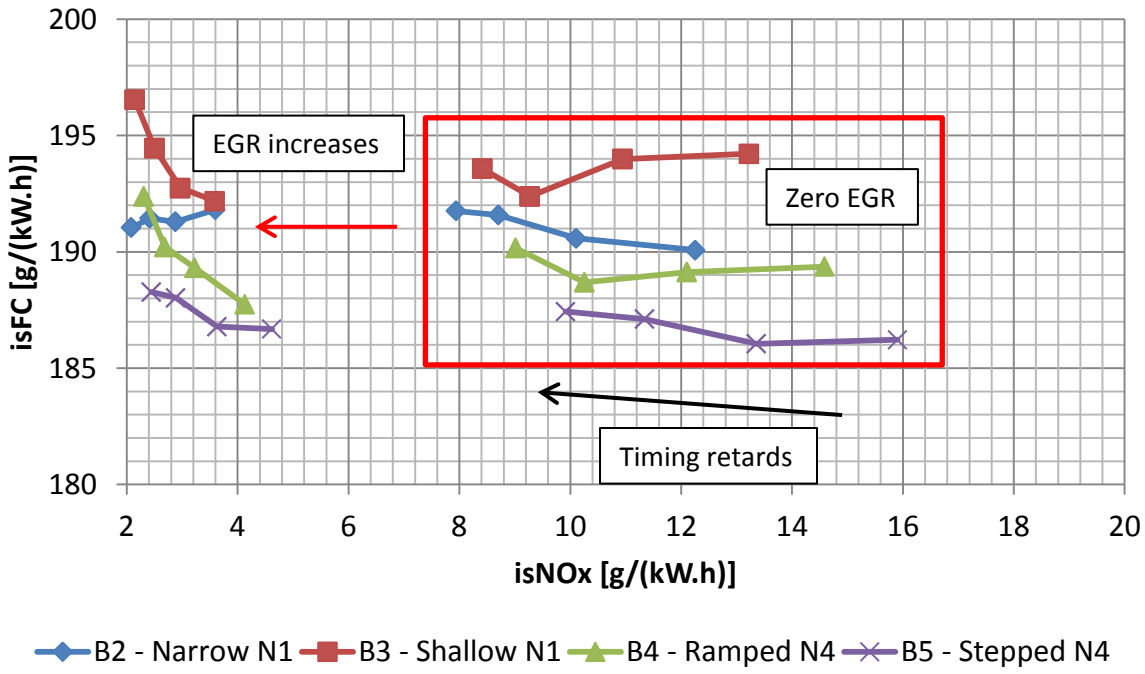

Figure 5.1 Illustration of the EGR and timing swings carried out at the part load keypoints. Illustration shows the first and second EGR conditions out of the four tested for illustration purposes

As a comparison, data from a Euro VI (Eu6) calibration of a vehicle using a 0.5 litre/cylinder (provided by Ricardo) is plotted on the zoomed in charts as a pale blue star (*). This is used to compare the performance of the unconventional systems to current production combustion system configurations.

Additionally this section includes a heat release calculation from the measured cylinder pressure data. The calculation itself was carried out as follows:

$$aHRR_{net} = \frac{1}{\gamma - 1}\left(\gamma P_i(V_{i+1} - V_{i-1}) + V_i(P_{i+1} - P_{i-1})\right)\frac{1}{(\theta_{i+1} - \theta_{i-1})}$$

Where γ is the ratio of specific heats at constant pressure and volume, P is the cylinder pressure, V is the cylinder volume and θ is the crank angle. The subscript i attached to each value is the value at the current crank angle. The value of used γ was 1.37 and the crank angle difference was 0.5 °.

5.1.1 KP3 Characterisation Test

Table 5.1 shows the test settings that were used for the KP3 test. Intake pressure, load (GIMEP), speed and fuel pressure were maintained at constant values in these tests in order to determine the performance of each bowl to EGR and SOIm. As the fuelling was adjusted to meet the load target the Air—to-Fuel Ratio (AFR) varied so nominal values are indicated in the table.

Test point	Speed	GIMEP	Intake pressure	EGR temp	Intake temp	Exhaust pressure	EGR %	AFR	Rail pressure	SOI_m
-	RPM	bar	barA	°C	°C	barA	%	-	bar	°ATDC
KP3 test	2000	9.00	1.47	31	33	2.57	0	28.8	1050	-9,-7,-5,-3
				63	37	2.15	18	23.4		
				70	42	1.92	26	20.0		
				72	44	1.85	30	18.8		

Table 5.1 KP3 test settings

Intake temperature varied due to the mixing of EGR with the air in the inlet. The Exhaust pressure dropped because the EGR back pressure valve was fixed for all tests whilst the EGR was regulated with a throttle located near the inlet plenum. AFR varied because EGR was effectively a thermal throttle that displaced air in the inlet when the manifold pressure remained constant.

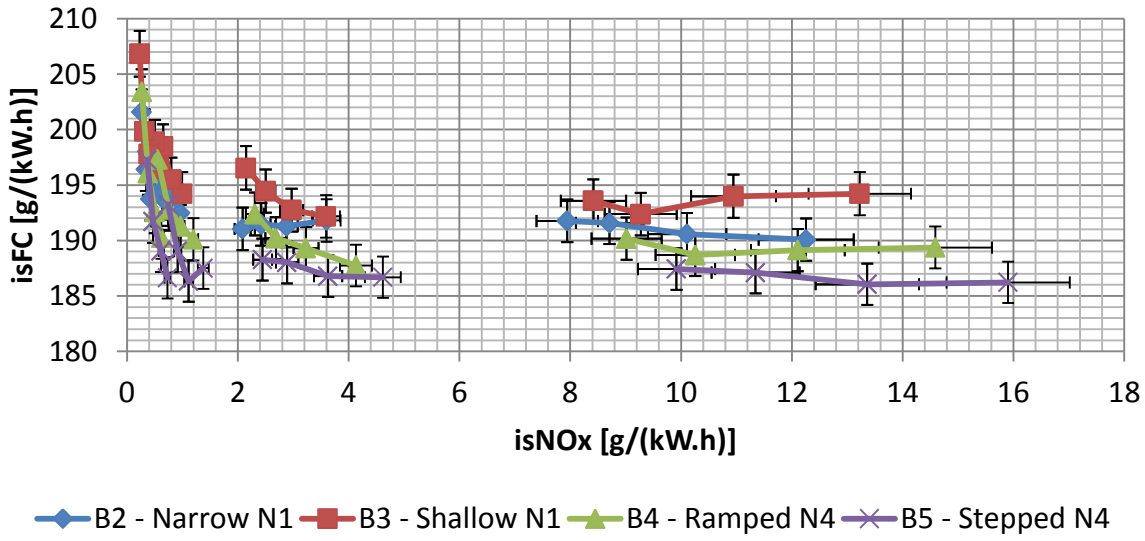

Figure 5.2 KP3 test EGR swing showing all 4 EGR conditions tested

Figure 5.2 shows that the unconventional bowls have lower isFC than the conventional bowls. B5 has the lowest overall isFC values for the EGR swing. At zero EGR (furthest right lines) and the most advanced SOIm timing (furthest right point), B5 is better than B2, B3 and B4 by 2.2 %, 4.3 % and 1.6 % respectively. At the same SOIm timing, isNOx levels are higher in general for the unconventional bowls.

This trend is the same at the higher levels of EGR as shown in Figure 5.3, although the isNOx emission is higher for the unconventional bowls. When retarding the combustion for the unconventional bowl to achieve equivalent isNOx (0.5 g/kWh), there is little difference between the fuel consumption values. B5 has the lowest value (192 g/kWh) and B2, B3 and B4 are 1.3 %, 2.5 % and 0.5 % higher. A retarded injection event results in lower efficiency, which reduces the fuel consumption benefit of the unconventional bowls. Alternative strategies would be required to reduce isNOx without penalising the fuel consumption. All bowls tested have better isFC than the Eu6 reference data (pale blue * on the graphs).

Bowl B5 has the best smoke performance. Even when the SOIm was retarded to the same leve of isNOx (0.5 g/kWh) the smoke number (0.54 FSN) is still better than all other bowls and the Eu6 comparison. Bowls B3 and B5 are comparable with a value of around 0.77 FSN, however bowl B4 deteriorates with a timing retard to 1.58 FSN at an isNOx value of 0.27 g/kWh. The smoke emission for bowl B2 is less sensitive to a timing retard, only increasing from 1.05 FSN to 1.22 FSN, however the initial smoke emission is higher.

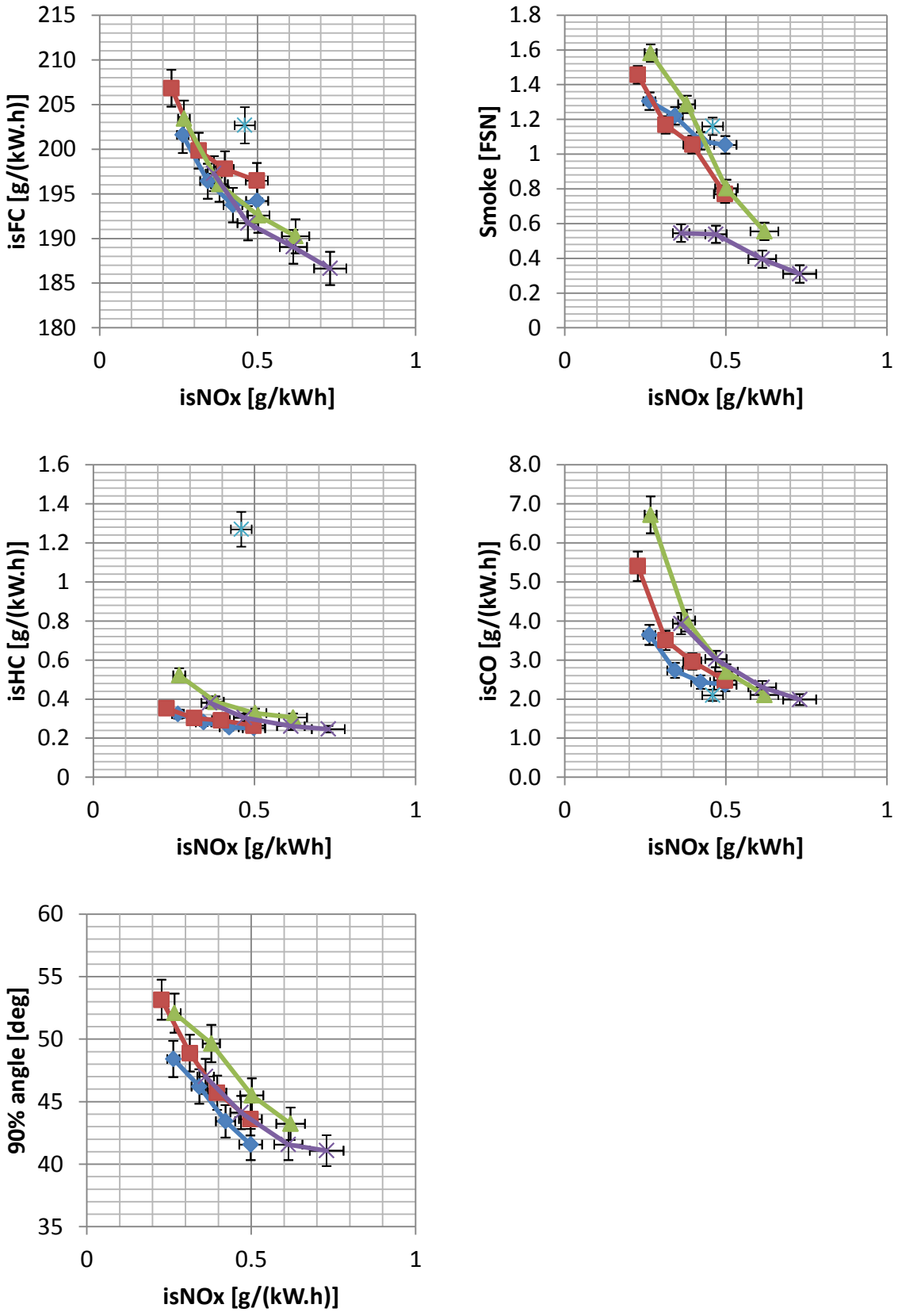

Figure 5.3 KP3 test data at 30 % EGR

isCO and isHC are generally comparable for all bowls however with the increase in isNOx emission associated with the unconventional bowls the emissions curves are better for the conventional designs. Comparing the bowls at the equivalent isNOx emission (0.5 g/kWh) bowl B2 has isHC emissions of 0.25 g/kWh and B3, B4 and B5 are 0.26 g/kWh, 0.33 g/kWh and 0.3 g/kWh respectively. In terms of isHC all bowls are better than the Eu6 reference.

The energy balance analysis helps to identify factors contributing to the bowl differences in performance. As Figure 5.4 shows, the indicated work is comparable for all bowls (7.48±0.06 kW and 9±0.05 bar GIMEP). Apart from B5 all of the exhaust heat rejection results are in the same range. This is due to the exhaust temperature being the lowest (434 °C) for bowl B5. The different heat rejection rates between the unconventional designs may be due to the differences in the in-cylinder flow regimes created due to the pip design and different toroidal radius.

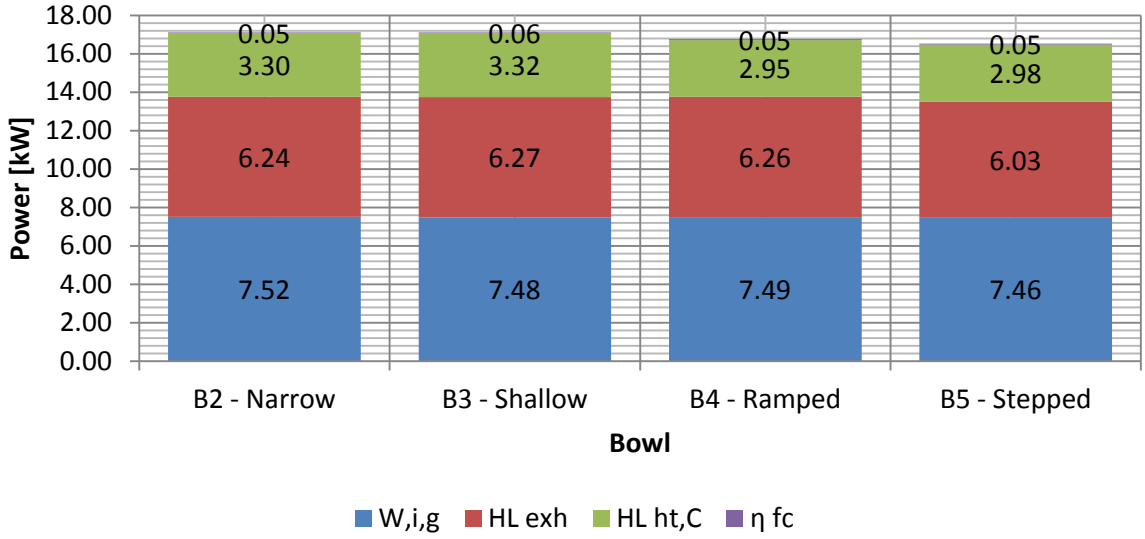

Figure 5.4 Fuel energy distribution identifying the areas affected by a change in bowl design. All bowls optimised washer, SOIm -9 °ATDC

The lower exhaust heat rejection shown in Figure 5.4 indicates a more rapid combustion process for B5. Looking at the apparent net heat release rate in Figure 5.5 shows that ignition for the unconventional bowls occurs sooner (0.8 °) after the end of the injection event than the conventional bowls. The highly premixed combustion has a long tail, which is similar for all bowls. The shorter ignition delay advances the combustion without making it more diffusive, which allows the combustion event to complete sooner.

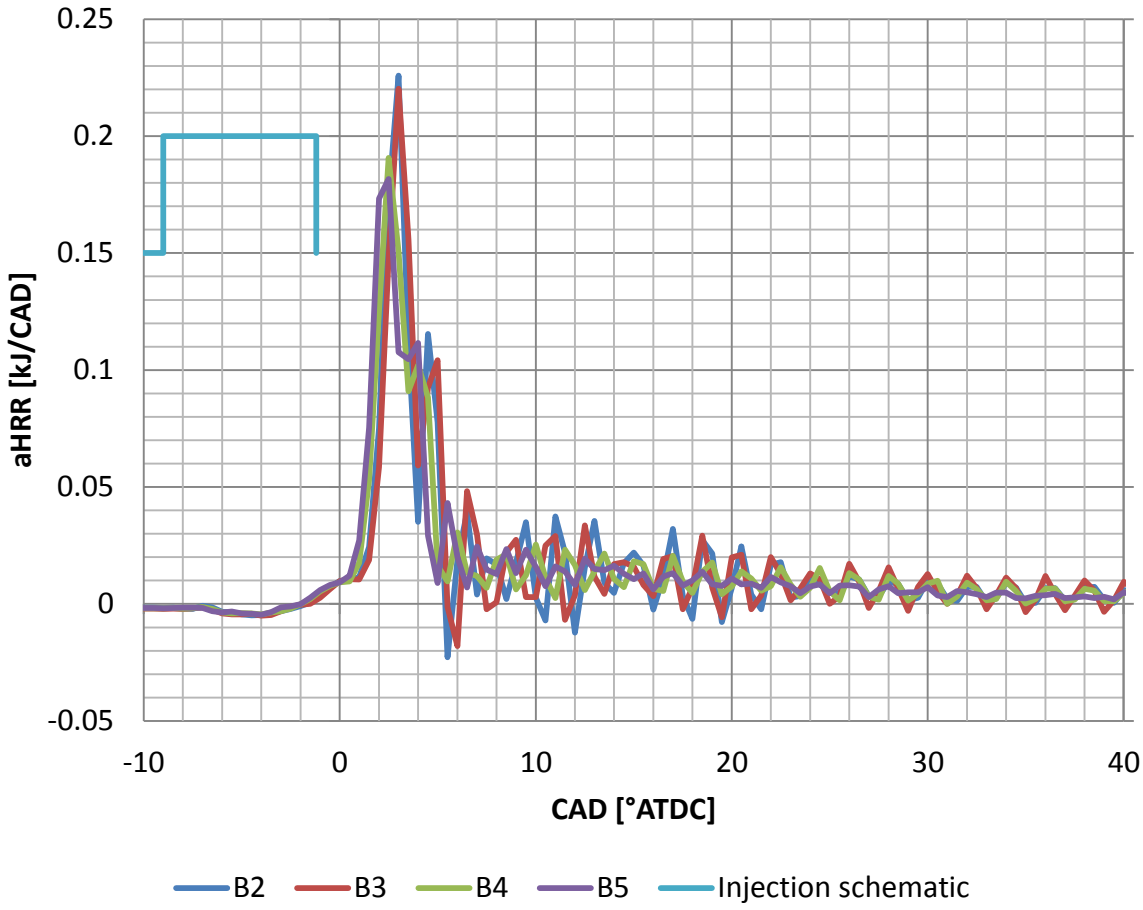

Figure 5.5 Apparent net heat release rate profiles for all of the bowls tested. KP3, 30 % EGR SOIm -9°ATDC

There is another difference between the conventional and the unconventional bowls at the most advanced SOIm timing. Looking again at Figure 5.4 the heat transfer and crevice losses are 10 % lower for the unconventional bowls. This is consistent with the behaviour observed in the protrusion experiments. This could be due to the lower surface area to volume ratio of the unconventional bowls as well as the differences in the in-cylinder turbulence, which both affect convective heat transfer losses.

Although the isNOx is higher for the unconventional bowls at this combustion phasing (-9°ATDC), as the EGR is increased the unconventional bowls achieve lower values of isFC, demonstrating an improved tolerance to EGR and indicating better pre-combustion mixing than the conventional bowls.

The difference in isNOx level indicates that the fuel air mixture is closer to a stoichiometric value in the unconventional designs before the onset of combustion. For the conventional toroidal designs the fuel is sprayed into the bowl and mixed to a rich equivalence ratio before combustion, resulting in less isNOx. Rich emissions formation is offset by oxidation due to the highly turbulent flow in the piston bowl. This approach relies on available oxygen concentration, temperature and turbulence for product oxidation. When increasing EGR to the levels required to meet proposed isNOx emissions standards, peak combustion temperature and oxygen concentration can be relatively low, which hinders the oxidation process.

The unconventional bowls are different because the turbulence created within the fuel spray interaction with the secondary pip entrains more air into the fuel spray. Even though there may be less turbulence induced in the bowl from squish flow, and toroidal supported swirl, it is not essential to achieve clean combustion because fewer products of incomplete combustion are formed. This is the strategy that the advanced combustion modes seemed to achieve; reducing particulates by balancing the trade-off between emissions formation and oxidation.

5.1.2 KP2 Characterisation Test

Table 5.2 shows the test settings used at KP2. Only the EGR rate and the SOIm were varied. Fuelling was adjusted to meet the load (GIMEP) target as the SOIm and EGR were varied. This key point differed from KP3 in both speed and load. The combustion phasing changed, requiring different SOIm to be used. The Rail pressure selected was lower than KP3 and this was chosen to be representative of current production engines operating at this key point.

Test point	Speed	GIMEP	Intake pressure	EGR temp	Intake temp	Exhaust pressure	EGR %	AFR	Rail pressure	SOI_m
	RPM	bar	barA	°C	°C	barA	%	-	bar	°ATDC
KP2 test	1500	6.00	1.16	30	32	1.55	0	30.3	800	-10,-8, -6,-4
				58	37	1.33	22	22.7		
				64	40	1.26	30	19.5		
				66	41	1.24	33	18.8		

Table 5.2 KP2 test settings used in the characterisation

Figure 5.6 shows the complete EGR swing for KP2. As with KP3, the unconventional bowls perform the best in terms of isFC. This trend diminishes as the EGR level increases for all bowls. Looking in more detail at isNOx<1.5 g/kWh in Figure 5.7 shows how all of the bowls compare against each other and the reference bowl at 33 % EGR.

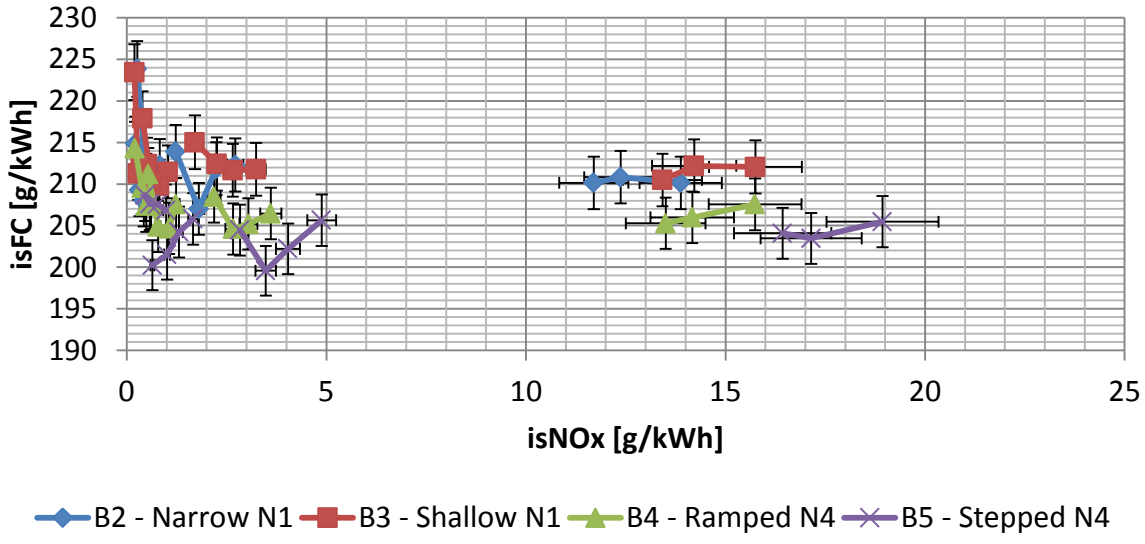

Figure 5.6 KP2 test EGR swing

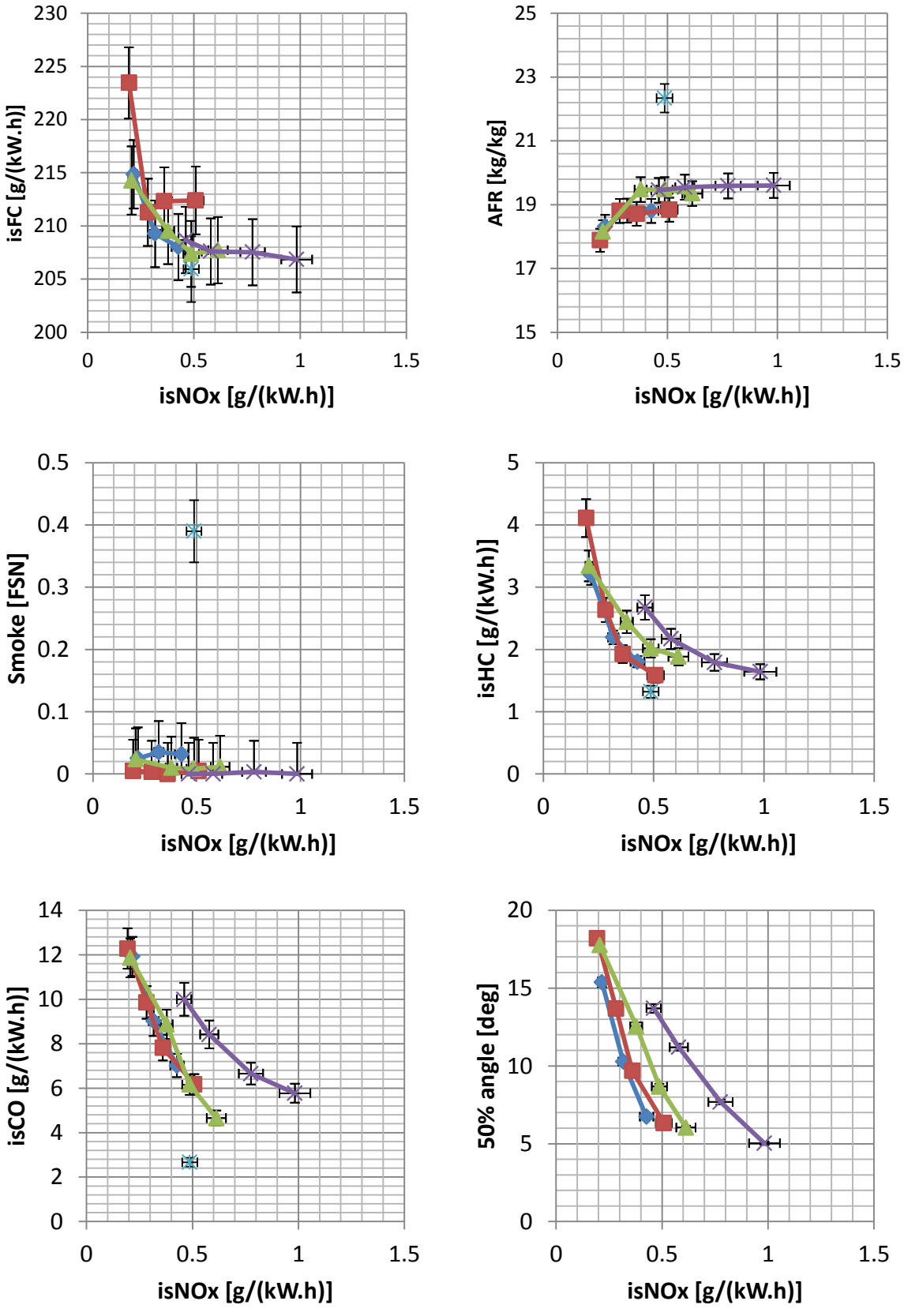

Figure 5.7 KP2 test 33 % EGR

Figure 5.7 shows the results of testing with the highest EGR rate (For all bowls: Average EGR=33 %, CoV on average EGR rate=0.6 %). There is little difference between bowls in terms of isFC. Bowl B3 has the highest initial isFC of 212 g/kWh at the most advanced timing. The response of B3 to a timing retard is relatively flat, varying less than 0.5 % up until the most retarded SOIm of -4°ATDC where isNOx is as low as 0.2 g/kWh and isFC increases by 5 % to 223 g/kWh. In comparison B5 is least sensitive to a retard in timing, only increasing by 2 g/kWh, which is around 1 % of the initial value. As with KP3, the isNOx is higher for the unconventional bowls. Bowl B5 has to be at the most retarded setting to achieve an isNOx of 0.46 g/kWh. Bowl B2 was not able to sustain combustion at the most retarded timing (-4°ATDC) hence only three points were logged. At this high EGR and low AFR condition bowl B2 is able to achieve the lowest isNOx level at the advanced SOIm of -10°ATDC.

At this condition few particulates are formed (the smoke number was below 0.05 FSN for all test points) and so only the isCO and isHC can be used as indicators of poor combustion. Even at an AFR of around 19; the highest particulate measured is 0.04 FSN for bowl B2 at isNOx 0.32 g/kWh. Smoke number improves for all bowls versus Eu6 data but there is a penalty on isCO, the Eu6 reference point having 2.67 g/kWh and the best performing bowls, B3 and B4, having around 6.2 g/kWh. Eu6 has higher AFR than all of the bowls tested, which would result in better fuel consumption and isCO. As a result of the higher AFR, a higher EGR rate (36 %) had to be used to achieve the same isNOx levels.

Due to the similarity in isFC at 33 % EGR, there is little difference in the energy distribution between conventional and unconventional systems. The energy balance in Figure 5.8 shows that there is no real trend for the behaviour between each piston bowl. The load target was met in each case and the best performing bowl in terms of heat rejection through the exhaust is bowl B5. The fuel conversion efficiency is comparable for all of the bowl designs (0.16 kW loss for B2 and 0.14 kW for B4/B5).

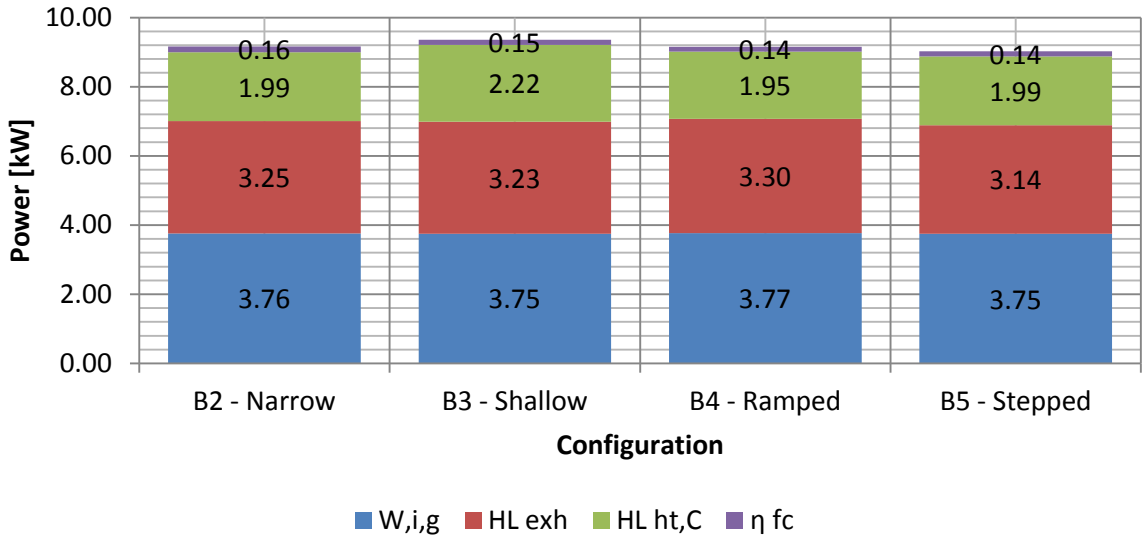

Figure 5.8 SOIm -10°ATDC, EGR 33 %

In order to understand why the smoke emission was so low at this key the combustion heat release rate for all bowls was examined. Figure 5.9 shows the $aHRR_{net}$ for all bowls at KP2. The injection schematic is based upon a typical injection duration (550-580 µs) required to meet the load condition in these tests.

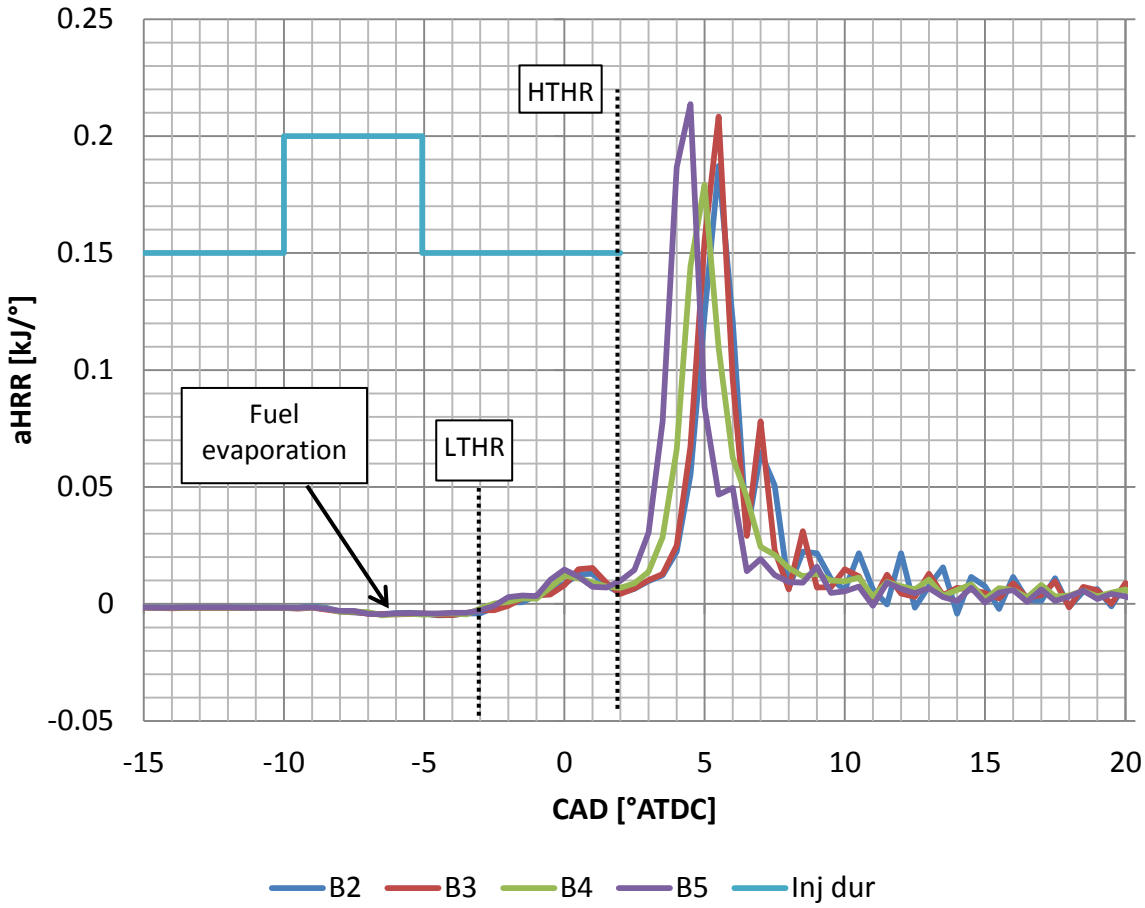

Figure 5.9 Apparent net heat release rate at KP2 30 % EGR, SOIm -10°ATDC.

Two lines are added to the figure to represent the approximate location of the low temperature heat release (LTHR) and high temperature heat release (HTHR). The LTHR is a small combustion rise prior to combustion of the majority of the fuel. The HTHR is the combustion of the remainder of the injected fuel. These regions are typical of premixed low temperature combustion (Dec, 2009), which can explain the low smoke output, even at this relatively high load of 6 bar GIMEP.

The ignition delay before the LTHR was approximately 4°, which at this speed represented approximately 444 µs. This is about 80 % of the injection duration, which is a significant period of time for the fuel spray to penetrate through the combustion chamber, evaporate and entrain air. A long period of time for the fuel and air to mix after the end of injection is beneficial to limiting the formation of particulates.

The unconventional bowls have a shorter ignition delay for the HTHR of around 8° (≈890 µs). B5 has the shortest delay between the end of injection and the peak of the heat release rate. The combustion of the conventional bowls is 1° more retarded than the unconventional bowls. A more retarded combustion event, due to the ignition delay, explains the differences between the isNOx levels seen in Figure 5.7. The ignition delay differences are greater than observed at KP3.

The protrusion optimisation demonstrated that fuel consumption and smoke improved by reducing the proportion of fuel entering the piston bowl at KP3. KP2 has benefitted from this optimisation because fuel rich regions that would have formed particulates have been avoided. The load is still high enough at this key point to avoid the fuel spray becoming too lean and producing high isCO and isHC emissions.

5.1.3 KP1 Characterisation Test

Table 5.3 shows the test conditions used at KP1. As with the previous test conditions the fuelling was adjusted to maintain the load target as the SOIm varied. All the other parameters were fixed for these tests and the AFR shown was the nominal value at each EGR level. This was the lowest load key point in the characterisation test programme. The rail pressure used was lower than the previous tests and was based upon representative pressures used in current production engines.

Test point	Speed	GIMEP	Intake pressure	Intake temp	Exhaust pressure	EGR %	AFR	Rail pressure	SOI_m
	RPM	bar	barA	°C	barA	%	-	bar	°ATDC
KP1 test	1500	3.00	1.03	32	1.41	0	50.1	600	-10,-9, -8,-7
				50	1.22	22	34.6		
				63	1.19	28	30.8		
				70	1.14	39	24.5		

Table 5.3 KP1 test settings used in the characterisation

Figure 5.10 shows the complete EGR swing from the testing at KP1. This is where the largest differences are seen between the conventional and unconventional combustion systems.

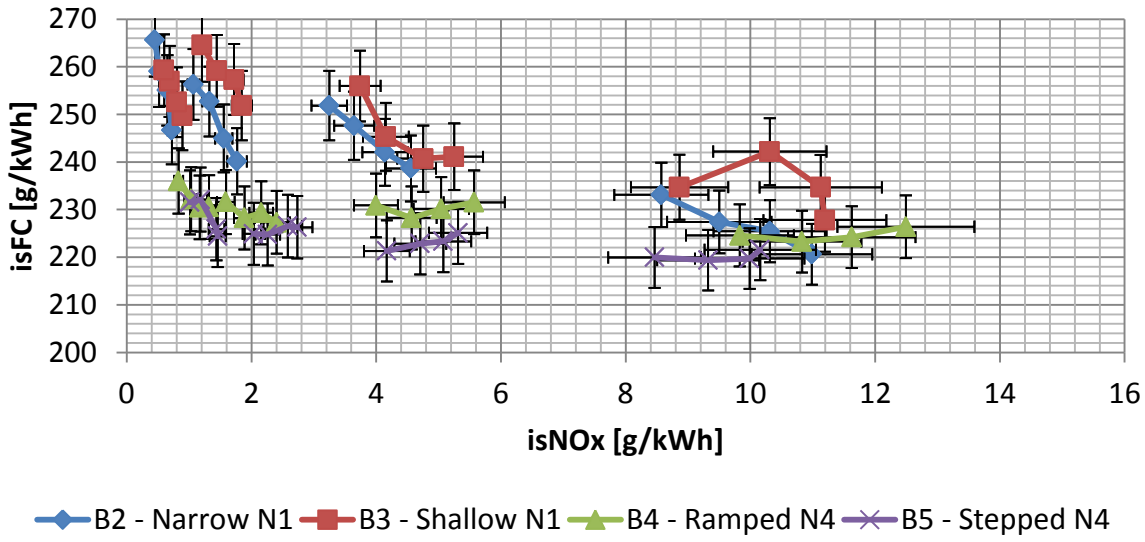

Figure 5.10 KP1 EGR swing

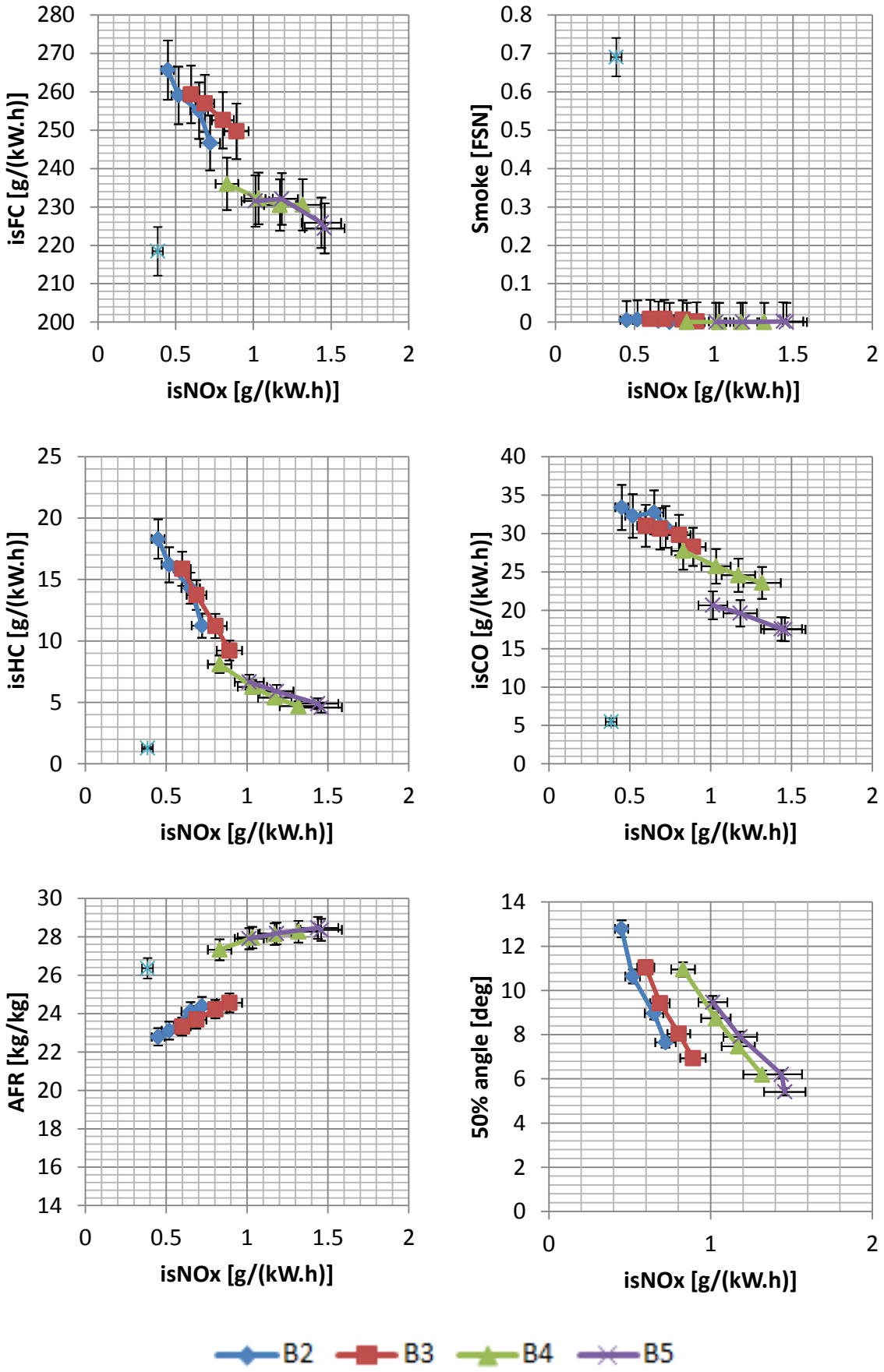

Figure 5.11 KP1 test results at 40 % EGR

Figure 5.11 shows the test results for this key point. The isNOx level is higher for the unconventional designs compared to the conventional designs for the same SOIm. When the same SOIm is used (-10°ATDC) the isFC for the unconventional bowls is approximately 10 % better than the conventional designs. With the same manifold conditions (hence similar air mass flow rates into the engine), less fuel is required to meet the load target thus the AFR is higher for the unconventional designs (27-28 AFR compared to 22-24 AFR). The Eu6 reference data has a higher AFR than the conventional designs but still achieves lower isNOx (0.38 g/kWh) than that measured by any bowl. The Eu6 data uses different test settings; importantly it uses a higher manifold pressure, which allows more charge flow (air+EGR) through the engine. The airflow is higher to maintain the AFR (26 AFR) and the EGR rate is higher (45 %) to reduce the isNOx. Overall the charge mass flow (air flow plus EGR flow) is higher for the Eu6 data (25.17 kg/h) compared to the test settings used in the characterisation (average flow 19.48 kg/h ±0.36 kg/h). Maintaining the AFR is key to good isFC, but detrimental to the isNOx output. The EU6 data suggests that an alternative inlet manifold condition could enable a simultaneous reduction in isNOx and isFC.

The emissions output for all of the bowls tested show similar tendencies to those observed at KP2. It is not possible to detect any smoke for either of the conventional or unconventional designs. From observation of the exhaust flow out of the exhaust pipe, the exhaust gas appearance was white, indicating moisture content and unburned fuel constituents. The Eu6 reference data has a smoke number of 0.7 FSN, showing a significant difference in the combustion behaviour from the bowls tested. This different combustion behaviour is reflected in the emission of isHC and isCO, which are significantly higher than the reference data. At the most advanced SOIm of -10°ATDC the unconventional bowls have the best isHC output of all bowls, of around 4.7 g/kWh, which deteriorates as the SOIm is retarded. This is 73 % higher than the reference data which has an isHC output of 1.27 g/kWh. Additionally, the isCO emissions are higher than the reference data for all bowls. Bowl B5 has the best output of 17.5 g/kWh which is 68 % higher than the reference data (5.48 g/kWh).

When the emissions of isCO and isHC are high relative to the smoke output at part load conditions, an assumption can be made that the fuel spray has typically become lean before combustion initiates (Ochoterena and Andersson, 2008). The load target in this test

condition is the lowest of the three part load conditions tested. The cylinder gas density is also low as a result of the low intake manifold pressure (1.03 barA). Cylinder gas density affects fuel spray penetration, the lower the cylinder gas density, the greater the fuel penetration (Karimi, 2007). The protrusion optimisation helps with fuel distribution at the key points when the load is high. However, when the load reduces this is detrimental to the combustion performance as can be seen in the energy balance in Figure 5.12.

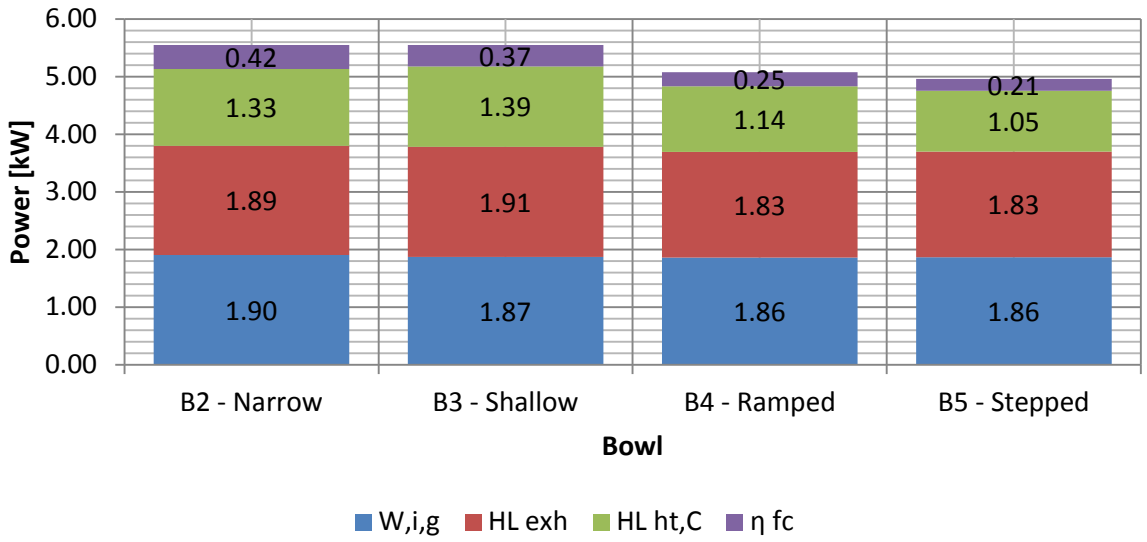

Figure 5.12 Fuel energy distribution identifying the areas affected by a change in bowl design. All bowls optimised washer, SOIm -10°ATDC

The differences between the conventional and unconventional bowls are significant at this test point. The biggest difference is with the heat transfer and crevice losses and the combustion loss. The combined loss of these two areas is highest for bowl B3 (1.76 kW), which is only just higher than bowl B2 by 0.1 kW. Bowl B5 is the best performing bowl with the lowest loss of 1.26 kW. This shows that the unconventional bowls are able to convert the fuel into heat more efficiently than the conventional bowls and lose less energy through heat transfer and crevice losses.

The maximum EGR used was highest at KP1, compared to the other test points. As a result ignition delay was the longest. The gas temperature calculated at TDC is within the same range as observed at KP2 (920-970 °K), although lower than that observed at KP3 (1000 °K).

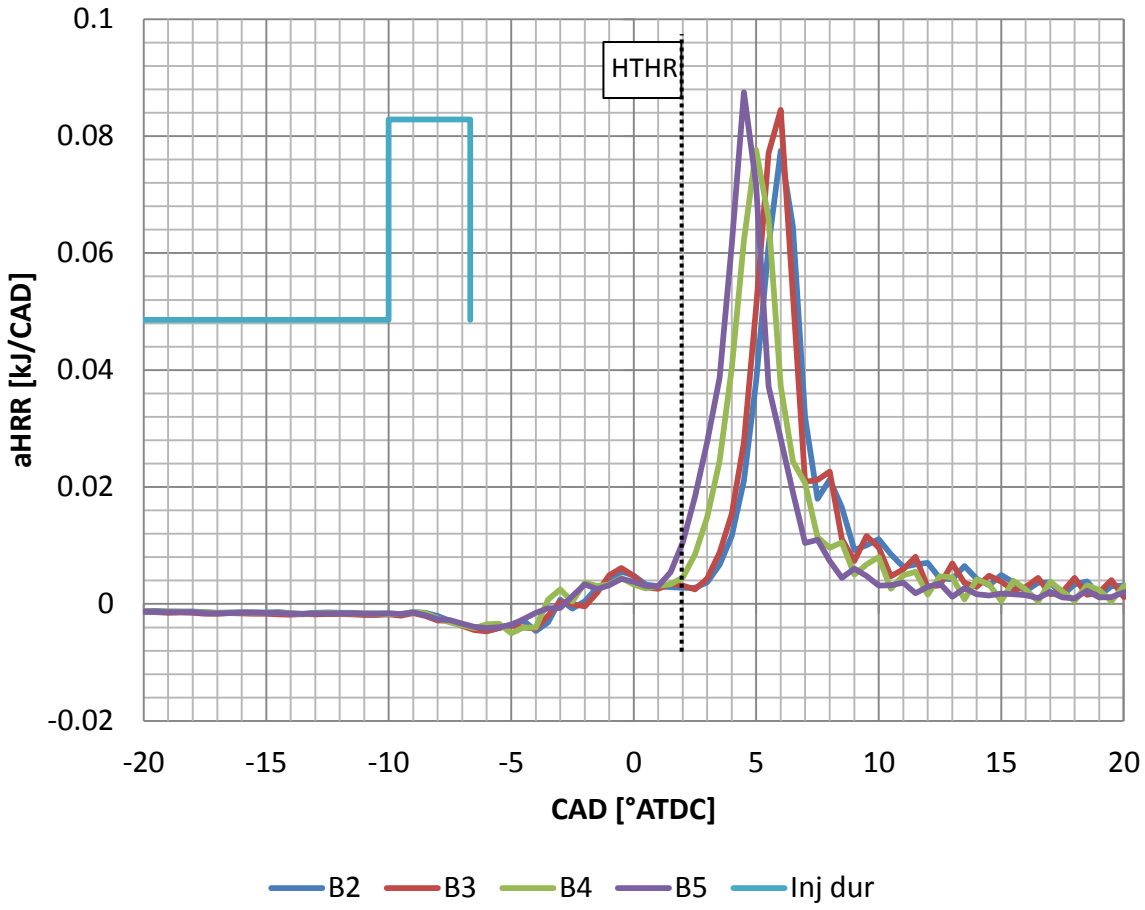

Figure 5.13 Apparent net heat release rate for all bowls at KP1. SOIm -10°ATDC

As observed at KP2, the unconventional bowls have the shortest ignition delay for the HTHR as shown in Figure 5.13. Bowl B5 has an ignition delay of 7.8° compared to bowl B2 and B3 of 9.8°. This 2° difference at the same SOIm helps to explain why the isNOx is higher for the unconventional designs. The long ignition delay also allows more time for fuel and air mixing before combustion begins. As a result the formation of particulates may be negated, by reducing the rich regions of fuel and air. Additionally, the lower load results in lower peak temperatures, which also helps to avoid the formation of particulates. The downside to this is that the products of lean and low temperature combustion, isCO and isHC, increase.

The difference in the conventional and unconventional bowls could be due to the fact that the wider unconventional bowls contains more of the fuel and air mixture than the conventional bowls. The presence of more rich regions in the unconventional bowl is beneficial for combustion by ensuring the mixture is not too lean, when the overall AFR is high at low load. If the protrusion washer increased the protrusion (say with a 2.1mm

washer) for the conventional bowls, thus focussing fuel spray into the bowl, this may have improved the combustion speed (reduced ignition delay) by concentrating an ignitable mixture in the bowl region.

5.1.4 Full Load Operation

An important aspect in the development of unconventional combustion systems is their potential to operate at a specific power output with an equivalent or better fuel efficiency than existing conventional designs. Currently, the development in automotive engine applications is towards high specific power outputs in terms of kW/litre as well as high specific torque for improved responsiveness and drivability (Thirouard et al., 2009). In general this is achieved with advanced boosting systems using compounded turbo charging systems or superchargers as well as injection systems that can deliver fuel at a higher rate and cylinders capable of higher maximum pressures. This enables downsizing of the engine whilst achieving the same power output, which has a number of benefits; improved part load fuel consumption, reduced engine weight and reduced engine friction.

5.1.4.1 4000FL Characterisation Test

Test Settings									
Test name	Speed	Load	Intake temp	Intake pressure	EGR rate	EGR temp	Pilot SOIm	Rail pressure	SOI range
	RPM	GIMEP	°C	barA	%	°C	-	bar	°ATDC
Protrusion – 4000FL	4000	21.4 (approx 35 kW)	45	2.4	NA	NA	NA	2000	-19, -7, -15, -3

Table 5.4 4000FL test settings used in the characterisation

At the full load test conditions the fuel rail pressure was increased to the maximum available for the fuel injection system. This was 2000 bar as indicated in the above Table 5.4. The test was carried out in a different way to the part load tests with only the SOIm changed. The fuelling was adjusted to meet the load target. The SOIm was set at the most advanced condition, which was dictated by the maximum cylinder pressure limit (P_{max}=200 bar) and retarded to either an exhaust temperature limit (750°C) or a smoke limit (4 FSN). The target manifold conditions were fixed and so dictated the air flow to the engine. Back pressure was set by installing a suitably sized restrictor in the exhaust pipe. The engine output and emissions were therefore dictated by the combustion duration. If the load target could not be met then the maximum load achieved was logged.

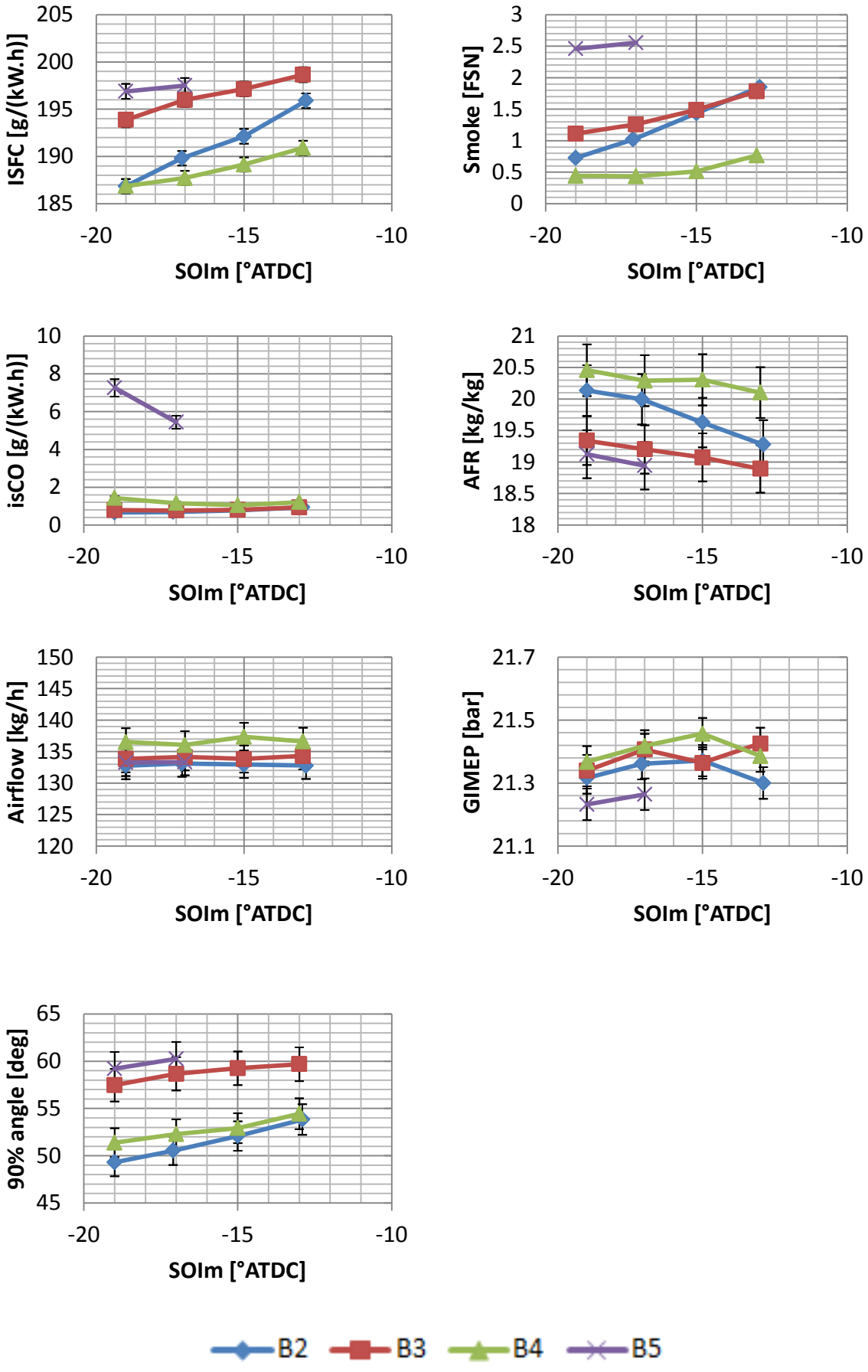

Figure 5.14 Full load test results at 4000FL

Figure 5.14 shows bowl B5 performed poorly at this condition and as a result the target load could only be achieved at 2 SOIm points. It was only possible to achieve an average load of 21.25 bar for the two points logged. The AFR differences observed between the bowls are a result of the different fuelling required to meet the load target for all but bowl B4. Airflow for bowl B4 (136.6 kg/h) is marginally higher than the other bowls tested (all bowls average 134.22 kg/h). The difference in air flow means that for the same fuel flow at the most advanced SOIm for B4 (6.67 kg/h) the AFR differs by 0.36 (AFR 20.5 with 136.6 kg/h, AFR 20.14 with 134.2 kg/h). This moderate difference may have an influence on the combustion behaviour of the bowl. The higher airflow may affect the isFC, smoke and isCO, bringing bowl B4 closer to the conventional bowls.

Smoke and isCO indicate that bowl B5 is the worst in terms of mixing the air and fuel prior to and during combustion. At the most advanced SOIm bowl B5 has the highest smoke output (2.46 FSN) and bowl B4 the lowest (0.44 FSN) which represents a significant difference in combustion behaviour. The combustion behaviour can be characterised by the plot of 90 % burn angle which shows that for both B2 and B4 combustion terminates sooner than bowl B3 and B5. This also explains the differences observed in isFC between both sets of bowls because combustion occurs more rapidly for bowls B2 and B4.

At this full load key point the unconventional bowl B4 performs well in terms of achieving the load target with a low isFC and low smoke and number. It performs as well as conventional bowl B2 and outperforms bowl B5 making it the best performing bowl at this condition.

5.1.4.2 2000FL Characterisation Test

Test Settings									
Test name	Speed	Load	Intake temp	Intake pressure	EGR rate	EGR temp	Pilot SOIm	Rail pressure	SOI range
	RPM	GIMEP	°C	barA	%	°C	-	bar	°ATDC
Protrusion – 2000FL	2000	24	50	2.4	NA	NA	NA	2000	-8, -6, -4, -2

Table 5.5 2000FL test settings used in the characterisation

As with 4000FL, the fuel rail pressure was increased to the maximum available for the fuel injection system. This was 2000 bar as indicated in the above Table 5.5. The SOIm was set at the most advanced condition, which was dictated by the maximum cylinder pressure limit (P_{max}=200 bar) and retarded to either an exhaust temperature limit (750 °C) or a smoke limit (4 FSN). If the load target could not be met then the maximum load achieved was logged.

The load target was met for all bowls as indicated in Figure 5.15. The resulting isFC shows that all bowls performed in a similar manner. Bowl B5 achieves the lowest isFC at a SOIm of -6°ATDC of 197.9 g/kWh, B4 is 197.7 g/kWh. At the same SOIm the isFC for bowl B3 is 1.2 % worse. With the most retarded SOIm the isFC for all bowls deteriorates, with bowl B5 having the worst isFC (203.8 g/kWh). The smoke emission follows this behaviour when the SOIm is retarded for all bowls but B4, which improves from 0.53 FSN at the most advanced timing to 0.4 FSN at the most retarded timing. Both of the conventional bowls have lower smoke emission than the unconventional bowls for all SOIm timings used.

Bowl B4 at this test condition has the lowest isFC across the range of SOIm timings used, lower than both conventional designs. The smoke number is highest at all but the most retarded timings, where the conventional bowls outperform the unconventional bowls.

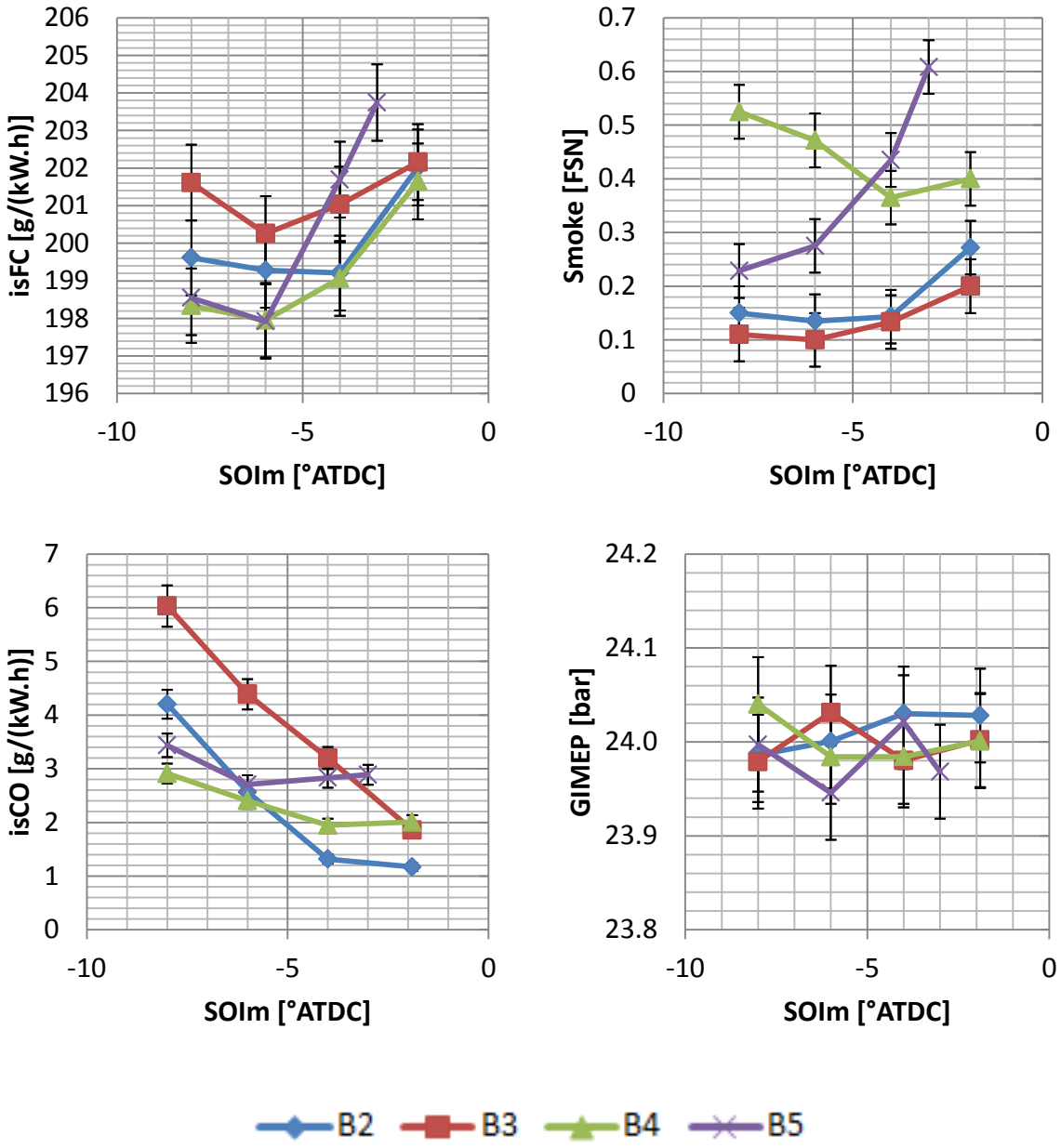

Figure 5.15 Full load test results at 2000FL

5.2 Optimised Bowl Selection

Based upon the characterisation of all bowls at the part load and full load conditions the best bowl was selected for further testing. The objective of this further testing was to investigate the response of the selected bowl to multiple injections. In addition it was hoped that an improved understanding of the fundamental factors affecting the combustion process in this system would assist in the development of strategies to simultaneously reduce fuel consumption and emissions.

Each bowl was scored for suitability from 1 to 4 at each one of the key points and a decision matrix was formed for the selection. The highest scoring bowl was selected. At the part load condition the criteria for the selection of the best bowl was based on of fuel consumption and regulated emissions. At the full load condition it was based upon whether the load target was achieved and the absolute value of fuel consumption.

Scoring each bowl for each parameter at each test point proved a challenge. Due to the complex nature of the response to a change of injection timing each parameter had to be judged by more than one consideration. When examining the response of each bowl for each of the regulated emissions the order of consideration used was first by the lowest absolute value and then the response to the change in SOIm of each bowl.

The following schematics in Figure 5.16 represent two examples of different responses that occurred and had to be judged in the bowl selection process. The y axis is the parameter being assessed.

Example (a) shows that the triangle series has the lowest absolute value and that the trend is for the value to increase with a retard in SOIm. The circle series improves its absolute value with a retard in SOIm however the overall result is that the triangle series is lower at all conditions. Therefore the triangle scores the highest.

Example (b) shows the circle series has the lowest absolute value. This is marginally lower than the triangle series, but none the less lower. The response to a retard in SOIm is a rapid increase of the parameter, beyond that of the triangle series. The triangle series is less sensitive to a retard in SOIm and is the same or lower than the second circle point for all

timings. In this case the triangle series would score the highest due to the lower sensitivity of the bowl to a variation in SOIm.

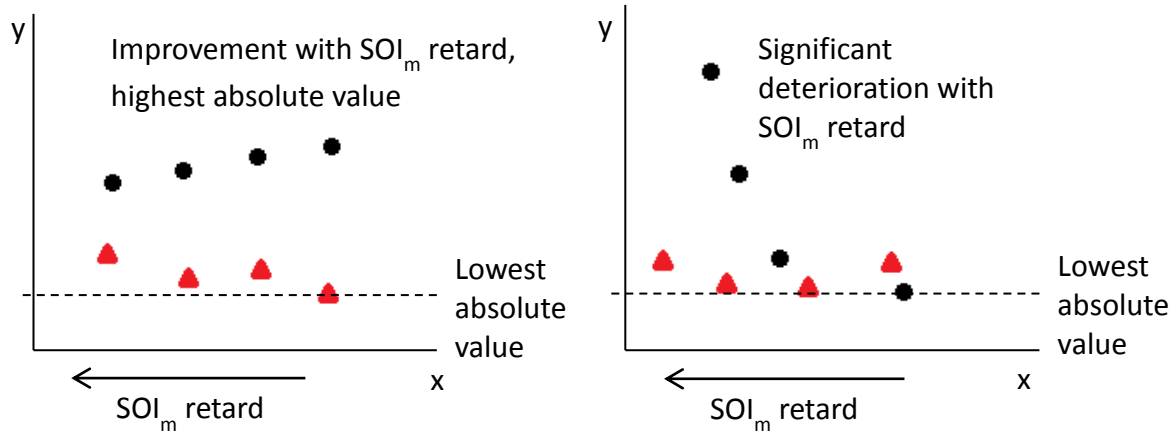

Figure 5.16 Schematics representing the variation in response of two different bowls. (a) is on the left, (b) is on the right.

Additionally, in cases where all of the bowls performed similarly or the difference was close to the uncertainty of the parameter (achieving the load target at the full load condition for example), all bowls were scored the same. When no smoke was detected at KP1 and KP2 all bowls were scored 4. The part load conditions were weighted in terms of importance by doubling the score. A 2 times factor was selected because it adequately represented the importance (in terms of normal vehicle use) of the regulated emissions without overemphasising them. The results can be seen in Table 5.6.

The first thing to note is that bowl B5 has the best performance at part load scoring 92 out of a possible 120 points. B4 is second with 84 and then the conventional bowl B2 with 76 and B3 last with 72. Bowl B5's strength is the fuel consumption performance; however this is achieved with consistently the highest isNOx output at all test points. The trend for the conventional bowls is that although the fuel consumption was consistently the worst across all bowls, the isNOx level measured was lower than the unconventional bowls. At KP1 and KP2 the conventional bowls are consistently the worst with CO and THC, which offsets the performance of the low isNOx output.

	KP1					KP2					KP3					2000FL				4000FL				Results		
Bowl	NOx	isFC	CO	THC	Smoke	NOx	isFC	CO	THC	Smoke	NOx	isFC	CO	THC	Smoke	GIMEP	isFC	Smoke	CO	GIMEP	isFC	Smoke	CO	PL weighted x2	FL weighted x1	Weighted total
B2	4	1	1	1	4	4	2	1	2	4	3	2	4	4	1	4	2	3	3	2	3	3	4	76	24	100
B3	3	2	2	2	4	3	1	2	1	4	4	1	2	3	2	4	1	4	2	3	2	2	3	72	21	93
B4	2	3	3	4	4	2	3	4	3	4	2	3	1	1	3	4	4	1	4	4	4	4	2	84	27	111
B5	1	4	4	3	4	1	4	3	4	4	1	4	3	2	4	4	3	2	1	1	1	1	1	92	14	106

Table 5.6 Selection matrix for the best performing bowl across all conditions tested in the characterisation.

The full load testing is where B5 struggles for performance scoring 14 out of 32. 4000FL is particularly bad as B5 struggles to meet the load target and performs the worst with the indicators of poor combustion (smoke and CO). B4 on the other hand scores the highest for the full load operation with 27 out of 32. The two conventional bowls perform well, which is to be expected with proven designs.

Overall, bowl B4 performs the best scoring 111 out of a possible 152. Bowls B5 is second, B2 third and bowl B3 is the worst bowl overall. If bowl B5 were to be optimised with the 3.1 mm washer to improve performance at the full load conditions (performance at full load improved with the 3.1 mm washer), the part load fuel consumption benefit would be lost and the isNOx emission would increase (refer to the protrusion test response in Chapter 3.7). Since KP1 and KP2 were not part of the protrusion evaluation tests, it is not possible to state whether the behaviour at KP3 would extend to these conditions. The bowl's performance may deteriorate at KP1 to a similar level as the conventional bowls, which when optimised with the 3.1 mm washer for low smoke and fuel consumption at KP3, suffer with excessive CO and HC and high fuel consumption at KP1. The only certainty is that making a change to the 3.1 mm washer would improve the performance at full load.

Judging the piston bowls solely on the part load response would have resulted in the selection of B5. This however would have compromised the operation at full load, which although unregulated nevertheless is still important. Further development of the design concept for bowl B5 would need to investigate how injector protrusion could be optimised so that the part load performance could be maintained whilst improving that at full load.

The unconventional design B4 worked well in the light duty Diesel engine, performing as well as and better than conventional designs. With the use of common rail fuel injection technology this bowl is able to operate at ever reducing isNOx emissions whilst maintaining good fuel economy. The next step to prove this design would be to evaluate its response to multiple injection strategies.

6 The Effect of Injector Design on Combustion and Emissions

The fuel injection equipment (FIE) available for the project allowed a comparison to be made between the design and operation of a conventional solenoid injector and a prototype, unconventional, direct acting injector. The comparison was made between the conventional injector N0 and prototype injector N1. These were closely matched in terms of nozzle characteristics having the same number and size of holes and a similar cone angle. The comparison between the operation of the conventional and the prototype injection system was only made with the conventional piston bowls because the spray angle of the conventional injector's nozzle (154°included angle) was matched to that design.

Due to the availability of hardware, the spray angle of the prototype design (155° included angle) differs from the conventional design by 1°. The k-factor of the prototype injector (k=2.5) was also different to the conventional design (k=2). This means that a direct comparison of the behaviour of the injector type cannot be made without taking into account the influence of these parameters.

6.1 Injector Characteristic

The operation of the prototype injector was fundamentally different to the operation of the conventional injector. As a result, being able to compare the operation of each injector required an understanding of the response of the injector to the injector demand signal. The prototype injector lifts the needle directly by a mechanical link to the piezo stack, whereas the conventional injector electronics lifts the needle by spilling fuel through a path in the injector. As a result, there is a difference in the delivery rate so the electrical demand for start of injection is different between each system.

Figure 6.1 shows the voltage and current traces measured for the prototype injection system during an injection event. The data shown in the trace was recorded at 0.1° resolution, using a combination of a current and voltage clamp. The numbers represent the 3 distinct phases of the injection event; 1) needle lift, 2) hold and 3) closing. The voltage relates to the voltage of the piezo stack with the trace being proportional to the needle lift. The current trace differs during the 3 phases; as the needle lifts the current becomes negative. As the needle approaches the maximum opening the current reduces to slow the rate of rise of the needle. Phase 2 is then reached where the current is zero. As the demand

to end the injection is sent in phase three, the current increases to a positive value to drive the needle closed, settling to zero again as the needle closes.

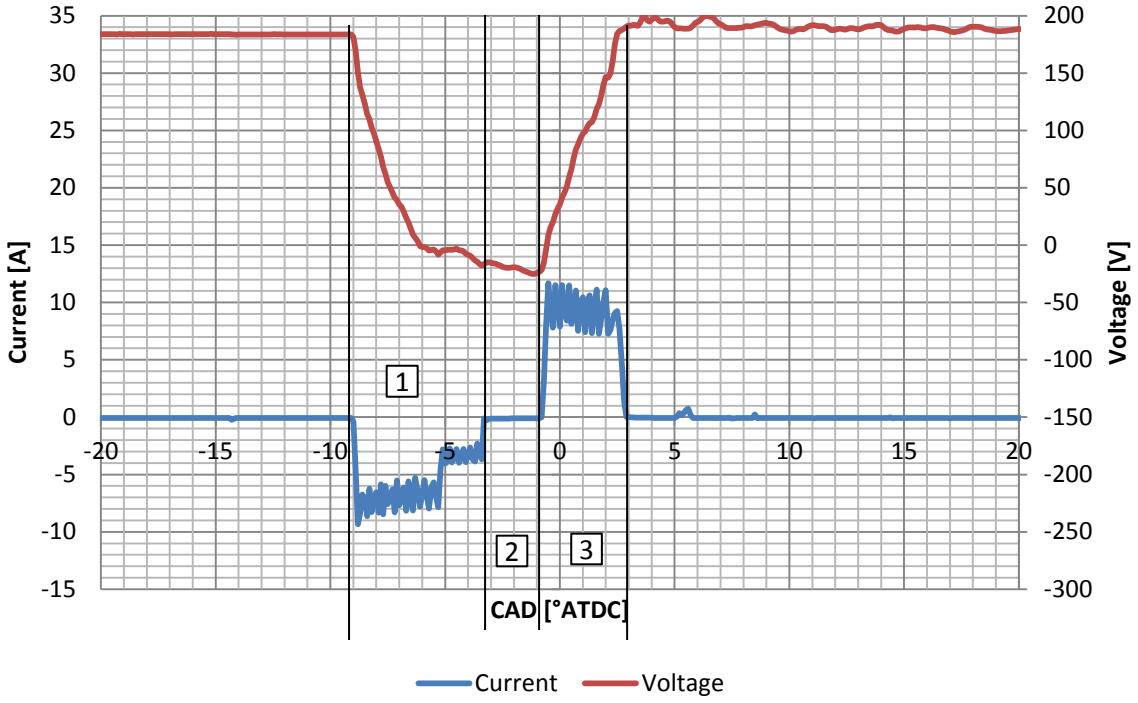

Figure 6.1 Current and voltage trace for the prototype fuel injection system.

Figure 6.2 shows the response of the engine to the different injectors with different demand signals sent to them. Flow rate characterisation of the injectors was not available for use during the project. They could have been characterised but time ran out before this could have been done. The first point of note is the difference in control of the fuel rail pressure. The positive spike on the fuel pressure trace for B2N1-9 is a result of the control strategy for the injection equipment as set by Delphi in the VISU control system supplied with the ECU (The fuel pressure for the conventional injector was controlled by the separate controller and injector driver Emtronix). The spike phases with the SOIm and occurs just as the needle begins to ascend. The delay from the demand means that a small increase in fuel pressure occurs as the bottom surface of the needle lifts from the nozzle body. The negative spike on this trace occurs just as the needle is in the closing phase.

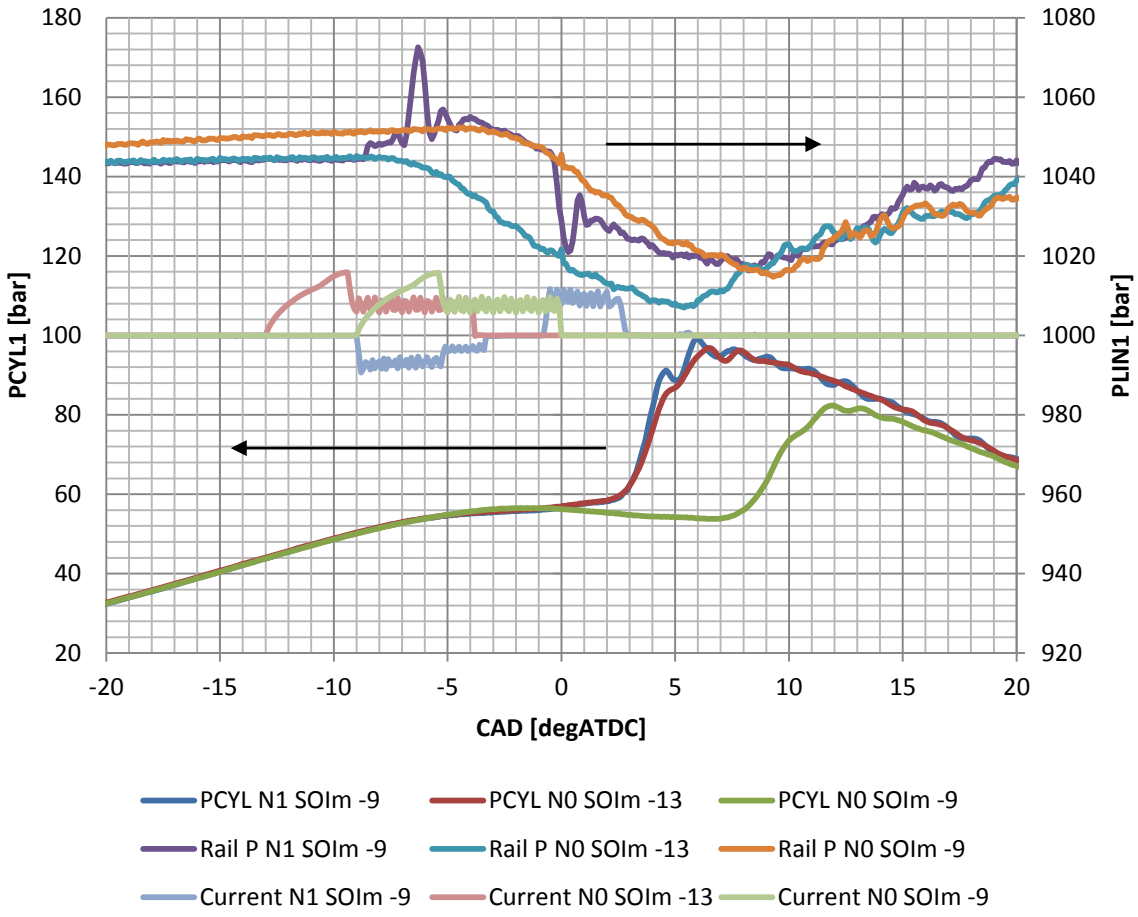

Figure 6.2 Cylinder (PCYL1) and fuel rail (PLIN1) pressure for the conventional (N1) and prototype (N0) injection equipment on the conventional bowl B2 at KP3 with 30 % EGR

The cylinder pressure traces indicate the differences in the injection rate of the injectors and the resulting effect on combustion. When the SOIm is timed the same at -9°ATDC, the start of combustion differs by 4°, with combustion initiating -2°ATDC for the prototype system and 2°ATDC for the conventional system. The combustion phasing requires the SOIm to be advanced for the conventional system. When set to 4° more advanced at -13°ATDC, the combustion start angle is comparable at -2°ATDC as shown in the figure. As a result, the electrical demand for the testing was set so that combustion was phased the same for each injection system.

6.2 Experimental Results

The comparison data that follows is based on the characterisation work for bowl B2, the best performing conventional bowl. The test process was exactly the same as described in the characterisation testing, with only the SOIm being varied for a constant load target at each EGR condition. Each plot that follows has 2 separate curves for each series; they represent the two different EGR rates used and each curve is made up of 4 points tested in the SOIm swing as shown in Figure 6.3. N0 is the conventional solenoid injector, with 7 holes and N1 is the prototype injector with 7 holes and matching flow rate.

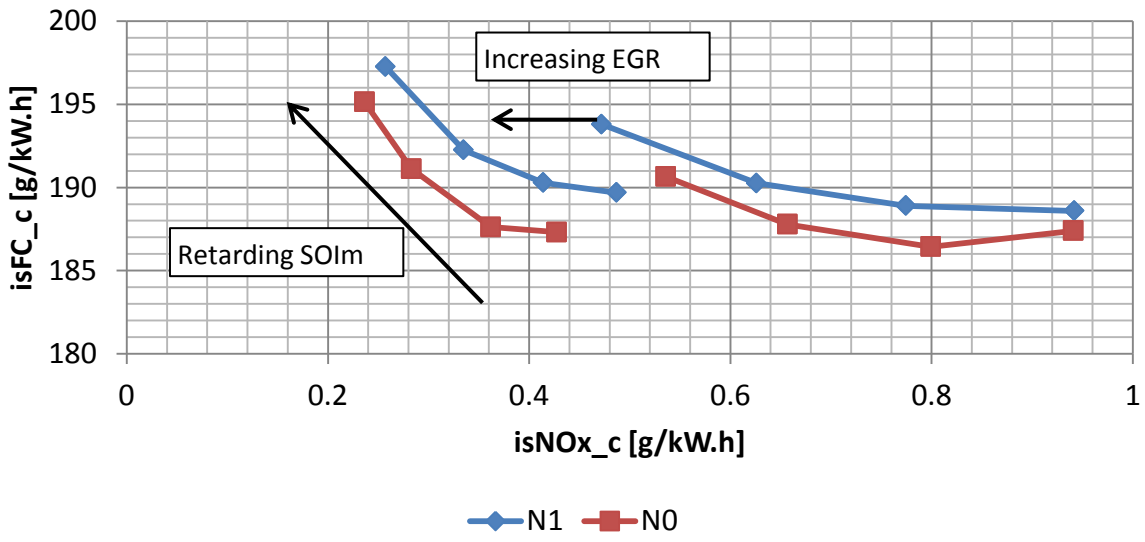

Figure 6.3 Illustration of the EGR and SOIm swing used in the comparison of the injector types

The fuel flow and exhaust flow were calculated from the value of airflow and AFR. This choice was made after observing the fluctuations in the fuel system that affected the fuel meter measurements for the conventional system. The calculated values are indicated with the suffix "_c" on the end of each parameter derived from these parameters.

6.2.1 KP3 Test

The following Table 6.1 shows the test settings that were used for the comparison of the injector type. The results are taken from the low isNOx end of the EGR swing at 27 % and 30 % EGR respectively and are plotted together.

Test name	Speed	Load	Intake temp	Intake pressure	EGR rate	EGR temp	Pilot SOIm	Rail pressure	SOI range
	RPM	GIMEP	°C	barA	%	°C	-	bar	°ATDC
KP3 test	2000	9	41	1.47	27	69	NA	1050	N0(-13, -11, -9, -7) N1(-9, -7, -5, -3)

Table 6.1 Test settings for the comparison of injector type at KP3

At 30 % EGR, the results indicate that the conventional injector N0 has the best efficiency with an isFC_c of 187.3 g/kWh at an isNOx_c of 0.43 g/kWh. At isNOx_c of 0.41 g/kWh, N1 has an isFC_c of 190.2 g/kWh which is a difference of 1.5 %. In terms of emissions output N0 is the best performing injector, consistently outperforming the prototype injection system. At the same test point (30 % EGR, isNOx_c 0.43 g/kWh) the smoke is 0.8 FSN for N0 and 1.08 FSN for N1. Each injector also demonstrates a different response to a change in SOIm; N1 consistently deteriorates with a retard in SOIm whereas the trend with N0 is an improvement at the most retarded timing. This is also demonstrated at 27 % EGR.

N0 has the best isCO_c output at 30 % EGR achieving 2 g/kWh compared to 2.4 g/kWh for N1. The two injectors match their responses across the SOIm used, at 27 % EGR. N0 has the lowest value of 1.23 g/kWh, by 0.04 g/kWh. The emission of isHC_c at 0.43 g/kWh isNOx_c, is lowest for N0, outputting 0.2 g/kWh. N1 was worse ati.25 g/kWh.

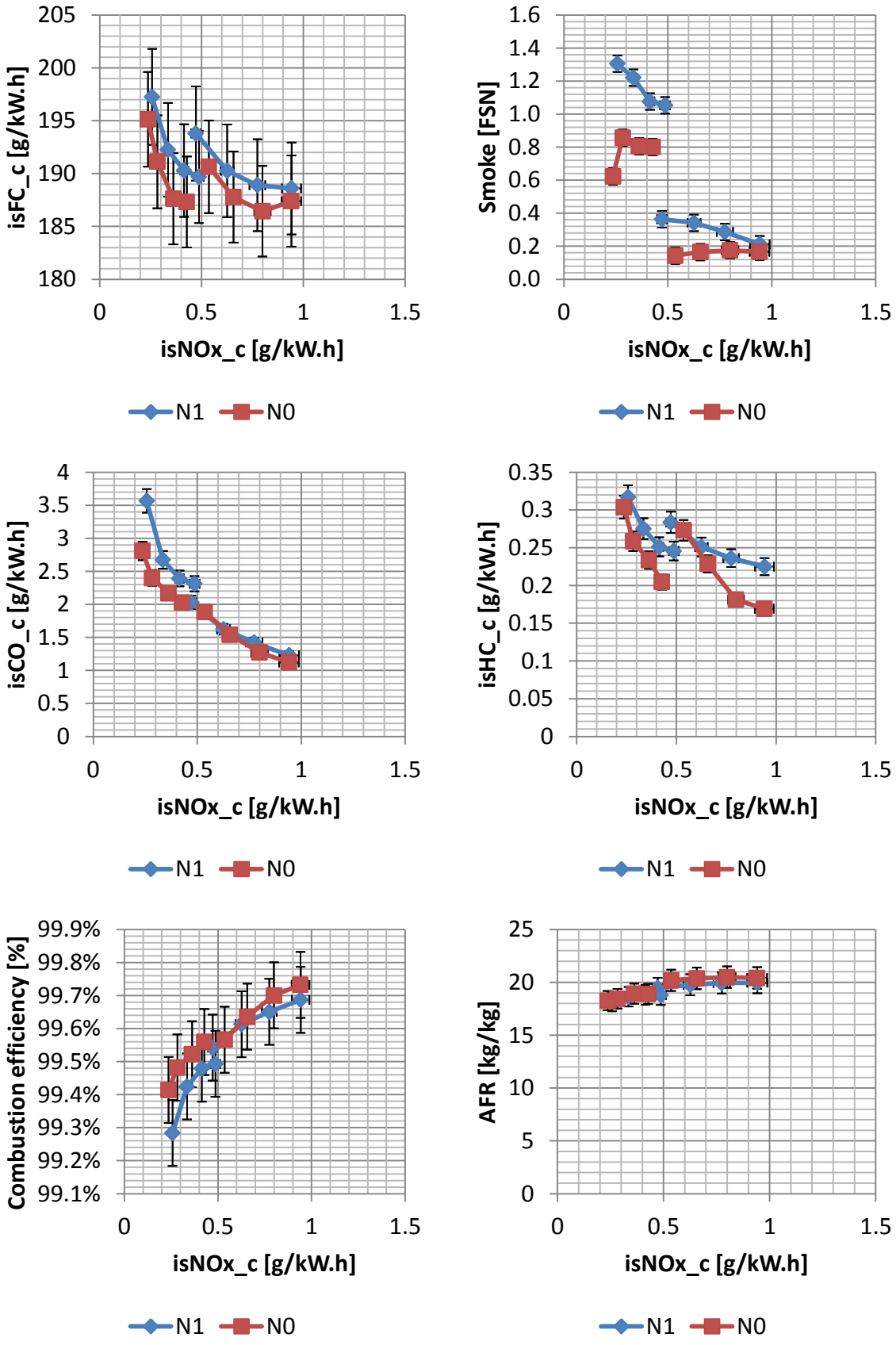

Figure 6.4 Results of testing of conventional and prototype injection systems at KP3 with bowl B2

The differences observed in the emissions outputs indicate a change in the fuel conversion efficiency between injector N0 and N1. This is not sufficient to completely explain the differences in isFC. The fuel conversion efficiency is different between N0 and N1, however in terms of fuel energy this is a small amount (0.02 kW) and the difference in performance is more significant. An examination of the in-cylinder behaviour in the following figure shows that the majority of the difference in isFC can be attributed to the differences in heat transfer and crevice losses. At the same start of combustion timing, N0 rejects 2.51 kW of heat through the combustion chamber during the working stroke up to EVO, compared to 2.82 kW with injector N1.

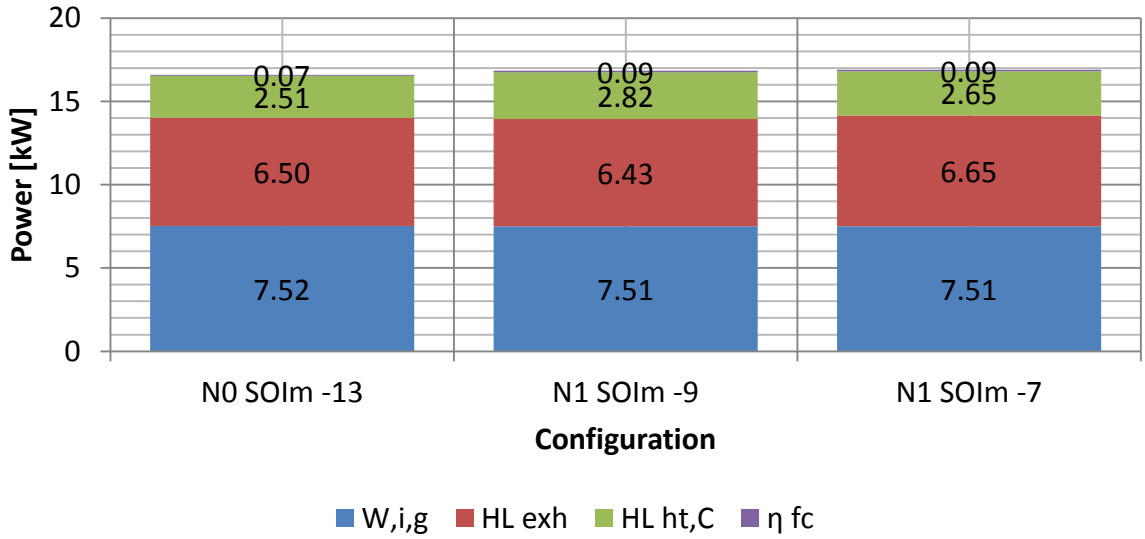

Figure 6.5 Energy balance at KP3 for the test of the effect of injector design with bowl B2

N1 rejects 6.43 kW of heat into the exhaust when the start of combustion occurs at the same time as N0. N0 rejects 6.5 kW of heat into the exhaust. When the start of combustion is retarded for injector N1, the heat transfer and crevice losses reduces to 2.65 kW and the heat rejection through the exhaust increases to 6.65 kW. These figures suggest that the duration of the combustion and the rate of heat release are affecting the efficiency of the engine in an unexpected manner; the slower combustion is beneficial to fuel consumption because the energy lost to the coolant is reduced without the penalty of increased heat losses to the exhaust. The change in fuel consumption is small (1.4 %); however it is above the uncertainty of the calculation of isFC using the air system (approx. 0.5 %).

The reduction of the smoke number with the conventional injector compared to the prototype system is unexpected. It is not possible to identify exactly why this effect occurs. It is possible that the reduced rate of rise of temperature due to the lower peak of heat release rate (0.05 kJ/deg) shown in Figure 6.6 potentially reduces the temperature during combustion resulting in a reduction in soot formation. This is speculative, however it was well established that lower combustion and flame temperatures reduce the formation of soot even in regions of rich air to fuel ratios (refer to the equivalence ratio versus temperature plots in Chapter 2.3.3 (Dec, 2009)).

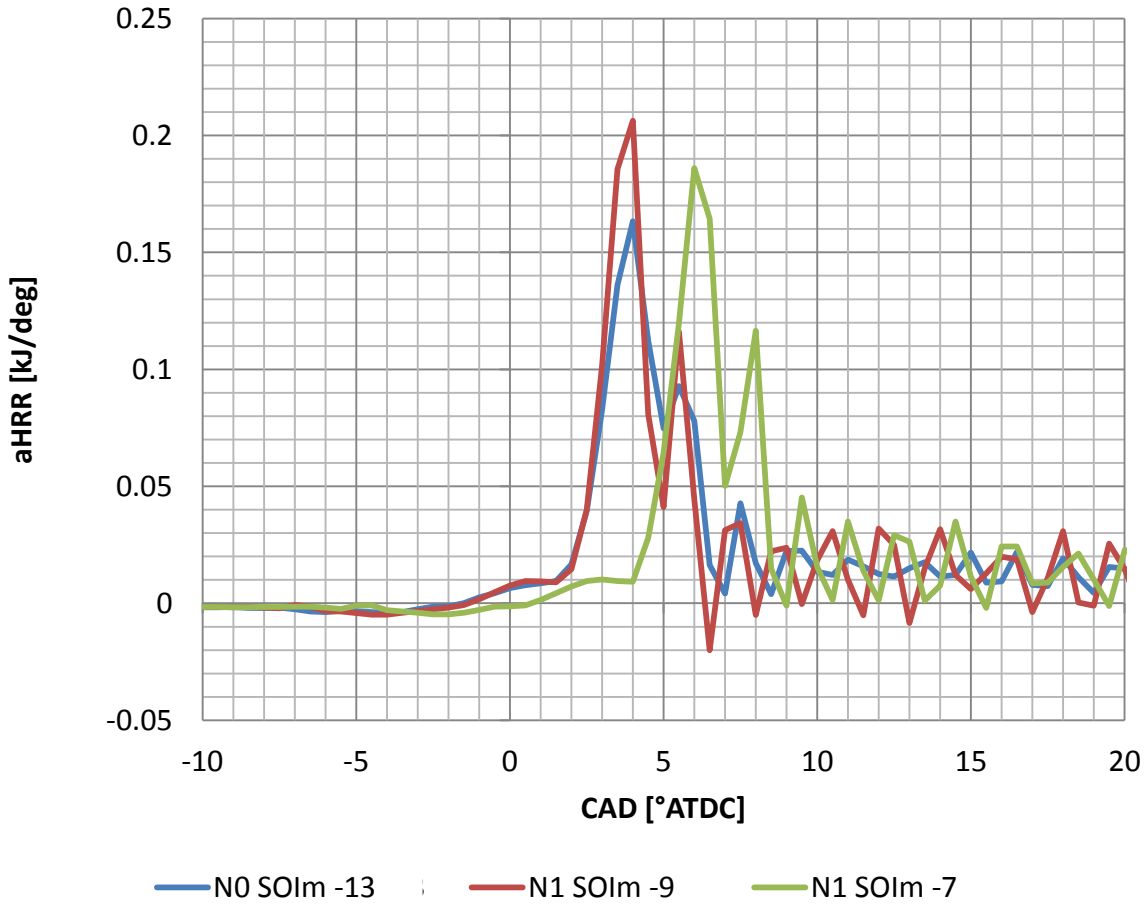

Figure 6.6 Apparent net heat release rate for bowl B2 with conventional(N0) and unconventional (N1) injection systems. The number following the injector type is the SOIm

Due to the efficiency difference, a lower mass of fuel was injected for N0. This may have reduced the regions of rich mixtures locally to the combustion. This may account for the

differences in the emissions output as either fewer pollutants were formed or there would be more oxygen available to oxidise the formed pollutants.

6.2.2 KP2 Test

The following Table 6.2 shows the test setting used at KP2 for the comparison of the injector type.

Test name	Speed	Load	Intake temp	Intake pressure	EGR rate	EGR temp	Pilot SOIm	Rail pressure	SOI range
	RPM	GIMEP	°C	barA	%	°C	-	bar	°ATDC
KP2 test	1500	6	41	1.16	30.5	65	NA	800	N0(-12, -10, -8, -7) N1(-10, -8, -6, -4)
			43		34	67			

Table 6.2 KP2 settings for the comparison of injector type at KP2

Observing Figure 6.7, at 30.5 % EGR, the conventional injector appears to have the lowest curve of isNOx_c against isFC_c. At 0.6 g/kWh isNOx_c the conventional injector has an isFC_c of 202.6 g/kWh. The prototype injection system has an isFC_c of 206.6 g/kWh at an isNOx_c of 0.48 g/kWh. This is a difference in isFC_c of 1.9 %.

The emissions of smoke are sufficiently low enough to be within the uncertainty of the measurement device (0.05 FSN). This indicates that the combustion was sufficiently premixed, the fuel spray was lean enough or that the rich regions were at sufficiently low enough temperature to avoid forming soot. The length of premixing time can be seen in the following combustion plot Figure 6.10.

The emissions of isCO_c and isHC_c are relatively similar for both injector types. The conventional injection system seems to have the best trade off curve at both EGR rates. This is reflected in the combustion efficiency plot.

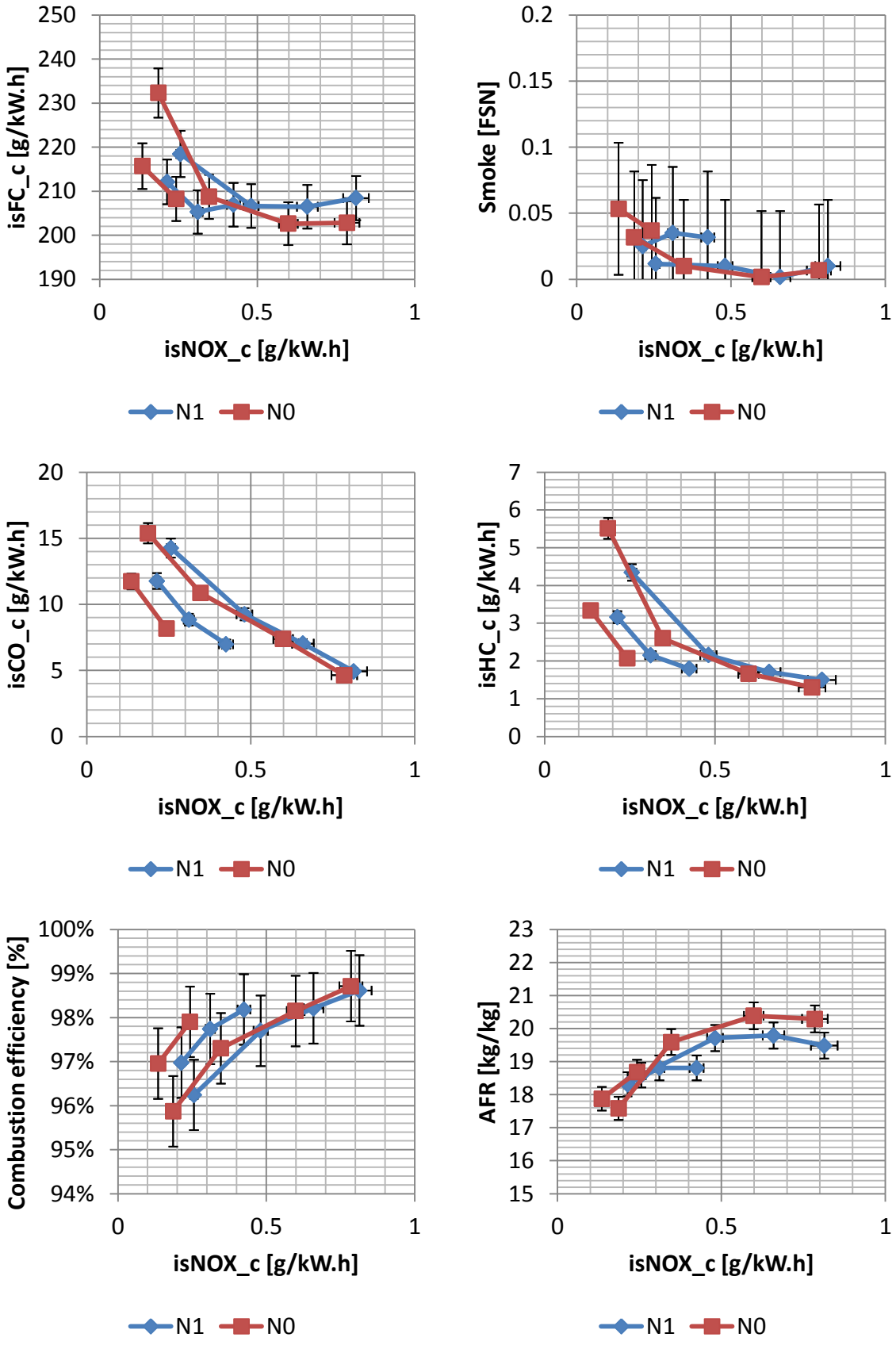

Figure 6.7 Test data for the comparison of injector type at KP2

The energy balance analysis shown in Figure 6.8 highlights the differences in the behaviour of each injector. At 30.5 % EGR, when the combustion phasing is the most advanced for each injector, the heat transfer and crevice losses are lower for the conventional injector (1.88 kW) compared to the prototype system (2.23 kW). This is the same combustion behaviour that was observed at KP3. The heat rejection through the exhaust is higher for the conventional system (3.23 kW) compared to the prototype system (3.15 kW), which indicates that a lower rate of heat release has the benefit of reducing heat transfer losses without a penalty on heat rejection to the exhaust.

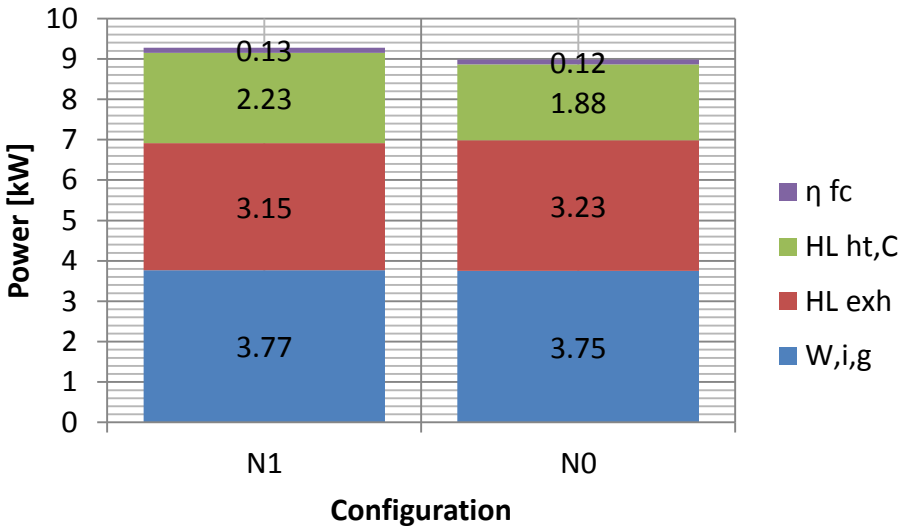

Figure 6.8 Combustion behaviour of each injector type at KP2

The points for comparison seen in Figure 6.8 are at the most advanced SOIm used. The apparent heat release rate for these points can be seen in Figure 6.9, where the peak of heat release occurs sooner for the prototype system (4.5°ATDC) compared to the conventional system (6°ATDC). At this point the combustion phasing differed by 1° i.e. the conventional system should have been set to SOIm =-13°ATDC. With the 1° compensation applied the peak of heat release for the conventional system lagged the prototype system by 0.5°. The peak of heat release is lowest for the conventional system and more retarded, which suggests a bias towards heat lost through the exhaust rather than heat lost through heat transfer and crevice losses.

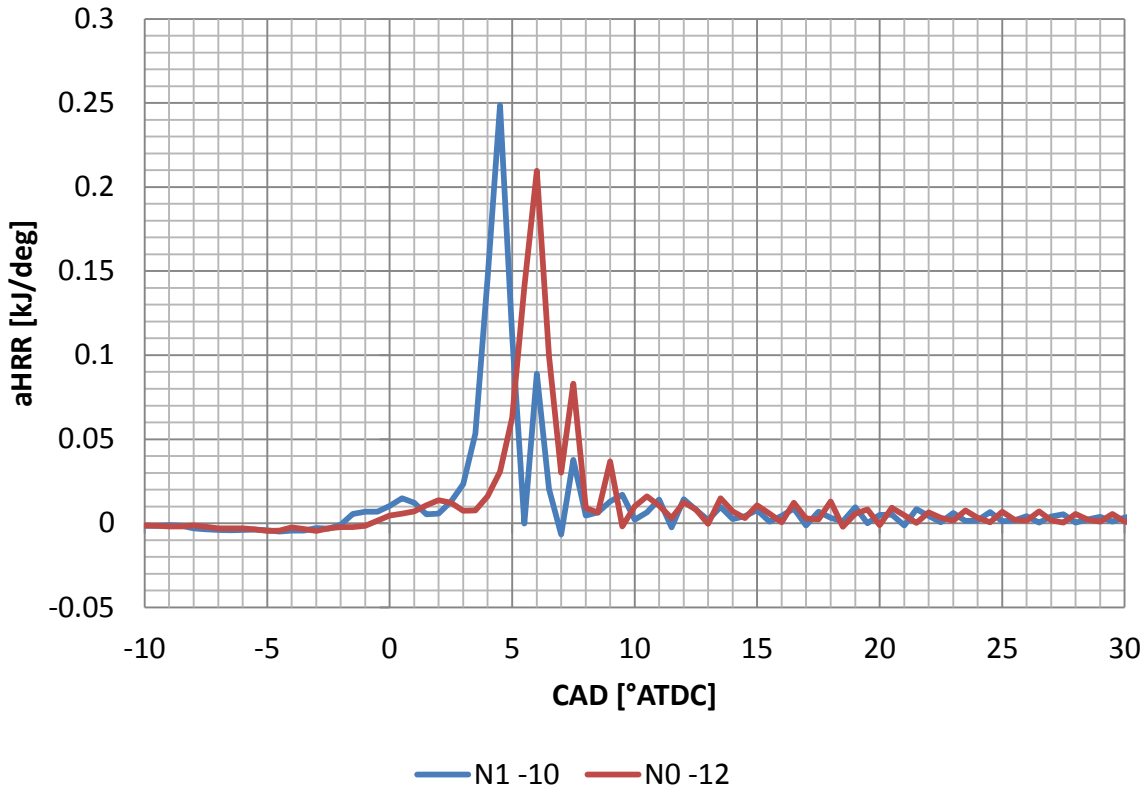

Figure 6.9 Apparent net heat release rate for comparison of injector types at KP2

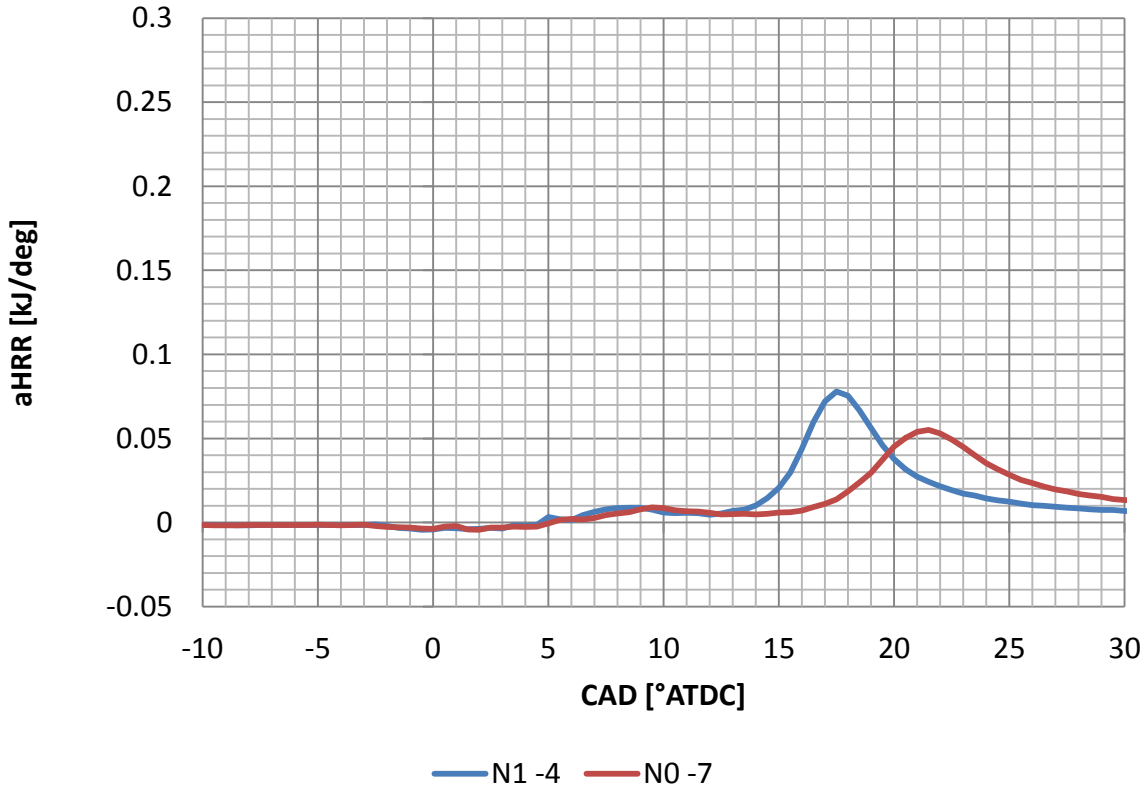

Figure 6.10 Apparent net heat release rate for the comparison of injector types at KP2

The variation in SOIm causes the isFC_c of the conventional injection system to change more rapidly than the prototype system. As the SOIm retards the main heat release retards more for the conventional system than the prototype system as shown in Figure 6.10. This figure shows that under the same conditions, the onset of the main high temperature heat release for the conventional injection system lags that of the prototype system after the initial low temperature heat release. The peak of high temperature heat release occurs at 17.5°ATDC for the prototype system compared to 21.5°ATDC for the conventional system. This difference of 4 degrees equates to 0.44 ms, which is similar in magnitude to the injection duration of the prototype system.

The combustion is longer and less efficient for the conventional system, requiring more fuel to meet the load target. There is a benefit to reducing the heat transfer losses with the conventional system at the advanced timing which is lost as the timing retards because the rate of mixture formation and combustion is significantly slower than the prototype system. As a result, the prototype system is able to maintain a lower isFC_c (218 g/kWh) than the conventional system (232.3 g/kWh) at the most retarded timing.

This demonstrates that at KP2, the conventional system benefits from an advanced timing combined with a slower combustion rate to maintain low isFC_c. The improved mixture formation of the prototype system allows the combustion timing to be retarded without a large fuel consumption penalty; however the rate of heat release needs to be reduced at the advanced timings to yield the isFC_c figures equivalent to the conventional system.

6.2.3 KP1 Test

The following Table 6.3 shows the test settings that were used for the comparison of the injector type at KP1.

Test name	Speed	Load	Intake temp	Intake pressure	EGR rate	Pilot SOIm	Rail pressure	SOI range
	RPM	GIMEP	°C	barA	%	-	bar	°ATDC
KP1 test	1500	3	64	1.03	33	NA	600	N0(-12, -11, -10, -9) N1(-10, -9, -8, -7)
			70		38.5			

Table 6.3 Test settings for the comparison of injector type at KP2

Figure 6.11 shows that at 33 % EGR the prototype nozzle has the lowest isFC_c (225 g/kWh) at the most advanced SOIm, however the curve of isNOx against isFC is better than the prototype system. At isNOx_c of 1 g/kWh the prototype system has an isFC_c of 239.8 g/kWh, whereas the conventional system has an isFC_c of 236.3 g/kWh at an isNOx of 0.92 g/kWh, which is a difference of 1.46 %.

When the EGR level is increased (38.5 %) the isNOx against isFC_c for both systems is similar. The prototype system has the lowest isFC_c (229.3 g/kWh) for an isNOx of 0.67 g/kWh, at the most advanced SOIm, compared to 234 g/kWh isFC at 0.68 g/kWh isNOx. As SOIm retards, the two injection systems follow the same curve. However, at the most retarded SOIm, combustion is more retarded for the conventional system, the isFC is higher and the isNOx is lower.

Smoke emissions are lower than the uncertainty of the measuring device (0.05 FSN) as observed at KP2, indicating that combustion was sufficiently premixed. This is also shown by the increase in CO and HC emissions which result from the fuel spray becoming overly lean before combustion occurs.

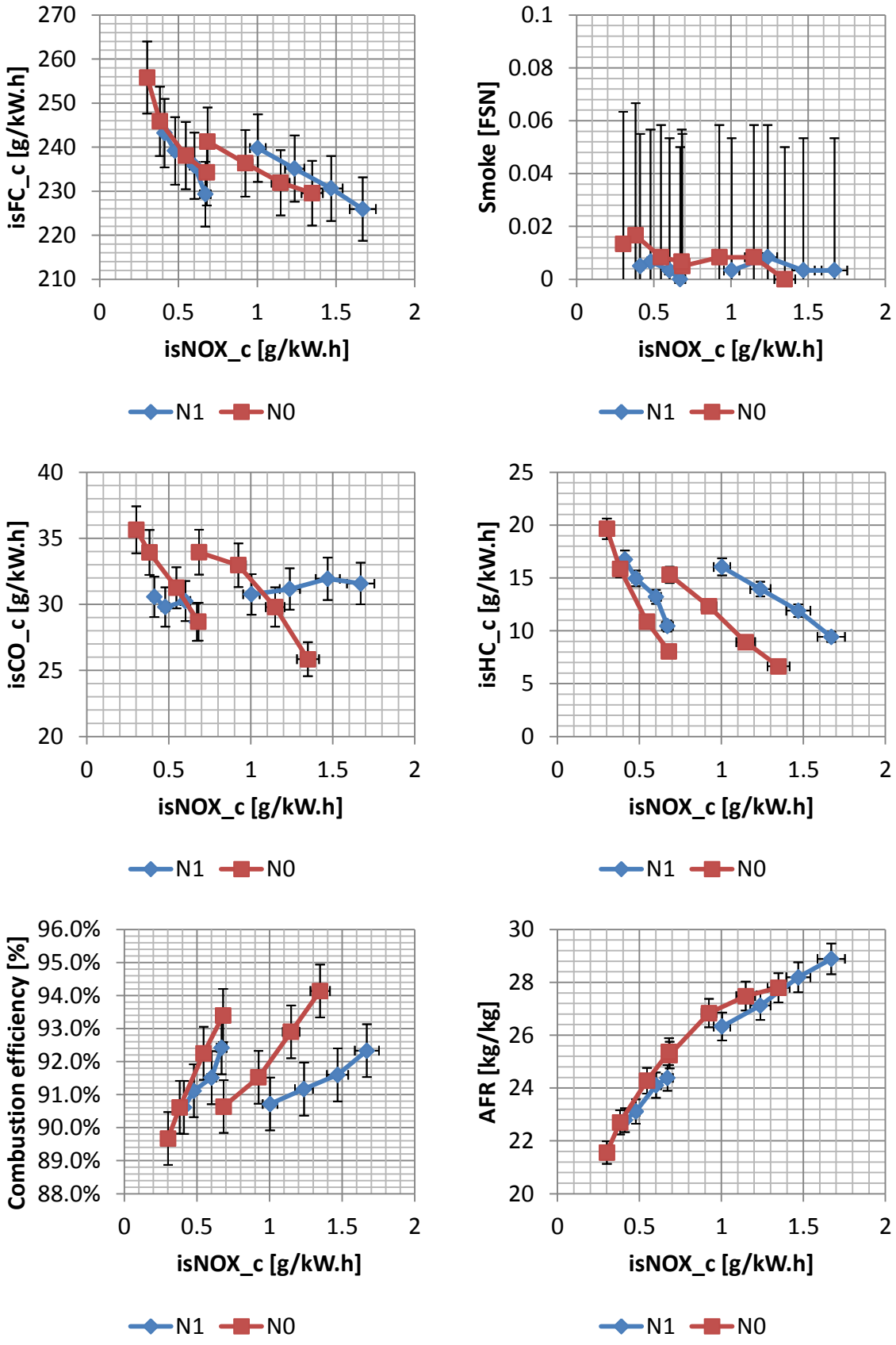

Figure 6.11 Test data for the comparison of injector type at KP1

The energy balance shown in Figure 6.12 has a similar trend trend to that observed at KP3 and KP2. The conventional system rejects more heat through the exhaust and less through in-cylinder heat transfer than the prototype system. The difference in the heat transfer loss at KP1 is 0.07 kW, the prototype system rejecting 0.93 kW compared to 0.86 kW for the conventional injection system. The major difference at this key point is how much energy was lost through incomplete combustion of the fuel, 0.48 kW compared to 0.44 kW for the prototype and conventional systems respectively. In terms of relative energy loss 9.3 % was lost by the prototype system and 8.5 % by the conventional system

The combustion aHRR trace for the 33 % EGR is shown in Figure 6.13. The combustion phasing for these points is the same. The peak of high temperature heat release is lower for the conventional injector (0.058 kJ/deg) compared to the prototype system (0.069 kJ/deg). Qualitatively the curves are very similar at the start and after the peak of heat release. As with the other key points tested the lower rate of heat is associated with lower heat transfer losses in general. For the best isFC, a balance has to be met between the reductions in rejected heat through heat transfer and the heat lost through the exhaust.

The most effective way of reducing isNOx_c is to increase EGR without incurring a fuel consumption penalty associated with a retard in SOIm. As a result, the speed of the mixture formation and combustion with the prototype system is the best way to achieve the lowest fuel consumption at this conditions; however as shown, this is only the case at the most advanced SOIm.

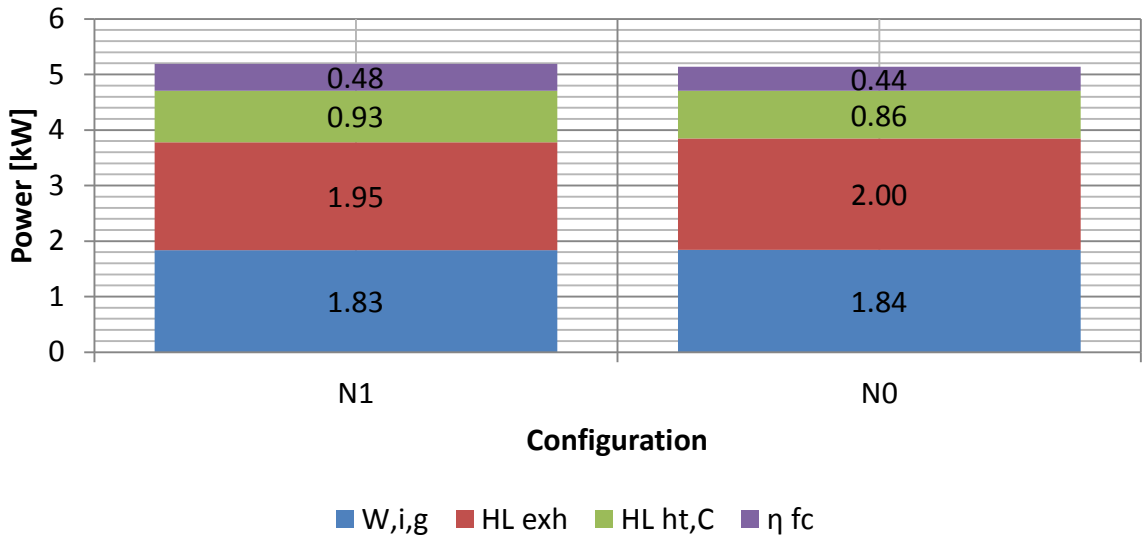

Figure 6.12 Plot of the energy balance for the conventional (N0) and prototype (N1) injection system at KP1

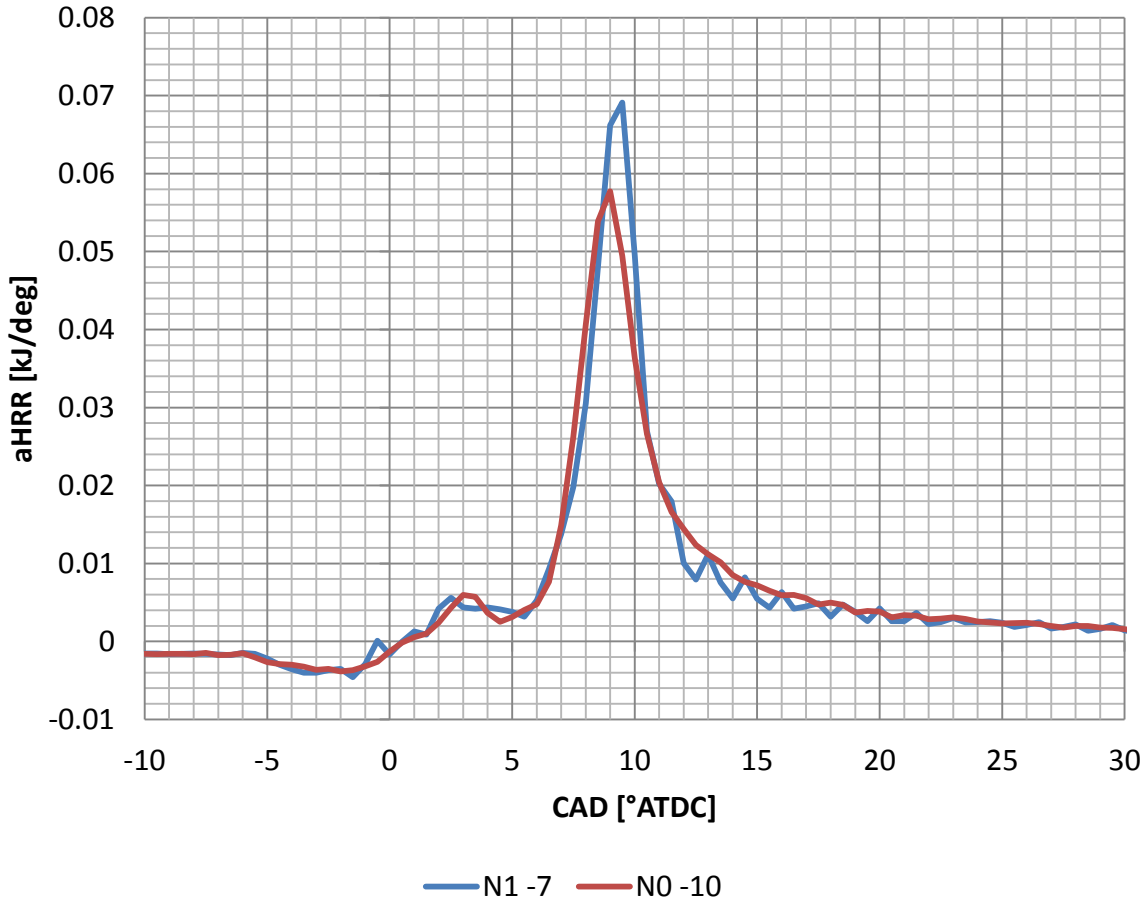

Figure 6.13 Apparent net heat release rate for the conventional (N0) and prototype (N1) injection system at KP1

6.2.4 4000FL Test

The following Table 6.4 shows the test settings that were used for the comparison of the injector types at 4000FL. The data was produced in the same way as in the previous full load testing. The test was a SOIm swing with fixed inlet manifold conditions and load target.

Test name	Speed	Load	Intake temp	Intake pressure	EGR rate	Pilot SOIm	Rail pressure	SOI range
	RPM	GIMEP	°C	barA	%	-	bar	°ATDC
4000FL	4000	21.4	50	2.4	NA	NA	2000	N0(-26, -25, -24, -22) N1(-19, -17, -15, -13)

Table 6.4 Test settings for the comparison of injector type at 4000FL

The first point to notice in Figure 6.14 is that the AFR against isFC_c curve is the best for the prototype system. The AFR is higher for the prototype system because for the same air flow (dictated by the intake manifold conditions) the fuel required to meet the load target is lower than for the conventional system. As a result, the isFC_c is lower for the prototype system (186 g/kWh) than the best point for the conventional system (193 g/kWh), for the same load target.

The smoke output of the engine reflects the combustion behaviour. The prototype system has the best curve of AFR versus smoke and the lowest smoke number of 0.73 FSN compared to a smoke number of 1.43 FSN at -26 °ATDC for the conventional system. The smoke number increases as the SOIm retards for both injector types. This could be a result of the increase in fuel required to meet the load target reducing the AFR, as well as a reduced amount of cycle time for any oxidation to take place.

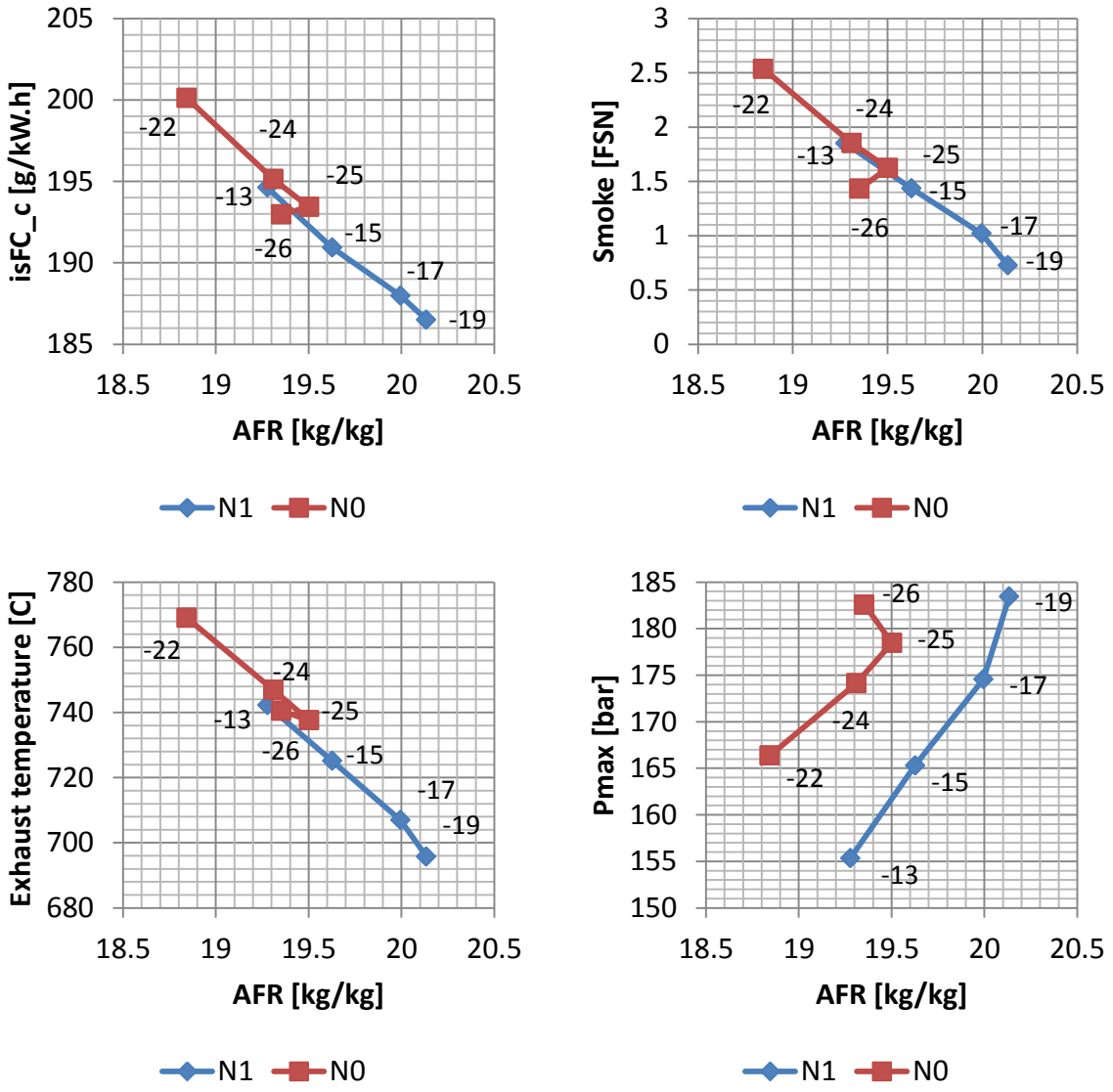

Figure 6.14 Test data for the comparison of injector type at 4000FL numbers indicate SOIm for both systems

The exhaust temperature follows the isFC_c curve well and indicates that the additional fuel being added to meet the load target is rejected into the exhaust. This suggests that for all SOIm used for the conventional system, the mixture formation and combustion process is slower. Even when the combustion phasing is the same between the injection systems (SOI_m=-22°ATDC N0, SOIm =-17°ATDC N1) the rejected heat to the exhaust is higher for N0.

This is illustrated in Figure 6.15, where the heat rejected to the exhaust is 33.8 kW for the conventional system and 30.9 kW for the prototype system. This is a difference of 8.8 % (2.97 kW). With the overall heat input increasing to meet the load target, a higher

proportion of heat is rejected in-cylinder through heat transfer losses. This is different to the effect observed at part load, primarily due to the fuel system being setup to achieve rapid mixture formation and hence a fast combustion process.

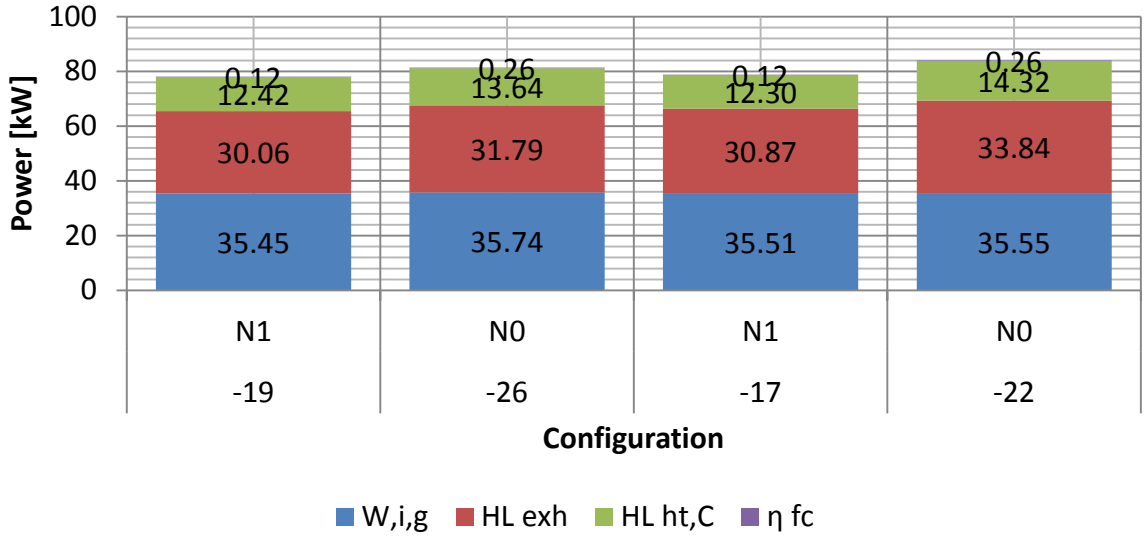

Figure 6.15 Energy balance for the conventional (N0) and prototype (N1) injection system at 4000FL

6.3 Conclusions of the Injector Evaluation

The results of the tests of the conventional and prototype injection systems on bowl B2 have shown how the injector type affects combustion and emissions. This has shown that the rate of fuel addition during the injection process with the conventional injector, can be beneficial to the fuel consumption and emissions of the engine at certain operating conditions.

At all of the part load conditions the conventional injection system is able to reduce isFC_c by reducing the peak of heat release rate without sacrificing overall efficiency due to the slower burn rate. The slower burn rate consistently results in higher heat rejection through the exhaust. This effect is consistent at all EGR levels for KP3 but was only observed at one EGR condition tested out of 4 at KP2 and KP1. When the EGR rate is increased to the point where the isNOx is around 0.5 g/kWh the difference between the conventional and prototype system was not significant. A low AFR has a larger influence on the engine emissions and efficiency than the design of the injection system.

At the full load condition, 4000FL, the higher injection rate of the prototype hardware results in the best smoke and isFC output for bowl B2. At the higher engine speed, the rate of mixture formation and combustion improves the engine efficiency. As a result fuelling is lower, which allows a higher AFR and lower smoke number.

The injection rate of the prototype system should be controlled at KP3 to yield low isNOx and isFC. The benefit of the high injection rate can be utilised under full load operation whilst the advanced features of the prototype system can be used to optimise the engine operation at the part load conditions.

Exactly why the operation of the conventional system reduces emissions and fuel consumption when compared to the prototype system is not clear from these tests. Certainly, the mixture formation process is not well understood in terms of the differences in spray structure that lead to a better trade-off on the emissions output particularly at KP3. The following Table 6.5 summarises the areas of the fuel spray formation that would need to be investigated to prove or disprove the hypotheses derived from these tests.

	Factor	Effect	Test
Penetration	The conventional system has lower overall penetration of liquid and vapour	Reduce the distribution of combustion products into quench regions avoiding product formation	Measure the penetration length of each injector type with the same test conditions in-cylinder i.e. Same gas pressure, temperature, composition (density), injection pressure, injection duration.
Atomisation	Assumed to be better for the unconventional system with rapid needle motion	Reduction of liquid droplets and improved air entrainment reducing rich regions in the fuel spray	Assess the liquid to vapour ratio in the spray under the same conditions mentioned above as well as assessing the difference in spray equivalence ratio.
Fuelling rate	Fuel addition rate diagrams showing when the fuel injection event is complete	indicates where liquid fuel addition ends relative to the combustion heat release	Measure the injection rate of each system with the same test conditions in-cylinder. Test the prototype injection equipment with variable fuelling rates.
Injection timing/Bowl interaction	Match the spray and bowl interaction with both injection systems	This may have inadvertently enhanced the mixing for the conventional system	Measure the injection rate differences of each injector and along with the penetration and atomisation information estimate the differences in fuel distribution

Table 6.5 Summarising the potential areas of influence on the mixture formation and combustion process of the different hardware types

From all of the factors listed in the above table, the fuelling rate is the one that could be investigated with the experimental equipment. Variations in the rate of injection could be achieved simply with multiple injections. The effect of multiple injections is interesting to investigate on this unconventional design, particularly as the majority of testing so far was carried out with a single injection strategy.

7 The Effect of Injector Nozzle Hole Size and Number of Holes on Combustion and Emissions

For the investigation of injector nozzle geometry the prototype peizo injection system was equipped with three different nozzle designs. The three different designs are shown in the following Table 7.1.

Nozzle	Actuator	Post hone vol flow	Hole size	Holes	Cone angle	k factor
ID	Type	(cm3/min)	mm	#	°	-
N4	Piezo	760	0.131	7	145	2.5
N5			0.123	8		
N6			0.116	9		

Table 7.1 Nozzle design characteristics used in the nozzle study

The only variation was the size of the holes and the number of the holes on the nozzle. The volume flow rate was maintained at 760 cm^3/min for each injector nozzle tested, and the spray angle was appropriate for bowl B4. The testing was carried out over similar conditions used in the characterisation testing, including part load, NEDC conditions as well as full load conditions.

7.1 Experimental Results

The cylinder pressure data in the following section (aHRR and PCYL) is shown with a non-dimensional trace that represents the needle lift profile of the prototype FIE. The traces are based on the measured voltage from the piezo stack. With a direct acting injector the needle lift is proportional to stack voltage. The traces are shown in Figure 7.1.

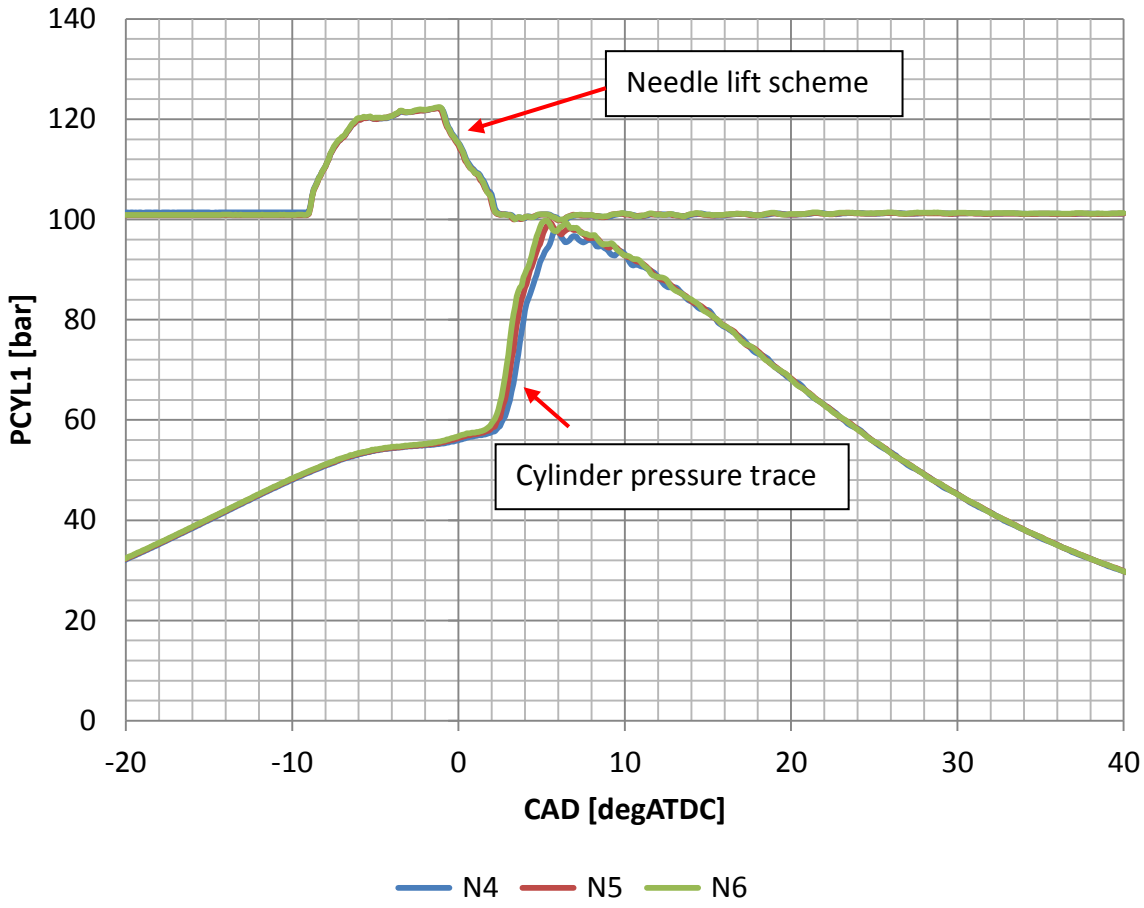

Figure 7.1 Example cylinder pressure data showing the single injection needle lift scheme

7.1.1 KP3 Test

The test conditions for the injector nozzle study are shown in the following Table 7.2. The two test points were part of an EGR swing at the highest EGR rates tested. The test was carried out using the same procedure as the characterisation process.

Test name	Speed	Load	Intake temp	Intake pressure	EGR rate	Exhaust pressure	Pilot SOI	Rail pressure	SOIm range
	RPM	GIMEP	°C	barA	%	barA	°ATDC	bar	°ATDC
KP3 test	2000	9	41.3	1.47	26.7	1.96	N/A	1050	-9,-7,-5,-3
			43.1		29.9	1.89			

Table 7.2 KP3 test settings used in the nozzle study

The following Figure 7.2 shows that there are some differences between the designs of the injector nozzles at this key point. The isFC curves appear to overlay each other with the 9 hole nozzle, N6 having a higher isFC at the most advanced timing for 26.7 % EGR. The isFC

for N6 at the most advanced timing is 189.7 g/kWh compared to 187.2 g/kWh for N4. This is a difference of 2.5 g/kWh or 1.34 %. The response to the variation in SOIm shows a smaller change for N6 than N4 and N5. Although the initial value of isFC is higher for nozzle N6, as combustion timing is retarded, isFC for all nozzles reaches a similar level with N6 being the lowest at 198.9 g/kWh (around 0.6 % less).

When the EGR level is higher at 29.9 %, the isFC is comparable for all injector nozzles. At an isNOx of 0.5 g/kWh, the isFC is around 190 g/kWh for all nozzles. As the SOIm retards to -3°ATDC the isFC is the lowest for nozzle N6 at 195.9 g/kWh. This is 2.8 % lower than N4, showing that the isFC of nozzle N6 is less sensitive to a retard in SOIm than nozzle N4.

The smoke emission a difference due to the injector nozzle designs. At 26.7 % EGR, there is a small difference between nozzle N4 compared to nozzles N5 and N6. N5 and N6 overlay each other and increase from 0.09 FSN to 0.14 FSN as the SOIm retards from -9°ATDC to -3°ATDC. N4 has a higher initial value of 0.17 FSN and is more sensitive to the SOIm retarding, resulting in a smoke number of 0.44 FSN.

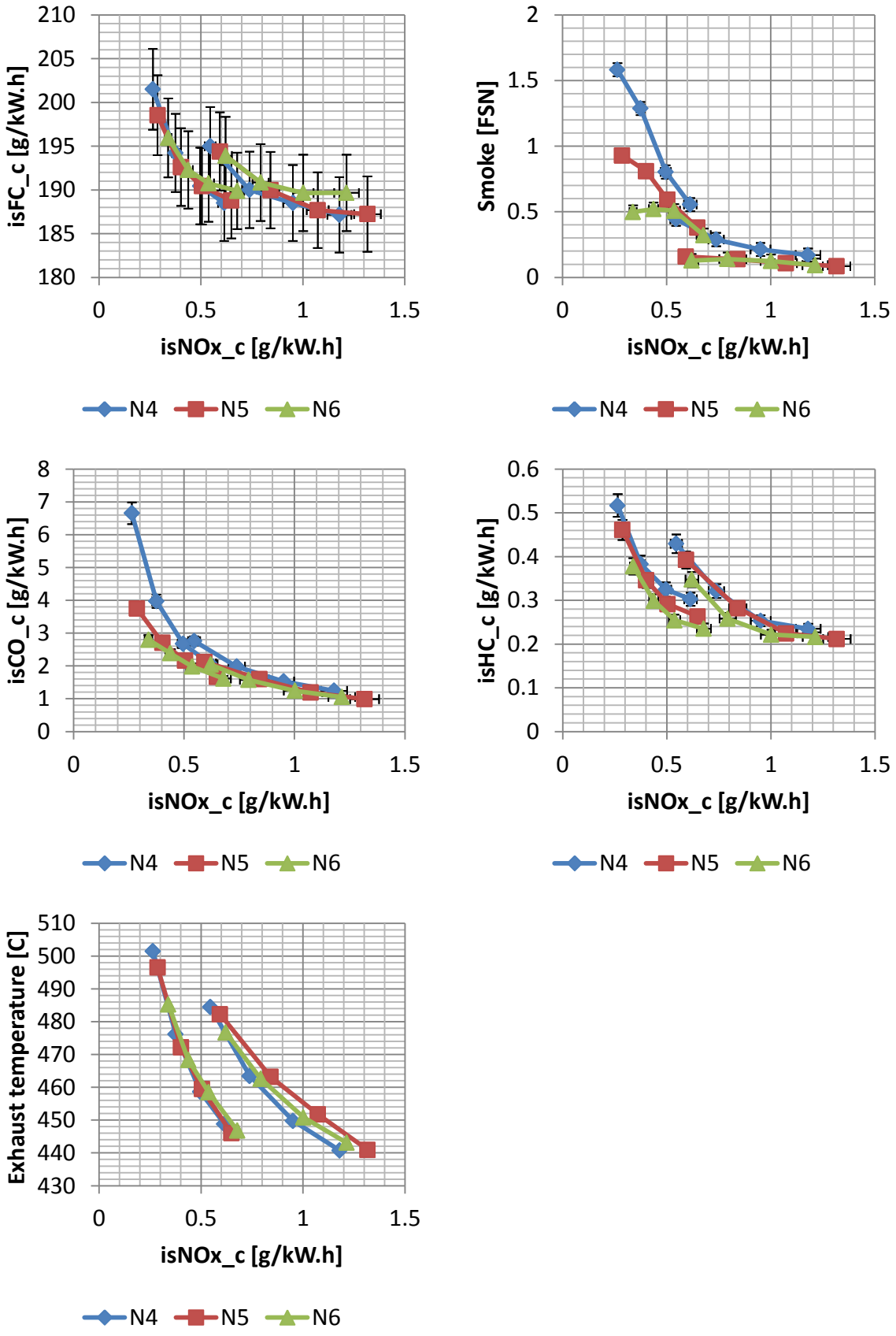

Figure 7.2 Test data for the comparison of nozzle design at KP3

When the EGR rate increases to 29.9 %, the difference between nozzles is more significant when the SOIm is retarded. Initially, at the most advanced timing, the best nozzle N6 has a smoke number of 0.32 FSN compared to 0.38 FSN for N5 and 0.56 FSN for N4. When the SOIm retards, the smoke number for both N4 and N5 increases relatively linearly, ending up at 1.58 FSN for N4 and 0.93 FSN for N5. N6 however increases from the initial smoke value to 0.51 FSN. As the SOIm timing retards further, the smoke number changes to 0.52 FSN (-5°ATDC) and then to 0.5 FSN (-3°ATDC). The response to a retard in SOIm indicates that the mixture formation process is different for each nozzle.

The emission of isCO is higher for N4 than both N5 and N6 across the range of SOIm timings used at both EGR conditions. At 0.5 g/kWh isNOx the emission of isCO for N6 is 1.98 g/kWh, this is lower than N5 by 0.18 g/kWh and lower than N6 by 0.69 g/kWh. The emission of isHC is best for N6 across the range of SOIm timings. This indicates that overall the mixture formation process is improved with the 9 holes nozzle compared to the 7 or 8 holes nozzle.

The exhaust temperature at 29.9 % EGR and the most retarded timing shows that less heat is rejected through the exhaust for N6. This indicates that for the same SOIm, the heat release is occurring sooner and results in lower exhaust temperatures.

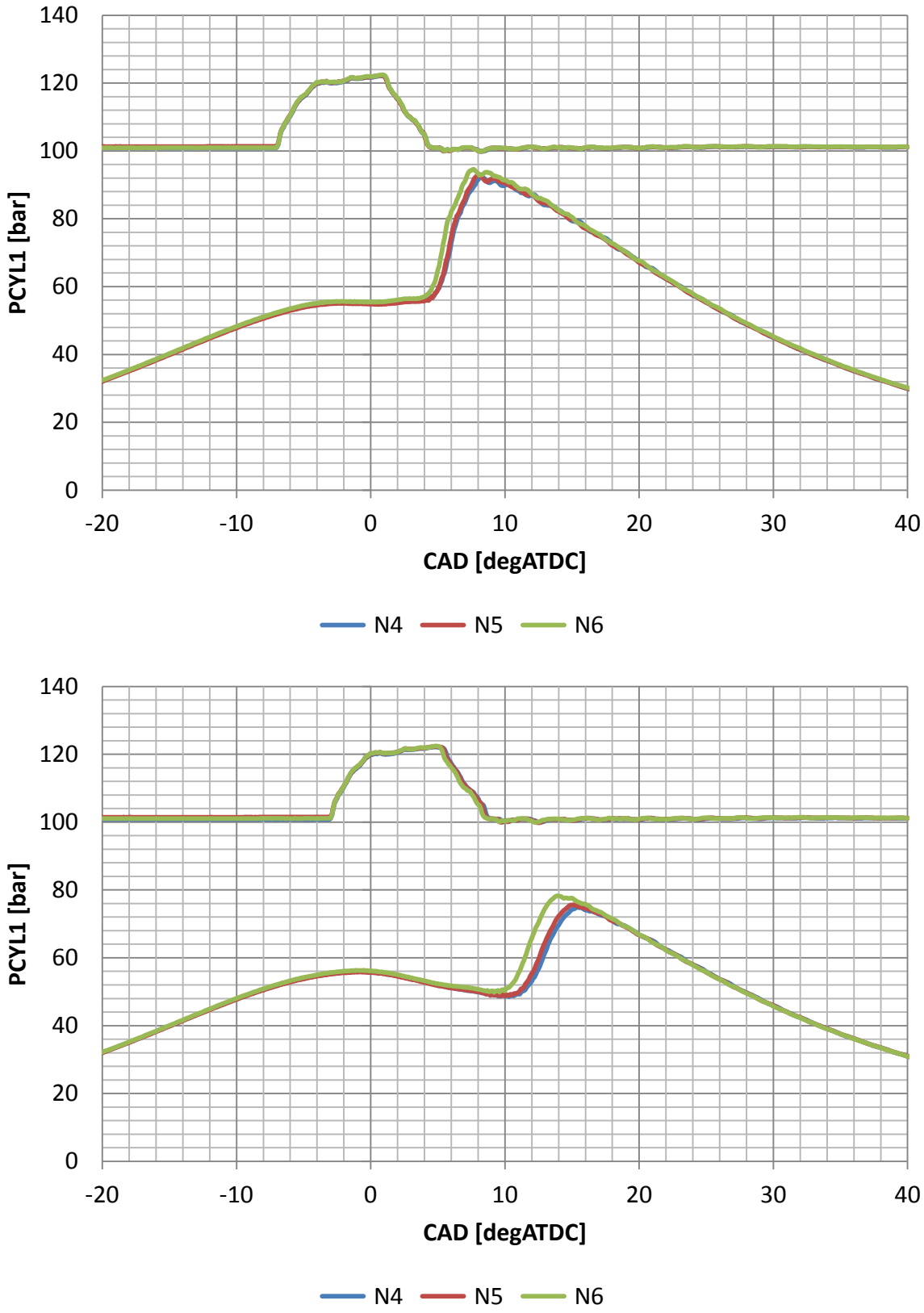

Figure 7.3 Cylinder pressure data for the nozzle study at KP3 with 30 % EGR. From top to bottom, SOIm-7 °ATDC and SOIm -3°ATDC

Figure 7.3 shows the in-cylinder pressure data for SOIm timings of -7°ATDC and -3°ATDC. The combustion at this key point is highly premixed, which is shown in the heat release plots (Figure 7.4) by the characteristic premixed spike, minimal diffusion phase and small tail phase. In each case the start of the cylinder pressure rise occurs earliest for the 9 holes injector, N6. This is most obvious when the SOIm is -3°ATDC. This shows that when the start of injection is the same for each injector, the 9 holes nozzle can form an ignitable mixture sooner under a single injection condition. This is the main reason why the exhaust temperature was lower when injector N6 was used. The trend is similar for each nozzle however with N6 appearing to promote more advanced combustion.

Figure 7.4 shows the heat release rate at the most advanced and the most retarded SOIm. At the most advanced SOIm the peak of the heat release rate is highest for N6. For all of the injector nozzles, the heat release occurs just as the needle begins to descend at the end of the injection event. The peak of heat release occurs 0.8° after the needle closes at the end of injection for N6, 1° for N5 and 1.3° for nozzle N4. When the SOIm retards to -3°ATDC, the heat release occurs later after the end of injection. For N6 this is 3.5° and 4.5 ° for N5 and N4. At the retarded SOIm, the longer ignition delay means there is more time for the fuel and air to mix before the high temperature heat release occurs.

At the most retarded SOIm, the 9 holes injector produced less smoke that the 7 holes injector. With more smaller holes, the fuel distribution around the cylinder is improved and the amount of liquid fuel or fuel that is heterogeneous is reduced. This has little effect on efficiency at the highest EGR rate used here, however overall emissions outputs of smoke isCO and isHC are improved.

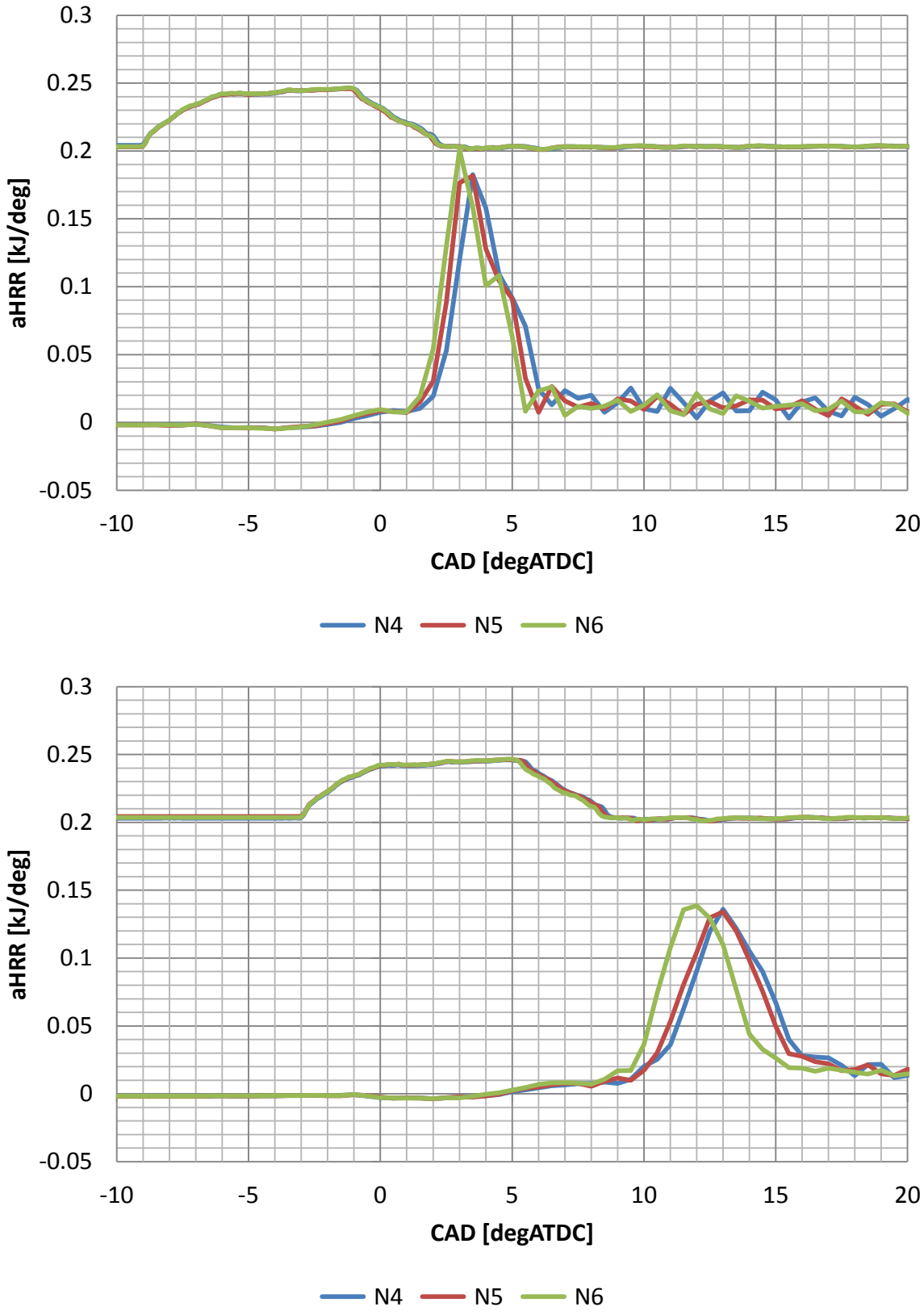

Figure 7.4 Apparent net heat release rate data for the nozzle study at KP3 with 30 % EGR. From top to bottom, SOIm -9°ATDC and SOIm -3°ATDC

7.1.2 KP2 Test

The testing was carried out in the same way as the characterisation process, the main variable changed was the injector nozzle number of holes and the hole diameter. At 33 % EGR, the most retarded timing that could be tested without misfiring was -5°ATDC. Details of the test point are shown in Table 7.3.

Test name	Speed	Load	Intake temp	Intake pressure	EGR rate	Exhaust pressure	Pilot SOI	Rail pressure	SOIm range
	RPM	GIMEP	°C	barA	%	barA	°ATDC	bar	°ATDC
KP2 test	1500	6	39.5	1.16	30	1.25	N/A	800	-10,-8,-6, (-5),-4
			40.7		33	1.23			

Table 7.3 KP2 test settings used in the nozzle study

Figure 7.5 shows the engine outputs for this test. At both EGR rates there is less than 0.5 % difference in isFC between the nozzles at the advanced injection timings of -10°ATDC, and -8°ATDC. Nozzle N6 has the lowest isFC of 203.8 g/kWh at 30 % EGR for the most retarded injection timing of -4°ATDC. N5 is 1.2 % higher and N4 is 2 % higher at this timing. At 33 % EGR N5 and N6 are within 0.5 % of each other across the entire range of SOIm, N5 has the lowest isFC at 204.8 g/kWh. Comparing nozzle N4 and N6 at the most retarded SOIm, the difference in isFC is as high as 3.3 %.

The smoke emission is low for all injector nozzles. The 0.05 FSN resolution of the smoke meter means that no discernible difference can be inferred from this testing. The smoke emission was low in the characterisation testing for all bowls because combustion at this key point was highly premixed. The long ignition delays and rapid pressure rise once the fuel ignites are ideal conditions to minimise the formation of particulates.

Figure 7.5 shows that there is no significant difference in isCO for the 8 holes and 9 holes injector nozzle until the most retarded SOIm at 33 % EGR. N6 has the lowest value of 8.5 g/kWh compared to 9.9 g/kWh for N5. N5 and N6 do sit on the same curve of isNOx against isCO possibly indicating a difference in combustion phasing at the same injection timing. N4 is worse than both of the 8 holes and 9 holes injectors for all SOIm timings. At the most retarded SOIm the isCO output is 11.9 g/kWh. N4 is around 20 % higher than N6 with 30 % EGR and 30 %-40 % higher at 33 % EGR.

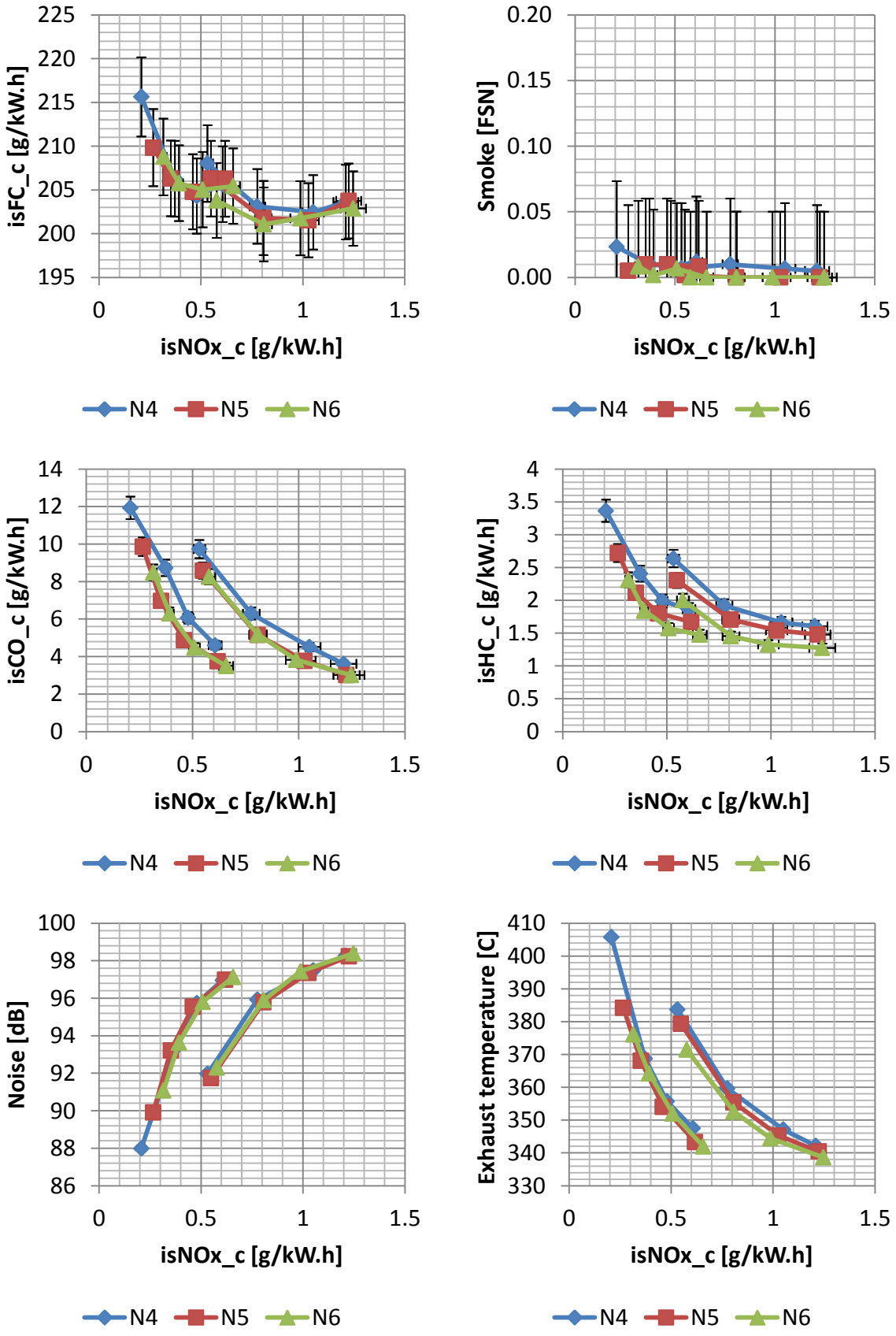

Figure 7.5 Test data for the comparison of nozzle design at KP2

The emission of isHC is the lowest for nozzle N6 at all conditions. The trend at 33 % EGR is that the curves begin to overlay at the most retarded SOIm. At 30 % EGR the lowest isHC is 1.3 g/kWh for 1.25 g/kWh isNOx. When the timing is retarded this increases to 2 g/kWh for 0.58 g/kWh isNOx. Nozzle N5 is 15 % higher and nozzle N4 is 25 %-30 % higher than N6 across the entire range of SOIm. This trend is also observed as the EGR rate increases.

The combustion noise output follows the same trend curves for all injector nozzles, at both EGR rates and nearly all SOIm timings. The exception occurs at the most retarded timing used at 33 % EGR. At this timing, N4 has the lowest noise output at 88 dB. N5 is 2.1 % higher and N6 is the highest at 91 dB (3.4 % higher than N4). Besides that test point, all of the nozzles follow the same curve varying less than 0.4 % across the entire range of SOIm timings.

The exhaust temperature is lowest for N6 for all conditions tested. This may explain why the isFC is marginally better for N6, with a reduction in heat rejected through the exhaust. When the EGR rate is at 33 % the curves for all nozzles are close together, N6 having lower exhaust temperature but slightly higher isNOx outputs as if the SOIm is slightly more advanced.

Figure 7.6 shows the cylinder pressure data with 33 % EGR, at a range of SOIm timings. The combustion is highly pre mixed indicated in the heat release plots (Figure 7.7) by the characteristic premixed spike, minimal diffusion phase and small tail phase.

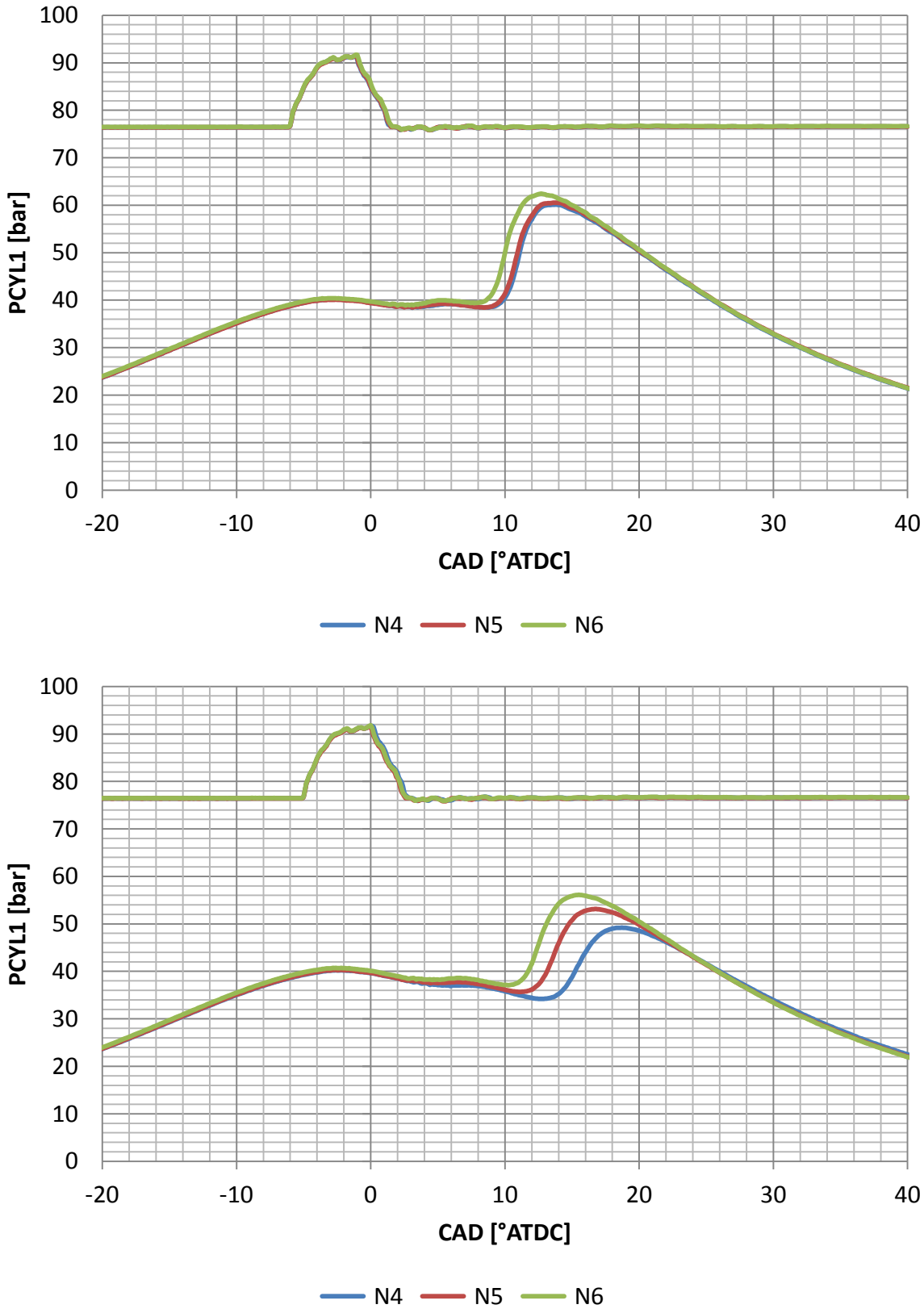

Figure 7.6 Cylinder pressure data for the nozzle study at KP2 with 33 % EGR. From top to bottom, SOIm-6 °ATDC and SOIm -5°ATDC

In each of the plots in Figure 7.6 the pressure trace for the 9 holes nozzle N6, has the most advanced phasing at each SOIm. The difference in phasing is present at KP3 and indicates that the 9 holes injector is forming an ignitable mixture sooner than the other injector nozzles. The effect is most exaggerated at -5°ATDC. The maximum pressure observed for the 9 holes injector occurs at 15.6°ATDC, whereas the 8 holes injector is 1.2° later and the 7 holes nozzle 3° later than N6. As a result, the heat rejected from the exhaust is lower and the exhaust temperature is lower.

The heat release analysis in Figure 7.7 shows that for the 9 holes injector at the most advanced timing, the start of combustion occurs 5° after the needle has closed. The remaining two injectors are 1° more retarded. This difference is more exaggerated at the most retarded timing; combustion for nozzle N6 initiates at 7° after the end of injection, N5 is 1° later and N4, 2° later.

At this key point, the injector nozzle design affects the mixture formation process. Smaller and more numerous holes result in a reduction in isCO and isHC as well as a small gain in efficiency up to a maximum of 2 % improvement at 33 % EGR from N4 to N6. The reduction in exhaust temperature, the emissions data and the cylinder pressure data suggests that for the same SOIm, the more holes the nozzle has, the earlier an ignitable mixture can be formed. The combustion phasing becomes more advanced, which explains why the 9 holes nozzle is less sensitive to a timing retard than the 7 hole injector.

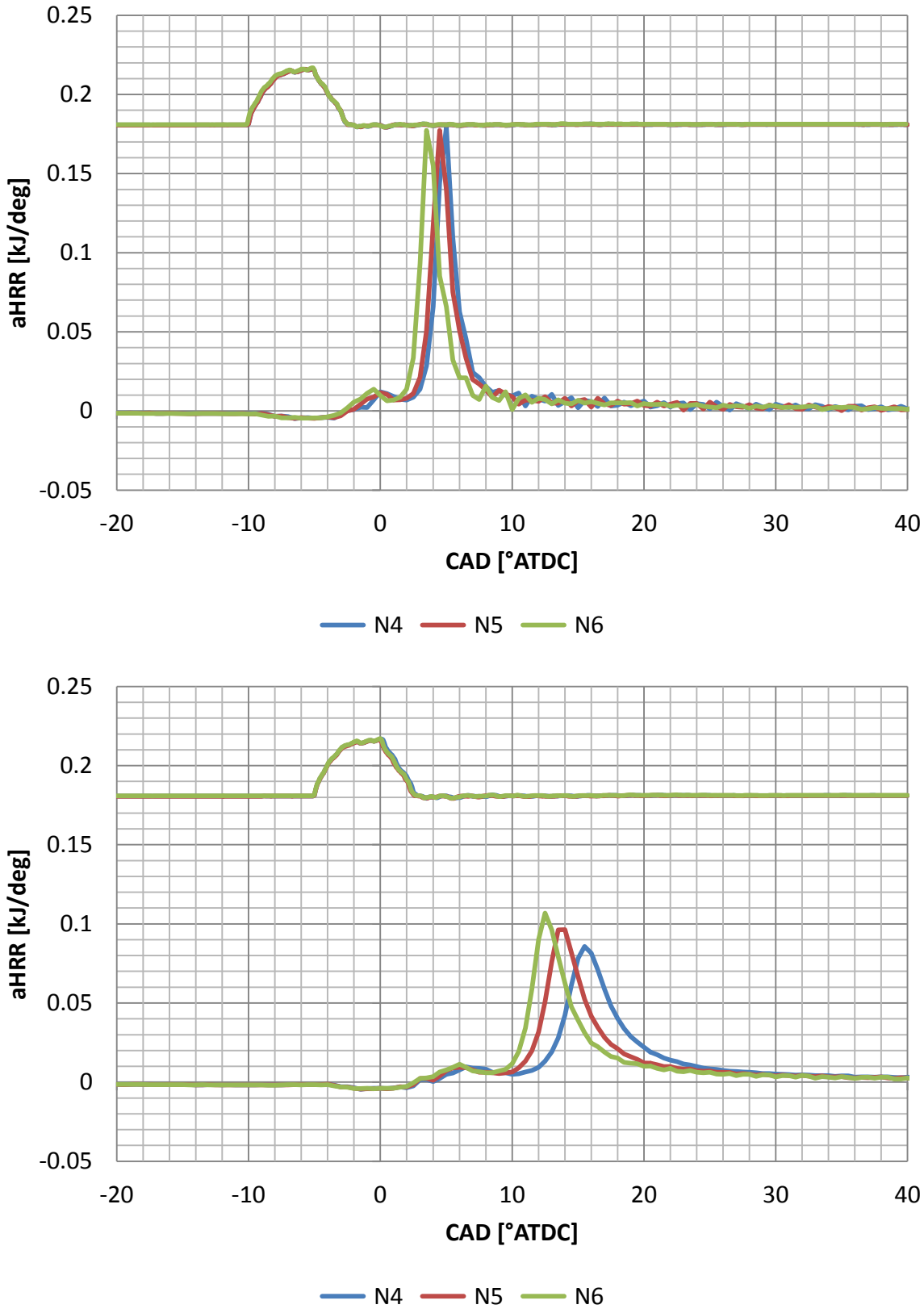

Figure 7.7 aparent net heat release data for the nozzle study at KP2 with 33 % EGR. From top to bottomSOIm-6 °ATDC and SOIm -5°ATDC

7.1.3 KP1 Test

The following table shows the test conditions used in the testing of the injector nozzles at KP1. The testing process was the same process used in the characterisation of the bowl designs. At this key point the SOIm was changed in increments of 1°.

Test name	Speed	Load	Intake temp	Intake pressure	EGR rate	Exhaust Pressure	Pilot SOI	Rail pressure	SOIm range
	RPM	GIMEP	°C	barA	%	°C	°ATDC	bar	°ATDC
KP1 test	1500	3	62.7	1.03	33.5	1.16	N/A	600	-10,-9,-8,-7
			70.2		38.2	1.14			

Table 7.4 KP1 test settings used in the nozzle study

The trend observed, at the other key points, for an improvement in either emissions output or isFC when the nozzle hole number increases from 7 holes change at KP1. The isFC was the lowest for nozzle N4 at both EGR rates apart from the most advanced timing for nozzle N6 at 33.5 % EGR. Across the entire range of SOIm at 38.2 % EGR, nozzle N6 isFC is 2.9 % to 3.5 % higher than nozzle N4, whilst at the most advanced timing, the isFC for nozzle N4 is 218 g/kWh compared to 224.5 g/kWh for nozzle N6. isNOx levels are comparable at 1.22 g/kWh for N6 and 1.25 g/kWh for N4. The trend is the same for the comparison of nozzle N4 with N5, but the magnitude of the difference is smaller, 2 % to 1.7 %. At the most advanced timing nozzle N5 has an isFC of 219.9 g/kWh, a difference of 0.8 %.

The smoke emission is low for all injector nozzles tested. The 0.05 FSN resolution of the smoke meter means that no discernible difference can be inferred from this testing. As with KP2, conditions are ideal to avoid forming particulates.

A result of the highly premixed combustion is that the emission of isCO and isHC increase. At KP1, isCO is the lowest for N4 across the range of SOIm timings at both EGR rates. At the highest EGR level, the emission of isCO for N6 is 15 % higher for all SOIm timings compared to N4. At the most retarded SOIm, where the difference is the largest, N4 has an isCO emission of 24.3 g/kWh compared to 27.9 g/kWh for N5 and 29.5 g/kWh for N6.

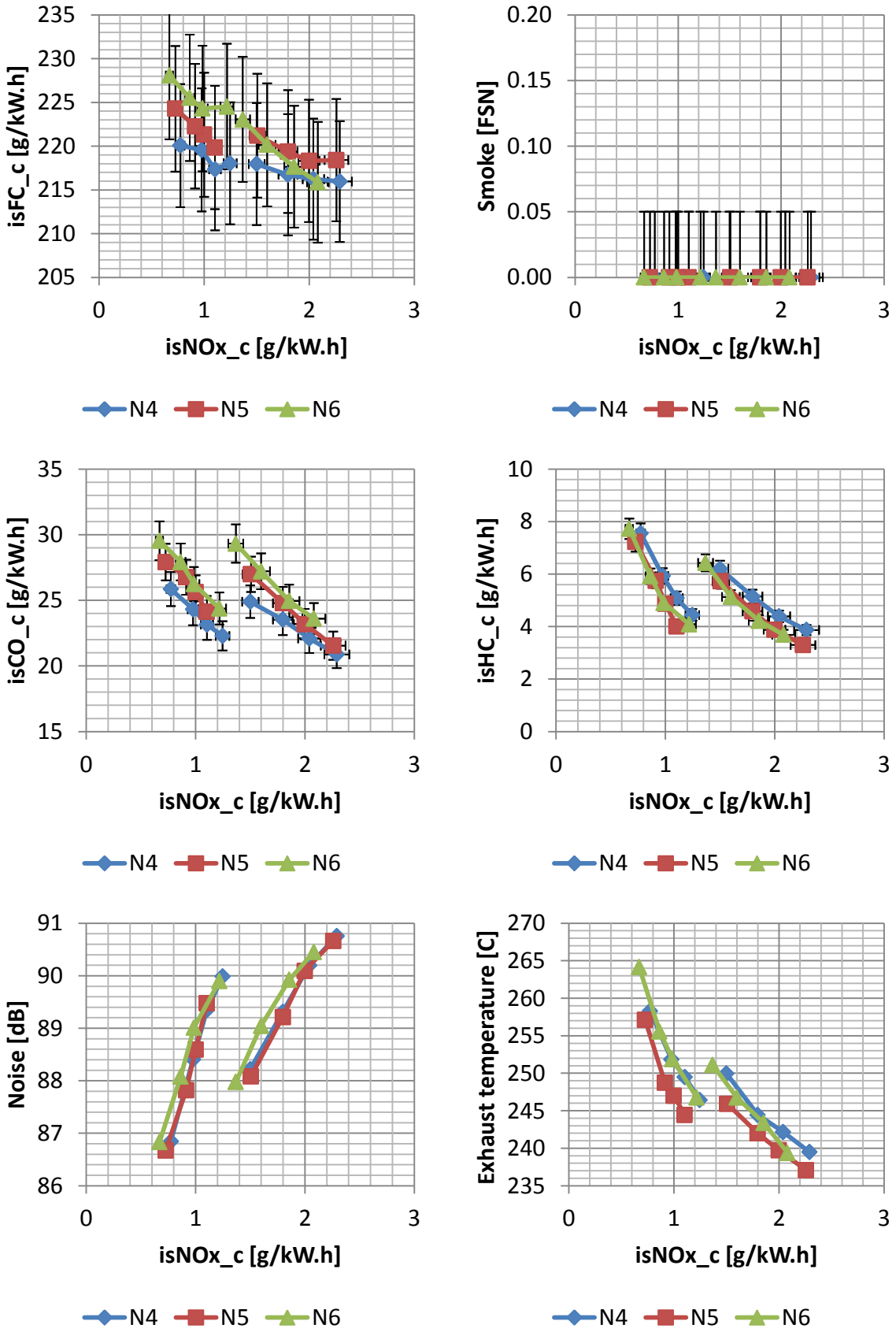

Figure 7.8 Test data for the comparison of nozzle design at KP1

The emission of isHC at this test point is the lowest for nozzle N5 at the most advanced SOIm, at 38 % EGR. The isHC is 4 g/kWh for N5 and 4.1 g/kWh for N6. This is a difference of 2 %. N4 isHC emission is 4.44 g/kWh which is 10.9 % higher than nozzle N5. The curve of isNOx against isHC with the variation in SOIm is similar for N5 and N6 whereas N4 is higher.

The noise emissions for all nozzles at the highest EGR rate are similar for all SOIm. At 33 % EGR N6 appears to be on a different curve of lower noise and isNOx for the same SOIm. The differences in the values are small indicating that combustion noise is not affected by nozzle geometry as significantly as the other parameters.

Figure 7.9 shows the in-cylinder pressure data for SOIm timings of -10 °ATDC and -7 °ATDC. At this key point the needle is not fully ascending during the injection event because the fuel injection period is short (around 550 µs to raise and lower the needle).

The pressure traces for both SOIm timings show only small differences between them compared to the previous key points. The delay between the needle closing and the peak pressure is larger at this key point, occurring 12° after the end of the injection event for the most advanced timing. At the most retarded timing the delay increases moderately to 12.5°ATDC.

Figure 7.10 shows the calculated rate of heat release data for all of the nozzles tested. At the most advanced timing, N4 and N6 has a peak value of 0.077 kJ/deg and N5 is lower at 0.074 kJ/deg. There is little difference in the traces at the most retarded SOIm, with the traces overlaying and achieving the same peak value 0.06 kJ/deg. Combustion at this key point is similar at all conditions, which makes the difference in emissions outputs of the engine difficult to interpret. Nozzle N4 is the best performing in terms of isFC, but it is not possible to identify the reasons why this is the case from this data.

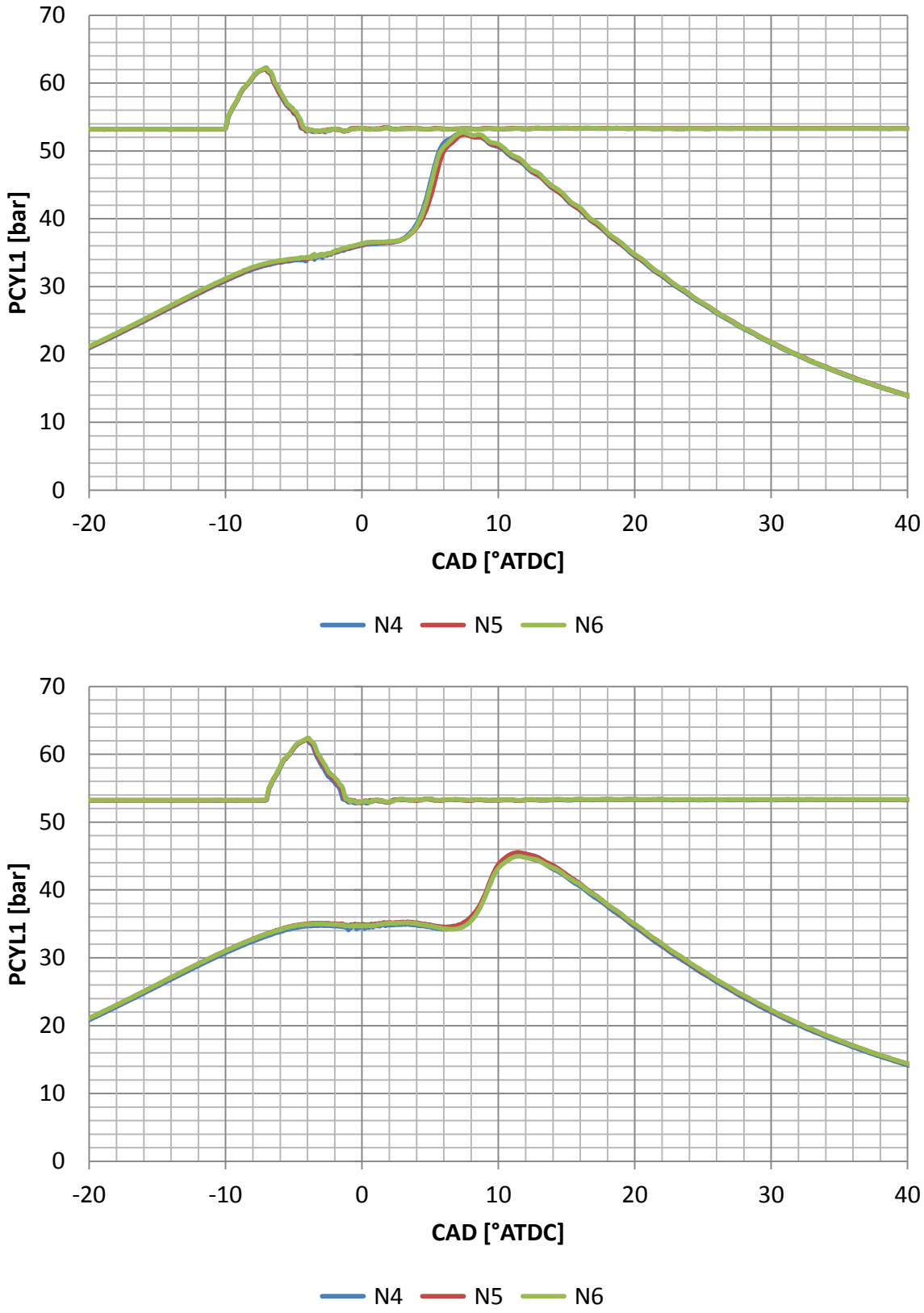

Figure 7.9 Cylinder pressure data for the nozzle study at KP1 with 38 % EGR. From top to bottom, SOIm -10 °ATDC and SOIm -7°ATDC

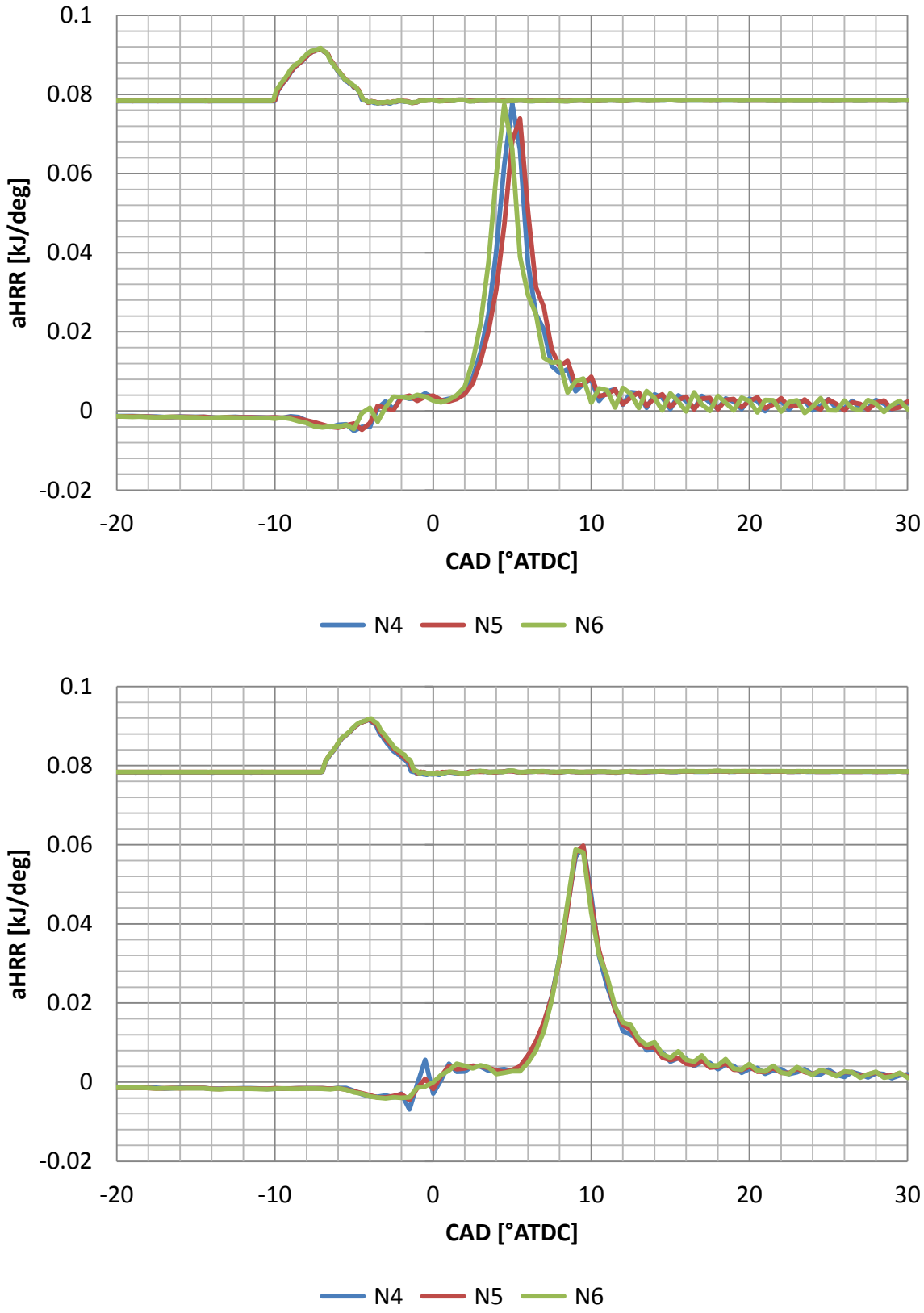

Figure 7.10 Apparent net heat release rate data for the nozzle study at KP1 with 38 % EGR. From top to bottom, SOIm SOIm-10 °ATDC and SOIm -7°ATDC

7.1.4 4000FL Test

The following Table 7.5 shows the test conditions at 400FL. The testing process was the same process used in the characterisation for the full load testing. At this key point the inlet manifold conditions were fixed and the SOIm was changed by increments of 2° at a time.

Test name	Speed	Load	Intake temp	Intake pressure	EGR rate	Exhaust Pressure	Pilot SOI	Rail pressure	SOIm range
	RPM	GIMEP	°C	barA	%	°C	°ATDC	bar	°ATDC
4000 FL	4000	21.4	46.5	2.38	N/A	2.58	N/A	2000	-19,-17, -15,-13

Table 7.5 Test settings used in the nozzle study at 4000FL

Figure 7.11 shows the engine data from the nozzle study at 4000FL. There is little difference in isFC at this test point, nozzle N6 has a fractionally higher output across the range of SOIm timings. N4 has the lowest isFC of 188.5 g/kWh at the most advanced SOIm increasing to 191.8 g/kWh at the most retarded timing. N6 is 0.6 % to 0.8 % higher for all but the most retarded SOIm where the difference increases to 1.7 %. N5 follows the curve of N4 within ±0.1 % until the most retarded timing where it is 0.48 % higher than N4.

The smoke response shows that for all but the most advanced SOIm N6 has the worst smoke output. At the most retarded timing the smoke number is 1.62 FSN compared to the best nozzle N4, which is 0.77 FSN. The response at the most advanced timing for N4 and N5 shows that N5 has the lowest overall smoke output of 0.35 FSN, but it is the most sensitive to the timing retard increasing to 1.54 FSN. N4 is more consistent in terms of smoke output, only increasing at -15°ATDC (0.51 FSN) and -13°ATDC (0.77 FSN).

N6 has the worst curve for isCO at all but the most advanced SOIm where the isCO is 1.37 g/kWh. At the advanced timing, the best isCO is N5 at 1.21 g/kWh and N4 is higher at 1.43 g/kWh. For nozzle N4, the isCO improves from the advanced timing for all but the most retarded timing even as the AFR was reducing. Nozzle N5 is similar but only improves as the timing is retarded by 2°.

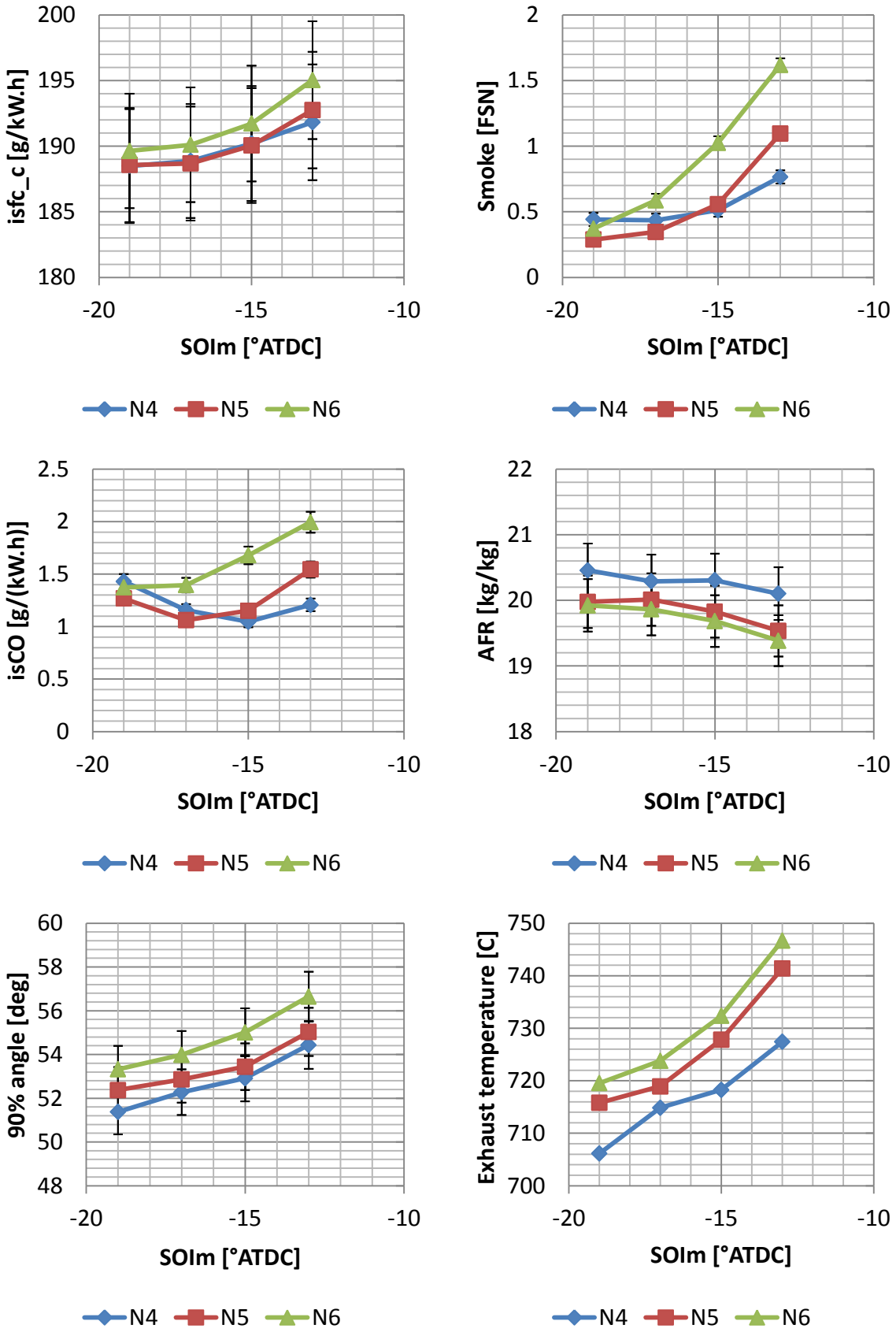

Figure 7.11 Test data for the comparison of nozzle design at 4000FL

The trend for exhaust temperature shows that as the nozzle hole number increases and the hole size reduces the exhaust temperature increases. More heat is rejected through the exhaust due to an increase in burn duration. The 90 % burn angle plot shows that combustion duration increases by 2° for N6 compared to N4.

Figure 7.12 shows the cylinder pressure data and the needle lift schematic for the most advanced and retarded SOIm timings at 4000FL. The injector is open for a significant period at this test point (1400 µs), which means that liquid fuel was being injected during the majority of the combustion event. The end of the injection event was at 25°ATDC for the most retarded SOIm tested. Combustion is highly diffusive, differing from the part load combustion behaviour.

In terms of the pressure traces seen in Figure 7.12, it appears that there is little difference between the nozzles at either operating condition. The combustion duration was marginally longer for the 9 holes injector (see Figure 7.11) leading to higher exhaust temperatures observed.

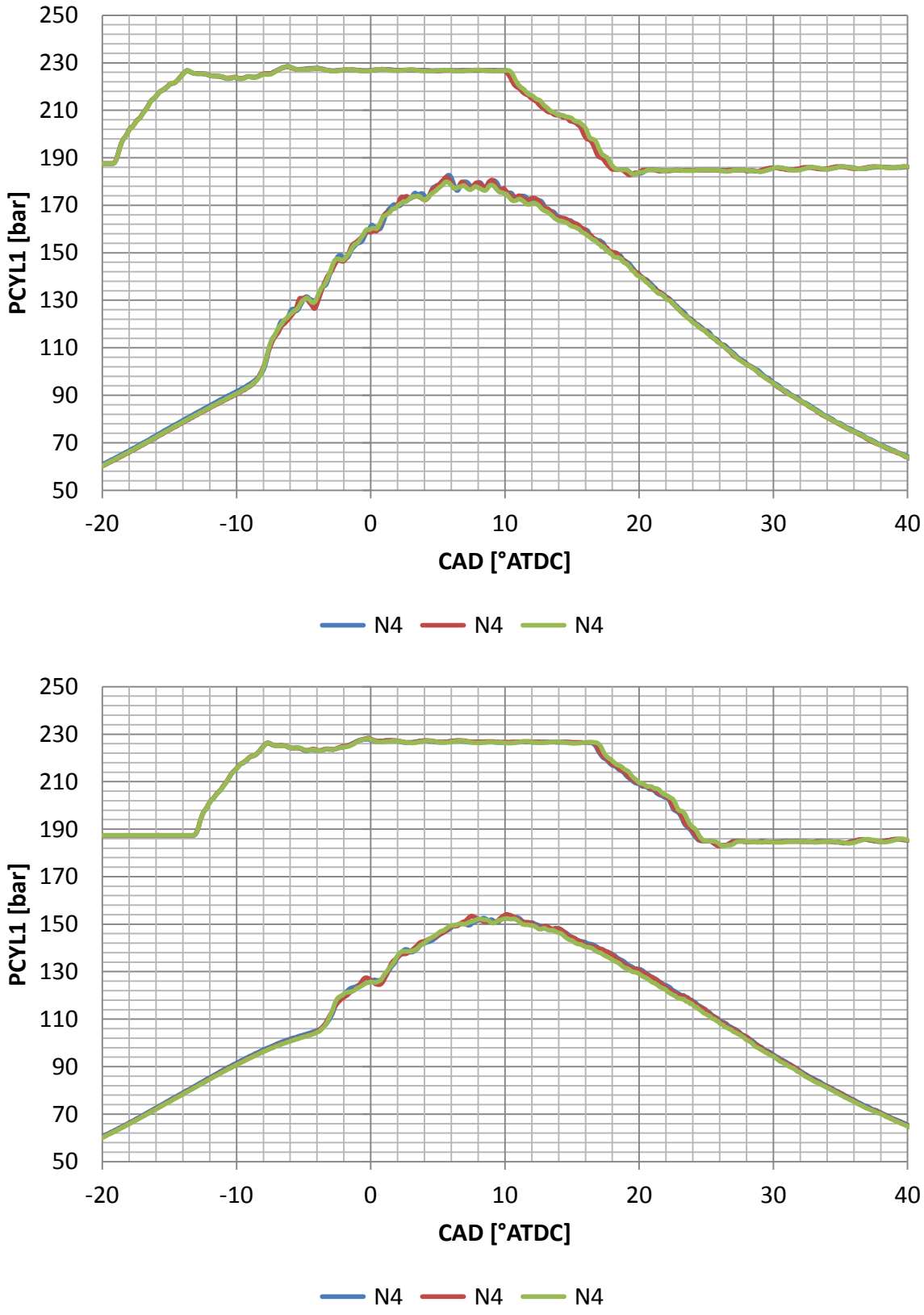

Figure 7.12 Cylinder pressure data for the nozzle study at 4000FL. From top to bottom, SOIm -19 °ATDC and SOIm -13°ATDC

7.1.5 2000FL Test

The following Table 7.6 shows the test conditions at 400FL. The testing process was the same process used in the characterisation for the full load testing. At this key point the inlet manifold conditions were fixed and the SOIm was changed by 2° at a time.

Test name	Speed	Load	Intake temp	Intake pressure	EGR rate	Exhaust Pressure	Pilot SOI	Rail pressure	SOIm range
	RPM	GIMEP	°C	barA	%	°C	°ATDC	bar	°ATDC
2000 FL	2000	24.0	52.4	2.41	N/A	1.45	N/A	2000	-8,-6,-4,-2

Table 7.6 Test settings used in the nozzle study at 4000FL

Figure 7.13 shows that nozzle N6 has the best isFC for all but the most advanced timing. N4 and N5 have similar curves with N5 having the highest isFC at all but the most retarded timing. N6 has the lowest isFC of 206 g/kWh at -6°ATDC, N4 is 0.4 % higher at 206.8 g/kWh and N5 is 0.7% higher than N6. There is no real trend for isFC with nozzle hole number and the differences in isFC are all less than 1 % at this key point.

The smoke plot at this key point shows that increasing the number of nozzle holes results in a reduction in smoke. Nozzle N4 has the highest smoke number of 0.5 FSN at the most advanced SOIm. For nozzles N4 and N5, the smoke number reduces up to the most retarded timing where it stays the same. For nozzle N6 the smoke number does not vary more than 0.02 FSN for all SOIm timing, indicating that SOIm has little effect on the smoke emission.

isCO reduces for nozzle N5 and N6 as the SOIm retards, nozzle N4 reduces and then increases again at the most retarded timing. Nozzle N6 has the highest isCO of 4.26 g/kWh at the most advanced timing but this reduces by 65 % as the SOIm retards.

At the most retarded timing for all injectors there is an increase in isFC and exhaust temperature, with a decrease in isCO and smoke. This indicates that as the SOIm retards the efficiency deteriorates as expected but the mixture formation process improves, reducing the fuel conversion efficiency losses. The exhaust temperature differences between each nozzle are small, less than ±1 % in all cases. Nozzle N4 has the highest exhaust temperature for all SOIm timings.

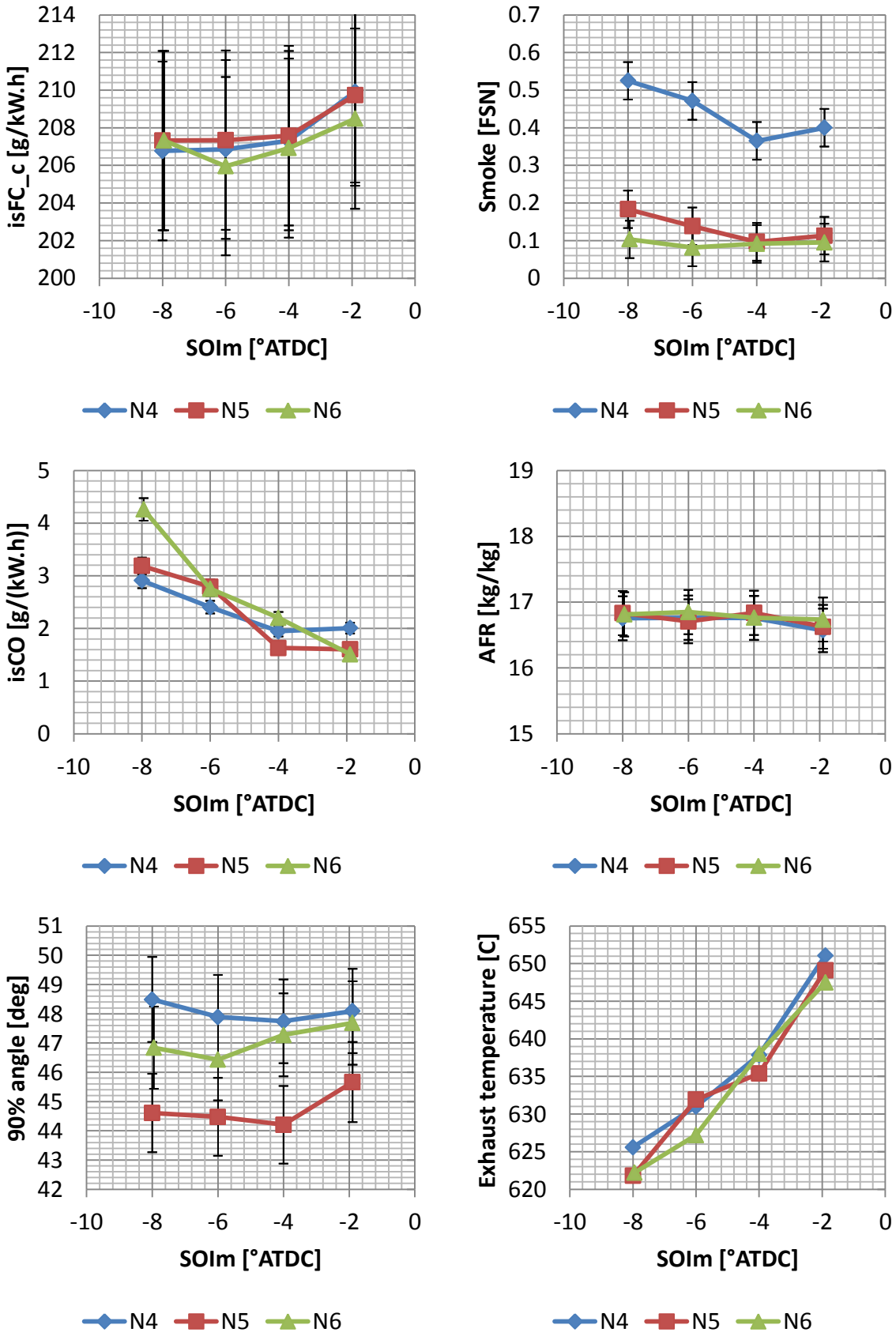

Figure 7.13 Test data for the comparison of nozzle design at 2000FL

The cylinder pressure data in Figure 7.14 shows the most advanced and most retarded SOIm timings. The injection duration at this key point is long (1500 µs) and liquid fuel is injected during the combustion event.

There are small differences in the pressure traces between each of the nozzles, with N4 having the lowest maximum cylinder pressure of 154.3 bar. Nozzle N6 has the highest cylinder pressure of 159.4 bar. Maximum cylinder pressure at all SOIm timings is around 2.8 % - 3.3 % higher for N6 than N4. Typically this indicates that combustion is more diffusive for nozzle N4, which could explain the difference in smoke output observed between both injectors.

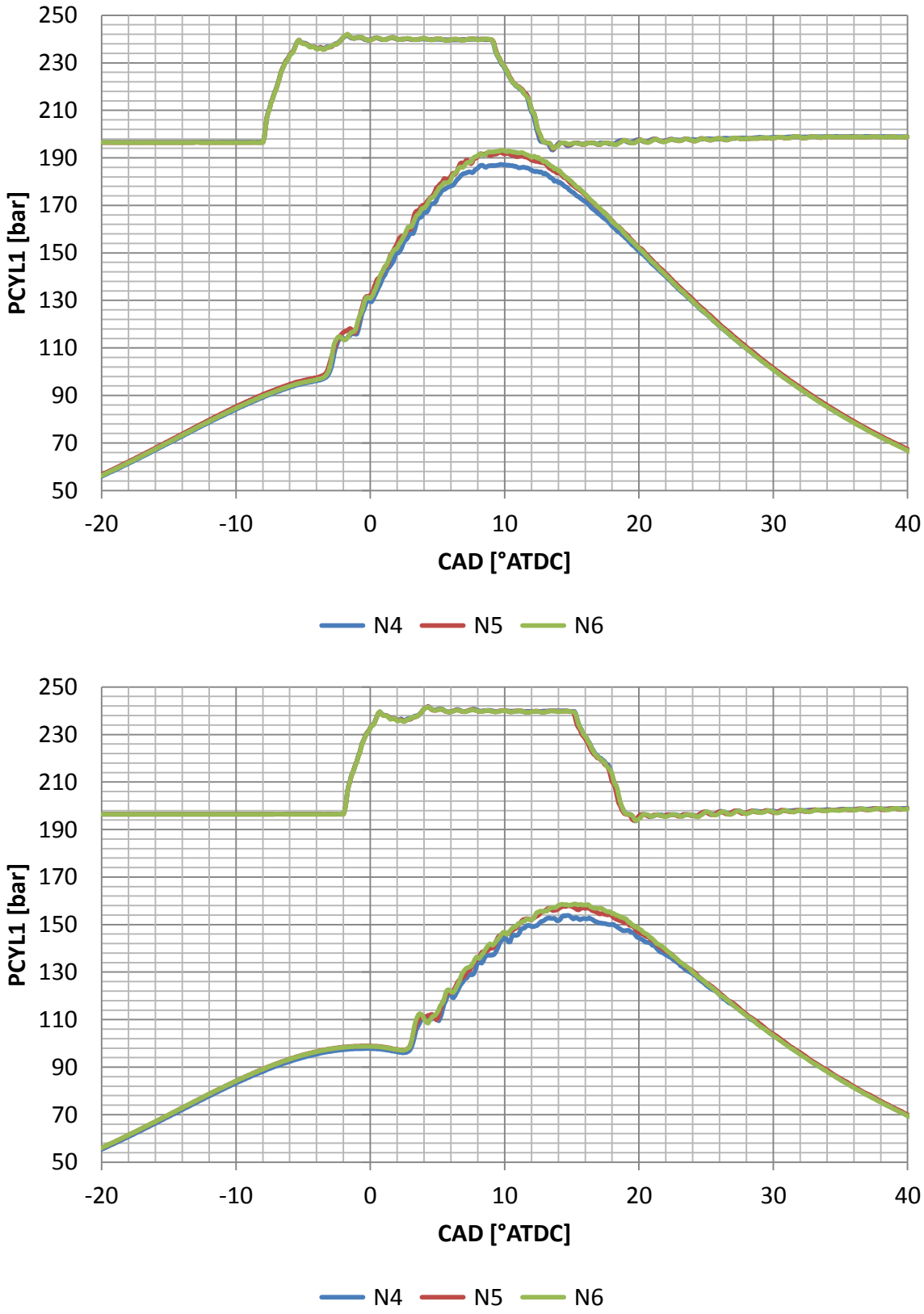

Figure 7.14 Cylinder pressure data for the nozzle study at 2000FL. From top to bottom, SOIm -8 °ATDC and SOIm -2°ATDC

7.2 Conclusions of the Injector Nozzle Study

In the nozzle study at part load, the data shows that generally there is little or no difference in the thermal behaviour of the engine, within the limits of accuracy, when the number and size of the holes in the injector nozzle of the prototype system are changed. For key points KP2 and KP3 the SOIm curves of isNOx versus isFC at each EGR conditions are similar for all nozzles.

At KP3, the isFC for the nozzle with 9 holes is higher by 1.34% at the lowest EGR rate, but as the EGR rate increases the isFC for all nozzles is similar until the timing is retarded. The isFC is better for the nozzle with 9 holes as it forms an ignitable mixture sooner than the other nozzles. This means that combustion is more stable with the 9 hole injector upon a timing retard. When the number of holes increases, the combustion mode appears to change to LTC, where isNOx and Smoke simultaneously reduce as the SOIm retards.

At KP2, the isFC for the 9 hole nozzle improves relative to the nozzles with 7 and 8 holes and in general as the number of holes increases then the isFC improves. The smoke number is small for all injectors at this key point meaning that there is no effect on smoke when the number of nozzle holes is reduced. The other pollutants, such as isCO and isHC reduce when the number of nozzle holes increases at this key point. For the same SOIm for each nozzle, the number of nozzle holes advances the combustion phasing, meaning that the combustion remains stable when the SOIm retards.

At the lowest load key point KP1 the trend is different to KP2, the isFC is highest for the nozzle with 9 holes at the highest EGR rate. When the EGR rate is 33.5 % the nozzle with 9 holes has the lowest isFC but as the timing retards the isFC is the highest. It is not clear as to why this occurs with the nozzle with 9 holes. The isFC at the highest EGR rate increases as the number of nozzle holes increases.

At 4000FL the isFC, smoke and isCO are highest for the 9 holes nozzle. There is no observable trend with increased hole numbers for the nozzles at this key point. Combustion is slower as the number of nozzle holes increases, which is reflected in the 90 % burn angle and the exhaust temperature. When the speed is the highest, the smaller droplets and increased number spray plumes is detrimental to the distribution of fuel and to the

combustion. This is not the case at 2000FL, even when the AFR is low due to the increased load, there is enough time for combustion to complete when the hole number increases.

Overall at part load, the increased number of holes results in the lowest pollutants but there is a compromise in isFC. When the load is lowest at KP1 there is no smoke production, which means there is no benefit having the 9 hole injector. As the load increases however the smoke number reduces at the most retarded SOIm for an equivalent isFC. Testing at higher part load speeds that are still NEDC relevant would indicate whether using the injector is suitable. At full load when the speed is 4000 RPM there is a marginal increase in isFC and smoke with the injector with 9 holes. This indicates an increase in the number of holes is detrimental at higher speeds and loads. As with the bowl selection there has to be a compromise between full load and part load operation. The priority for vehicle certification has to be with the performance of the injector nozzle holes at the part load condition, which means that for lower engine output emissions the nozzle with more holes is better.

8 The Effect of Pilot Injection Event on Unconventional Combustion Systems

The following section presents the results of the investigation into the performance of the optimum combustion system bowl B4, with a pilot injection added. The objective of the characterisation process, reported in chapter 5, was to identify the combustion chamber design which had the best combination of efficiency and emissions over the range of speed and load conditions tested. In this investigation a single injection event was used with the start of injection SOIm and fuel quantity varied, and all other engine variables fixed. In this chapter results from an investigation into the effects of pilot timing, pilot size and separation on the response of the unconventional combustion system are reported.

The characterisation study identified the control of the fuel penetration and ignition delay as the keys to clean and efficient operation. The optimisation of the combustion system spray targeting at KP3 (in the protrusion tests) meant that the resulting response at KP1 and KP2 had higher than normal CO and HC emissions with a resulting fuel consumption penalty (due mostly to the low fuel conversion efficiency). This was more pronounced with the conventional bowl designs. This could be a consequence of the in-cylinder conditions at KP1 and KP2 resulting in the fuel penetration being high. When coupled with poorly matched spray targeting this would cause the fuel to be distributed away from the main bowl region. This phenomenon would have the effect of increasing the ignition delay and in turn allowing the fuel to penetrate further into the quench region.

In this chapter methods for controlling the ignition delay were investigated so that when employing the idealised fuel spray targeting for KP3 the engine outputs at the lower load conditions could be improved. It was expected that this would lead to an improvement in the fuel distribution of the main injection process. Additionally, the response at KP3 was examined to establish whether any further gains in performance could be made at this condition.

8.1 Method and Definitions

Pilot size and separation were tested, with a fixed main SOIm timing. For each size and separation, a timing swing of the pilot and main was carried out to assess their interaction. Three sizes of pilot were selected; one conventional small size pilot used for noise reduction and two larger pulses used in advanced combustion modes (Tanaka et al., 2002, Carlucci et al., 2005, Choi et al., 2005, Mancaruso et al., 2008, Benajes et al., 2008, Anselmi et al., 2010). The pilot separation was selected from zero separation so that the interaction of the pilot combustion with the main injection varied.

The size of the injection can either be defined in terms of injected mass or the total duration of the injection event, which includes the opening and closing of the needle. The latter method was used in this work to define all injection events as no flow data was available for the injector. The size of the smallest pilot was selected by increasing the injection duration until the minimum opening that has an influence on the combustion process that could be achieved. The pilot size was established by measuring the fuel consumption with and without a pilot using a fixed injection duration. The in-cylinder conditions matched the key points tested for injector nozzle back pressure purposes. The pilot injected mass was calculated by taking the mass difference between a pilot and single injection. The separation for each injection was defined as the time between the end of the pilot injection event and the demand for the main injection event and is shown in the following Figure 8.1.

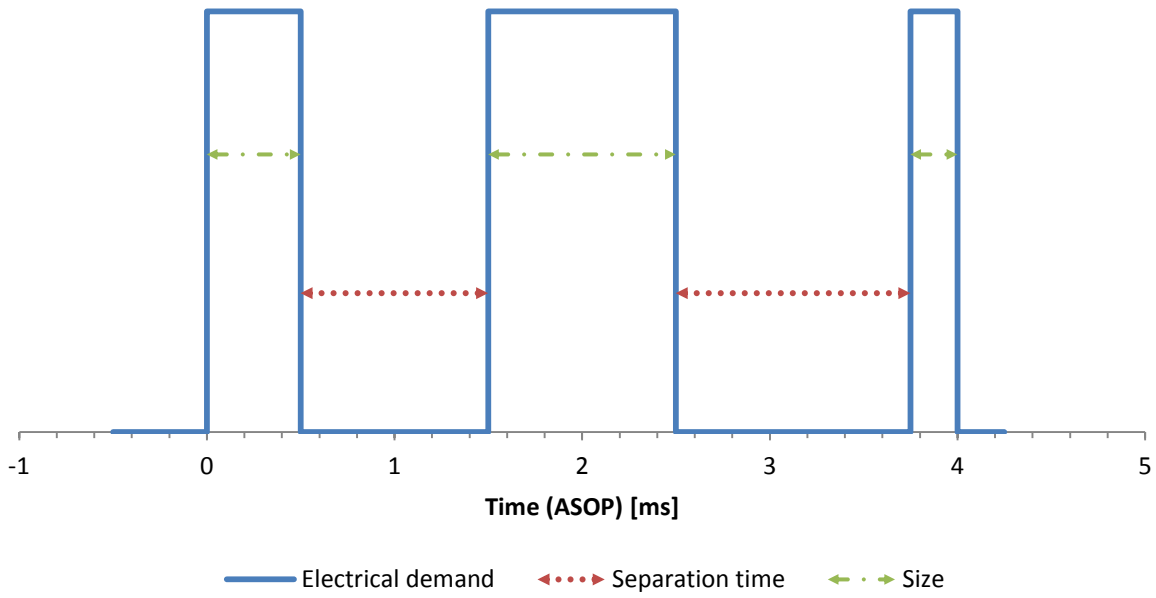

Figure 8.1 Definition of separations that were used in the study. The electrical demand for; the pilot injection is on the left, the main in the middle and the post on the right.

In order to ensure the same starting in-cylinder conditions for the pilot injection the start timing is the same for all pilot sizes. Adding a pilot has the effect of advancing the combustion process because fuel is introduced earlier in the engine cycle and the ignition delay reduces. As a result the main injection timing was retarded at each engine key point compared to the single injection case. This enabled the phasing of the combustion process to be matched with the single injection case. The pilot injection cases are compared with the single injection case from the characterisation process to assess the effect of multiple injections and the response of the unconventional piston bowl to a multiple injection strategy.

Once the pilot size and separation was set then the whole configuration, pilot and main separation and duration, was phased to perform a SOIm swing as demonstrated in Figure 8.2. The pilot injection timing was not fixed and enabled the response of the pilot to be examined over a range of in-cylinder conditions and spatial relationships with the piston bowl.

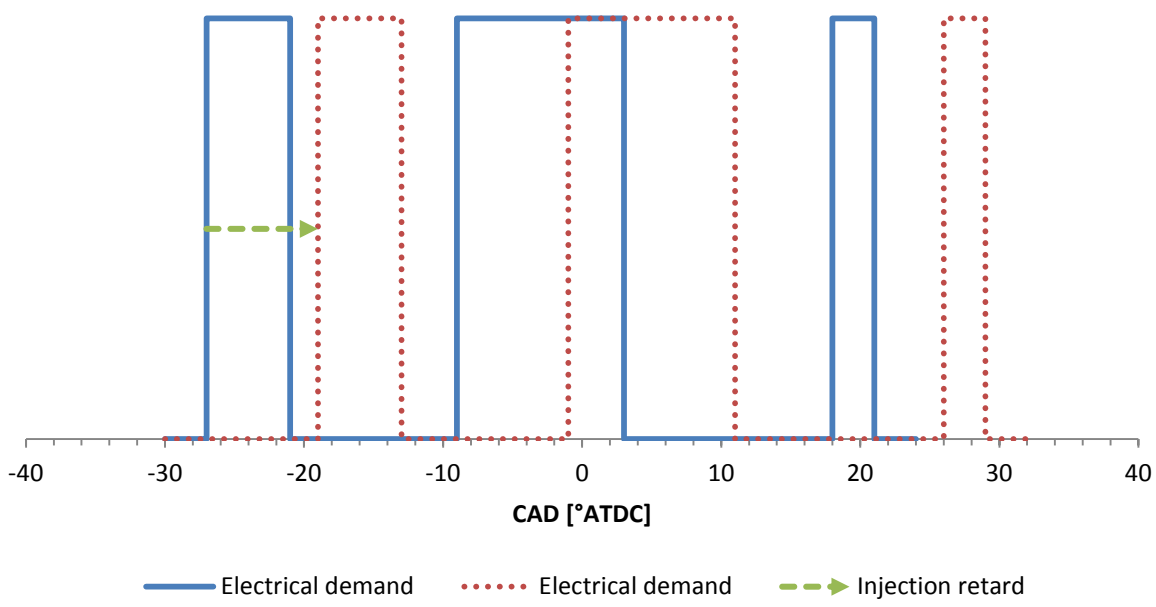

Figure 8.2 Schematic showing the process of retarding the injection event, The blue trace shows the initial set up and the dotted trace shows the set up as the timing is retarded.

8.2 Experimental Results

The cylinder pressure data in the following section is shown with a schematic of the needle lift trace for the injection event. The trace is intended to show the needle lift during the pilot injection event. An example is shown in Figure 8.3.

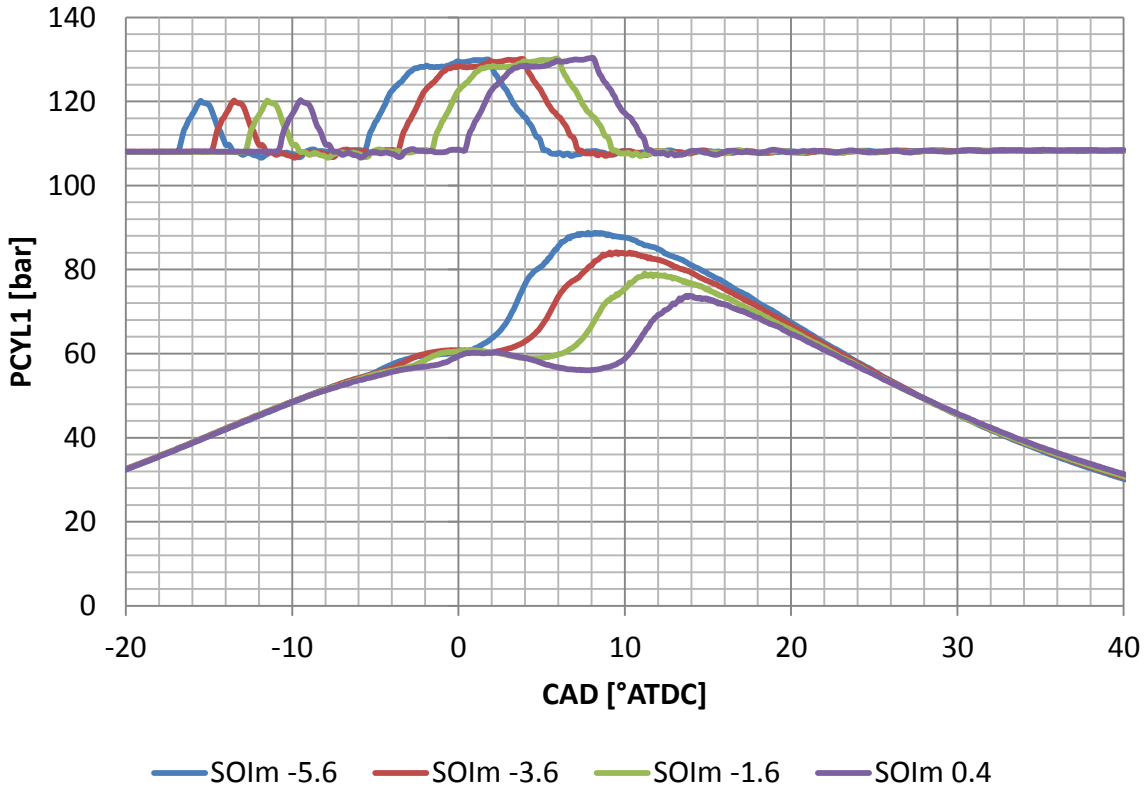

Figure 8.3 Example cylinder pressure data with pilot injection needle schematic

8.2.1 KP3 Test

The comparison points at KP3 were taken when the separation to the main injection was 800 µs and the pilot was 1.3 mg/injection. The test point data was logged and is presented in the following Table 8.1.

Test name	Speed	Load	Intake temp	Intake pressure	EGR rate	Pilot size	Pilot sep	Rail pressure	SOIm range
	RPM	GIMEP	°C	barA	%	mg	µs	bar	°ATDC
KP3 test	2000	9	41.7	1.47	26.9	N/A	N/A	1050	-9,-7, -5,-3
KP3 test-a3			42.2	1.47	27	1.3	800		-5.6,-3.6, -1.6,0.4

Table 8.1 KP3 multiple injection test settings

The pressure traces in Figure 8.4 show the differences between a single injection event and a pilot injection event. As with the protrusion and characterisation tests, the single injection event pressure trace shows that the majority of the injection event is complete before start of the pressure rise. The delay between the end of the injection event and the start of combustion increases as the injection event is retarded.

When a pilot is added and the main injection is retarded, a small proportion of heat release occurs around TDC. This causes a pressure rise and a temperature rise. The temperature rise reduces the ignition delay of the main injection event leading to more diffusive combustion. The peak of the pressure rise for the single injection event at the most advanced injection timing occurs at 5.5°ATDC with a magnitude of 101 bar compared to a peak of pressure that occurs at 8.1°ATDC with a magnitude of 89.4 bar for the most advanced multiple injection test. The gradient of the main combustion pressure rise is shallower for the pilot injection event, which is due to diffusive combustion.

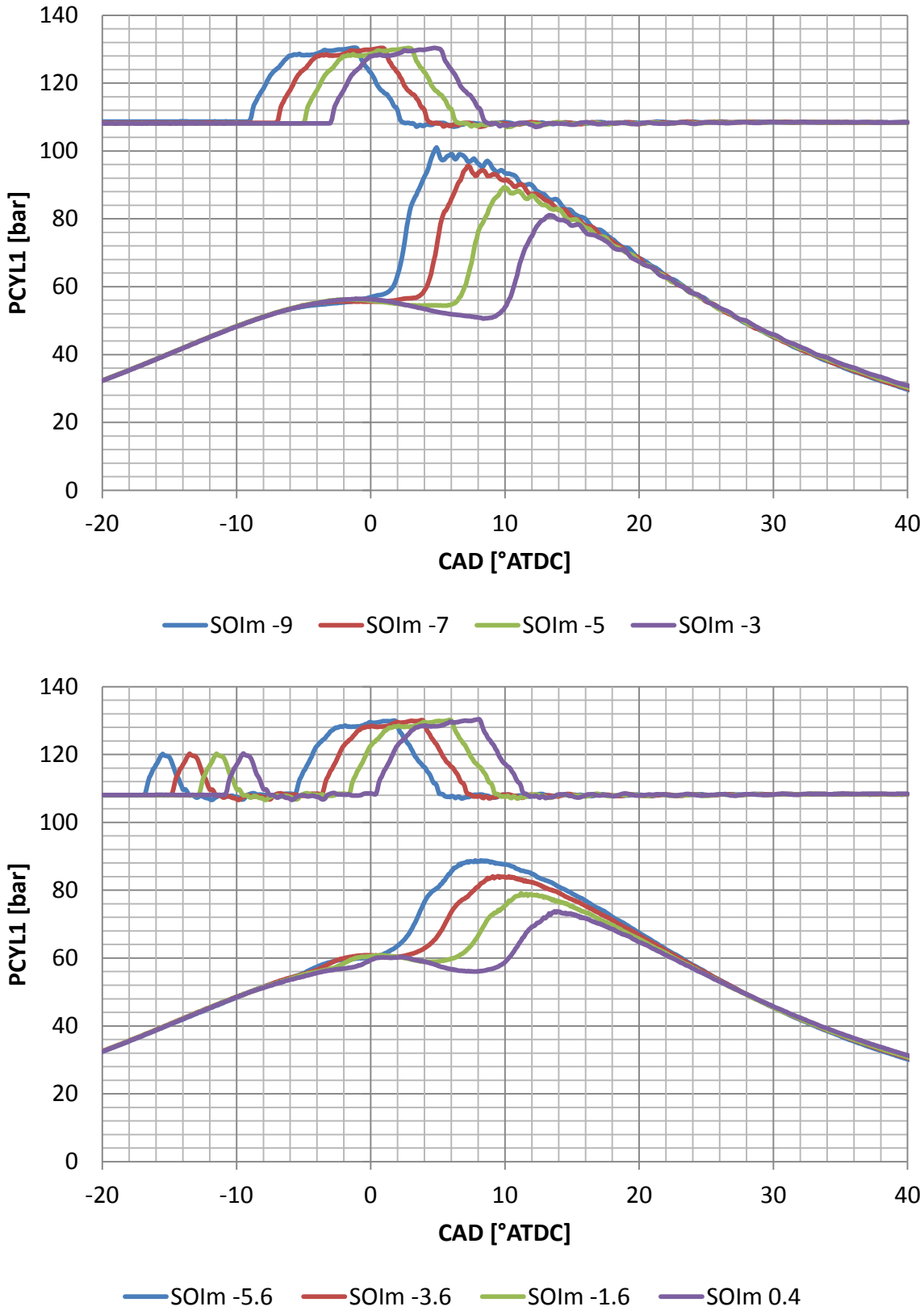

Figure 8.4 Cylinder pressure traces and injection schematics for the single (top) and pilot (bottom) cases

Figure 8.5 shows the combustion analysis for the single and the pilot injection at two SOIm conditions. The first shows the high temperature heat release starting at the same time (-2°ATDC). In the second case the SOIm was similar (-5°ATDC for the single event and -5.6°ATDC for the pilot and main event).

The first comparison shows that a small heat release occurs at -5°ATDC for the pilot injection. It also shows that the peak of heat release rate is lower for the pilot injection event. The peak is fractionally later and the tail proportion appeared larger for the pilot injection event.

When compared at a similar SOIm, the shorter ignition delay caused by the pilot injection event is apparent. The combustion of the single injection event initiates at 2°ATDC, which is a delay of 4° compared to the pilot injection event. The emissions results from the testing can be seen in the following Figure 8.6.

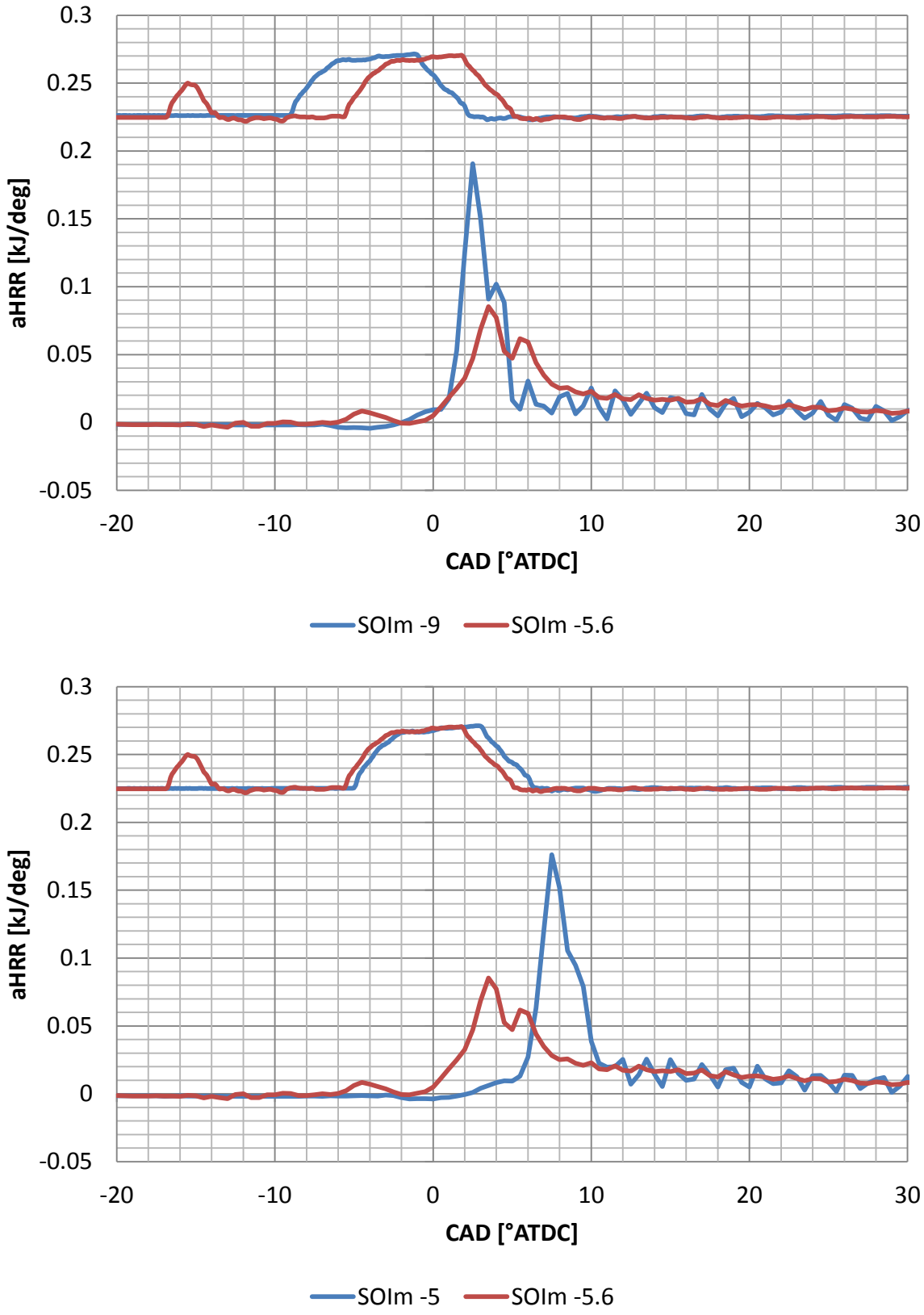

Figure 8.5 Apparent net heat release rate traces and injection schematics for the single (blue) and pilot (red) injection cases. Plots show approximately the same phasing (top) and the same SOIm (bottom)

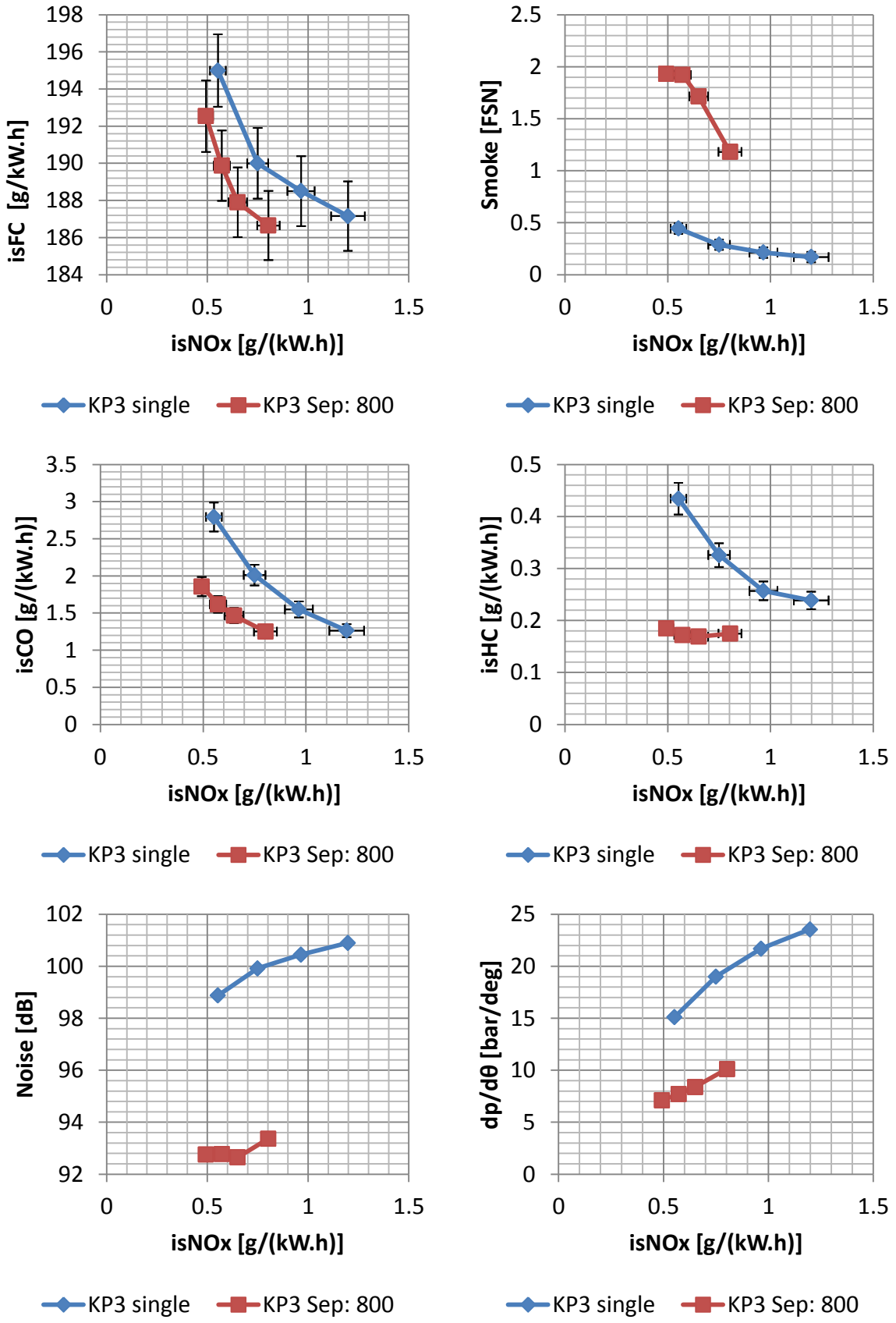

Figure 8.6 Performance and emmissions data for the single and pilot injection case at KP3

The pilot injection changes the characteristic of the emissions output compared to the single injection case. The indicators of premixed combustion for the single injection case are the low smoke number and the high HC and CO.

Figure 8.6 shows that the addition of the pilot improves the isFC by 1.5 % to 2 % over the SOIm range. When the combustion rate of heat release is reduced the heat rejection in heat transfer losses in-cylinder ($HL_{ht,C}$) is reduced thus increasing engine efficiency. At the same time, because the combustion rate is reduced, the pilot injection case is more sensitive to the timing retard meaning more heat is rejected through the exhaust. This is the same observation as the injector type test, where the lower rate of injection of the conventional system results in an improvement in isFC because heat transfer and crevice losses were reduced.

Figure 8.6 shows that the pilot injection results in rich combustion leading to the formation of particulates. At all combinations of SOIm the smoke emissions are greater than the single injection event, the largest value, 1.93 FSN occurs at 0.49 g/kWh isNOx. This is significantly higher than the single injection event which reached a maximum of 0.44 FSN at 0.55 g/kWh isNOx (SOI_m=-3°ATDC). The smoke number appears to plateau as the injection timing is retarded; the last two smoke numbers are 1.92 FSN and 1.93 FSN at 0.52 g/kWh and 0.49 g/kWh respectively.

isCO and isHC are lower than the single injection event which suggests that the combustion mode has become diffusive. Long ignition delays lead to the fuel spray becoming too lean and products of incomplete combustion such as CO and HC are formed. The isCO of the pilot injection case is 0.65 g/kWh to 1.6 g/kWh lower than the single injection case for all SOIm. The emission of isHC did not change significantly for the pilot injection case for the range of SOIm. The value varies from 0.17 g/kWh to 0.19 g/kWh, which is lower than the single injection case.

The observed reductions in pressure rise rate results in a noise reduction which is observed for all SOIm timings. At the most retarded timings for the pilot injection, the noise value is 92.8dB compared to 98.8dB for the single injection event. The reduction in combustion

noise is due to the reduction in the premixed peak, which reduces the pressure rise rate during combustion.

8.2.2 KP2 Test

The comparison points at KP2 were taken when the separation to the main injection was 1200 µs and the pilot was 6.8 mg/injection. The test points that were logged are presented in the following Table 8.2.

Test name	Speed	Load	Intake temp	Intake pressure	EGR rate	Pilot size	Pilot sep	Rail pressure	SOI_m range
	RPM	GIMEP	°C	barA	%	mg	µs	bar	°ATDC
KP2 test	1500	6	41	1.16	33	0	0	800	-10,-8,-6, -5
KP2 test - a4			42.7	1.16	33.9	6.8	1200		-4.7,-2.7, -0.7,1.3

Table 8.2 KP2 multiple injection test settings

The pressure traces in Figure 8.7 show the single and pilot injection case with EGR at KP2. For the single injection case, the combustion process is highly premixed and the injection event completes before combustion starts. At the most retarded SOIm the main pressure rise does not occur until 10° after the needle has closed. At the most advanced SOIm (-4.7°ATDC) for the pilot injection case, combustion of the main proportion of fuel initiates closer to the end of the main injection event compared to the single injection case. With the pilot, the first observed pressure rise occurs around -2°ATDC. The pressure and temperature rise reduces the ignition delay of the main injection event. The pilot injection is 41 % of the total fuel injected which makes the heat release of the pilot injection significant.

The pressure rise rate is suppressed by the pilot injection when compared to the single injection case. At the most retarded single injection condition, combustion is significantly retarded initiating at 12°ATDC. The pressure rise is suppressed at this condition because the piston expansion is significant. This is the only condition where the suppression of the pressure rise rate is less for the single injection case but this is an extreme case with a significant ignition delay for the single injection case due to the high EGR rate and retarded injection timing.

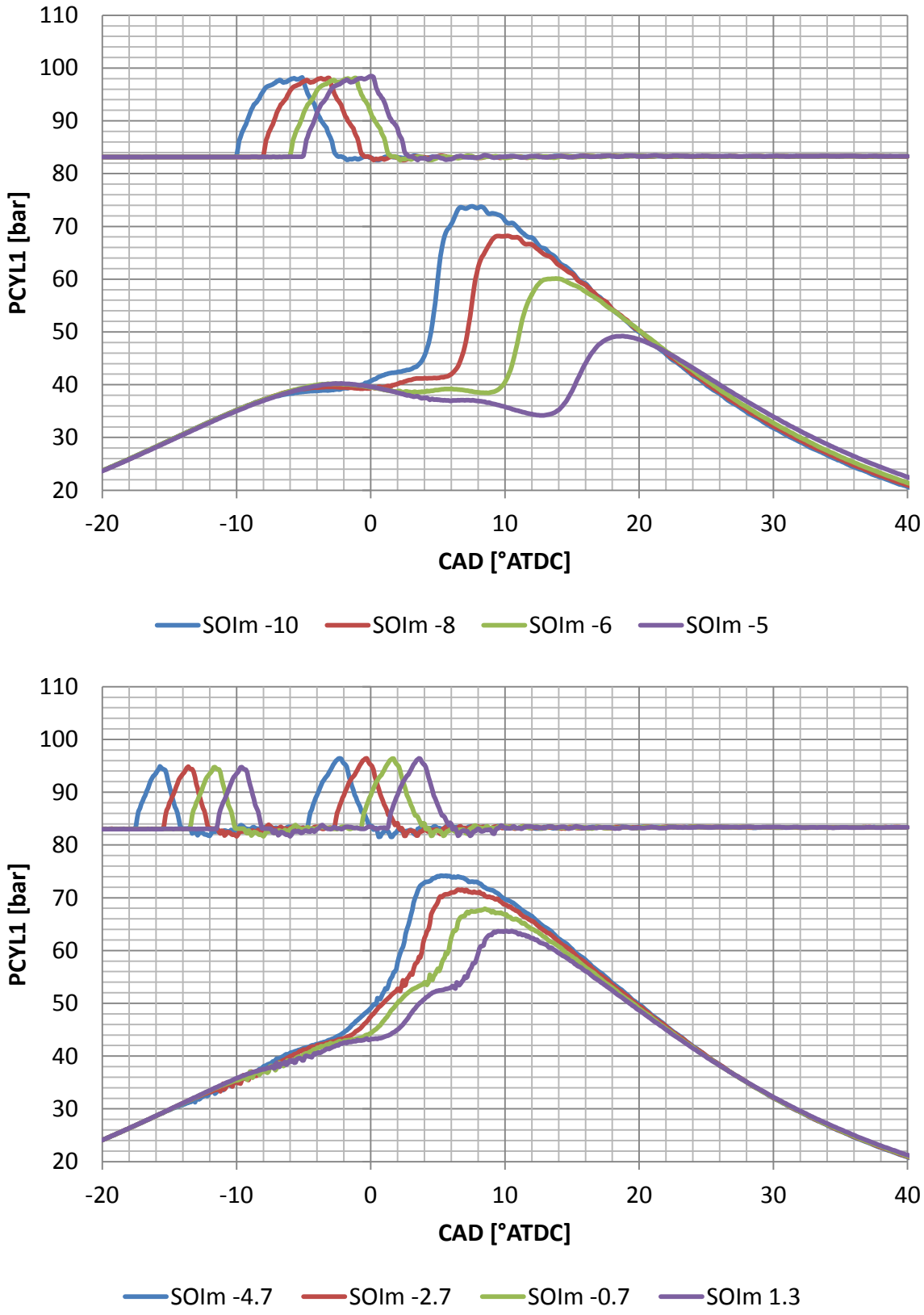

Figure 8.7 Cylinder pressure traces and injection schematics for the single (top) and pilot (bottom) injection cases

Combustion analysis shows the effect of the pilot injection. The comparison at this key point is made at two different single injection conditions. The first is the most advanced SOIm for the single injection and the pilot injection with an SOIm of -2.7°ATDC. These test points were closest in terms of combustion initiation. Figure 8.8 shows that the pilot combustion actually occurs at the beginning of the main injection event. The main injection ignites due to the combustion of the pilot, which reduces the amount of time for the mixture formation process. As a result, the peak of heat release rate is reduced, which explains the slower pressure rise rate of the pilot injection case.

The second comparison shows when the main injection of both the pilot and single injection case is approximately the same (-5°ATDC for the single case and -4.7°ATDC for the pilot case). The single injection case has an extremely long ignition delay relative to the pilot injection event. This is due to a combination of the fuel spray being lean, the lower temperature as the cylinder expands and the effect of the low oxygen concentration due to the EGR. The peak of the heat release rate is lower than the pilot injection case as the heat release rate is suppressed by the lower temperature after TDC. The effect of this change in the combustion characteristic can be seen in the emissions results that follow.

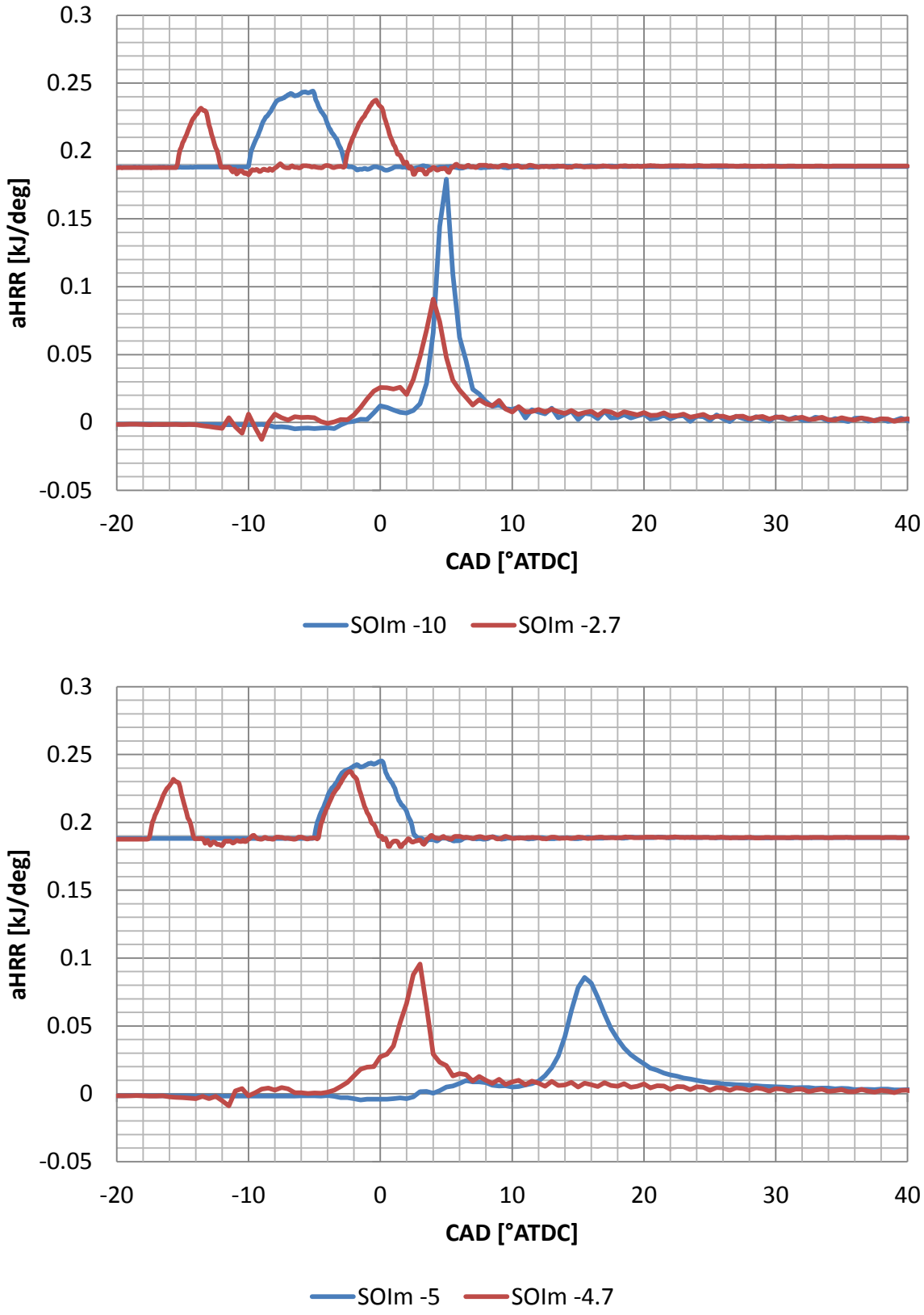

Figure 8.8 Apparent net heat release rate traces and injection schematics for the single (blue) and pilot (red) injection cases. Plots show approximately the same phasing (top) and the same SOIm (bottom)

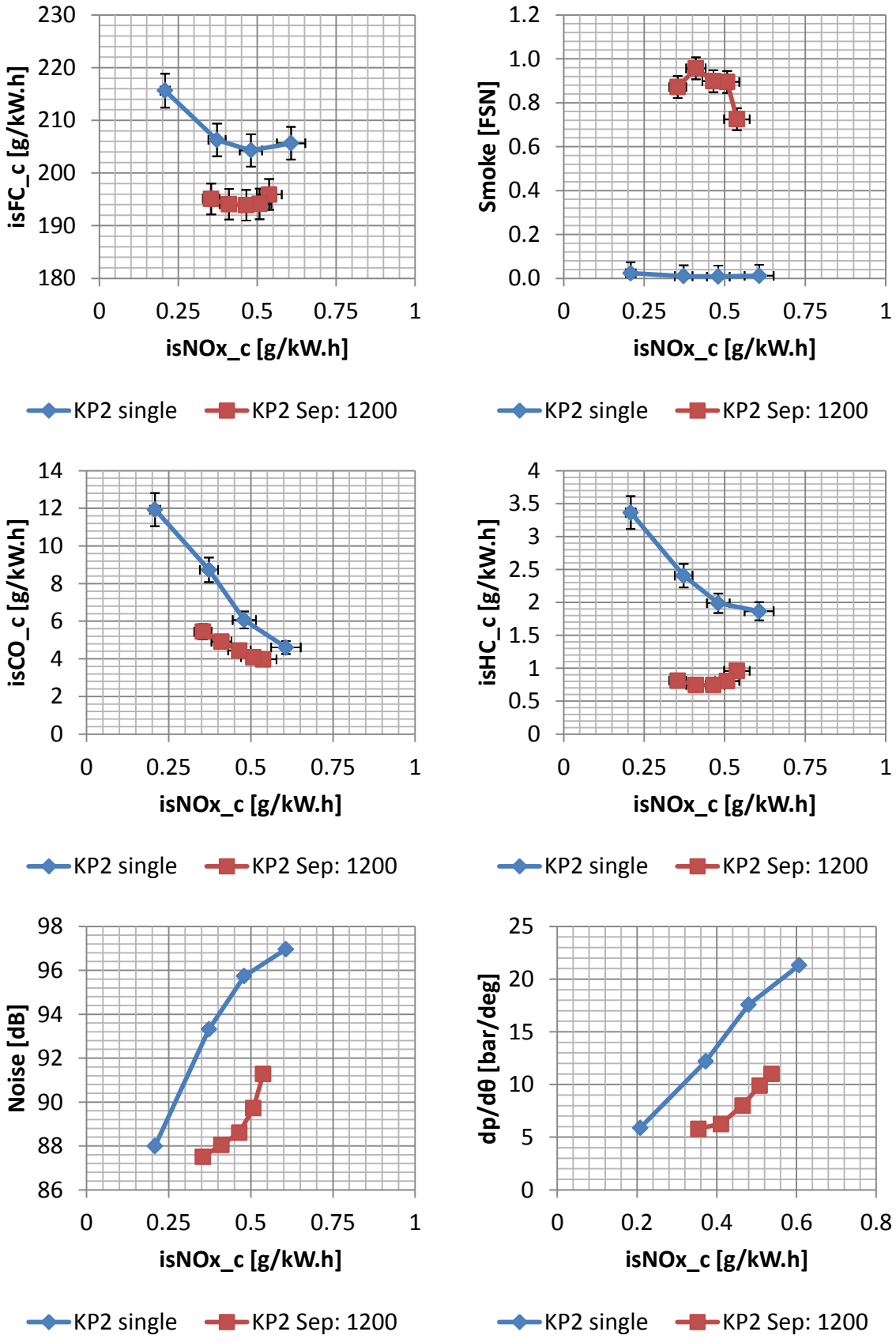

Figure 8.9 Performance and emmissions data for the single and pilot injection case at KP2

Adding a large pilot (6.8mg/injection) to the injection set up results in a significant benefit to the fuel consumption. At around 0.48 g/kWh isNOx for the single injection event, the isFC is reduced by 5.1 % by adding a pilot. The response to a retard in SOIm of the main injection (with a fixed pilot separation) is flat, varying less than 0.5 % from the most advanced to the most retarded injection.

The cylinder pressure trace indicates that this is due to the fact that combustion does not phase in the same way with the SOIm. For the single injection case, when the SOIm is retarded from -10°ATDC to -8°ATDC, -8°ATDC to -6°ATDC and -6°ATDC to -5°ATDC, the angle that the maximum pressure occurrs at (apMax) phases 2.5°, 3.7° and 4.9° respectively with each step in SOIm. For the pilot injection case, when the SOIm is retarded by 2°, apMax phases at 0.9°, 1.6° and 1.8° respectively. Combustion does not retard significantly in the pilot injection case meaning that more heat is available for conversion into work rather than being rejected into the exhaust.

For the single injection case the emission of carbon was mainly CO and HC with little smoke emission. Indeed the level of smoke measured was within the uncertainty of the smoke meter. The combustion data reflects this as the ignition delay was long and the combustion highly premixed. When adding a large pilot the effect on the smoke was significant. At 0.48 g/kWh isNOx the smoke number was 0.9 FSN for the pilot injection compared to 0.01 FSN for the single injection. The smoke number increases up to the point that the SOIm is the most retarded, when the smoke number again begins to fall.

The pilot reduces CO and HC simultaneously. The CO emission at 0.48 g/kWh isNOx falls from 6.1 g/kWh to 4.4 g/kWh. HC reduces from 2 g/kWh to 0.75 g/kWh. This was expected as the ignition delay was reduced, limiting the fuel spray penetration and over mixing before combustion initiates.

Finally, the pressure rise rate and the noise output were reduced with a pilot injection. This effect diminished as the combustion of the single injection case retarded and the pressure rise was suppressed by the gas expansion after TDC.

8.2.3 KP1 Test

The comparison points at KP1 were taken when the separation to the main injection was 1200 µs and the pilot was 1 mg/injection. The logged test points are in the following Table 8.3.

Test name	Speed	Load	Intake temp	Intake pressure	EGR rate	Pilot size	Pilot sep	Rail pressure	SOIm range
	RPM	GIMEP	°C	barA	%	mg	µs	bar	°ATDC
KP1 test	1500	3	71.4	1.03	38.2	0	0	600	-10,-9, -8,-7
KP1 test - a4			73.3	1.03	38.7	1	1200		-5.6,-4.6, -3.6,-2.6

Table 8.3 KP1 multiple injection test settings

The pressure traces in Figure 8.10 show the effect of adding a pilot injection to a single injection at KP1. The single injection cylinder pressure trace indicates that the combustion is highly premixed with a long delay between the needle closure and the main rise of the cylinder pressure. The delay is 6° for the most advanced SOIm and 8° for the most retarded SOIm.

With the pilot injection there is a shorter delay between the end of the main injection and the start of the cylinder pressure rise due to pilot combustion. The delay between the end of the injection and the start of the main heat release for the most advanced SOIm is 0.5°. It is the same delay at all SOIm. The pressure rise rate and maximum cylinder pressure are both reduced by adding a pilot injection when the combustion is phased identically. For the single injection case, at an SOIm of -10°ATDC the maximum cylinder pressure of 52.7 bar occurs at 7.4°ATDC, for the pilot injection, the maximum cylinder pressure is 49.7 bar and occurs at 8.2°ATDC.

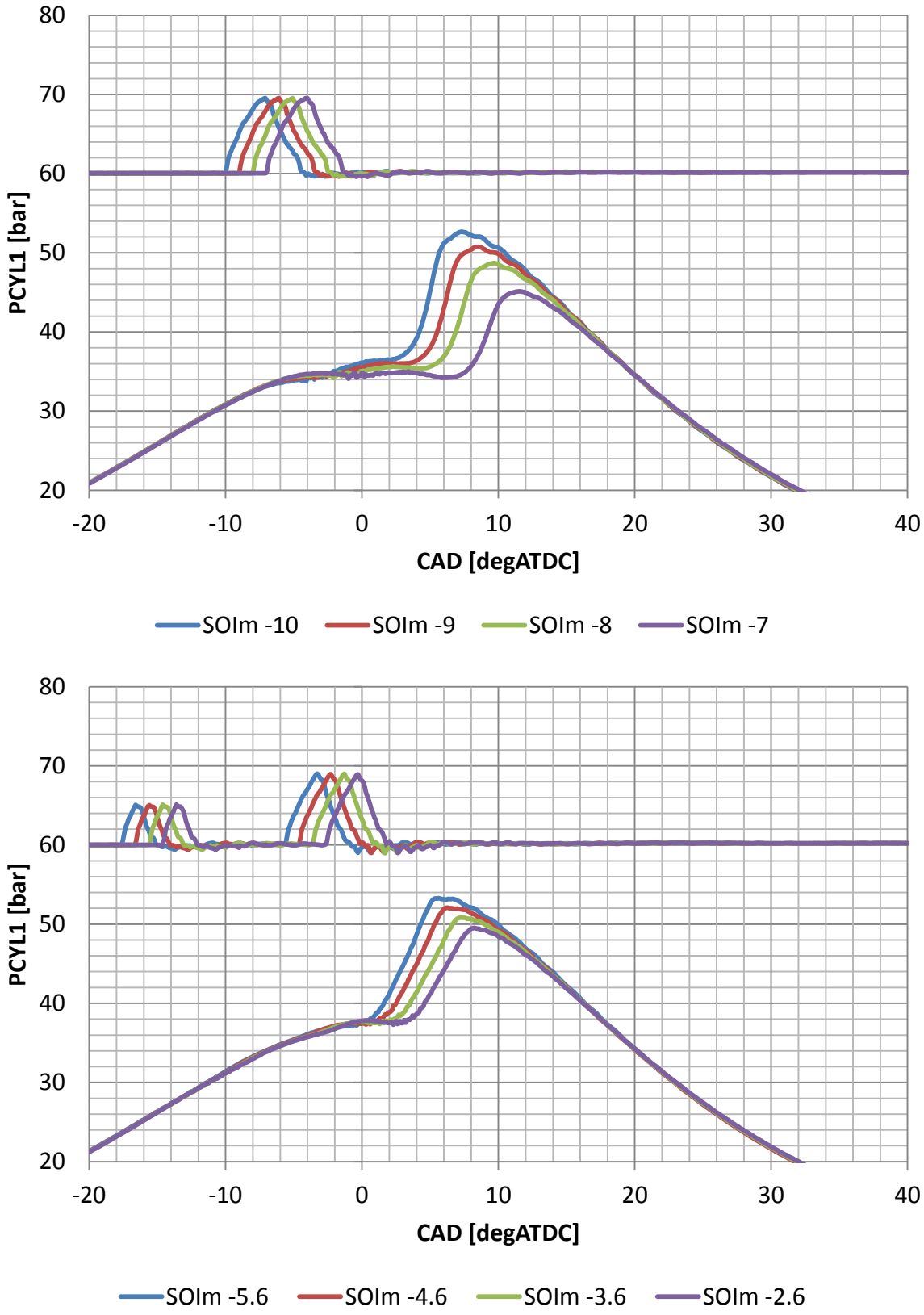

Figure 8.10 Cylinder pressure traces and injection schematics for the single (top) and pilot (bottom) injection cases

Combustion analysis shows the effect of adding a small pilot to KP1. Figure 8.11 shows that when combustion is phased the same the peak of heat release is lower for the pilot injection. The pilot injection appears to release heat just before TDC around the time of the main injection event. The reduced ignition delay of the main injection reduces the time available for fuel spray penetration and over mixing.

When the SOIm of the single and the pilot injection are approximately the same (-7°ATDC for the single injection and -5.6° ATDC for the pilot injection was the best available comparison) the combustion is significantly retarded for the single injection. The peak of the heat release rate occurs at 9.5°ATDC for the single injection case compared to 4°ATDC for the pilot case. This is 10° and 4.5° after the end of injection for the single and pilot case respectively.

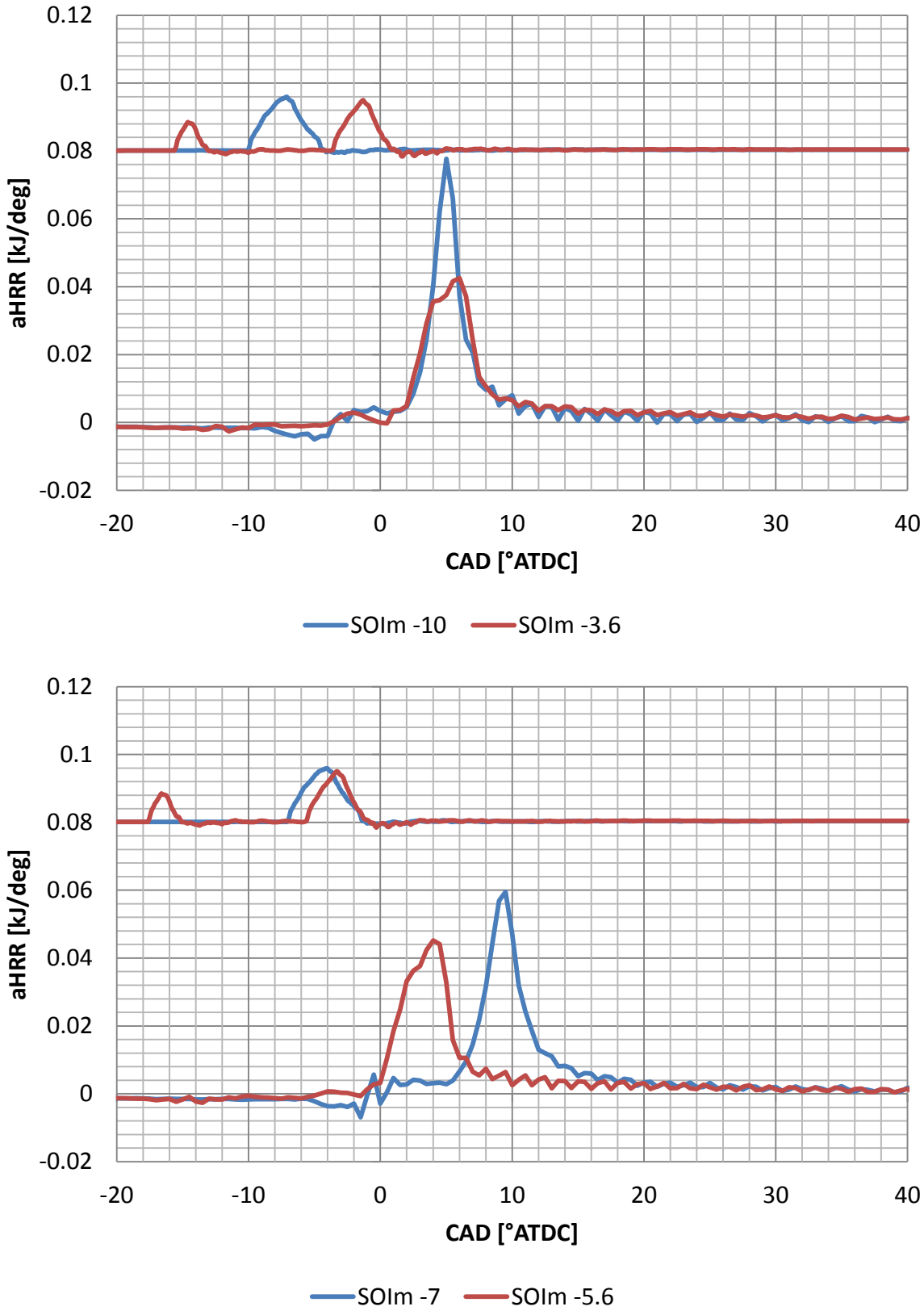

Figure 8.11 Apparent net heat release rate traces and injection schematics for the single (blue) and pilot (red) injection cases. Plots show approximately the same phasing (top) and the same SOIm (bottom)

The effect of the change in combustion on emission and fuel consumption can be seen in the following Figure 8.13. The addition of the pilot at all of the SOIm, results in improvement of isFC_c. The most retarded SOIm for the pilot injection is the lowest isFC_c at 203 g/kWh for an isNOx of 0.95 g/kWh. The single injection case is 8.2 % higher at 219.6 g/kWh at an isNOx of 0.98 g/kWh. The pilot injection case isFC_c continues to improve as the SOIm retards. This could be due to the more advanced combustion initiated by the pilot injection.

Based on the cylinder analysis the reason for the improvement in isFC_c can be identified. When combustion is phased the same (SOIm -10°ATDC for the single injection and SOIm -3.6°ATDC for the pilot injection case), the biggest improvement in the efficiency is from the increase in the conversion of fuel into heat. The pilot injection case fuel conversion efficiency improves by 0.13 kW (2.7 %) for the pilot injection. This is due to the fuel penetration being reduced by the shorter ignition delay, localising combustion and reducing the amount of fuel in the main injection that is too lean to ignite. The rate of heat release is suppressed with the pilot combustion and the heat lost through heat transfer is reduced by 0.11 kW (2.3 %) from the single to the pilot injection case when combustion is phased the same.

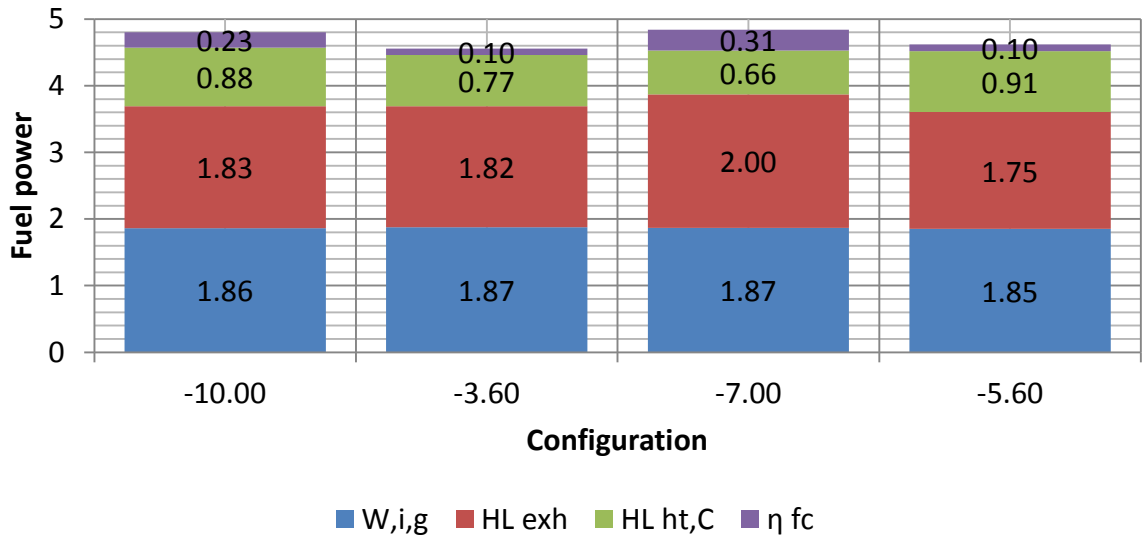

Figure 8.12 Energy diagram for the comparison of the effect of pilot injection on combustion

When the start of the main injection is phased similarly (SOI_m at -7°ATDC for the single injection, SOIm at -5.6°ATDC for the pilot injection case), there is a reduction of 4.3 % in fuel

conversion losses from the single injection event. The rejected heat for both cases is the same (2.66 kW) however the distribution changes between the single and the pilot case. For the single injection case 2 kW is rejected through the exhaust compared to 1.75 kW for the pilot case. The retarded combustion timing seen with the single injection case explains why more heat is rejected through the exhaust.

The difference in heat transfer and crevice loss is 0.24 kW between the two cases. The combustion characteristic of the pilot injection case means the temperature is higher and increases closer to TDC. Generally the heat transfer and crevice losses are higher when combustion occurrs closer to TDC in an SOIm swing.

As observed with the addition of a pilot injection at KP3 and KP2, the smoke emission increases due to the heat release of the pilot whilst fuel is injected in the main event. Time for adequate evaporation and mixing is not available leading to the formation of particulates and a reduction in CO and HC. The smoke number increases to 0.1 FSN from being undetectable with a single injection. The increase in smoke number is less significant than the previous test points, possibly due to the higher AFR at the reduced load and smaller quantity of fuel injected.

The pilot injection reduces the ignition delay and fuel spray penetration before combustion inititates. Over penetration of the fuel prior to combustion is thought to be the cause of the excessive HC and CO emissions due to the fuel spray becoming overly lean and the temperature being too low (Miles, 2010). Figure 8.13 shows that the CO emission is reduced by 65 % from 25.7 g/kWh 9 g/kWh at 0.98 g/kWh. HC is reduced by 71.5 % from 6.27 g/gkWh to 1.79 g/kWh.

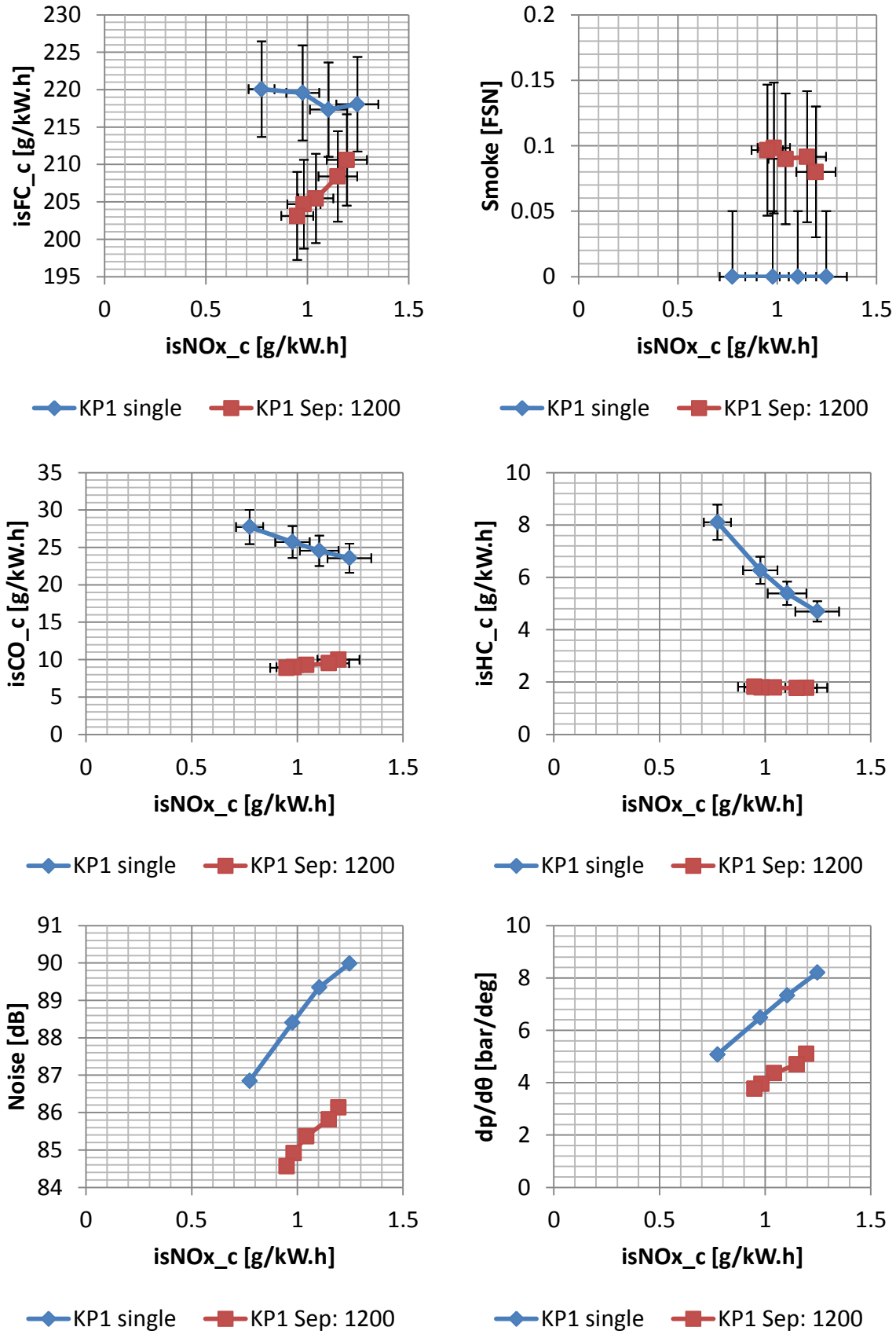

Figure 8.13 Performance and emmissions data for the single and pilot injection case at KP1

8.3 Conclusion of the Pilot Injection Study

The characterisation results demonstrated that at the part load key points selected the single injection strategy leads to highly premixed combustion, with a high rate of heat release and rapid pressure rise rates. This resulted in emissions of CO and HC at KP1 and KP2 but no measureable emission of smoke at these key points. Testing with a pilot injection has shown that the isFC and emissions of CO and HC can be reduced but at the expense of the smoke output.

The reason for this is that the pilot injection causes some heat release to occur around the main injection event. This reduces the time for the fuel and air to mix before combustion initiates, causing the fuel to break down in a high temperature fuel rich environment. The fuel spray penetration is reduced by the shortened ignition delay, which reduces the distribution of fuel further into the combustion chamber. At KP1 and KP2 this is important because the load is low enough that the fuel spray can become overly lean.

At all key points the fuel consumption was improved by the addition of a pilot injection. This was either due to a smaller amount of energy being lost through the exhaust or through heat transfer to the coolant. The heat transfer to the coolant was reduced in some cases because the rapid pressure and temperature rise was suppressed by the combustion becoming diffusive due to the heat release of the pilot injection.

Testing at KP3 and KP2 demonstrated that when a pilot is added and the SOIm retards, the Smoke numbers either reduce or stay the same. This is an indicator that combustion is switching to a low temperature mode where NOx and smoke are reduced simultaneously. Further tests have shown that low temperature combustion is possible on the unconventional bowl design and this is presented in the following section.

8.4 Low Temperature Combustion with a Retarded Injection

At KP3 there is an interesting response observed as the start of injection timing is retarded beyond the normal window used for testing. Figure 8.6 shows that as the SOIm is retarded the smoke response reaches a maximum value. There is potential for further retarding without an increase in smoke number. Therefore a test was conducted where the SOIm was retarded further to observe whether there would be a reduction in smoke by running in a late injection low temperature Diesel combustion mode.

Test name	Speed	Load	Intake temp	Intake pressure	EGR rate	Exhaust pressure	Rail pressure	Pilot size	Pilot separation	SOIm range
	RPM	GIMEP	°C	barA	%	barA	bar	mg/inj	µs	°ATDC
KP3 test	2000	9	42.4	1.47	27.1	2.05	1050	1.3	0, 400, 800, 1200	-9,-7,-5,-3 -5.7,-3.7, -1.7,0.3, 2.3

Table 8.4 Test data for the pilot injection test at KP3.

Table 8.4 contains the test data used when retarding the SOIm beyond the normal window. The smallest pilot (1.3 mg/injection) was used, the SOIm and the separation of the main injection and the pilot were fixed and a timing retard was carried out using the same procedure as the characterisation tests. These tests were defined by the separation of the pilot to the main injection. The pilot tests were compared to the single injection case. Figure 8.14 shows the experimental data from these tests.

All of the pilot injection cases result in an improvement in isFC. This was previously observed with the single pilot test seen in 8.2.1. When the timing was retarded, the isFC deteriorates in the same way for all pilot cases with little difference observed between the individual curves. At the most retarded condition the isFC is the highest (197.5 g/kWh) when the separation is fixed at 400 µs, but the isNOx is the lowest at 0.42 g/kWh.

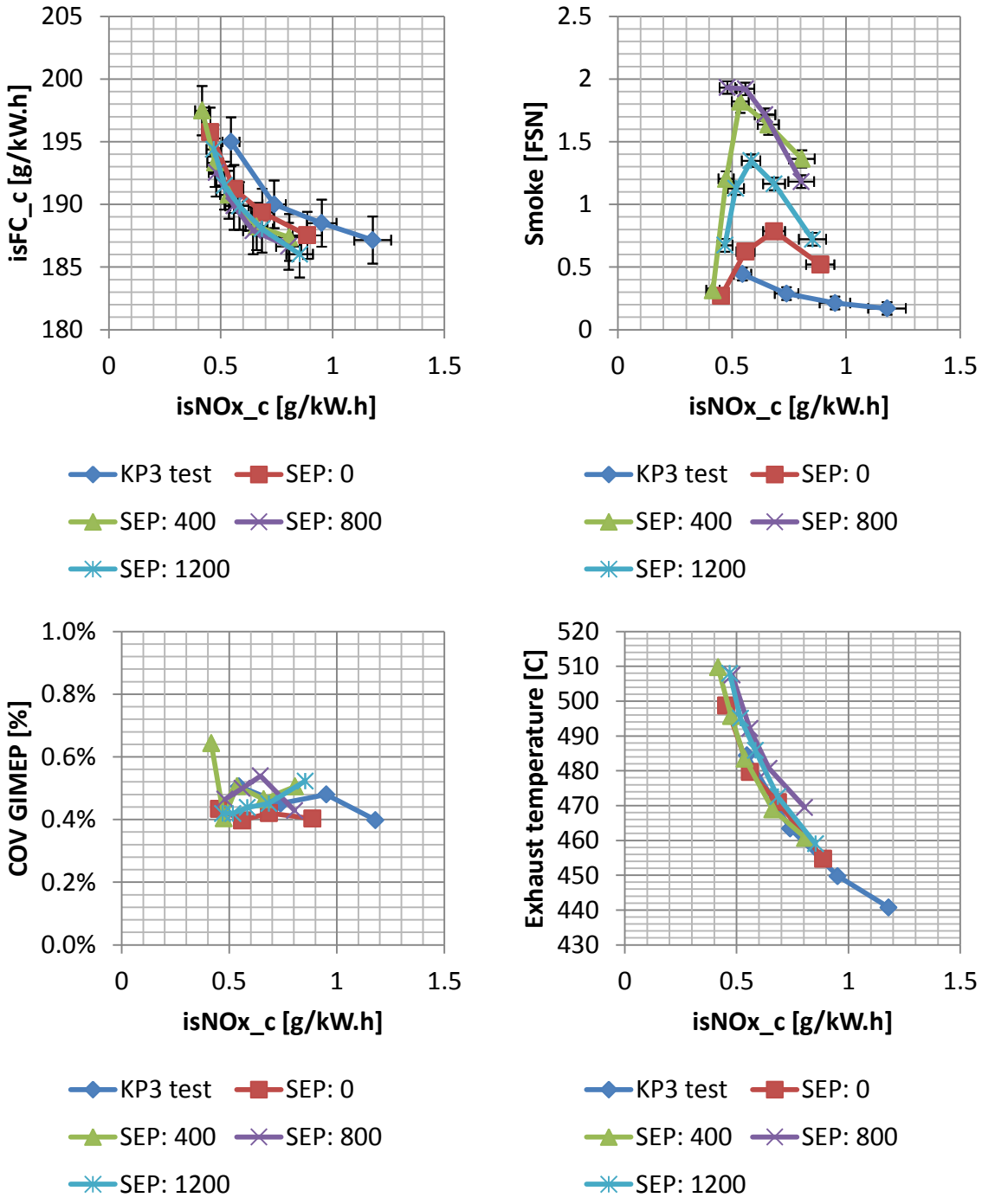

Figure 8.14 Performance and emissions data for the LTC with retarded injection timings

When the separation to the main injection is set at 0 µs, the smoke output is the lowest of all the pilot cases, 0.52 FSN with 0.89 g/kWh isNOx at the most advanced timing. The trend curve is lower than the other pilot injection cases when the timing retards. When the SOIm timing is set to the most retarded timing of 2.3°ATDC, the smoke number reduces to 0.27 FSN at 0.45 g/kWh isNOx. The prototype fuel injection hardware means the pilot

spacing is set without a delay between the end of the pilot and the start of the main injection. The pilot injection does not release heat during the main injection event. The pilot injection cases have similar efficiency as the timing was retarded, but there is an improvement over the single injection case.

Combustion with a 400 µs separation between the pilot and the main injection results in the largest reduction in smoke as the timing is retarded. The peak smoke number is 1.82 FSN which occurs at 0.54 g/kWh when the SOIm is -1.7°ATDC. As the timing is retarded by 2° the smoke number reduces to 1.2 FSN at 0.47 g/kWh isNOx. A further retard of 2° results in a reduction of smoke to 0.32 FSN at 0.42 g/kWh. This is lower than the highly premixed single injection case, in which smoke begins to increase as the SOIm is retarded. The single injection case has an output of 0.44 FSN at 0.55 g/kWh isNOx.

The apparent heat release rate shown in Figure 8.15 is for the 400 µs separation of the pilot to the main injection event. The figure shows that asthe injection timing is retarded the peak of the main injection heat release occurs later after the end of the injection. At the two most advanced timings the peak of heat release rate occurs at 0.7° before the end of the main injection event (EOIm). This reduces to 0.3° before EOIm for an SOIm of -1.7°ATDC, increases to 1.1° after EOIm for SOIm of 0.3°ATDC and eventually increases to 3.5° after EOIm for an SOIm of 2.3°ATDC.

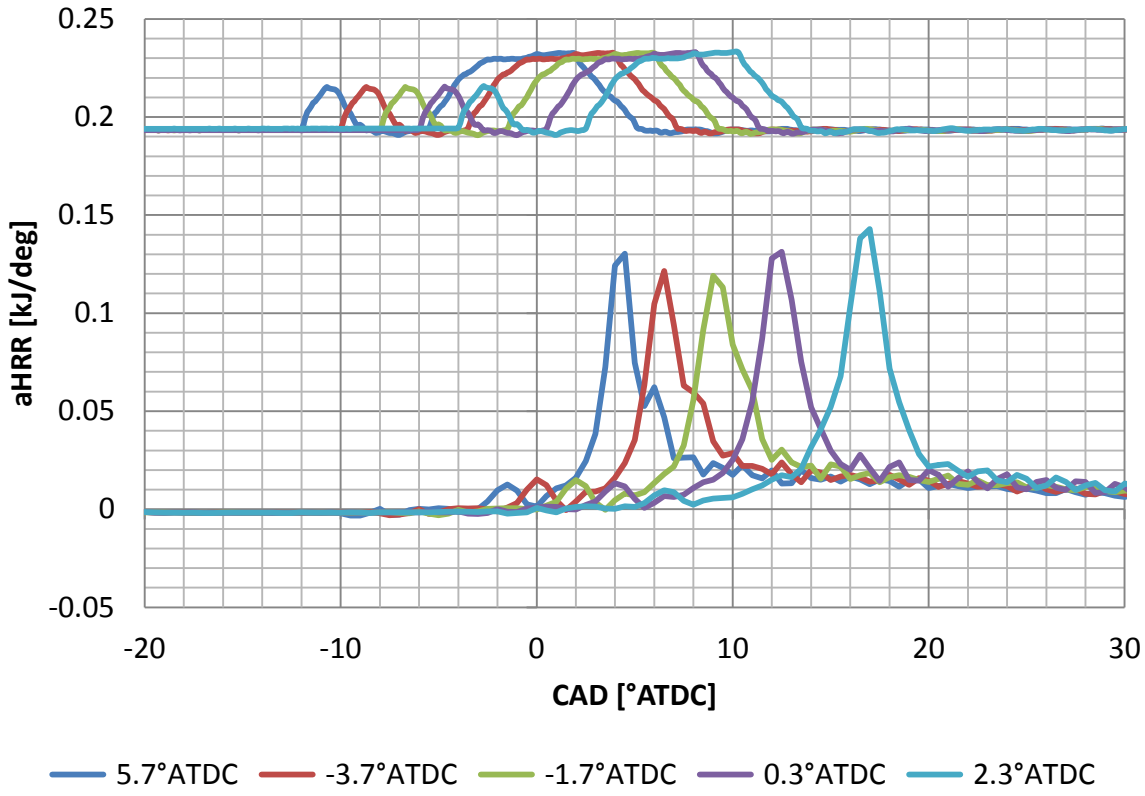

Figure 8.15 Apparent net heat release rate traces and injection schematics for the low temperature combustion case

The process of retarding the main injection event with a fixed separation results in a reduction in the rate of combustion of the main injection heat release as well as a reduction in the peak of the pilot combustion. A reduction in the combustion rate as well as the delay after the end of the main injection event correlates well with the reduction in the smoke number observed. It appears that retarding the injection in this way results in the combustion of the main injection of fuel happening after the pilot combustion, allowing more time for the fuel and air to mix. The expansion of the gases after top dead centre results in a temperature reduction during combustion, helping to reduce the smoke number through low temperature combustion (Dec, 2009).

The smoke response shows that as the pilot separation increases from 0 µs to 1200 µs the smoke number increases and then reduces for all but the most retarded SOIm. This trend is shown in Figure 8.16. The most retarded SOIm, 2.3°ATDC, has the lowest emission of smoke relative to all of the advanced timings used for each separation, but has a different

relationship between smoke and separation. The phasing of the combustion of the pilot fuel quantity influences the mixture formation process.

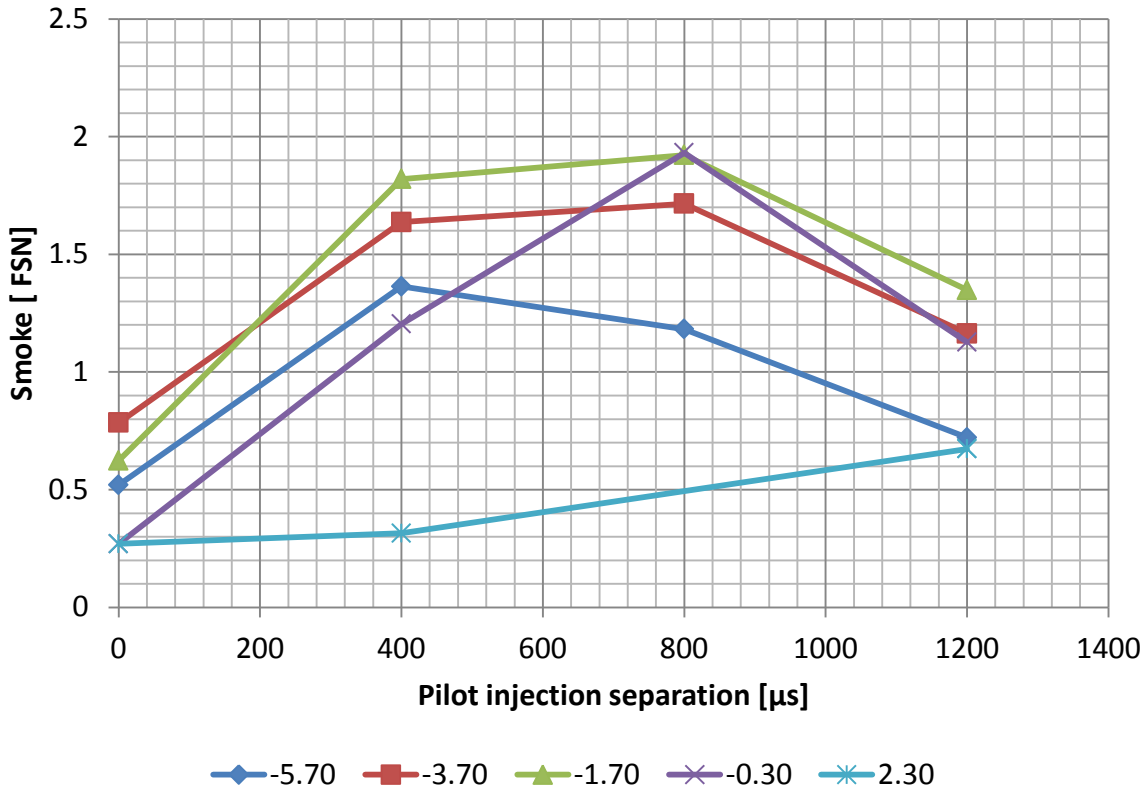

Figure 8.16 Smoke versus pilot injection separation at each SOIm tested

The apparent net rate of heat release shown in Figure 8.17 shows that as the pilot separation increases from the 0 µs there is a small amount of pilot releasing heat during the main injection event. For the 400 µs separation the pilot heat release starts at -2°ATDC, just as the needle reaches maximum lift. As the separation increases to 800 µs the pilot combustion advances to -5°ATDC, just after the SOIm (-5.7°ATDC). Additionally, the peak of the rate of heat release was lower than the 400 µs case.

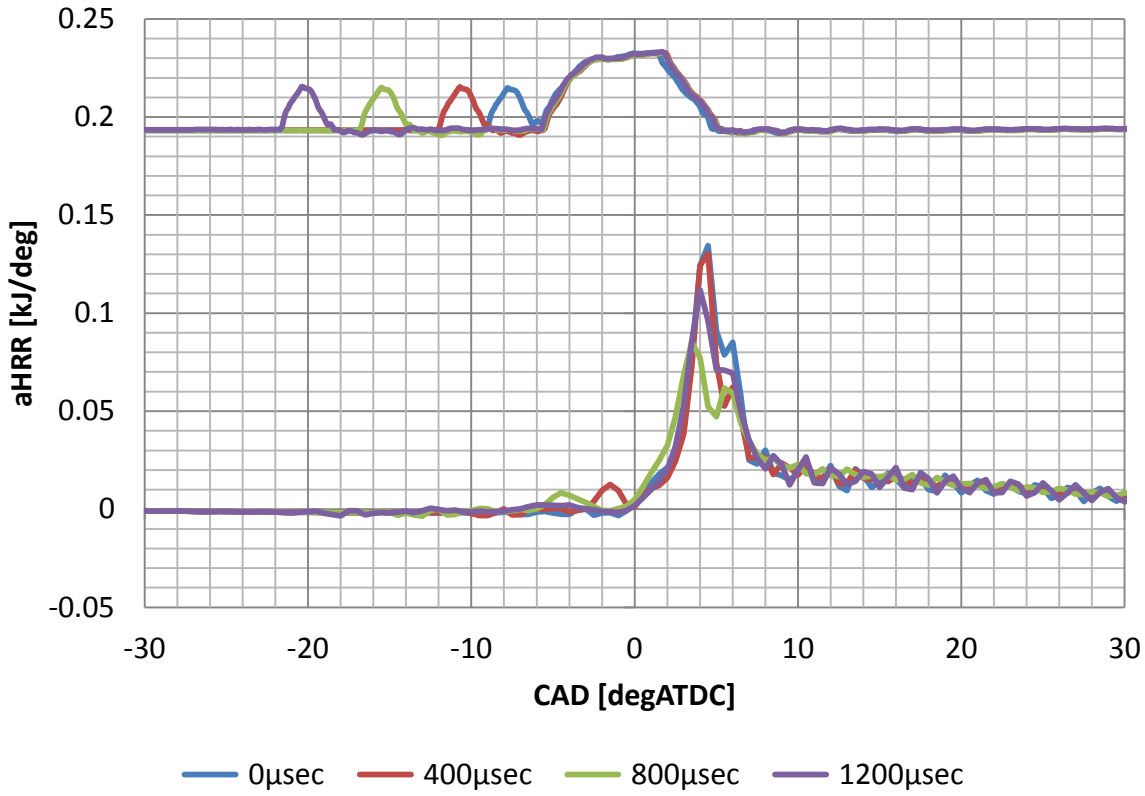

Figure 8.17 Apparent net heat release rate traces and injection schematics for the pilot injection separation test

As the pilot injection separation increases to 1200 µs, the peak of the heat release of the pilot is lower than the 400 µs and 800 µs pilot separations. A smaller proportion of the pilot injection releases heat which reduces the temperature at the start of the main injection event compared to the other cases. When the separation is either 0 µs or 1200 µs there is little or no combustion for the pilot injection compared with the other two pilot separations. The smoke number was lower here because there was no heat release from the pilot injection during the combustion of the main injection event.

8.6 Conclusions of Retarded Injection Timing Study

In carrying out the tests where the timing of the pilot injection cases were retarded further after top dead centre, it was possible to achieve late injection low temperature combustion on the unconventional piston bowl. The addition of the pilot meant that the combustion could be retarded further compared to the single injection event where lower combustion temperatures could be achieved avoiding the formation of smoke through temperature suppression.

The prototype fuel injection hardware allowed the pilot spacing to be set without a delay between the end of the pilot and the start of the main injection. This resulted in the lowest smoke number for the range of SOIm timings tested because the pilot injection did not release heat during the main injection event. The pilot injection cases showed similar efficiency as the timing was retarded, but there was an improvement over the single injection case.

The single injection case was highly premixed and it was found that the curve of isNOx versus smoke increased as the timing was retarded. The only occasion the single injection case achieved a reduction in smoke with a retard of the SOIm timing was when the hole size was reduced and the hole number increased.

9 Conclusions

This thesis documents the research carried out on a light duty Diesel engine, using conventional and unconventional piston bowl designs and conventional and prototype fuel injection equipment. The research has shown that unconventional Diesel piston bowl designs were more thermally efficient than the conventional designs, whilst still achieving low levels of engine out emissions. The research has also shown that the prototype fuel injection equipment could be used to achieve late injection low temperature combustion, with no separation between the pilot and the main injection. Finally the research has added further insight into the process of Diesel combustion through the analysis of engine gas flows and in-cylinder pressure data from protrusion testing and characterisation testing.

The first step in this investigation was to examine the influence of the position of the fuel spray centre on combustion system performance. Each of the piston bowls was tested over a range of engine operating points with combustion system performance evaluated in terms of regulated emissions (NOx, CO, HC and smoke) as well as fuel conversion efficiency. Based upon the performance of the combustion system (combination of piston bowl shape and position of the fuel spray centre) over all test conditions, an injector nozzle protrusion was selected. For three of the bowls tested (B2, B3 and B4) a small protrusion (determined by the use of a 3.1 mm washer installed on the injector) achieved the best overall performance. The testing has shown that the benefit of using the 3.1 mm washer compared to the next best washer for each bowl was; 2.4 %, 1.6 % and 0.5 %, for bowls B2, B3 and B4 respectively. The exception was bowl B5 which required greater protrusion (using a 2.6 mm washer). Optimising bowl B5 with the 3.1 mm washer to benefit Protrusion – 4000FL would have sacrificed the fuel consumption improvement of approximately 1.6 % that was observed at Protrusion – KP3. Increasing protrusion led to the deterioration of the combustion process.

For bowls B2, B3 and B4, the data suggested that the fuel spray entrained less air as the protrusion was increased. This was indicated by the increase in smoke and CO as well as a reduction in NOx. An analysis of the fuel spray impingement over the range of fuel injection timings suggests that this was due to the fuel spray being concentrated in the bowl region, without interacting with either the lip feature for the conventional bowls (B2 and B3) or the pip feature for the unconventional bowl (B4). This analysis supports the conclusions of the

performance assessment that identified a small protrusion (using the 3.1 mm washer) as optimal for these combustion systems.

Spray analysis for bowl B5 suggests that the location of the secondary pip was such that the combustion system performed poorly when the fuel spray was too far above the pip region. This indicates that bowl B5 would require a larger protrusion than the other bowls as was determined from the evaluation of the combustion system performance.

At higher engine outputs, the protrusion test has shown a definite separation in behaviour between the conventional and unconventional piston bowls. There was an increase in emissions and fuel consumption as the protrusion was increased for the unconventional piston bowls (B4 and B5). Fuel consumption was the lowest for the 3.1 mm washer for both bowls; 1 % better than the 2.6 mm washer for B4 and 2 % better than the 2.6 mm washer for bowl B5. The two conventional bowls (B2 and B3) were insensitive to protrusion at high loads; the fuel consumption for bowl B2 did not differ by more than 0.5 % between all washers. Bowl B3 has the same trend apart from the 1.6 mm washer, which resulted in a 3 % difference.

Once the location of the fuel spray centre had been determined for each combustion chamber shape (piston bowl) an extended set of tests was conducted. In this characterisation, it was found that the selected protrusion resulted in the fuel spray becoming overly lean at the lower part load conditions used in the protrusion study. This suggests that an extended protrusion test programme including a wider range of combustion modes should be used to identify an appropriate injector protrusion.

With the selection of the washer established, the characterisation testing was carried out. This testing has shown a separation between the engine outputs of the conventional and unconventional designs. The unconventional bowls had the characteristic that the emission of NOx was higher for the same injection setting. Analysis has shown that combustion was slightly more advanced (0.5 ° to 2 ° in some cases) for the same start of injection timing, indicating that the unconventional bowls had a different mixture formation process. It was thought that the unconventional bowls worked with a fuel spray closer to stoichiometric than the conventional designs. Conventional design mixture formation resulted in a richer

fuel spray, leading to lower NOx emissions. Any formed particulates were oxidised by the turbulent flows in-cylinder.

The unconventional designs were more thermally efficient than the conventional designs. The biggest differences in isFC at part load were observed at KP3 and KP1. At KP3 for the same isNOx of 0.5 g/kWh, B5 had the lowest isFC and B2, B3 and B4 were 1.3 %, 2.5 % and 0.5 % higher. Combustion had to be retarded for the unconventional bowls (B5 by 4 ° and B4 by 2 °) to achieve this isNOx point. A retarded injection event resulted in reduced efficiency which disguised the fuel consumption benefit of the unconventional bowls. Alternative strategies would be required to reduce isNOx without penalising the fuel consumption. At KP1, the isNOx was not comparable for conventional and unconventional bowls, however at the most retarded timing the unconventional bowls B4 and B5 were better than the conventional bowls in terms of isFC by 4 % and 6 % respectively.

The improvement in fuel consumption that was observed with the unconventional designs was as a result of a reduction in the heat transfer energy losses in-cylinder. When the combustion phasing was compared at the same time, the heat transfer losses were generally lower for the unconventional designs for all test conditions. The biggest difference was observed at KP1 where the heat transfer loss percentage was around 1.5 % lower. This effect could be attributed to the difference in the surface area to volume ratio of the piston bowls being favourable for the unconventional designs. Additionally this may also have been due to a reduction in turbulence associated with open chamber piston bowl designs. Without in cylinder flow studies it was not possible to say this with any certainty. Following this, the unconventional bowl, B4, was selected for further testing because it performed better at the full load condition than bowl B5. At 4000FL the fuel consumption was 5 % better for bowl B4 and the smoke output was lower by 2 FSN.

The prototype injector hardware was used in both the protrusion and the characterisation process. A conventional injector type with a similar nozzle specification to one of the prototype injectors was also available. This conventional injector was used in a set of tests with the conventional bowl B2 which matched the injector spray angle. In these tests it was found that at part load the fuel consumption and emissions output was better than with the prototype injector with a similar nozzle. The isFC was 1.34 % lower and the smoke was

0.2 FSN lower. From an analysis of the combustion process it was shown that the combustion rate was slower for the conventional injector type, when compared to the prototype system. The rate of heat release peak was 0.2 kJ/°CA for the prototype injector and 0.05 kJ/°CA less for the conventional injector. This was due to the fact that for the same fuel pressure setting, the fuelling rate was higher for the prototype system due to the ability of the injector to lift the needle directly and without having to spill pressurised fuel.

With a higher fuelling rate, the mixture formation process occurred more rapidly and led to faster combustion. In this case, at part load, the fuel consumption was worse for the prototype injector, because the faster combustion process resulted in more heat being rejected through heat transfer in cylinder. This difference varied in magnitude at each key point; 1.6 % at KP3, 3.1 % at KP2 and 1.2 % at KP1.

The faster mixture formation and combustion process that the prototype injection system generated was beneficial at the higher load condition resulting in an improvement in fuel consumption by 3 % and a reduction in smoke by 0.3 FSN. In particular, the lower emissions of particulates would be an advantage at the higher loads as this would result in a reduction in particle filter loading in vehicle applications. While the shape of the injection rate of the prototype injectors can be modified by controlling the needle velocity, this function was not available in this study. It could enable this injector to match the performance of the conventional injector at part load conditions by reproducing the same needle lift profile.

The nozzle testing carried out during in the characterisation process compared the effect of a prototype injector nozzle with 7 holes, 8 holes and 9 holes on each bowl. The results were only shown for bowl B4 as it was selected in the characterisation process. The results have shown that at part load condition KP3, there was a reduction in smoke output with the 9 hole injector, without any penalty on fuel consumption. The smoke number was 0.5 FSN lower for the 9 hole injector at the most retarded SOIm. The smoke reduction was a result of the fuel spray reducing in size when the size of the hole decreased, thus reducing the rich regions in the fuel spray. The 9 holes injector was comparable to the other injectors in terms of fuel consumption and emission at the remaining part load key points. The assessment of the smoke benefit of the 9 holes nozzle was difficult at the remaining key points because combustion was highly premixed due to the lower loads and longer ignition delay. Premixed

combustion tended to result in either no smoke forming or complete oxidation of the formed particulates. The 9 holes injector suffered as the engine speed increased beyond 2000 RPM to 4000 RPM and the load increased to the maximum tested. The isFC was 0.8% worse than a 7 holes injector and the smoke number was 0.6 FSN worse at the most retarded timing. Before saying definitively that the 9 holes injector should be selected for a reduction in engine out smoke it is recommended that testing at higher load NEDC points should be carried out.

Multiple injection strategies are common in production Diesel engines. In order to contain the time required to complete the characterisation tests only single injection events were employed in this phase of the study. Following the selection of the best performing bowl from the characterisation tests, bowl B4, the effect of pilot injection strategies on this combustion system were investigated.

The results of the pilot injection study show that the unconventional bowl can operate using this type of injection strategy. The unconventional bowl B4 does not react unusually to pilot injection timing. The effect of the pilot injection on the unconventional bowl at the part load condition was a reduction in HC and CO emission at the expense of the smoke output for conventional injection timings. At KP3 HC and CO were reduced by 0.2 g/kWh and 0.5 g/kWh respectively but this was where the largest increase in the smoke emission was observed (from 0.7 to 1.5 FSN). The smoke output increased at the part load conditions when the pilot injection timing resulted in combustion of the fuel added by the pilot during the main injection. The emissions of HC and CO were reduced because of a decrease in the ignition delay caused by the combustion of the fuel added by the pilot. This minimised the lean regions in the fuel spray thus improving the emissions. It was also observed that the fuel consumption improved when a pilot injection was added. The improvements were as much as 2.1 %, 5.4 % and 7.4 % at KP3, KP2 and KP1 respectively. The speed of the mixture formation slowed and thus the combustion process, which reduced the heat losses due to heat transfer in-cylinder. At KP1, when combustion of the main portion of fuel was phased the same as the single injection the heat losses due to heat transfer were reduced by 1.4 %. This improvement was observed up to the point where the fuel consumption deteriorated

because the slower combustion led to heat being rejected through the exhaust when combustion retarded.

When the injection timing was retarded further at KP3 the combustion mode switched to a late low-temperature type resulting in a simultaneous reduction in NOx and smoke, achieving 0.27 FSN at isNOx 0.45 g/kWh compared to the single injection case that had 0.44 FSN at isNOx of 0.55 g/kWh. This demonstrates the potential of the unconventional bowl designs for use with low temperature combustion strategies.

In conclusion, this research has shown that unconventional bowl designs, operated with a prototype injection system and using a mixture of combustion strategies can produce improvements in fuel consumption and emission when compared to conventional piston bowl designs. The combination of an open combustion chamber with a secondary pip to aid the mixture formation process and high flow rate fuel injectors produced the best combustion system. This combination was suitable for all round performance at both part load and high load. The injector nozzle could be selected with more holes of a smaller size for an emission benefit at the medium load conditions.

10 Future Work

The protrusion optimisation should be tested at both higher and lower key points to create a map of the effects of protrusion over a wider range of conditions. This study has shown that the optimisation at one part load key point can lead to poor performance at lower load conditions. It would be useful to test protrusion at higher loads seen on the NEDC as well as lower loads, such as KP1.

Work should be carried out to understand the mixture formation effect of the unconventional designs. It was postulated that the secondary pip aided the entrainment of air into the fuel spray leading to combustion that resulted in a reduction in particulate formation at part load. The in-cylinder behaviour understanding needs to improve as there was not enough information available from the engine testing to establish why unconventional piston bows were different at the full load protrusion test.

The testing of the unconventional bowl could only be carried out with the prototype piezo injectors and should be tested with the conventional solenoid design to examine the effect of that combination. The prototype injectors were probably the most suitable due to the process of mixture formation relying on fuel spray energy rather than turbulence in cylinder to enhance combustion. The prototype fuelling rate could be investigated to demonstrate the impact on emissions and fuel consumption for the unconventional bowls.

Further work should be carried out with the fuelling rate of the prototype injectors to assess whether the performance of the conventional injector can be replicated in terms of the smoke and fuel consumption output. This could be both multiple injection testing and rate shaping. Testing at higher part load points should be carried out to examine the limit of the effect of rate control because there was a limit to the benefit a full load.

References

ABRAHAM, J., KHAN, A. & MAGI, V. (1999) Jet-jet and jet-wall interactions of transient jets from multi-hole injectors. *SAE Technical Paper 1999-01-0513*.

AKAGAWA, H., MIYAMOTO, T., HARADA, A., SASAKI, S., SHIMAZAKI, N., HASHIZUME, T. & TSUJIMURA, K. (1999) Approaches to solve problems of the premixed lean diesel combustion. *SAE TRANSACTIONS,* 108**,** 120-132.

AKIHAMA, K., TAKATORI, Y., INAGAKI, K., SASAKI, S. & DEAN, A. M. (2001) Mechanism of the smokeless rich diesel combustion by reducing temperature. *SAE TRANSACTIONS,* 110**,** 648-662.

AMAGAI, K., MARUYAMA, Y., SAITO, M. & ARAI, M. (2003) Spray-to-Spray Interactions after Wall Impingement. *SAE Technical Paper 2003-01-1835*.

ANSELMI, P., KASHDAN, J., BRESSION, G., FERRERO-LESUR, E., THIROUARD, B. & WALTER, B. (2010) Improving Emissions, Noise and Fuel Economy Trade-Off by using Multiple Injection Strategies in Diesel Low Temperature Combustion (LTC) Mode. *SAE Technical Paper 2010-01-2162*.

BAE, C., YU, J., KANG, J., KONG, J. & LEE, K. O. (2002) Effect of nozzle geometry on the common-rail diesel spray. *SAE Technical Paper 2002-01-1625*.

BENAJES, J., MOLINA, S., NOVELLA, R. & DERUDDER, K. (2008) Influence of injection conditions and exhaust gas recirculation in a high-speed direct-injection diesel engine operating with a late split injection. *Proceedings of the Institution of Mechanical Engineers, Part D: Journal of Automobile Engineering,* 222**,** 629-641.

BICKERSTAFFE, S. (2009) No one ideal solution. *Automotive Engineer.* Caspian Media.

BOSCH, R. (2000) *Automotive Handbook,* Stuttgart, Bentley Publishers.

CARLUCCI, P., FICARELLA, A. & LAFORGIA, D. (2005) Effects on combustion and emissions of early and pilot fuel injections in diesel engines. *International Journal of Engine Research,* 6**,** 43-60.

CARR, R. (2014) Paxman Diesel Engines since 1934. *http://www.paxmanhistory.org.uk/images/comethd.gif*.

CHOI, D., MILES, P. C., YUN, H. & REITZ, R. D. (2005) A Parametric Study of Low-Temperature, Late-Injection Combustion in a HSDI Diesel Engine. *JSME International Journal Series B,* 48**,** 656-664.

CLEYNEN, O. (2011) Cutaway of a MAN V8 Diesel engine. *http://en.wikipedia.org/wiki/File:Cutaway_of_a_MAN_V8_Diesel_engine.jpg*.

DAVIS, N. (2011) Diesel-Emission-Control. *http://autorepair.about.com/library/graphics/42003930.gif*.

DEC, J. (1997) A Conceptual Model of DI Diesel Combustion Based on Laser-Sheet Imaging. *SAE Technical Paper 970873*.

DEC, J. (2009) Advanced compression-ignition engines--understanding the in-cylinder processes. *Proceedings of the Combustion Institute,* 32**,** 2727-2742.

DOUG, W. (2009) Wärtsilä (Sulzer) Low-Speed Engines. *Pounder's Marine Diesel Engines and Gas Turbines (Ninth edition).* Oxford, Butterworth-Heinemann.

FANG, T., COVERDILL, R. E., LEE, C. F. & WHITE, R. A. (2008a) Effects of injection angles on combustion processes using multiple injection strategies in an HSDI diesel engine. *Fuel,* 87**,** 3232-3239.

FANG, T., COVERDILL, R. E., LEE, C. F. F. & WHITE, R. A. (2008b) Low temperature premixed combustion within a small bore high speed direct injection (HSDI) optically accessible diesel engine using a retarded single injection. *International Journal of Automotive Technology,* 9**,** 551-561.

FANG, T. G., COVERDILL, R. E., LEE, C. F. F. & WHITE, R. A. (2008c) Low-sooting combustion in a small-bore high-speed direct-injection diesel engine using narrow-angle injectors. *Proceedings of the Institution of Mechanical Engineers, Part D: Journal of Automobile Engineering,* 222**,** 1927-1937.

FRENKLACH, M. & WANG, H. (1994) Soot Formation in Combustion: Mechanisms and Models. *Ed. Bockhorn, H. Kazakov, A. and Frenklach M.(1998) Combustion and Flame,* 114**,** 484-510.

HAN, Z., ULUDOGAN, A., HAMPSON, G. J. & REITZ, R. D. (1996) Mechanism of soot and NOx emission reduction using multiple-injection in a diesel engine. *SAE TRANSACTIONS,* 105**,** 837-852.

HASEGAWA, R. & YANAGIHARA, H. (2003) HCCI Combustion in DI Diesel Engine. *SAE Technical Paper 2003-01-0745*.

HEISLER, H. (2002) *Advanced vehicle technology*, Butterworth-Heinemann.

HEYWOOD, J. B. (1988) *Internal combustion engine fundamentals,* New York, McGraw-Hill.

IIDA, N., YAMASAKI, Y. & SATO, S. (2004) The Key Points of HCCI Combustion Controls. Editions TECHNIP.

IKEGAMI, M., FUKUDA, M., YOSHIHARA, Y. & KANEKO, J. (1990) Combustion chamber shape and pressurized injection in high-speed direct-injection diesel engines. *SAE Technical Paper 900440*.

KAMIMOTO, T. & BAE, M. H. (1988) High combustion temperature for the reduction of particulate in diesel engines. *SAE Technical Paper 880423*.

KARIMI, K. (2007) Characterisation of multiple-injection diesel sprays at elevated pressures and temperatures. School of Engineering, University of Brighton.

KIDOGUCHI, Y., YANG, C. & MIWA, K. (1999) Effect of high squish combustion chamber on simultaneous reduction of NOx and particulate from a direct-injection diesel engine. *SAE Technical Paper 1999-01-1502*.

KIM, D., EKOTO, I., COLBAN, W. F. & MILES, P. C. (2008) In-cylinder CO and UHC Imaging in a Light-Duty Diesel Engine during PPCI Low-Temperature Combustion. *SAE Int. J. Fuels Lubr.,* 1**,** 933-956.

KIMURA, S., AOKI, O., KITAHARA, Y. & AIYOSHIZAWA, E. (2001) Ultra-clean combustion technology combining a low-temperature and premixed combustion concept for meeting future emission standards. *SAE Technical Paper 2001-01-0200*.

KIMURA, S., AOKI, O., OGAWA, H., MURANAKA, S. & ENOMOTO, Y. (1999) New combustion concept for ultra-clean and high-efficiency small DI diesel engines. *SAE Technical Paper 1999-01-3681*.

KITAMURA, T., ITO, T., SENDA, J. & FUJIMOTO, H. (2002) Mechanism of smokeless diesel combustion with oxygenated fuels based on the dependence of the equivalence ration and temperature on soot particle formation. *International Journal of Engine Research,* 3**,** 223-248.

KOOK, S., BAE, C., MILES, P. C., CHOI, D. & PICKETT, L. M. (2005) The Influence of Charge Dilution and Injection Timing on Low-Temperature Diesel Combustion and Emissions. *SAE Technical Paper 2005-01-3837*.

LAGUITTON, O. (2005) Advanced Diesel Combustion Strategies for Ultra-Low Emissions. Brighton, University of Brighton.

LAGUITTON, O., CRUA, C., COWELL, T., HEIKAL, M. R. & GOLD, M. R. (2007) The effect of compression ratio on exhaust emissions from a PCCI diesel engine. *Energy Conversion and Management,* 48**,** 2918-2924.

LECHNER, G. A., JACOBS, T. J., CHRYSSAKIS, C. A., ASSANIS, D. N. & SIEWERT, R. M. (2005) Evaluation of a narrow spray cone angle, advanced injection timing strategy to achieve partially premixed compression ignition combustion in a diesel engine. *SAE Technical Paper 2005-01-0167*.

LÜ, X.-C., CHEN, W. & HUANG, Z. (2005) A fundamental study on the control of the HCCI combustion and emissions by fuel design concept combined with controllable EGR. Part 1. The basic characteristics of HCCI combustion. *Fuel,* 84**,** 1074-1083.

MANCARUSO, E., MEROLA, S. S. & VAGLIECO, B. M. (2008) Study of the multi-injection combustion process in a transparent direct injection common rail diesel engine by means of optical techniques. *International Journal of Engine Research,* 9**,** 483-498.

MARTYNOV, S. (2005) Numerical simulation of the cavitation process in diesel fuel injectors. Brighton, The University of Brighton.

MASON, D., BEGG, S., COOPER, B. & JACKSON, N. (2008) A low compression ratio low NOx diesel combustion system. *DIESEL ENGINES: The Low CO2 and Emissions Reduction Challenge.* Rouen, France.

MIDDLEMISS, I. D. (1978) Characteristics of the Perkins 'Squish Lip' Direct Injection Combustion System. *SAE Technical Paper 780113*.

MILES, P. (2007) Sources and mitigation of CO and UHC emissions in low-temperature diesel combustion regimes: Insights obtained via homogeneous reactor modeling. *Diesel Engine Efficiency and Emissions Research (DEER).* Detroit, Michigan.

MILES, P. (2010) Sources of UHC and CO in Low Temperture Automotive Diesel Combustion Systems. *Directions in Engine-Efficiency and Emissions Research (DEER)* Detroit, Michigan.

MINATO, A., TANAKA, T. & NISHIMURA, T. (2004) Investigation of premixed lean diesel combustion with ultra high pressure injection. *Isuzu Technical Journal,* 112**,** 57-63.

MOLLENHAUER.K & TSCHOEKE.H (2010) *Handbook of Diesel Engines,* Berlin Heidelberg, Springer-Verlag.

MONTAJIR, R. M., TSUNEMOTO, H., ISHITANI, H. & MINAMI, T. (2000) Fuel spray behavior in a small DI diesel engine: effect of combustion chamber geometry. *SAE Technical Paper 2000-01-0946*.

MOUKAIDECHE, F. (2009) *Oracle Hydra Build Book*, Ricardo Consulting Engineers.

OCHOTERENA, R. L. & ANDERSSON, S. (2008) Time and Spatially Resolved Temperature Measurements of a Combusting Diesel Spray Impinging on a Wall. *SAE Int. J. Fuels Lubr.,* 1**,** 970-983.

OKUDE, K., MORI, K., SHIINO, S. & MORIYA, T. (2004) Premixed compression ignition (PCI) combustion for simultaneous reduction of NOx and soot in diesel engine. *SAE Technical Paper 2004-01-1907*.

ONISHI, S., JO, S. H., SHODA, K., DO JO, P. & KATO, S. (1979) Active Thermo-Atmosphere Combustion (ATAC) - A New Combustion Process for Internal Combustion Engines. *SAE Technical Paper 790501*.

PARK, S. W. & REITZ, R. D. (2009) Optimization of fuel/air mixture formation for stoichiometric diesel combustion using a 2-spray-angle group-hole nozzle. *Fuel,* 88**,** 843-852.

PAYRI, R., SALVADOR, F. J., GIMENO, J. & DE LA MORENA, J. (2011) Influence of injector technology on injection and combustion development - Part 1: Hydraulic characterization. *Applied Energy,* 88**,** 1068-1074.

PAYRI, R., SALVADOR, F. J., GIMENO, J. & ZAPATA, L. D. (2008) Diesel nozzle geometry influence on spray liquid-phase fuel penetration in evaporative conditions. *Fuel,* 87**,** 1165-1176.

PICKETT, L. M. & LOPEZ, J. J. (2005) Jet-wall interaction effects on diesel combustion and soot formation. *SAE TRANSACTIONS,* 114**,** 803-817.

PICKETT, L. M., SIEBERS, D. L. & IDICHERIA, C. A. (2005) Relationship between ignition processes and the lift-off length of diesel fuel jets. *SAE Technical Paper 2005-01-3843*.

RYAN, T. (2007) HCCI – A Technical Review and Progress Report 2006.

RYAN, T. W., CALLAHAN, T. J. & MEHTA, D. (2004) HCCI in a variable compression ratio engine-effects of engine variables. *SAE Technical Paper 2004-01-1971*.

SAITO, T., DAISHO, Y., UCHIDA, N. & IKEYA, N. (1986) Effects of combustion chamber geometry on diesel combustion. *SAE Technical Paper 861186*.

SCHÖPPE, D. & ZÜLCH, S. (2009) Future Trends in Light Duty Diesel Fuel Injection Systems. *18. Aachener Kolloquium Fahrzeug- und Motorentechnik 2009.* Aachen.

SHIMAZAKI, N., TSURUSHIMA, T. & NISHIMURA, T. (2003) Dual mode combustion concept with premixed diesel combustion by direct injection near top dead center. *SAE TRANSACTIONS,* 112**,** 1060-1069.

SJÖBERG, M. & DEC, J. E. (2005) An investigation into lowest acceptable combustion temperatures for hydrocarbon fuels in HCCI engines. *Proceedings of the Combustion Institute,* 30**,** 2719-2726.

SOM, S., RAMIREZ, A. I., LONGMAN, D. E. & AGGARWAL, S. K. (2011) Effect of nozzle orifice geometry on spray, combustion, and emission characteristics under diesel engine conditions. *Fuel,* 90**,** 1267-1276.

STONE, R. (1999) *Introduction to internal combustion engines*, Palgrave Macmillan.

TANAKA, T., ANDO, A. & ISHIZAKA, K. (2002) Study on pilot injection of DI diesel engine using common-rail injection system. *JSAE Review,* 23**,** 297-302.

THIROUARD, M., MENDEZ, S., PACAUD, P., CHMIELARCZYK, V., AMBRAZAS, D., GARSI, C., LAVOISIER, F. & BARBEAU, B. (2009) Potential to improve specific power using very high injection pressure in HSDI Diesel engines. *SAE Technical Paper 2009-01-1524*.

THRING, R. H. (1989) Homogeneous charge compression ignition engine. *SAE 890268*.

WALTER, B. & GATELLIER, B. (2002) Development of the High Power NADITM Concept Using Dual Mode Diesel Combustion to Achieve Zero NOx and Particulate Emissions. *SAE technical Paper 2002-01-1744*.

YAO, M., ZHENG, Z. & LIU, H. (2009) Progress and recent trends in homogeneous charge compression ignition (HCCI) engines. *Progress in Energy and Combustion Science,* 35**,** 398-437.

ZHENG, Z. & YAO, M. (2009) Charge stratification to control HCCI: Experiments and CFD modeling with n-heptane as fuel. *Fuel,* 88**,** 354-365.

Appendix A Fuel Specification

PETROCHEM CARLESS

CERTIFICATE OF ANALYSIS

MATERIAL: Carcal 725A (Marked) †

PRODUCT CODE: 17106

BATCH NUMBER: 09/123
CERTIFICATION DATE: 11/01/10
CERTIFICATE NUMBER: 2846

PROPERTY (UNITS)	SPECIFICATION Min	Max	RESULT	METHOD
Cetane Number *	52.0	54.0	52.8	D613
Density @ 15°C, g/ml	0.833	0.837	0.8348	D4052
Distillation, °C				D86
IBP	TBR		199.0	
10% Recovered	TBR		218.0	
50% Recovered	245.0	280.0	273.0	
90% Recovered	TBR		326.5	
95% Recovered	345.0	350.0	347.5	
FBP		370.0	354.5	
Cetane Index	50.0		54.2	D4737
Aromatic Content, %v/v	TBR		31.0	D1319
Olefin Content, %v/v	TBR		3.3	D1319
Saturate Content, %v/v	TBR		65.7	D1319
Pensky Closed Flash, °C	55.0		86	D93
Polycyclic Aromatics, %m/m *	3.0	6.0	4.0	IP391
Fatty Acid Methyl Ester, %v/v		Prohibited	NIL	EN14078
Strong Acid Number, mg KOH/g *		0.02	0	D974
Oxidation Stability, mg/100ml *		2.5	0.7	D2274
Copper Corrosion, 3hrs @ 100°C		Class 1	1b	D130
Viscosity @ 40 °C, cSt	2.3	3.3	2.70	D445
Sulphur Content, mg/kg	6.0	10.0	9.3	IP531
Lubricity, µm *		400	323	ISO12156
Conradson Carbon Residue on 10% Dist. Residue, %m/m *		0.2	0.01	D189
Ash Content, %m/m *		0.01	0.001	D482
Cloud Point, °C *		-5	-20	D2500
Cold Filter Plugging Point, °C		-15	-16	EN116
Water and Sediment, %v/v *		0.02	0	D2709
Oxygen Content, %m/m *	TBR		<0.04	Elem. Analysis
Carbon Content, %m/m *	TBR		86.45	D5291
Hydrogen Content, %m/m *	TBR		13.55	D5291
H/C Atomic Ratio	TBR		1.88	Calculation
O/C Atomic Ratio	TBR		<0.0003	Calculation
Carbon Weight Fraction	TBR		0.8645	Calculation
Gross Calorific Value, MJ/kg *	TBR		45.62	IP12
Net Calorific Value, MJ/kg	TBR		42.75	IP12
Net Calorific Value, Btu/lb	TBR		18379	IP12

The results marked with an asterisk were obtained from a subcontracted test house. † Marked in accordance with current C&E regulations. All other tests were carried out by Petrochem Carless.

ISSUED BY	S. Calver	POSITION	RCR Chemist
CHECKED BY	J. Thrower		
ISSUING SIGNATURE	.....	ISSUE DATE	30/6/10